CRANFIELD UNIVERSITY

KANMING WANG

ANAEROBIC MEMBRANE BIOREACTORS IN UPFLOW ANAEROBIC SLUDGE BLANKET CONFIGURATION FOR ENERGY NEUTRAL SEWAGE TREATMENT

SCHOOL OF WATER, ENERGY AND ENVIRONMENT

PhD

Academic Year: 2014 - 2018

Supervisor: Dr. Ewan McAdam and Dr. Ana Soares
March 2018

CRANFIELD UNIVERSITY

SCHOOL OF WATER, ENERGY AND ENVIRONMENT

PhD

Academic Year 2014 - 2018

KANMING WANG

ANAEROBIC MEMBRANE BIOREACTORS IN UPFLOW ANAEROBIC SLUDGE BLANKET CONFIGURATION FOR ENERGY NEUTRAL SEWAGE TREATMENT

Supervisor: Dr. Ewan McAdam and Dr. Ana Soares
March 2018

This thesis is submitted in partial fulfilment of the requirements for the degree of Doctor of Philosophy

ABSTRACT

Anaerobic membrane bioreactors (AnMBRs) are emerging as a promising technology to offer the prospect to achieve energy neutral sewage treatment. The key challenges limiting full-scale application of AnMBR for municipal wastewater treatment are high operational cost of energy demand for fouling control and high capital cost of membrane investments. This thesis explores a novel pseudo dead-end gas sparging regime for membrane fouling control, enabling a high sustainable flux (15 L m^{-2} h^{-1}) with low energy demand (0.14 kWh m^{-3}) in upflow anaerobic sludge blanket (UASB) configured AnMBR, sufficient to achieve energy neutral sewage treatment. However, this strategy is only possible within low solids environment, emphasising the importance of solids management in the UASB reactor. Solids accumulated in the sludge blanket enhances UASB treatment efficiency during the steady-state operation, indicating to control the sludge blanket at a threshold between the sludge blanket development and steady-state period. The granular inoculum has good stability which exerts a positive influence on reactor stability and sustained permeability, whilst the flocculent inoculum enables to deliver similar sustained membrane operation provided the sludge blanket is controlled. Low temperatures (average temperature of 10 °C) cause the instability of UASB reactor especially for the one with flocculent inoculum biomass. It is therefore proposed to keep relatively high upflow velocity (V_{up}) of 0.8-0.9 m h^{-1} in the UASB reactor for granular AnMBR to promote the stratification of particular and granular material, whilst reducing V_{up} to 0.4 m h^{-1} for flocculent AnMBR to minimise solids washout and sustain membrane operation at low temperatures. The potential for permeability recovery following peak flow (diurnal peaks and storm water flows) has been investigated and evidenced, suggesting that membrane surface area for AnMBR can be specified based on average flow, providing a considerable (67 %) capital cost reduction compared with the design based on peak flows (three times of average flow). Importantly, this thesis promotes UASB configured AnMBR as a highly reliable and more economically viable technology, facilitating to achieve the energy neutral sewage treatment at ambient temperature.

Key words: Cost, gas sparging regime, inoculum biomass, MBR, membrane fouling, operational resilience, peak flow, pseudo dead-end filtration, sludge blanket stability, solids accumulation, unsteady-state

ACKNOWLEDGEMENTS

My first acknowledgement goes to my supervisor Dr. Ewan McAdam, for guiding me through this three-year PhD project, overcoming all the challenges (not problems) and pushing me to think more about the mechanisms and the underpinning science. Thanks to Dr. Ana Soares for her continuous encouragement and positive point of view during my research. Additional thanks to Professor Bruce Jefferson, who always provides constructive suggestions during my progress review and industry sponsor meetings.

Thanks also go to my industry sponsors: Anglian Water, Scottish Water, Severn Trent Water and Thames Water for their financial and technical support.

I would like to thank all the technicians for their technical support especially Jane Hubble and Nigel Janes. Thanks to Nigel for all his help to look after my experimental rigs when I was away and I quite enjoyed working with you in the pilot hall.

I also want to thank Joana Manuel Silva Dias, my pilot hall plant neighbour and good friend. Thank you for your support and encouragement all the way through my PhD. To Edwina Mercer, I will always be thankful for all your help and support especially for your proof reading of this thesis.

Finally, thanks to my parents, grandparents, uncle, aunt and little brother for their continuous support and encouragement. Thanks all my friends in Cranfield especially Philani, Lawson, Sabrina, Carlos, Lloyd, Judith, Salvatore, Sam, Xiangfang and Chenglei for their moral support.

TABLE OF CONTENTS

ABSTRACT i
ACKNOWLEDGEMENTS iii
LIST OF FIGURES ix
LIST OF TABLES xv
ABBREVIATIONS xvii
NOTATIONS xix
GREEK LETTERS xxi
1 Introduction 3
1.1 Background 3
1.2 Aim and objectives 8
1.3 Thesis structure 9
1.4 References 11
2 Comparison of fouling between aerobic and anaerobic MBR treating municipal wastewater 19
2.1 Introduction 20
2.2 Biomass characteristics 22
2.2.1 Mixed liquor suspended solids 23
2.2.2 Particle size distribution 26
2.2.3 Organic fouling by EPS 28
2.3 Fouling control strategies 33
2.3.1 Specific gas demand and operation flux 33
2.3.2 Physical and chemical cleaning: Reversible, irreversible and irrecoverable fouling 35
2.4 Establishing the energy profile of AnMBR for municipal application 39
2.4.1 Towards energy neutral wastewater treatment 39
2.4.2 Emerging engineered solutions to constrain energy demand within AnMBR 43
2.5 Conclusions 44
2.6 Acknowledgements 46
2.7 References 46
3 Evaluation of the impact of solids accumulation in granular and flocculent upflow anaerobic sludge blanket (UASB) reactors for settled municipal wastewater treatment under temperate conditions 67
3.1 Introduction 68
3.2 Materials and methods 70
3.2.1 UASB pilot plants 70
3.2.2 Statistical analysis 72
3.2.3 Analytical methods 73

3.3 Results 75
3.3.1 Impact of sludge blanket stability on solid and organic separation 75
3.3.2 Impact of sludge blanket stability on biogas production 77
3.3.3 Impact of temperature on sludge blanket stability 79
3.3.4 Adjustment of V_{up} to maintain sludge blanket stability 86
3.4 Discussion 88
3.5 Conclusions 91
3.6 Acknowledgements 92
3.7 References 92
3.8 Supplementary data 97
4 Comparison of granular and flocculent upflow anaerobic sludge blanket configured anaerobic membrane bioreactors for municipal wastewater treatment 101
4.1 Introduction 102
4.2 Material and methods 104
4.2.1 UASB and UASB configured AnMBR pilot plants 104
4.2.2 Analytical methods 108
4.3 Results 110
4.3.1 Comparison of granular and flocculent UASB and UASB configured AnMBR 110
4.3.2 Membrane operation comparison between G-AnMBR and F-AnMBR 112
4.3.3 Impact of temperature on G-AnMBR and F-AnMBR system resilience 114
4.3.4 Alternative pseudo dead-end gas sparging strategy 116
4.4 Discussion 120
4.5 Conclusions 123
4.6 Acknowledgements 124
4.7 References 124
5 Identification of gas sparging regimes for granular anaerobic membrane bioreactor to enable energy neutral municipal wastewater treatment 133
5.1 Introduction 134
5.2 Material and methods 136
5.2.1 Anaerobic MBR pilot plant 136
5.2.2 Analytical methods 140
5.3 Results 141
5.3.1 Anaerobic MBR characterisation and critical flux determination 141
5.3.2 Continuous filtration and continuous gas sparging 142
5.3.3 Continuous filtration and intermittent gas sparging 143
5.3.4 Pseudo dead-end filtration using intermittent filtration and intermittent gas sparging 146
5.4 Discussion 149

5.5 Conclusions 156
5.6 Acknowledgements 157
5.7 References 157
6 Sustaining membrane permeability during unsteady-state operation of anaerobic membrane bioreactors for municipal wastewater treatment following peak-flow 165
6.1 Introduction 166
6.2 Material and methods 169
6.2.1 Anaerobic MBR pilot plant 169
6.2.2 Analytical methods 173
6.3 Results 174
6.3.1 Characterisation of AnMBR bulk sludge, treatment and critical flux determination 174
6.3.2 Impact of gas sparging on AnMBR membrane permeability following peak flow 175
6.3.3 Impact of peak flux on AnMBR permeability 177
6.3.4 Impact of peak length and multiple peak events on AnMBR permeability 180
6.3.5 Alternative hydrodynamic conditions 182
6.4 Discussion 183
6.5 Conclusions 187
6.6 Acknowledgements 188
6.7 References 188
6.8 Supplementary data 193
7 Overall discussion 197
7.1 Can UASB configured AnMBR provide permeate quality compliance to International discharge standard? 200
7.2 Does UASB configured AnMBR provide a robust and resilient system for municipal wastewater treatment? 202
7.3 Is UASB configured AnMBR a low energy demand and low operational cost technology for municipal wastewater treatment? 204
7.4 What are the implications of this research on cost of AnMBR technology for municipal wastewater treatment? 205
7.5 References 206
8 Conclusions and future works 213
8.1 Conclusions 213
8.2 Future works 214
Appendices 219
9.1 Appendix 1: Images of pilot scale experimental rigs 219
9.2 Appendix 2: Images of lab-scale membrane cell 221

LIST OF FIGURES

CHAPTER 1

Figure 1-1. Schematics of anaerobic membrane bioreactor (AnMBR) in completely stirred tank reactor (CSTR) and upflow anaerobic sludge blanket (UASB) configuration. 6

Figure 1-2. Highlight the thesis objectives and related chapters. 9

CHAPTER 2

Figure 2-1. Combined headspace and dissolved methane production rates from anaerobic MBR treating: (a) settled sewage; and (b) crude sewage. Where dissolved methane data was not provided, the dissolved fraction was estimated using Henry's law. Energy data was normalised assuming 40 % CHP conversion efficiency. 42

Figure 2-2. Comparison of membrane energy demand to the average (0.34 kWh m^{-3}, dashed line) and maximum (0.80 kWh m^{-3}, continuous line) energy production reported in the literature to date for anaerobic MBR treating settled wastewater. 43

CHAPTER 3

Figure 3-1. Schematics of pilot scale G-UASB and F-UASB. 71

Figure 3-2. (a) Temporal variation of UASB sludge blanket height (X)/Effluent height (XT) ratio and reactor temperature. (b) Impact of sludge blanket on particulate COD separation. Stage I, sludge blanket development (0-40 d for G-UASB, 0-42 d for F-UASB); Stage II, steady-state operation (41-86 d for G-UASB, 43-65 d for F-UASB); Stage III, breakthrough (87-120 d for G- UASB, 66-120 d for F-UASB). 76

Figure 3-3. (a) Headspace CH_4 production from G-UASB and F-UASB and reactor temperatures. (b) Effluent SCOD concentrations in G-UASB and F-UASB. Stage I, sludge blanket development (0-40 d for G-UASB, 0-42 d for F-UASB); Stage II, steady-state operation (41-86 d for G-UASB, 43-65 d for F-UASB); Stage III, breakthrough (87-120 d for G-UASB, 66-120 d for F-UASB). 78

Figure 3-4. Residual energy production through BMP tests from primary sludge and the sludge blanket under different desludge strategy (for 70 days, because the low sludge blanket height, samples were only taken from 90 cm port; for 140 days, the mixed sludge samples were from three sampling ports: 90 cm, 120 cm and 150 cm from the bottom of the UASB reactor). 79

Figure 3-5. Impact of temperature on sludge blanket stability and particulate COD separation. 81

Figure 3-6. Impact of temperature on particle settling velocity in G-UASB and F-UASB (the average temperature when sampling particles from G-UASB and F-UASB reactors was 19.6±0.5 °C). Grey line represents V_{up} liquid (0.8 m h^{-1}, 222 μm s^{-1}),

dashed grey line represents V_{up} mixed gas and liquid (1.22 m h^{-1}, 339 μm s^{-1}). Black line represents linear trend line of predicted settling velocity at 20 °C calculated from the particle settling velocity at 10 °C. Dashed black line represents confidence interval range (95 %). Impact of temperature on particle settling velocity for (a) flocculent sludge above granules in G-UASB and (b) flocculent sludge in F-UASB at water temperatures of 10 and 20 °C. Comparison of particle settling velocity between flocculent sludge above granules in G-UASB and flocculent sludge in F-UASB at a water temperature of (c) 10 °C and (d) 20 °C. 82

Figure 3-7. (a) Major bacterial phyla and their relative abundance of inoculum sludge in G-UASB and F-UASB (bacterial phyla with abundance over 1 %). (b) Relative abundance of all archaea at genus level..... 85

Figure 3-8. The spatial distribution of granules by fluorescence in situ hybridisation (FISH) analyses viewed by confocal laser scanning microscope (CLSM). Cells in green are bacteria hybridised by the Bacteria (EUB338-I, EUB338-II, EUB338-III) probe and cells in purple are methanosaeta co-hybridised by the Archaea (ARCH915) and the Methanosaeta (MX825) probes. 86

Figure 3-9. Impact of upflow velocity (0.8 and 0.4 m h^{-1}) on sludge blanket stability and particulate COD separation. 87

Figure S3-1 Impact of sludge blanket on particulate COD separation (Stage I, sludge blanket development (0-40 d for G-UASB, 0-42 d for F-UASB), Stage II, steady-state operation (41-86 d for G-UASB, 43-65 d for F-UASB), Stage III, breakthrough (87-120 d for G-UASB, 66-120 d for F-UASB). 97

CHAPTER 4

Figure 4-1. Schematics of G-UASB and F-UASB (top) and G-AnMBR and F-AnMBR (bottom). 106

Figure 4-2. Schematics of membrane cell for critical flux test in the laboratory (ambient temperature around 20 °C). 109

Figure 4-3. Critical flux tests of UASB effluent and membrane tank bulk sludge (2 L m^{-2} h^{-1} per step; 15 mins step), sampled at the wastewater average temperature of 10.2-13.1 °C. 112

Figure 4-4. (a) G-AnMBR and (b) F-AnMBR membrane fouling curves using filtration/relaxation (10 min on/1 min off) and cyclic gas sparging (10 s on/10 s off, SGD_m=1.12 m^3 m^{-2} h^{-1} and SGD_{mnet}=0.56 m^3 m^{-2} h^{-1}). Flux has been normalised to 20 °C. 113

Figure 4-5. G-AnMBR and F-AnMBR membrane fouling curves. Filtration/relaxation (10 min on/1 min off), cyclic gas sparging (10 s on/10 s off) with same $J_{20\ net}$=12 L m^{-2} h^{-1}. Inset the critical flux tests of F-AnMBR (samples taken at different reactor temperatures). The tests were run in the laboratory (ambient temperature around 20 °C). 115

Figure 4-6. G-AnMBR and F-AnMBR membrane fouling curves under different upflow velocity (V_{up}). Filtration/relaxation (10 min on/1 min off), cyclic gas sparging (10 s on/10 s off) with same $J_{20\ net}$=12 L m^{-2} h^{-1}. 116

Figure 4-7. G-AnMBR and F-AnMBR membrane fouling curves using two hydrodynamic conditions with $J_{20\ net}$=7.5 L m^{-2} h^{-1}: (a) Standard, Filtration/relaxation (10 min on/1 min off) and gas sparging (10 s on/10 s off), SGD_m=1.12 m^3 m^{-2} h^{-1} and SGD_{mnet}=0.56 m^3 m^{-2} h^{-1}; (b) Pseudo dead-end (DE), Intermittent filtration (10 min on/1 min off) and intermittent gas sparging (1 min on/10 min off), SGD_m=1.12 m^3 m^{-2} h^{-1} and SGD_{mnet}=0.102 m^3 m^{-2} h^{-1}. Flux has been normalised to 20 °C. 117

Figure 4-8. (a) Impact of temperature on G-AnMBR and F-AnMBR transmembrane pressure under pseudo dead-end gas sparging regime. (b) Cake fouling rate (r_f, dP/dt) analyses under pseudo dead-end gas sparging regime. Intermittent filtration (10 min on/1 min off) and intermittent gas sparging (1 min on/10 min off) with $J_{20\ net}$ = 7.5 L m^{-2} h^{-1}, SGD_m=1.12 m^3 m^{-2} h^{-1} and SGD_{mnet}=0.102 m^3 m^{-2} h^{-1}. The data of the inset is transmembrane pressure after 100 h. Flux has been normalised to 20 °C. 118

Figure 4-9. Total biopolymer (TBP) (protein + carbohydrates in mg m^{-2}) and hydraulic resistances from three fouling layer fraction of G-AnMBR and F-AnMBR after long term run. Intermittent filtration (10 min on/1 min off, J_{20}=8.25 L m^{-2} h^{-1}, $J_{20\ net}$=7.5 L m^{-2} h^{-1}) and intermittent gas sparging (1 min on/10 min off, SGD_m=1.12 m^3 m^{-2} h^{-1}, SGD_{mnet}=0.102 m^3 m^{-2} h^{-1}). Each system filtered for 200 h with about 1500 L wastewater..... 119

CHAPTER 5

Figure 5-1. Energy consumption of AnMBR for different fluxes and specific gas demand per unit membrane area (SGD_m). Data compared to energy recovered from this sewage using AnMBR (0.275 kWh m^{-3}, biogas from UASB and dissolved CH_4) (Cookney et al., 2016). Black break line illustrates average energy recovery from municipal AnMBR literature (0.34 kWh m^{-3}) (Cookney et al., 2016; Gouveia et al., 2015a, 2015b; Shin et al., 2014)..... 135

Figure 5-2. Schematic of the anaerobic membrane bioreactor (AnMBR). 138

Figure 5-3. Critical flux determination under different specific gas demand per unit membrane area (SGD_m) (3 L m^{-2} h^{-1} per step; 10 mins step). 142

Figure 5-4. Impact of flux (specific gas demand per unit membrane area (SGD_m), 0.2 m^3 m^{-2} h^{-1}) and SGD_m (fixed flux, J_{20} =13.5 L m^{-2} h^{-1}) on membrane fouling rate using continuous filtration and continuous gas sparging. Filtration to 24 h or TMP_{max} (550 mbar)..... 144

Figure 5-5. Impact of specific gas demand per unit membrane area (SGD_m) and gas sparging frequency ($\Theta_{gs,f}$) (10 s on time fixed) on membrane fouling rate using continuous filtration and intermittent gas sparging: (a) J_{20}= 5 L m^{-2} h^{-1}; (b) 10 L m^{-2} h^{-1}; (c) 13.5 L m^{-2} h^{-1}. Filtration to 24 h or TMP_{max} (550 mbar). 145

Figure 5-6. Impact of gas sparging frequency ($\Theta_{gs,f}$) and gas sparging on time ($\theta_{gs,on}$) on membrane fouling rate using continuous filtration and intermittent gas sparging at fixed flux (J_{20}=13.5 L m^{-2} h^{-1}, SGD_m=2.0 m^3 m^{-2} h^{-1}). Filtration to 24 h or TMP_{max} (550 mbar)..... 146

Figure 5-7. Impact of specific gas demand per unit membrane area (SGD_m) on membrane fouling rate using pseudo dead-end gas sparging regime: 9 min on/1 min off; $J_{20\ net}$= 5, 10, 13.5 L m^{-2} h^{-1}. Gas sparging introduced once filtration has stopped. Filtration to 24 h or TMP_{max} (550 mbar). 147

Figure 5-8. Impact of filtration off time (gas sparging on time) and filtration on time (gas sparging off time) on membrane fouling rate using pseudo dead-end gas sparging regime (J_{20}=13.5 L m^{-2} h^{-1}, $J_{20\ net}$ varied): (a) fixed filtration on time (9 min); (b) fixed filtration off time (1 min). Filtration to 24 h or TMP_{max} (550 mbar). 148

Figure 5-9. Internal residual fouling resistance (R_{if}, calculated from pressure at onset of filtration) and cake fouling rate (r_f, dP/dt) analyses under pseudo dead-end gas sparging regime. J_{20}, 13.5 L m^{-2} h^{-1}; filtration 4 min on/1 min off, 9 min on/1 min off, 14 min on/1 min off. Gas sparging introduced once filtration has stopped: SGD_m, 2.0 m^3 m^{-2} h^{-1}..... 149

Figure 5-10. Comparison of membrane fouling under same specific gas demand per membrane area (SGD_m) and same net SGD_m ($SGD_{m\ net}$) with different gas sparging regimes ($J_{20\ net}$= 13.5 L m^{-2} h^{-1}). Con. (Continuous), Inter. (Intermittent); CGS (continuous gas sparging), IGS (intermittent gas sparging), DE (pseudo dead-end gas sparging). Detailed test parameters can be referred to Table 5-2. 151

Figure 5-11. Impact of specific energy demand on membrane fouling (based on 3 m hydraulic head). CGS, continuous gas sparging; IGS, intermittent gas sparging; DE, pseudo dead-end. Black, grey and white data represent fluxes (J_{20}) of: 5, 10 and 13.5 L m^{-2} h^{-1}. Lines represent energy recovered from biogas and dissolved CH_4 using: sewage from the present study (grey solid line) (Cookney et al., 2016); average from the municipal AnMBR literature (black broken line) (Cookney et al., 2016; Gouveia et al., 2015a, 2015b; Shin et al., 2014). 156

CHAPTER 6

Figure 6-1. Schematic of the pilot granular anaerobic membrane bioreactor (G-AnMBR). 169

Figure 6-2. Gas sparging strategies tested to manage peak flow during continuous filtration. 172

Figure 6-3. Comparison of continuous filtration and continuous gas sparging ($Filt_{Cont.}$ + $Gas_{Cont.}$, CGS) with pseudo dead-end (DE) operation, comprising intermittent filtration (9 min on/1 min off) and intermittent gas sparging (1 min on/9 min off) ($Filt_{Inter.}$ + $Gas_{Inter.}$). 173

Figure 6-4. Critical flux determined using specific gas demand per unit membrane area (SGD_m) of 0.5 and 2 m^3 m^{-2} h^{-1} (flux step, 3 L m^{-2} h^{-1} per step; step length, 10 mins.). 174

Figure 6-5. Impact of doubling flow (peak, 2Q) on transmembrane pressure at different initial fluxes using a fixed specific gas demand per unit membrane area (SGD_m) of 0.5 m^3 m^{-2} h^{-1} throughout. 176

Figure 6-6. Impact of doubling flow (peak, 2Q) on transmembrane pressure at different initial fluxes. Specific gas demand per unit membrane area (SGD_m) increased from 0.5 to 2.0 m^3 m^{-2} h^{-1} during peak flow. 176

Figure 6-7. Impact of different gas sparging strategies on relative membrane permeability after flow was doubled (peak, 2Q). Initial flux, 6 L m^{-2} h^{-1}; Peak flux, 12 L m^{-2} h^{-1}. Constant specific gas demand per unit membrane area (SGD_m) of 0.5 m^3 m^{-2} h^{-1} during steady-state, and increased from 0.5 to 2.0 m^3 m^{-2} h^{-1} for set periods during specific trials (see Figure 6-2). 177

Figure 6-8. Impact of peak flow ratio on transmembrane pressure when: (a) Initial flux, 6 L m^{-2} h^{-1}; (b) Initial flux, 10 L m^{-2} h^{-1}. Specific gas demand per unit membrane area (SGD_m) increased from 0.5 to 2.0 m^3 m^{-2} h^{-1} during peak flow. 179

Figure 6-9. Impact of peak length on membrane permeability recovery. Initial flux, 6 L m^{-2} h^{-1}; Peak flux, 18 L m^{-2} h^{-1} (Peak, 3Q). Specific gas demand per unit membrane area (SGD_m) increased from 0.5 to 2.0 m^3 m^{-2} h^{-1} during peak flow. 180

Figure 6-10. Impact of peak length on membrane permeability recovery for two different peak flow ratios. Initial flux, 6 L m^{-2} h^{-1}; Peak flux, 12 L m^{-2} h^{-1} (2Q) or 18 L m^{-2} h^{-1} (3Q). Specific gas demand per unit membrane area (SGD_m) increased from 0.5 to 2.0 m^3 m^{-2} h^{-1} during peak flow. 181

Figure 6-11. Impact of multiple peak flow events on transmembrane pressure. Initial flux, 6 L m^{-2} h^{-1}; Peak flux, 18 L m^{-2} h^{-1} (3Q). Specific gas demand per unit membrane area (SGD_m) increased from 0.5 to 2.0 m^3 m^{-2} h^{-1} during peak flow. 181

Figure 6-12. Comparison of two hydrodynamic conditions subject to peak flow: continuous filtration and continuous gas sparging (CGS); pseudo dead-end (DE) comprising intermittent filtration (9 min on/1 min off) and intermittent gas sparging (9 min off/ 1 min on). (a) Initial flux, 6 L m^{-2} h^{-1}; Peak flux, 12 L m^{-2} h^{-1} (2Q); (b) Initial flux, 10 L m^{-2} h^{-1}; Peak flux, 20 L m^{-2} h^{-1} (2Q). Constant specific gas demand per unit membrane area (SGD_m) of 0.5 m^3 m^{-2} h^{-1} applied throughout trial. See Figure 6-3. 182

Figure S6-1 Impact of different gas sparging strategies on relative membrane permeability after flow was tripled (peak, 3Q). Initial flux, 6 L m^{-2} h^{-1}; Peak flux, 18 L m^{-2} h^{-1}. Constant specific gas demand per unit membrane area (SGD_m) of 0.5 m^3 m^{-2} h^{-1} during steady-state, and increased from 0.5 to 2.0 m^3 m^{-2} h^{-1} for set periods during specific trials (see Figure 6-2). 193

CHAPTER 7

Figure 7-1. The proposed UASB configured AnMBR for municipal wastewater treatment. 197

Figure 7-2. Schematics diagram of proposed flowsheet integration with anaerobic membrane bioreactor (AnMBR) (Adapted from Martin-Garcia (2010)). 202

APPENDICES

Figure A-1. 70 L upflow anaerobic sludge blanket (UASB) reactors with granular and flocculent inoculum biomass (Chapter 3 and Chapter 4). 219

Figure A-2. Sludge blanket in granular UASB reactor. 219

Figure A-3. 70 L granular and flocculent UASB reactor coupled with 30 L membrane tank (Chapter 4). 220

Figure A-4. 42.5 L granular UASB reactor coupled with 30 L membrane tank (Chapter 5 and Chapter 6). 220

Figure A-5. ZW-10 membrane module. 221

Figure A-6. Lab scale membrane cell (Chapter 4). 221

LIST OF TABLES

CHAPTER 2

Table 2-1.Overview of operating conditions and membrane performance in immersed anaerobic MBRs treating municipal wastewater. 25

Table 2-2. Particle size distribution of sludge/biomass in aerobic and anaerobic MBRs in contact with the membrane. 27

Table 2-3. Concentration and composition of EPS in aerobic and anaerobic MBR sludge/biomass..... 31

Table 2-4. Concentration and composition of soluble microbial products in aerobic and anaerobic MBRs..... 32

Table 2-5. Hydrodynamic conditions and specific energy demand of immersed anaerobic MBRs treating municipal wastewater (real and synthetic). 37

Table 2-6. Overview of operating conditions and membrane performance in side-stream anaerobic MBRs..... 38

Table 2-7. Biogas production from anaerobic MBRs treating municipal wastewater (real and synthetic)..... 41

CHAPTER 3

Table 3-1. Impact of temperature on G-UASB and F-UASB treatment performance including sludge blanket development, steady-state operation and breakthrough. 83

Table 3-2. UASB performance under different upflow velocity (0.8 and 0.4 m h^{-1}) including sludge blanket development, steady-state operation and breakthrough, average temperature of 15.0-15.4 °C..... 88

CHAPTER 4

Table 4-1. Impact of membrane addition on the overall system performance..... 110

Table 4-2. Impact of membrane addition on bulk sludge characteristics. 111

Table 4-3. Colloidal SMP fractionation in UASB effluent and membrane tank bulk sludge (n=3)..... 112

Table 4-4. Impact of temperature on G-AnMBR and F-AnMBR bulk sludge characteristics. 115

CHAPTER 5

Table 5-1. Influent characteristics, G-AnMBR treatment performance and bulk sludge characteristics..... 142

Table 5-2. Comparison of different gas sparging regimes under same specific gas demand per membrane area (SGD_m) and same net SGD_m ($SGD_{m\,net}$). 151

CHAPTER 6

Table 6-1. AnMBR removal efficiency, wastewater and membrane bulk sludge characterisation. 174

Table 6-2. Comparison of fouling rate before and after peak flow when SGD_m was either fixed to 0.5 $m^3\ m^{-2}\ h^{-1}$ or increased from 0.5 to 2.0 $m^3\ m^{-2}\ h^{-1}$ during peak flow (two hour peak). 177

Table 6-3. Fouling rate determined before and after peak flow for initial fluxes of 6 and 10 L $m^{-2}\ h^{-1}$. SGD_m was increased from 0.5 to 2.0 $m^3\ m^{-2}\ h^{-1}$ during peak flow (two hour peak). 178

CHAPTER 7

Table 7-1. Proposed engineered solutions arising from the research to promote sustained operation and limit both operational and capital cost. 198

ABBREVIATIONS

ABR	Anaerobic baffled reactor
AD	Anaerobic digester
AeMBR	Aerobic membrane bioreactor
AFBR	Anaerobic fluidised bed reactor
AFMBR	Anaerobic fluidised bed membrane bioreactor
AnMBR	Anaerobic membrane bioreactor
ANOVA	Analysis of variance
ARMBR	Anaerobic rotate disk membrane bioreactor
ASP	Activated sludge process
AT	Ambient temperature
BMP	Biochemical methane production
BNR	Biological nutrient removal
BOD_5	Five-day biochemical oxygen demand
BSA	Bovine serum albumin
BW	Backwash
CFV	Crossflow velocity
CGS	Continuous gas sparging
CHP	Combined heat and power
CLSM	Confocal laser scanning microscope
CAS	Conventional activated sludge
COD	Chemical oxygen demand
COD_t	Total chemical oxygen demand
CSTR	Completely stirred tank reactor
DE	Dead-end
DNA	Deoxyribonucleic acid
EBCT	Empty bed contact time
eEPS	Extracted extracellular polymeric substances
EGSB	Expanded granular sludge bed
EPS	Extracellular polymeric substances
F:M	Food to microorganism ratio
FISH	Fluorescence in situ hybridisation
FS	Flat sheet

F-AnMBR	Flocculent anaerobic membrane bioreactor
F-UASB	Flocculent upflow anaerobic sludge blanket
GA	Glucose addition
GAC	Granular activated carbon
GHG	Greenhouse gas
G-AnMBR	Granular anaerobic membrane bioreactor
G-UASB	Granular upflow anaerobic sludge blanket
HF	Hollow fibre
HFMC	Hollow fibre membrane contactor
HPLC	High performance liquid chromatography
HRT	Hydraulic retention time
IAFMBR	Integrated anaerobic fluidised-bed membrane bioreactor
IEX	Ion exchange
IGS	Intermittent gas sparging
MBR	Membrane bioreactor
MLSS	Mixed liquor suspended solids
MT	Multiple tube
MWCO	Molecular weight cut off
OLR	Organic loading rate
PAC	Powered activated carbon
PAN	Polyacrylonitrile
PCOD	Particulate chemical oxygen demand
PE	Polyethylene
PES	Polyethersulfone
PF	Plate and frame
PTFE	Poly-tetrafluoroethylene
PVDF	Polyvinylidene fluoride
rRNA	ribosomal ribonucleic acid
SAF-MBR	Staged anaerobic fluidised membrane bioreactor
SCOD	Soluble chemical oxygen demand
SMP	Soluble microbial product
SRT	Solids retention time
SS	Suspended solids

SSR	Sum of square of residuals
STP	Standard temperature and pressure
TMP	Transmembrane pressure
TOC	Total organic carbon
TS	Total solids
UASB	Upflow anaerobic sludge blanket
VFA	Volatile fatty acid
VS	Volatile solids

NOTATIONS

A	reactor cross-sectional area	m^2
a	membrane surface area	m^2
A^2/O	anaerobic/anoxic/aerobic	
C_b	MLSS concentrations	kg m^{-3}
CH_4	methane	
d_{50}	equivalent diameter corresponding to 50 % of cumulative volume undersize (μm)	μm
d_p	particle diameter	μm
d*P*/dt	fouling rate	kPa s^{-1}
e	compressor efficiency, 0.70-0.90	
g	gravity constant	m s^{-2}
J	permeate flux	L m^{-2} h^{-1}
J_{20}	flux normalised to 20 °C	L m^{-2} h^{-1}
$J_{20\ net}$	net flux normalised to 20 °C	L m^{-2} h^{-1}
J_c	critical flux	L m^{-2} h^{-1}
J_T	flux at T °C	L m^{-2} h^{-1}
k	constant, k=1.4 for nitrogen	
K_H	proportion of volume of filter/volume of sludge bed	
K_{20}	permeability normalised to 20 °C	L m^{-2} h^{-1}
$K_{20,ppr}$	peak permeability recovery normalised to 20 °C	%
$K_{20,tpr}$	total permeability recovery normalised to 20 °C	%
LMH	L m^{-2} h^{-1}	

$\dot{m}$	mass flow rate	kg s^{-1}
$M_{critical}$	critical mass	g m^{-2}
N	Number of data points	
n	constant	
P_1	inlet pressure	Pa
P_2	outlet pressure	Pa
P_a	the pressure required to obtain a specific cake resistance twice as high as α_0	mbar
P_{power}	power requirement	kW
Q	flow rate	m^3 s^{-1}
Q_g	gas flow rate	m^3 s^{-1}
Q_l	Liquid flow rate	m^3 s^{-1}
Q_{peak}	Peak flow	m^3 s^{-1}
Q_w	wastewater flow	m^3 h^{-1}
R	gas constant, 8.314	J K^{-1} mol^{-1}
r_f	cake fouling rate	mbar h^{-1}
R_{if}	internal residual fouling resistance	m^{-1}
R_m	clean membrane resistance	m^{-1}
R_{rvf}	reversible fouling resistance	m^{-1}
R_t	total resistance	m^{-1}
SAD_m	Specific air demand per unit membrane area	m^3 m^{-2} h^{-1}
SGD_m	Specific gas demand per unit membrane area	m^3 m^{-2} h^{-1}
$SGD_{m\ net}$	net specific gas demand per unit membrane area	m^3 m^{-2} h^{-1}
SGD_p	specific gas demand per unit permeate	m^3 m^{-3}
SMP P/C	protein to carbohydrate ratio	
SMP_c	carbohydrate concentration	kg m^{-3}
SMP_{COD}	soluble microbial product (measured as COD concentration)	kg m^{-3}
SMP_p	protein concentration	kg m^{-3}
SMP_{p+c}	soluble microbial product (measured as sum of protein and carbohydrate concentrations)	kg m^{-3}
SSR_1	Sum of square of residual of first group regression	
SSR_2	Sum of square of residual of second group regression	

SSR_p	Sum of square of residual of pooled regression	
t	filtered time	min
T_1	temperature	K
TMP_{ave}	average transmembrane pressure	mbar
TMP_i	initial transmembrane pressure for each filtration cycle	mbar
TMP_{max}	maximum transmembrane pressure	mbar
TMP_t	transmembrane pressure at the end of pseudo dead-end filtration cycle	mbar
V_{crit}	critical filtered volume	L
V_{filter}	volume of wastewater filtered	m^3
V_{mix}	mixed gas and liquid velocity	m h^{-1}/μm s^{-1}
V_p	particle settling velocity	μm s^{-1}
V_{up}	upflow velocity	m h^{-1}/μm s^{-1}
W	specific energy demand	kWh m^{-3}
w	weight of flow of gas	kg s^{-1}
X	sludge blanket height	m
X_T	effluent height	m

GREEK LETTERS

α	specific cake resistance	m kg^{-1}
α_0	specific cake resistance at zero pressure	m kg^{-1}
α_{TBP}	specific biopolymer resistance	m kg^{-1}
ΔTMP_c	pressure drop of cake layer	mbar
$\Theta_{gs,f}$	gas sparging frequency	
$\theta_{gs,on}$	gas sparging on time	s
$\theta_{gs,off}$	gas sparging off time	s
μ	permeate viscosity/liquid viscosity	Pa s
ρ_g	gas density	kg m^{-3}
ρ_l	liquid density	kg m^{-3}
ρ_{mix}	mixed gas and liquid density	kg m^{-3}
ω	solids concentration in the cake per unit filtrate volume	kg m^{-3}

CHAPTER 1

Introduction

1 Introduction

1.1 Background

The water industry is currently an energy-intensive endeavour which accounts for about 2-3 % of the total electricity demand in countries such as the UK and the US (Environment Agency, 2009a; EPA Office of Water, 2006; Gude, 2015). Energy demand in the water industry has been increasing (Water UK, 2012) due to population growth and the requirements to meet more stringent consents (Copeland and Carter, 2017). Consequently, although greenhouse gas (GHG) emissions have declined in the UK over the past ten years, GHG emissions from the water industry have increased by about 30 % (Environment Agency, 2009b; McAdam et al., 2011). Whilst the investment into renewable energy production has been continuously increased in recent years to lower GHG emissions within the water industry (Water UK, 2012), more must be done to further reduce the energy demand and GHG emission, making greater contribution towards the GHG emission reduction goal by 80 % from 1990 levels by 2050 in the UK (OFWAT, 2010).

The energy demand of a typical flowsheet comprising aerobic treatment with an activated sludge process (ASP) coupled with anaerobic digestion (AD) of primary and secondary sludge, is about 0.3-0.6 kWh m^{-3} (McCarty et al., 2011; Tchobanoglous et al., 2003). More than half of this energy is for aeration (Gude, 2015; Tchobanoglous et al., 2003). A paradigm shift is now underway to regard municipal wastewater as a resource rather than a waste from which water, energy and nutrient fertiliser (nitrogen and phosphorus) can be recovered (McCarty et al., 2011). It has been estimated that a maximum potential energy of 1.9 kWh m^{-3} can be recovered from the oxidation of organic matter in municipal wastewater, comprising chemical oxygen demand (COD) of around 500 mg L^{-1} (McCarty et al., 2011). Therefore, new flowsheets have been developed, aiming at achieving energy sustainability based on the intrinsic carbon (rather than sludge imports), coupled with water and nutrient recovery, while minimising residual solids production (i.e. biomass) and GHG emission (Sutton et al., 2011; McAdam et al., 2011).

The flowsheet integration with anaerobic membrane bioreactor (AnMBR) seems promising as it offers the prospect to achieve energy neutral sewage treatment, which is regarded as the principal advantage for this technology (Pretel et al., 2014, 2015; Smith et al., 2014). In order to maximise the overall energy production from AnMBR even at low temperatures with low solids (particulate matter) hydrolysis rate, it is proposed to introduce primary sedimentation to divert solids toward AD and leave only settled wastewater to be processed by AnMBR (McAdam et al., 2011). As nutrients (ammonia and phosphorus) are not removed with AnMBR, this flowsheet requires further nutrient removal through downstream biological treatment (Eusebi et al., 2013) or recovery through physico-chemical separation (McAdam et al., 2011; Sutton et al., 2011). Compared with conventional anaerobic processes treating municipal wastewater, membrane integration overcomes the main challenges of preventing biomass washout (Robles et al., 2012), which decouples the sludge retention time (SRT) and hydraulic retention time (HRT) (Gouveia et al., 2015a; Liao et al., 2006; Smith et al., 2013), therefore enabling complete biomass retention. Additionally, AnMBR provides permeate compliant for biological oxygen demand (BOD), COD and total suspended solids (TSS) even at low temperatures (Martin Garcia et al., 2013; Smith et al., 2013). Whilst the membrane enables process intensification, the AnMBR matrix is considerably more heterogeneous and complex than conventional aerobic MBR (AeMBR), which increases fouling rate and reduces attainable flux (Martin-Garcia et al., 2011). Consequently, the main challenges of full-flow AnMBR applications for municipal wastewater treatment are membrane fouling and low flux, thus high operational cost for energy demand associated with fouling control and high capital cost for membrane investment (Ozgun et al., 2013a; Ruigómez et al., 2016).

Many attempts have been made to reduce membrane fouling in AnMBR, which is affected by reactor configuration, membrane characterisation, feeding and biomass properties, and operational conditions (Dong et al., 2015; Gouveia et al., 2015b; Martin Garcia et al., 2013; Ozgun et al., 2013a; Robles et al., 2013; van Voorthuizen et al., 2008). Reactor configuration is proposed to be an important factor that can change the AnMBR fouling propensity (Ozgun et al., 2013b, 2015b). By far, most of the pilot scale AnMBRs

treating municipal wastewater are in completely stirred tank reactor (CSTR) configuration, similar to AeMBR (Dong et al., 2015; Giménez et al., 2014; Martinez-Sosa et al. , 2012; Robles et al., 2013). However, upflow anaerobic sludge blanket (UASB) configured AnMBRs have been increasingly investigated (Gouveia et al., 2015a, 2015b, Ozgun et al., 2015a, 2015b) due to less tenacious fouling than CSTR configured AnMBR (Figure 1-1) and therefore to be conducive to reduce energy demand for fouling control (Martin Garcia et al., 2013; van Voorthuizen et al., 2008). The authors attributed this to the lower solids concentrations from >10,000 mg L^{-1} in CSTR configuration to 300-500 mg L^{-1} within the membrane tank (Liao et al., 2006), which is evidenced to limit cake layer growth at the membrane surface (Liao et al., 2006; Ozgun et al., 2015b). However, the advantage of UASB configured AnMBR is strongly dependent upon the resilience and stability of the UASB reactor as soluble organic matter and solids removal in the UASB is directly linked to the downstream membrane bulk sludge characteristics. Due to the superior settling characteristics leading to less biomass washout, the granular inoculum in an UASB reactor can be inferred to be beneficial to AnMBR resilience compared with flocculent inoculum. However, few studies have applied granular inoculum in AnMBR (Chu et al., 2005; Gouveia et al., 2015b; Martin Garcia et al., 2013). The comparison between granular and flocculent biomass, to infer an advantage of one inoculum over another, is scarce and generally not centred on municipal application at low temperatures (Lettinga et al., 1983; Sabry, 2008). This is crucial as the flocculent biomass is readily available from anaerobic digested sludge or wasted activated sludge (Chong et al., 2012) whilst granular inoculum biomass is limited in supply with high cost between 500 and 1000 USD per ton wet weight (Liu et al., 2002). Therefore, investigation into the impact of granular and flocculent inoculum biomass on downstream membrane permeability in UASB configured AnMBR is required. Both SS and COD removal efficiencies have been noted to reduce with temperature decrease in UASB reactors (Lew et al., 2004; Syutsubo et al., 2011; Uemura and Harada, 2000), leading to solids washout sufficient to affect membrane permeability. Accordingly, further research is required to improve the UASB configured AnMBR resilience by reducing the solids loading to the downstream membrane and maintaining the stability of the UASB reactor.

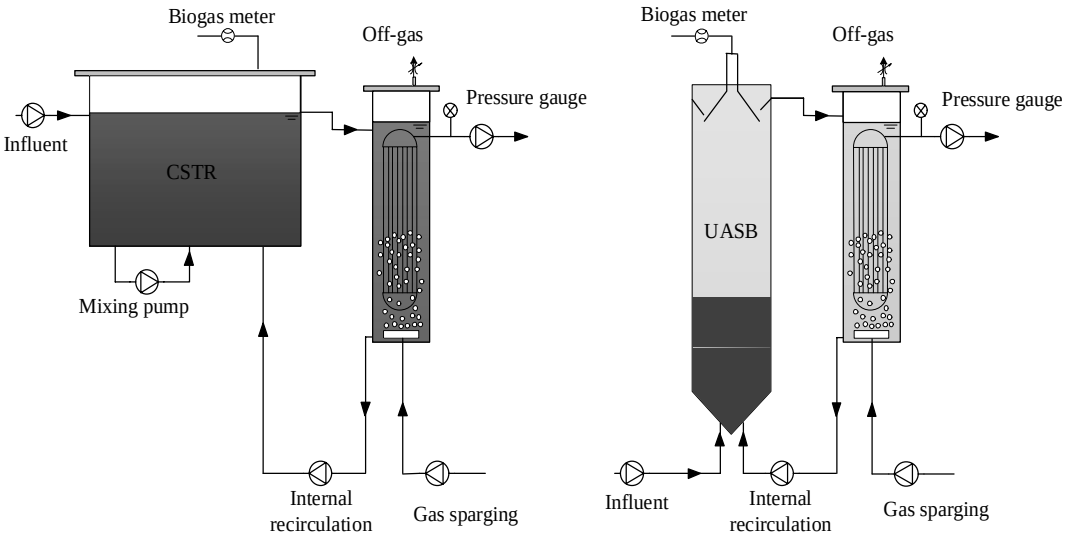

Figure 1-1. Schematics of anaerobic membrane bioreactor (AnMBR) in completely stirred tank reactor (CSTR) and upflow anaerobic sludge blanket (UASB) configuration.

Immersed membranes are predominantly studied in AnMBR, as lower specific energy demand around 0.25-1.0 kWh m^{-3} was reported compared with 3.0-7.3 kWh m^{-3} in external cross-flow configuration (Liao et al., 2006; Martin-Garcia et al., 2011). The use of gas sparging in immersed membrane system has been established as an appropriate fouling control strategy, which is dominately used in commerial AeMBR applications and widely used in AnMBRs (Dong et al., 2015; Gouveia et al., 2015a, 2015b; Lin et al., 2011; Martin Garcia et al., 2013; Robles et al., 2013; Smith et al., 2013). Due to the complex bulk sludge matrix in AnMBR leading to comparatively low fluxes and high specific gas demand for fouling control, gas sparging remains a significant contributor to the energy demand (Pretel et al., 2014) and hence operational cost (Lin et al., 2011; Martin et al., 2011; Mathioudakis et al., 2012) in immersed AnMBR. Therefore, low energy demand gas sparging regimes for fouling control become the key to potentially approach to energy neutral sewage treatment. Most of the current AnMBR studies still applied continuous gas sparging (Dong et al., 2015; Fox and Stuckey, 2015; Giménez et al., 2011; Gouveia et al., 2015a, 2015b, Robles et al., 2012, 2013, Smith et al., 2013, 2015; van Voorthuizen et al., 2008). Limited trials on cyclic gas sparging (10 s on/10 s off) (Martin-Garcia et al., 2011; Martin Garcia et al., 2013) were conducted, which are

commonly applied in commercial immersed AeMBR to save about 50 % of the energy demand. Some other low energy demand gas sparging regimes were also preliminary studied (Cerón-Vivas et al., 2012; Martin-Garcia et al., 2011; Martin Garcia et al., 2013). However, further research is required to identify the low energy demand gas sparging regimes that can sustain membrane operation using less energy than produced by an AnMBR treating municipal wastewater. This would indicate whether the energy neutral sewage treatment with AnMBR can be realised. At full-scale, one of the main challenges for AnMBR treating municipal wastewater is handling unsteady-state peak flow (diurnal peaks and storm water flows), which presents similar problems to the commercialised AeMBR. This can be overcome by sustaining an average flux at peak flow through an increase in membrane surface area or by temporarily increasing flux during peak flow period. The latter option will constrain the capital investment in membrane surface area, but its viability depends upon the membrane permeability recovery after the peak flow. Whilst this has yet to be studied in AnMBR, a limited number of controlled studies were conducted in AeMBR on the temporary increase in permeate flux to cope with peak flow. The results have demonstrated that response to peak flow is plausible without sacrificing membrane permeability (Hirani et al., 2010; Lebegue et al., 2008; Syed et al., 2009). Consequently, research is required to determine whether analogous operational considerations can be drawn with AnMBR, which presents a more complex bulk sludge matrix. This provides the potential to specify the AnMBR membrane area based on average flow rather than peak flow, therefore substantially reduces the capital costs and promotes AnMBR a more resilient and economically viable technology for municipal wastewater treatment.

1.2 Aim and objectives

The aim of this thesis is to establish how to improve the operational resilience of UASB configured AnMBR treating municipal wastewater at ambient temperature, in order to deliver energy neutral sewage treatment. Accordingly, series objectives were identified and highlighted (Figure 1-2).

1. A comprehensive literature review to investigate the characterisation of biomass properties within AnMBRs for municipal wastewater, evaluating their impact on membrane fouling and comparing to those in AeMBR to ascertain the main factors that determine differences in fouling behaviour and characteristic between AnMBR and the commercially successful AeMBR.
2. To evaluate the impact of solids accumulation in both granular and flocculent UASB, in order to ascertain whether sludge blanket stability can be sustained during low temperature treatment of settled municipal wastewater.
3. To compare the impact of granular and flocculent inoculum selection on membrane permeability in UASB configured AnMBR to determine whether the proposed advantage of granular biomass outweighs the risks to cost and supply, and further to identify whether membrane inclusion can dissipate the apparent disadvantages associated with flocculent biomass.
4. To evaluate different gas sparging regimes within UASB configured AnMBR, to identify controlling parameters that govern sustained permeability within each gas sparging regime whilst simultaneously identifying their capacity to deliver energy neutral operation.
5. To evaluate the impact of a temporary increase in AnMBR flux, in response to peak flow, to ascertain whether AnMBR membrane surface area can be specified based on average flow rather than peak flow in order to diminish capital investment.

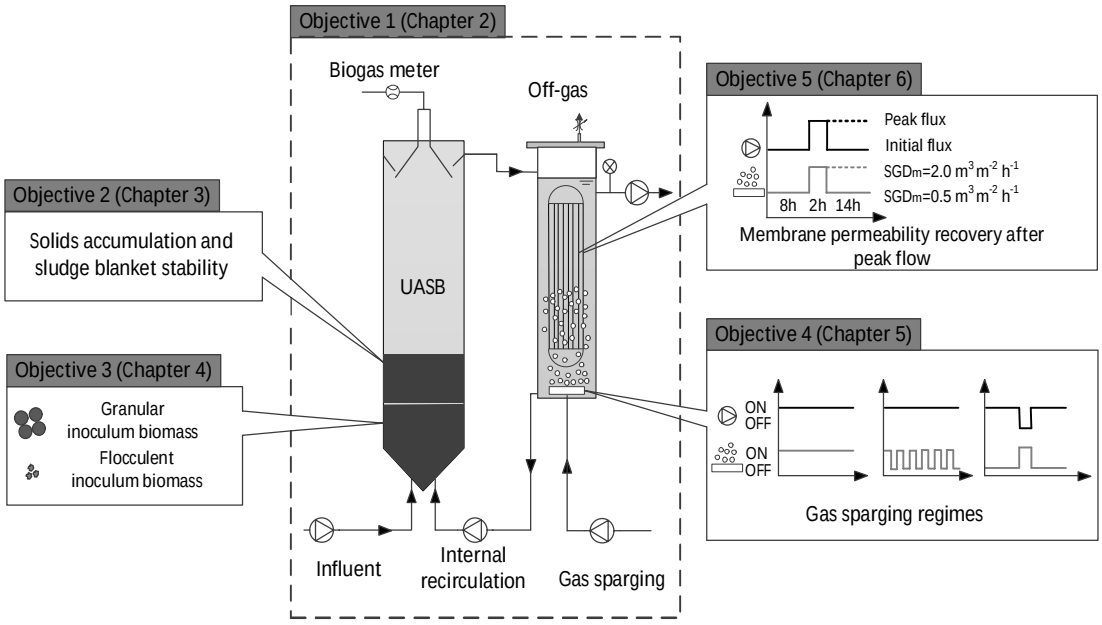

Figure 1-2. Highlight the thesis objectives and related chapters.

1.3 Thesis structure

This thesis is presented in paper format. All papers have been written by the first author Kanming Wang and edited by two supervisors Dr. Ewan McAdam and Dr. Ana Soares. The experimental work was completed by Kanming Wang in collaboration with Diego Cingolani from Marche Polytechnic University (Ancona, Italy) who contributed to the data collections for Chapter 5. The fluorescence in-situ hybridisation (FISH) and microbial diversity analyses in Chapter 3 were conducted by external contractors. The FISH analyses samples were collected by Dr. Yolanda Aguilera Torrico, whilst the microbial diversity data interpretation was carried out by Dr. Gregg Iceton from Prokarya limited.

Chapter 2 is a literature review to investigate the characterisation of biomass properties within AnMBRs for municipal wastewater treatment, evaluating their impact on membrane fouling and comparing to those in AeMBR, to ascertain the main factors that determine differences in fouling behaviours and characteristics between AnMBRs and AeMBRs. Additionally, the energy production from AnMBR for municipal wastewater treatment and membrane specific energy demand from the literature were

analysed to ascertain the position of the existing literature with respect to the 'energy neutral' sewage treatment. Chapter 2 - *K. M. Wang, N. Martin Garcia, A. Soares, B. Jefferson, E.J. McAdam. Comparison of membrane fouling of aerobic and anaerobic MBRs treating domestic wastewater*. Submitted to *H_2Open Journal*.

Chapter 3 evaluates the impact of solids accumulation in both granular and flocculent UASB and in order to ascertain whether sludge blanket stability can be sustained during low temperature treatment of settled municipal wastewater. Chapter 3 - *K. M. Wang, Y. Aguilera, A. Soares, B. Jefferson, E. J. McAdam. Evaluation of the role of sludge blanket on granular and flocculent upflow anaerobic sludge blanket (UASB) reactors for municipal wastewater treatment at low temperatures.* In preparation to be submitted to *Water Research.*

Chapter 4 compares the impact of inoculum selection on membrane permeability in UASB configured AnMBR, in order to determine whether the proposed advantage of granular biomass outweighs the risks to cost and supply, and further to identify whether membrane inclusion can dissipate the apparent disadvantages associated with flocculent biomass. Chapter 4 - *K. M. Wang, B. Jefferson, A. Soares, E. J. McAdam. Comparison of granular and flocculent upflow anaerobic sludge blanket configured anaerobic membrane bioreactors for municipal wastewater treatment.* In preparation to be submitted to *Separation and Purification Technology.*

Chapter 5 evaluates conventional (continuous and intermittent) and non-conventional gas sparging regimes (pseudo dead-end) within UASB configured AnMBR, to identify controlling parameters that govern sustained permeability within each gas sparging regime whilst simultaneously identifying their capacity to deliver energy neutral operation. Chapter 5 - *K. M. Wang, D. Cingolani, A. L. Eusebi, A. Soares, B. Jefferson, E. J. McAdam (2018) 'Identification of gas sparging regimes for granular anaerobic membrane bioreactor to enable energy neutral municipal wastewater treatment', Journal of Membrane Science, 555, pp. 125-133*. Published in *Journal of Membrane Science.*

Chapter 6 investigates the impact of peak flow and the strategy to increase permeability recovery after the temporary flux increase to cope with peak flow, in order

to determine whether AnMBR membrane surface area can be designed based on average flow instead of peak flow. Chapter 6 - *K. M. Wang, B. Jefferson, A. Soares, E. J. McAdam.* Sustaining membrane permeability during unsteady-state operation of anaerobic membrane bioreactors for municipal wastewater treatment following peak-flow. In press in *Journal of Membrane Science.*

Chapter 7 is overall discussion which presented the key aspects that support the practical implementation of UASB configured AnMBR for municipal wastewater treatment.

1.4 References

Cerón-Vivas, A., Morgan-Sagastume, J.M.M. and Noyola, A. (2012) 'Intermittent filtration and gas bubbling for fouling reduction in anaerobic membrane bioreactors', *Journal of Membrane Science*, 423–424, pp. 136–142.

Chong, S., Sen, T.K., Kayaalp, A. and Ang, H.M. (2012) 'The performance enhancements of upflow anaerobic sludge blanket (UASB) reactors for domestic sludge treatment - A State-of-the-art review', *Water Research*, 46, pp. 3434–3470.

Chu, L.B., Yang, F.L. and Zhang, X.W. (2005) 'Anaerobic treatment of domestic wastewater in a membrane-coupled expended granular sludge bed (EGSB) reactor under moderate to low temperature', *Process Biochemistry*, 40, pp. 1063–1070.

Copeland, C. and Carter, N.T. (2017) *Energy-Water Nexus : The Water Sector's Energy Use*. US.

Dong, Q., Parker, W. and Dagnew, M. (2015) 'Impact of FeCl3 dosing on AnMBR treatment of municipal wastewater', *Water Research*, 80, pp. 281–293.

Environment Agency (2009a) *Evidence: Renewable energy potential for the water industry, SC070010/R5*. Bristol, UK.

Environment Agency (2009b) *Evidence: A Low Carbon Water Industry in 2050, Report: SC070010/R3*. Bristol, UK.

EPA Office of Water (2006) *Wastewater Management Fact Sheet, Energy conservation*. Washington DC.

Eusebi, A.L., Martin-Garcia, N., Mcadam, E.J., Jefferson, B., Lester, J.N. and Cartmell, E. (2013) 'Nitrogen removal from temperate anaerobic-aerobic two-stage biological systems: Impact of reactor type and wastewater strength', *Journal of Chemical Technology and Biotechnology*, 88, pp. 2107–2114.

Fox, R.A. and Stuckey, D.C. (2015) 'The effect of sparging rate on transmembrane pressure and critical flux in an AnMBR', *Journal of Environmental Management*, 151, pp. 280–285.

Giménez, J.B., Martí, N., Robles, A., Ferrer, J. and Seco, A. (2014) 'Anaerobic treatment of urban wastewater in membrane bioreactors: evaluation of seasonal temperature variations', *Water Science & Technology*, 69, pp. 1581–1588.

Giménez, J.B., Robles, A., Carretero, L., Durán, F., Ruano, M.V., Gatti, M.N., Ribes, J., Ferrer, J. and Seco, A. (2011) 'Experimental study of the anaerobic urban wastewater treatment in a submerged hollow-fibre membrane bioreactor at pilot scale', *Bioresource Technology*, 102, pp. 8799–8806.

Gouveia, J., Plaza, F., Garralon, G., Fdz-Polanco, F. and Peña, M. (2015a) 'Long-term operation of a pilot scale anaerobic membrane bioreactor (AnMBR) for the treatment of municipal wastewater under psychrophilic conditions', *Bioresource Technology*, 185, pp. 225–233.

Gouveia, J., Plaza, F., Garralon, G., Fdz-Polanco, F. and Peña, M. (2015b) 'A novel configuration for an anaerobic submerged membrane bioreactor (AnSMBR)', *Bioresource Technology*, 198, pp. 510–519.

Gude, V.G. (2015) 'Energy and water autarky of wastewater treatment and power generation systems', *Renewable and Sustainable Energy Reviews*, 45, pp. 52–68.

Hirani, Z.M., DeCarolis, J.F., Adham, S.S. and Jacangelo, J.G. (2010) 'Peak flux performance and microbial removal by selected membrane bioreactor systems', *Water Research*, 44, pp. 2431–2440.

Lebegue, J., Heran, M. and Grasmick, A. (2008) 'MBR functioning under steady and unsteady state conditions. Impact on performances and membrane fouling dynamics', *Desalination*, 231, pp. 209–218.

Lettinga, G., Roersma, R. and Grin, P. (1983) 'Anaerobic treatment of raw domestic sewage at ambient temperatures using a granular bed UASB reactor', *Biotechnology and Bioengineering*, 25, pp. 1701–1723.

Lew, B., Tarre, S., Belavski, M. and Green, M. (2004) 'UASB reactor for domestic wastewater treatment at low temperatures: A comparison between a classical UASB and hybrid UASB-filter reactor', *Water Science & Technology*, 49, pp. 295–301.

Liao, B.Q., Kraemer, J.T. and Bagley, D.M. (2006) 'Anaerobic membrane bioreactors: applications and research directions', *Critical Reviews in Environmental Science and Technology*, 36, pp. 489–530.

Lin, H., Chen, J., Wang, F., Ding, L. and Hong, H. (2011) 'Feasibility evaluation of submerged anaerobic membrane bioreactor for municipal secondary wastewater treatment', *Desalination*, 280, pp. 120–126.

Liu, Y., Xu, H.L., Show, K.Y. and Tay, J.H. (2002) 'Anaerobic granulation technology for wastewater treatment', *World Journal of Microbiology and Biotechnology*, 18, pp. 99–113.

Martin-Garcia, I., Monsalvo, V., Pidou, M., Le-Clech, P., Judd, S.J., McAdam, E.J. and Jefferson, B. (2011) 'Impact of membrane configuration on fouling in anaerobic membrane bioreactors', *Journal of Membrane Science*, 382, pp. 41–49.

Martin, I., Pidou, M., Soares, A., Judd, S. and Jefferson, B. (2011) 'Modelling the energy demands of aerobic and anaerobic membrane bioreactors for wastewater treatment', *Environmental Technology*, 32, pp. 921–932.

Martin Garcia, I., Mokosch, M., Soares, A., Pidou, M. and Jefferson, B. (2013) 'Impact on reactor configuration on the performance of anaerobic MBRs: Treatment of settled sewage in temperate climates', *Water Research*, 47, pp. 4853–4860.

Martinez-Sosa, D., Helmreich, B. and Horn, H. (2012) 'Anaerobic submerged membrane bioreactor (AnSMBR) treating low-strength wastewater under psychrophilic temperature conditions', *Process Biochemistry*, 47, pp. 792–798.

Mathioudakis, V.L., Soares, A., Briers, H., Martin-Garcia, I., Pidou, M. and Jefferson, B. (2012) 'Treatment and energy efficiency of a granular sludge anaerobic

membrane reactor handling domestic sewage', *Procedia Engineering*, 44, pp. 1977–1979.

McAdam, E.J., Luffler, D., Martin-Garcia, N., Eusebi, A.L., Lester, J.N., Jefferson, B. and Cartmell, E. (2011) 'Integrating anaerobic processes into wastewater treatment', *Water Science & Technology*, 63, pp. 1459–1466.

McCarty, P.L., Kim, J. and Bae, J. (2011) 'Domestic wastewater treatment as a net energy producer – Can this be achieved?', *Environmental Science & Technology*, 45, pp. 7100–7106.

OFWAT (2010) *Playing our part- reducing greenhouse gas emissions in the water and sewerage sectors: Supporting information*. Birmingham, UK.

Ozgun, H., Dereli, R.K., Ersahin, M.E., Kinaci, C., Spanjers, H. and van Lier, J.B. (2013a) 'A review of anaerobic membrane bioreactors for municipal wastewater treatment: Integration options, limitations and expectations', *Separation and Purification Technology*, 118, pp. 89–104.

Ozgun, H., Ersahin, M.E., Tao, Y., Spanjers, H. and van Lier, J.B. (2013b) 'Effect of upflow velocity on the effluent membrane fouling potential in membrane coupled upflow anaerobic sludge blanket reactors', *Bioresource Technology*, 147, pp. 285–292.

Ozgun, H., Gimenez, J.B., Evren, M., Tao, Y., Spanjers, H. and van Lier, J.B. (2015a) 'Impact of membrane addition for effluent extraction on the performance and sludge characteristics of upflow anaerobic sludge blanket reactors treating municipal wastewater', *Journal of Membrane Science*, 479, pp. 95–104.

Ozgun, H., Tao, Y., Ersahin, M.E., Zhou, Z., Gimenez, J.B., Spanjers, H. and van Lier, J.B. (2015b) 'Impact of temperature on feed-flow characteristics and filtration performance of an upflow anaerobic sludge blanket coupled ultrafiltration membrane treating municipal wastewater', *Water Research*, 83, pp. 71–83.

Pretel, R., Robles, A., Ruano, M.V., Seco, A. and Ferrer, J. (2014) 'The operating cost of an anaerobic membrane bioreactor (AnMBR) treating sulphate-rich urban wastewater', *Separation and Purification Technology*, 126, pp. 30–38.

Pretel, R., Shoener, B.D., Ferrer, J. and Guest, J.S. (2015) 'Navigating environmental, economic, and technological trade-offs in the design and operation of submerged anaerobic membrane bioreactors (AnMBRs)', *Water Research*, 87, pp. 531–541.

Robles, A., Ruano, M.V., García-Usach, F. and Ferrer, J. (2012) 'Sub-critical filtration conditions of commercial hollow-fibre membranes in a submerged anaerobic MBR (HF-SAnMBR) system: the effect of gas sparging intensity', *Bioresource Technology*, 114, pp. 247–254.

Robles, A., Ruano, M.V., Ribes, J. and Ferrer, J. (2013) 'Factors that affect the permeability of commercial hollow-fibre membranes in a submerged anaerobic MBR (HF-SAnMBR) system', *Water Research*, 47, pp. 1277–1288.

Ruigómez, I., Vera, L., González, E. and Rodríguez-Sevilla, J. (2016) 'Pilot plant study of a new rotating hollow fibre membrane module for improved performance of an anaerobic submerged MBR', *Journal of Membrane Science*, 514, pp. 105–113.

Sabry, T. (2008) 'Application of the UASB inoculated with flocculent and granular sludge in treating sewage at different hydraulic shock loads', *Bioresource Technology*, 99, pp. 4073–4077.

Smith, A.L., Skerlos, S.J. and Raskin, L. (2013) 'Psychrophilic anaerobic membrane bioreactor treatment of domestic wastewater', *Water Research*, 47, pp. 1655–1665.

Smith, A.L., Skerlos, S.J. and Raskin, L. (2015) 'Anaerobic membrane bioreactor treatment of domestic wastewater at psychrophilic temperatures ranging from 15 °C to 3 °C', *Environmental Science: Water Research & Technology*, 1, pp. 56–64.

Smith, A.L., Stadler, L.B., Cao, L., Love, N.G., Raskin, L. and Steven, J. (2014) 'Navigating wastewater energy recovery strategies: A life cycle comparison of anaerobic membrane bioreactor and conventional treatment systems with anaerobic digestion', *Environmental Science & Technology*, 48, pp. 5972–5981.

Sutton, P.M., Rittmann, B.E., Schraa, O.J., Banaszak, J.E. and Togna, A.P. (2011) 'Wastewater as a resource: A unique approach to achieving energy sustainability', *Water Science & Technology*, 63, pp. 2004–2009.

Syed, W., Zhou, H., Sheng, C., Mahendraker, V., Adnan, A. and Theodoulou, M. (2009) 'Effects of hydraulic and organic loading shocks on sludge characteristics and its effects on membrane bioreactor performance', *Proceedings of WEFTEC*. Orlando, FL.

Syutsubo, K., Yoochatchaval, W., Tsushima, I., Araki, N., Kubota, K., Onodera, T., Takahashi, M., Yamaguchi, T. and Yoneyama, Y. (2011) 'Evaluation of sludge properties in a pilot-scale UASB reactor for sewage treatment in a temperate region', *Water Science & Technology*, 64, pp. 1959–1966.

Tchobanoglous, G., Burton, F.L. and Stensel, H.D. (2003) *Wastewater Engineering Treatment and Reuse*. 4th edn. New York: McGraw-Hill Companies.

Uemura, S. and Harada, H. (2000) 'Treatment of sewage by a UASB reactor under moderate to low temperature conditions', *Bioresource Technology*, 72, pp. 275–282.

van Voorthuizen, E., Zwijnenburg, A., van der Meer, W. and Temmink, H. (2008) 'Biological black water treatment combined with membrane separation', *Water Research*, 42, pp. 4334–4340.

Water UK (2012) *Sustainability indicator 2010/2011*. London, UK.

CHAPTER 2

Comparison of fouling between aerobic and anaerobic MBR treating municipal wastewater

2 Comparison of fouling between aerobic and anaerobic MBR treating municipal wastewater

K. M. Wang[a], N. Martin Garcia[a], A. Soares[a], B. Jefferson[a], E.J. McAdam[a,*]
[a]Cranfield Water Science Institute, Vincent Building, Cranfield University, Bedfordshire, MK43 0AL, UK

Abstract

Anaerobic membrane bioreactors (AnMBR) have been realised at commercial scale for industrial wastewater treatment. Development of AnMBR technology for municipal wastewater is less mature, requiring a very different set of challenges to be resolved before implementation. The key driver for this technology is in enabling the transition to energy neutral wastewater treatment. However, municipal wastewater delivers a comparatively constrained methane yield, which means energy conservation must be prioritised to achieve the proposed energy neutral ambition. A critical focus on membrane fouling is therefore warranted, as membrane operation represents the primary energy demand in MBRs. This review seeks to quantify the characteristics of the prevailing AnMBR biological suspension and to ascertain whether knowledge transfer exists between fouling characteristics in aerobic and anaerobic MBRs for municipal applications. In doing so, this will help inform how best to reduce and control fouling through optimisation of membrane operation. Analysis of literature data revealed that the level of extractable extracellular polymeric substrate is slightly higher in aerobic MBRs than in anaerobic MBRs. However, AnMBR comprises considerably higher soluble microbial product concentrations, which have been widely reported to increase fouling propensity in aerobic systems. More distinct is the difference in the colloidal and fine solids fraction (between 1 and 10-15 μm). This highly dispersed matrix is likely to dominate fouling in anaerobic systems and limit knowledge transfer from aerobic MBRs. Literature data on energy production was compared to that employed for membrane operation, and evidences that despite the challenging character of the particle matrix, energy neutral operation is achievable for AnMBR applied to municipal wastewater treatment.

Keywords: membrane bioreactor, biomass characteristics, energy demand, biogas

2.1 Introduction

Anaerobic membrane bioreactors (AnMBRs) hold significant potential to reduce the overall energy demand of municipal (domestic) wastewater treatment through mediating organic biodegradation in the absence of oxygen which obviates the need for aeration and increases energy recovery through methane production. The lower secondary sludge production is also practically advantageous (Martin-Garcia et al., 2011). Several reviews have been published on AnMBR over the past ten years. Liao et al. (2006) provided a comprehensive overview of AnMBR technology, which strongly focused on high strength industrial wastewater treatment. More recent reviews have since updated the position of AnMBR for industrial treatment (Dvořák et al., 2016; Lin et al., 2013; Skouteris et al., 2012), which include a particularly insightful narrative on the thirty years of AnMBR commercial development for industrial application (Lin et al., 2013).

Development of AnMBR for municipal wastewater treatment has been comparatively limited. This can be attributed to the past perception that municipal wastewater could not be treated anaerobically since the low organic concentration was insufficient to support microbial growth (Lester et al., 2013). Integrating membrane technology into anaerobic systems helps respond to this challenge by decoupling hydraulic retention time (HRT) from solids retention time (SRT) thereby diminishing washout. The capability of AnMBR to achieve chemical oxygen demand (COD) and suspended solids compliance to International discharge standards has since been experimentally demonstrated on municipal wastewater (Martin Garcia et al., 2013; Stuckey, 2012). The impact of reactor configuration and operating conditions on organic biodegradation, coupled with a description of potential methods for integrating AnMBR technology into the flowsheet for municipal wastewater is presented in recent reviews (Ozgun et al., 2013; Smith et al., 2012).

Whilst the capability of AnMBRs to treat municipal wastewater has been demonstrated, the principal driver for their implementation is in enabling the transition toward energy neutral wastewater treatment. McAdam et al. (2011) demonstrated this conceptually for anaerobic treatment of temperate settled wastewater, evidencing COD reduction and around 0.28 kWh m^{-3} of additional energy production (including recovery of both headspace and dissolved methane fractions) (Cookney et al., 2016). This

demonstrates the considerable impact of anaerobic systems on the energy balance. However, through comparison of the typical energy demand of membrane operation in commercial aerobic MBR technology (0.19-0.70 kWh m^{-3}) (Itokawa et al., 2014; Judd, 2011; Krzeminski et al., 2012), it can also be evidenced that to achieve the proposed energy neutral ambition, energy conservation must be prioritised. Consequently, membrane fouling can be considered one of the critical barriers in achieving commercially viable AnMBR for municipal wastewater treatment, as this governs the energy demand (Judd, 2006; Mathioudakis et al., 2012).

The mechanisms underpinning membrane fouling in aerobic MBR (AeMBR) for municipal wastewater have been studied extensively, and are comprehensively summarised elsewhere (Drews et al., 2006; Le-Clech et al., 2006; Meng et al., 2009). The factors that influence membrane fouling in both aerobic and anaerobic MBR can be generally defined by the membrane characteristics, biomass properties, reactor and membrane operational conditions. The biomass properties influence the membrane fouling potential depending on the characteristics of the bacterial flocs, colloidal species, dissolved organics, and inorganic compounds all of which can increase the resistance to filtration (Chang et al., 2002). Very few studies have directly compared aerobic and anaerobic MBR experimentally, for either municipal wastewater or blackwater (Achilli et al., 2011; Baek and Pagilla, 2006; Martin Garcia et al., 2011; van Voorthuizen et al., 2008). These studies acknowledge an important distinction in fouling behaviour between aerobic and anaerobic systems, however, an in-depth characterisation and comparison of foulants has not yet been completed. What is clear from the literature is that size distribution and organics concentration in the AnMBR mixed liquor determines the characteristics and mechanisms of fouling. Providing greater resolution on the characterisation can thus inform the most effective fouling control strategies, as compared with the more extensively studied AeMBRs. This review therefore proposes to complement existing knowledge through characterisation of biomass properties within AnMBRs for municipal wastewater treatment, evaluating their impact on membrane fouling and comparing to those in AeMBR, so as to ascertain the main factors that determine differences in fouling behaviour and characteristics between these two

systems. Since membrane fouling strongly influences energy demand, published data on both energy production from AnMBR for municipal wastewater treatment and membrane specific energy utilisation was further analysed to ascertain the position of the existing literature relative to the aspiration of 'energy-neutral' wastewater treatment.

2.2 Biomass characteristics

Differences in characteristics between aerobic and anaerobic sludge are most readily attributed to the different mechanisms involved in the biological process. Aerobic biological suspensions mainly comprise microorganisms, decay products and influent solids forming microbial aggregates which are held together by high molecular weight polymers secreted by bacteria. This allows them to exist at high population densities (Laspidou and Rittmann, 2002) in virtue of their high biomass yield and growth rates. It has been reported that the structure, morphology and surface properties of such suspensions can be altered by changes in physiological state of the biomass induced by changes in bioreactor operational parameters such as SRT and food to microorganism (F:M) ratio (Liao et al., 2001).

On the other hand anaerobic degradation of wastewater with dissolved, colloidal and particulate organic matter, involves several sequential steps such as hydrolysis, acidogenesis, acetogenesis and methanogenesis (Batstone, 2006). Hydrolysis is thought to be an extracellular reaction where solids are converted to simple monomers by extracellular enzymes secreted by hydrolytic and fermentative bacteria (Sanders et al., 2000; Vavilin et al., 2008). As a result and due to the low hydrolysis rates and biomass yield of anaerobic bacteria in high rate anaerobic reactors, the reactor solids inventory is considered to be mainly constituted by influent particles (Soto et al., 1993) that are of reduced particle size (Elmitwalli et al., 2001) and density (Lant and Hartley, 2007). Therefore, as opposed to aerobic systems, sludge properties are probably more dependent on influent characteristics than on bioreactor operational parameters.

2.2.1 Mixed liquor suspended solids

Although sludge flocs are not considered the main contributors to fouling under low flux operation, mixed liquor suspended solids (MLSS) concentration has shown to negatively affect membrane fouling in AnMBRs (Table 2-1). For instance, Jeison and van Lier (2006) found that changing biomass concentration had a greater impact on the formation of a cake layer than varying gas sparging intensity. Robles et al. (2013a) also indicated that higher MLSS concentration led to lower membrane permeability, which supports the observations of Jeison and van Lier (2006). Martin Garcia et al. (2013) compared a flocculent AnMBR configured as a completely stirred tank reactor (CSTR) and a granular AnMBR configured as an upflow anaerobic sludge blanket (UASB) reactor for settled municipal wastewater treatment, which presented MLSS concentrations for membrane filtration of 7.7 g L^{-1} and 0.1-0.6 g L^{-1}, respectively. Higher fouling rates and lower critical fluxes have been determined for the CSTR configured AnMBR comprising more concentrated flocculent sludge. In AeMBR, Le Clech et al. (2003) also reported that the effect of MLSS was higher than gas sparging in an AeMBR. However, in their study, critical flux increased at a higher biomass concentration of 12 g MLSS L^{-1} as compared to the lowest MLSS concentration of 4 g L^{-1}.

The contradicting influence that MLSS concentration has on membrane hydraulic performance between aerobic and anaerobic MBRs can be attributed to differences in the relationship between biomass and dissolved/colloidal compounds in the mixed liquor. In AeMBRs, it has been widely reported that higher levels of soluble microbial products are found at lower MLSS when short SRTs are applied (Lee et al., 2003; Liang et al., 2007; Lousada-Ferreira et al., 2015; Massé et al., 2006) while in anaerobic systems, soluble microbial products (SMP) tend to accumulate together with biomass (Harada et al., 1994) or at high sludge ages.

For AnMBR, Ghyoot and Verstraete (1997) reported that permeate fluxes at concentrations below 13 g L^{-1} total solids (TS) appeared to be higher than those recorded at 20 and 25 g TS L^{-1}. Analysis of the characteristics of digested primary sludge in the membrane revealed that, on increasing the biomass concentration from 6 g L^{-1} to 25 g L^{-1} the colloidal COD (8 µm filtered) increased from 69 to 716 mg L^{-1}. Beaubien et al. (1996) who studied the impact of transmembrane pressure (TMP), crossflow velocity

(CFV) and suspended solids (SS) concentration on membrane flux observed that permeability decreased from 0.6 to 0.2 μm s^{-1} kPa^{-1} as MLSS concentrations increased from 0.4 g L^{-1} to 2.5 g L^{-1} remaining constant thereafter. Since permeability appeared to be independent of CFV at *Reynolds* numbers between 2000 and 15000, the author attributed this trend to higher concentrations of pore plugging particles rather than viscosity and concentration polarisation.

Table 2-1.Overview of operating conditions and membrane performance in immersed anaerobic MBRs treating municipal wastewater.

Source	Reactor type/Sludge	Reactor size RE.	Reactor size Fl.	Material/ Geo./ Pore size	MLSS	SGD	J_c	$J_{c,20}$	Flux	TMP	Fouling rate		T_{op}	Ref.
		L		µm	g L^{-1}	m^3 m^{-2} h^{-1}	L m^{-2} h^{-1}		L m^{-2} h^{-1}	mbar	mbar min^{-1}	kPa h^{-1}	h	
Crude[a]	UASB/F	17.7[d]		PE/HF/0.03	16-21.5	0	-	-	5,10	<700	0.033,0.058	0.200,0.350	336,144	Wen et al.,1999
Crude[b]	CSTR/F	1300	800	PVDF/HF/0.05	10-30	0.23	-	-	9-13.3	-	-	-	14400	Robles et al., 2013b
Crude[b]	CSTR/F	-	50	PVDF/HF/0.04	21.3	1.3	10-12	10-12	10	<140	0.002-0.075	0.012-0.45	60	Ruigómez et al., 2016b
Crude[b]	CSTR/F	-	50	PVDF/HF/0.04	21.3	0	12-14	12-14	10	<140	0.001-0.027	0.007-0.16	>200	Ruigómez et al., 2016b
Crude[a]	CSTR/F	550	80	PVDF/HF/0.04	12.8[f]	0.146	-	-	17	<215	0.002	0.010	2160	Dong et al.,2015
Crude[a]	CSTR/F	550	80	PVDF/HF/0.04	5.6[f]	0.146	-	-	17	<88	0.001[j]	0.004[j]	2160	Dong et al.,2015
Crude[a]	CSTR/F	550	80	PVDF/HF/0.04	11.3-23	0.146	21-27	20-25	17	<250	0-0.004	0.001-0.025	4272	Dong et al., 2016a
Crude[a]	CSTR/F	60[d]		PVDF/FS/140[f]	6.4-9.3	0.12	-	-	12	-	-	-	-	Lin et al., 2011
Crude[c]	IAFMBR	7.6[d]		-/HF/0.4	-	0	-	-	11.3	<300	0.014	0.086	348	Gao et al., 2014b
Crude[c]	IAFMBR	7.6[d]		-/HF/0.4	-	0	-	-	11.3	<300	0.009[k]	0.052[k]	576	Gao et al., 2014b
Crude (GA)	CSTR/F	350	-	PES/FS/0.038	15	-	7	7	7	<280	<0.002	0.001-0.011	2352	Martinez-Sosa et al., 2011
Black	UASB/F	5	-	PVDF/Tub/250[e]	-	-	-	-	10[g]	-	-	-	-	van Voorthuizen et al. , 2008
Black	CSTR/F	4[d]		PVDF/Tub/250[e]	-	-	-	-	8[g]	-	-	-	-	van Voorthuizen et al. , 2008
Settled	UASB/F	160	150	PVDF/HF/0.045	0.5,5-7[f]	0.2, 0.4-1.0	-	-	2.5,10-15	50, <550	-	-	4320	Gouveia et al., 2015a
Settled	UASB/G	326	175	PVDF/HF/0.045	2, 12-14[f]	0.07-0.13	-	-	12, 15.7	-	0.001-0.013	0.004-0.079	-	Gouveia et al., 2015b
Settled	UASB/G	94	31	PVDF/HF/0.04	0.1-0.6	1.2	4.3-13.4	4.6-14.2	6[g]	<100	0.001	0.004-0.013	>300	Martin Garcia et al., 2013
Settled	CSTR/F	900	300	PVDF/HF/0.04	7.7	0.4	1.9-9.7	2.0-10.3	6[g]	<700	0.033	0.198	<200	Martin Garcia et al., 2013
Settled	CSTR/G	40[d]		-/HF/0.1	6.5-6.8	-	-	40	-	-	0.004-0.007	0.025-0.042	-	Fawehinmi, 2006
Settled	CSTR/F	5	1	PES/PF/0.45	8.0-13.6	-	-	-	-	<300	0.005-0.014	0.031-0.083	360-960	Huang et al., 2013
Settled	SAF-MBR/F	0.245	0.245	PVDF/HF/0.1	-	0	-	-	9	<400	<0.001-0.035	0.002-0.213	9500	Yoo et al., 2014
Settled	SAF-MBR/F	990	770	PVDF/HF/0.03	0.6-1.2[f]	0	-	-	4.1-7.5[g]	<500	-	-	11640	Shin et al., 2014
Synthetic	UASB	-		PVDF/FS/0.22	-	1.8	-	-	25	<300	0.055-0.530[l]	0.330-3.180[l]	-	Wu et al., 2009
Synthetic	UASB/G	4.7[d]		PE/0.1	-	0	-	-	-	-	-	-	480	Chu et al., 2005
Synthetic	UASB/F	30[d]		PVDF/FS/0.22	0.14	0-1.2	-	-	25	<300	0.417-1.250	2.5-7.5	4-12	An et al., 2010
Synthetic	CSTR/F	5	1	PES/PF/0.45	5.6-10.5	-	-	-	5.3-7.9	<300	<0.006	0.002-0.036	840-2400	Huang et al., 2011
Synthetic	CSTR/F	3[d]		PE/FS/0.4	4.3-4.8	3	-	-	20	<270	0.003-0.005[k]	0.018-0.031[k]	384	Hu and Stuckey, 2007
Synthetic	CSTR/F	3[d]		PE/FS/0.4	6-19,12-16	3	-	-	10	120-230	-	-	360	Akram and Stuckey, 2008
Synthetic	CSTR/F	7[d]		PES/FS/0.2	-	7.24	-	-	7	-	<0.001[m]	<0.001[m]	720	Smith et al., 2013
Synthetic	AFBR+AFMBR	0.245	0.245	PVDF/HF/0.1	0.09-0.13[f]	0	-	-	9	<100	-	-	2400	Bae et al., 2014
Synthetic	ABR+AFMBR	3.93	2.0	PVDF/HF/0.1	-	0	-	-	7	30[h], 320[i]	0.444[i]	2.667[i]	-	Kim et al., 2011
Synthetic	ARMBR	4[d]		PE/FS/0.22	5.5	0	-	-	11	<50	-	-	2400	Kim et al., 2014

a. Crude: after screening; b. Crude: Pre-treatment including screening, degritter and grease removal; c. Crude: from septic tank; d. Membrane submerged in the anaerobic reactor; e. MWCO (kDa); f. reported MLVSS; g. Net flux; h- With GAC; i-Without GAC; j. With $FeCl_3$ addition; k. With GAC (granular activated carbon) or PAC (powdered activated carbon) addition; l. With addition of PAC (powdered activated carbon)/zeolite/polyamide/polyaluminum chloride; m. Backwash 4min every 4h.
Acronyms: ABR+AFMBR- anaerobic baffled reactor + anaerobic fluidised bed membrane bioreactor; AFBR- anaerobic fluidised bed reactor; ARMBR- anaerobic rotate disk MBR; BW-backwash; CSTR-completely stirred tank reactor; F-flocculent sludge; Fl-filtration; FS-flat sheet; G-granular sludge; GA -glucose addition; HF-hollow fibre; IAFMBR- integrated anaerobic fluidised-bed; MWCO-molecular weight cut off; PE- Polyethylene; PES-polyethersulfone; PF-plate and frame; PVDF-polyvinylidene fluoride; RE. anaerobic reactor; SAF-MBR -staged anaerobic fluidised MBR; SGD_m-specific gas demand; T_{op}- time of performance; Tub- tubular; UASB-upflow anaerobic sludge blanket

2.2.2 Particle size distribution

According to Hartley and Lant (2007) anaerobic sludge particle sizes are one order of magnitude lower than aerobic flocs (activated sludge floc), even though the range of particle sizes covers three orders of magnitude as opposed to only one for aerobic biomass. Data collated from the literature identified similar median particle size ranges of 5.2 to 220 µm and 0.8 to 138 µm in aerobic and anaerobic MBRs respectively (Table 2-2), however, a significant difference is the presence of a population of fine colloidal matter in AnMBR which has been shown to negatively affect membrane performance. This was confirmed by Martin-Garcia et al. (2011) who found a higher colloidal content in a flocculent AnMBR (CSTR) and a granular AnMBR (UASB), when compared directly with an AeMBR. The authors attributed the higher degree of dispersive growth to higher fouling propensity.

Particle size analysis in AnMBRs (Table 2-2) indicates that externally configured (side-stream) membrane systems yield considerably lower particle sizes when compared to immersed systems using gas sparging (Bailey et al., 1994; Hu and Stuckey, 2006; Imasaka et al., 1989; Jeison and van Lier, 2006). This can be attributed to the shear imposed by the pumping demanded to maintain cross-flow velocity (Imasaka et al., 1989; Jeison et al., 2009). Analogous effects have been demonstrated following conversion of conventional anaerobic reactors to AnMBR (Ho and Sung, 2009; Ozgun et al., 2015a) and it is suggested that such particle reduction can also decrease biomass activity (Brockmann and Seyfried, 1997).

Apart from hydrodynamic conditions, operating temperature has been shown to influence biomass characteristics. Comparison of mesophilic and thermophilic AnMBRs operated at similar MLSS concentration (8 g L^{-1}) showed that the latter contained a higher fraction of fine solids between 1 and 15 µm and provided a 5 to 10 fold increase in cake layer resistance over that of the mesophilic system (Lin et al., 2009). Ozgun et al. (2015b) also observed a reduction in median particle size from 80-137 µm to 25-88 µm when the temperature was reduced from 25 to 15 °C during the treatment of synthetic municipal wastewater. This was corroborated by Robles et al. (2013a) following the transition from mesophilic to psychrophilic conditions. The authors proposed that the smaller particle sizes led to lower cake layer porosities, and higher cake layer tortuosity,

which resulted in considerable cake layer resistance. Transients in particle size distributions have been noted in both anaerobic and aerobic MBR systems following changes to SRT. Huang et al. (2011, 2013) reported a decrease in median particle size for AnMBR when SRT increased from 30 to 60 d, which is similar to the observations of Martin Garcia et al. (2011). Similar effects of particle size reduction in AeMBR in response to an increase in SRT have been observed (Huang et al., 2001; Martin-Garcia et al., 2011).

Table 2-2. Particle size distribution of sludge/biomass in aerobic and anaerobic MBRs in contact with the membrane.

Source	Reactor Type	Geo./Mode/Config.	Temp °C	SRT d	Average d_{p50} µm	Ref.
			Anaerobic MBRs			
Industrial [a]	CSTR	PF/pumped/Side	53-55	-	3-16	Choo and Lee, 1998
Industrial [b]	CSTR	Tubular/pumped/Side	52	-	0.8,4.0	Imasaka et al., 1989
Settled	UASB	HF/gas sparged/Sub	-	30,200	60,1.4	Martin-Garcia et al., 2011
Settled	CSTR	HF/gas sparged/Sub	-	30,200	43,7.6	Martin-Garcia et al., 2011
Settled	CSTR	PF/gas sparged/Sub	25-30	30,60	28,21	Huang et al., 2013
Synthetic	UASB	Tubular/pumped/Side	30	-	36,16[d]	Bailey et al., 1994
Synthetic [c]	UASB	FS/pumped/Side	-	-	75,13[d]	Cho and Fane, 2002
Synthetic	UASB	Tubular/pumped/Side	25	-	465,138[e]	Ozgun et al., 2015a
Synthetic	UASB	Tubular/pumped/Side	25	-	80-137[f]	Ozgun et al., 2015b
Synthetic	UASB	Tubular/pumped/Side	15	-	25-88[f]	Ozgun et al., 2015b
Synthetic	CSTR	-/pumped/Side	35	-	13	Elmaleh and Abdelmoumni, 1997
Synthetic	CSTR	Tubular/pumped/Side	25	90-360	51,25[d]	Ho and Sung, 2009
Synthetic	CSTR	Tubular/gas sparged/Sub	30,55	-	70-90[g]	Jeison and van Lier, 2006
Synthetic	CSTR	FS/gas sparged/Sub	35	250	23.5	Akram and Stuckey, 2008
Synthetic	CSTR	FS/gas sparged/Sub	35	250	9.6-16.3[h]	Akram and Stuckey, 2008
Synthetic	CSTR	FS,HF/gas sparged/Sub	35	-	60-65	Hu and Stuckey, 2006
Synthetic	CSTR	PF/gas sparged/Sub	25-30	30-∞	24-31	Huang et al., 2011
			Aerobic MBRs			
Industrial + Crude	CSTR	HF/gas sparged/Sub	>10	-	32-36	Sun et al., 2011
Crude	CSTR	MT/pumped/Side	20	60	50	Defrance et al., 2000
Crude	CSTR	HF/gas sparged/Sub	9-21	5,20,40	14,48,31	Huang et al., 2001
Settled	CSTR	HF/gas sparged/Sub	20	10	120-220	Massé et al., 2006
Settled	CSTR	HF/gas sparged/Sub	20	30	70-100	Massé et al., 2006
Settled	CSTR	HF/gas sparged/Sub	-	30,200	32.4,14.0	Martin-Garcia et al., 2011
Synthetic	CSTR	HF/gas sparged/Sub	-	20,40,60	5.2-6.6	Lee et al., 2003
Synthetic	CSTR	HF/gas sparged/Sub	-	30	57.6	Zhou et al., 2014

a. Alcohol-distillery wastewater; b. Concentrated thermophilic fermentation broth of evaporator condensate discharged from a kraft pulp mill; c. Not mention synthetic, but assume according to the influent characteristics; d. Particle size before and after shear induction; e. UASB sludge particle size before and after membrane addition; f. Particle size in the UASB effluent; g. Estimate from graph; h. With addition of PAC (powdered activated carbon)
Acronyms: CSTR- completely stirred tank reactor; FS-flat sheet; HF-hollow fibre; MT-multiple tube; PF-plate and frame; UASB-upflow anaerobic blanket reactor

2.2.3 Organic fouling by EPS

Extracellular polymeric substances (EPS) have been widely reported as being responsible for organic fouling in both aerobic (Fan et al., 2006; Lesjean et al., 2005; Pollice et al., 2005; Rosenberger et al., 2006) and anaerobic MBRs (Cho and Fane, 2002; Harada et al., 1994; Hu and Stuckey, 2006; van Voorthuizen et al., 2008). These biopolymers, composed mainly of polysaccharides, proteins and lipids, which have been fractionated according to whether they are found in the sludge supernatant as SMP or bound to the sludge flocs and are thus extracted from the cell walls (eEPS). Although the term SMP implies that these substances are of bacterial origin, they may also be the result of recalcitrant or partially transformed influent organics. This is particularly the case for anaerobic systems at lower temperatures where lower biodegradation rates apply, which increases SMP concentrations above those of aerobic biomass (Lettinga et al., 2001). However, independent of their origin, analysis of eEPS and SMP has contributed to further characterisation both of the solid and the colloidal/soluble fractions of biological suspensions respectively.

2.2.3.1 Bound/extractable EPS

The surface properties of the sludge are primarily determined by eEPS. The hydrophobicity and surface charge have been correlated with the total EPS concentration and the ratio of proteins to carbohydrates in both conventional activated sludge and MBR systems (Lee et al., 2003; Liao et al., 2001). For instance, a higher ratio of proteins to carbohydrates in activated sludge has been reported to enhance bioflocculation through the reduction of surface charge and increase in hydrophobicity. On the other hand, high proportions of carbohydrates in the eEPS are associated with a more dispersed sludge structure due to the greater repulsion between sludge particles and interaction with the aqueous phase resulting from the higher negative surface charge and reduced hydrophobicity (Liao et al., 2001).

Literature data regarding surface properties of anaerobic sludge do not correlate as consistently as those from aerobic systems, and no conclusions can be drawn regarding comparative concentrations of eEPS and fractions thereof, to allow comparison between aerobic and anaerobic sludges with respect to surface charge and

hydrophobicity. Morgan et al. (1990) reported that aerobic sludge was more negatively charged, contained higher levels of total eEPS and lower ratios of proteins to carbohydrates than anaerobic sludge. Similarly, analysis of eEPS literature data from MBR operated with municipal wastewater (Crude, Settled and Synthetic) demonstrates a considerably higher protein to carbohydrate ratio in AnMBR when compared to AeMBR (Table 2-3). In terms of specific eEPS concentration, the distinction between aerobic and anaerobic systems is less clear. Comparison between anaerobic and aerobic MBRs operated with complete retention of solids and fed with settled sewage (Baek and Pagilla, 2006) showed a continuous decrease of levels of EPS. In a further study on AnMBR, Lee et al. (2008) attributed the rapid onset of fouling after stable operation of 28 days to a sudden increase in eEPS from 30 to 235 mg TOC L^{-1}. A similar trend was reported by Fawehinmi et al. (2004) who observed an increase in specific resistance to filtration as the eEPS content of crushed granular sludge increased from 20 to 130 mg g VSS^{-1}. Ceron-Vivas et al. (2012) demonstrated the highest eEPS values above 200 mg g VSS^{-1} in a synthetic wastewater. Analysis of the arising cake layer revealed that the specific eEPS deposited on the membrane surface was twice that found in the granular sludge with higher eEPS protein to carbohydrate ratio on the membrane (Chu et al., 2005). Whilst Lin et al., (2009) reported a lower eEPS protein to carbohydrate ratio in the fouling layer when compared to the bulk material. Regardless of the major fouling component, the discrepancies between biomass and cake layer eEPS composition found in these studies suggest that soluble or colloidal compounds are also responsible for the increase in membrane resistance in AnMBRs.

2.2.3.2 Soluble-colloidal EPS: SMP

It has been reported that soluble organic matter in the effluent from the biological treatment processes is predominantly SMP which comprises the soluble cellular components released during cell lysis, lost during synthesis, or otherwise secreted for some purposes (Laspidou and Rittmann, 2002). Soluble microbial products are classified according to their origin as products associated with biomass growth and are produced at a rate proportional to substrate utilisation and non-growth associated products related to cell lysis. In conventional (i.e. non-membrane based) systems, the

concentration of SMP normalised to influent COD is higher in aerobic than anaerobic processes (Barker and Stuckey, 1999). This can be explained by the lower biomass uptake and decay rates of anaerobic microorganisms compared to aerobic biomass.

The SMP concentration within aerobic and anaerobic MBR is higher than for conventional processes (Aquino et al., 2006; Massé et al., 2006). Ozgun et al. (2015a) directly compared the SMP of conventional UASB with UASB coupled with membrane and reported that SMP increased over 3 times after membrane addition from about 37 mg L^{-1} to 120 mg L^{-1}. This is due to an increased retention of the high molecular weight organic fraction by the membrane (Massé et al., 2006) as well as an increase in net SMP productivity through endogenous decay and cell lysis which are enhanced by long SRT and high organic loading rates (Harada et al., 1994). Anaerobic MBRs have considerably higher SMP concentrations than are present in aerobic MBR (Table 2-4). Normalising literature SMP_{COD} data to influent COD (w/w), suggests arising SMP_{COD} ranges from 10-48 % and from 9-59 % for aerobic and anaerobic MBRs, respectively. This has been confirmed through comparative experimental study of anaerobic and aerobic MBR systems for municipal wastewater treatment, which has evidenced SMP concentrations up to five times higher in anaerobic MBR (Martin-Garcia et al., 2011). The higher colloidal content within AnMBR, compared with that of AeMBR, may reflect the higher levels of free bacteria in mixed liquor, together with the lower biodegradation rates or SMP biodegradability expected under anaerobic conditions (Ince et al., 2000). There is also evidence of high molecular weight polymeric material of up to 1000 kDa being retained by the cake layer in AnMBRs, which presumably decreases permeability and potentially increases rejection capability (Harada et al., 1994). Feed temperature is also a factor, where decreased temperature from 25 to 15 °C in an AnMBR, increased SMP_{COD} from 50 to 150 mg L^{-1} (Ho and Sung, 2010).

Table 2-3. Concentration and composition of EPS in aerobic and anaerobic MBR sludge/biomass.

Source	Reactor type/sludge	Config.	Temp. °C	SRT d	HRT h	MLSS g L^{-1}	EPS_{tot} mg g VSS^{-1}	EPS_p mg g VSS^{-1}	EPS_c mg g VSS^{-1}	Ratio EPSp/EPSc	Ref.
Anaerobic MBRs											
Crude[a]	CSTR/F	Sub	20	70	24.5	18-28	98[h]	74	24	7.0 (3.1)[o]	Robles et al., 2013a
Crude[a]	CSTR/F	Sub	33	70	5.5-16.5	14-32	155[h]	121	34	16.4 (3.6)[o]	Robles et al., 2013a
Crude[a]	CSTR/F	Sub	17-29	28.6-41.1	12.1-28.4	10-25	161[i]	126	35	3.6	Giménez et al., 2014
Settled	CSTR/G	Sub	12	120[f]	6	5.9	11-32[i,n]	10.1-31.5[n]	0.9[n]	10.7-33.3	Fawehinmi, 2006
Settled	CSTR/F	Sub	25-30	30-90	10	8.0-13.6	42-50[i]	32-40	10	4-5	Huang et al., 2013
Synthetic	UASB/G	Sub	11-25	-	3.5-5.7	-	5-7.7[i,j]	0.6-1.6	4.4-6.1	0.18-0.25	Chu et al., 2005
Synthetic	UASB/G	Sub	11-25	-	3.5-5.7	-	17.4-20.4[i,k]	5.8-7.0	11.6-13.4	0.48-0.55	Chu et al., 2005
Synthetic	UASB/G	Sub	21-24	-	8	-	219[i,l]	108-244	27-60	4.1	Cerón-Vivas et al., 2012
Synthetic	UASB/F	Side	25	-	6	-	4[i]	3.7	0.3	12.3	Ozgun et al., 2015a
Synthetic	CSTR/F	Sub	15	300	16	-	57-81[h,k]	32-46	25-35	1.3	Smith et al., 2013
Synthetic	CSTR/F	Sub	25-30	30	8-12	5.6-7.1	55.5[i]	38-48	10-15	2.5-2.85	Huang et al., 2011
Synthetic	CSTR/F	Sub	25-30	60	8-12	5.7-8.9	55.5[i]	37-45	11-18	2.0-2.85	Huang et al., 2011
Synthetic	CSTR/F	Sub	25-30	∞	8-12	6.5-10.5	49.5[i]	35-42	11	2.5	Huang et al., 2011
Synthetic	IAFMBR[d]/F	Sub	35	-	6	-	60[i,m]	45[m]	15[m]	3	Gao et al., 2014b
Synthetic	IAFMBR[d]/F	Sub	35	-	6	-	37.5-42.5[i,m]	30-35[m]	5-10[m]	4.3	Gao et al., 2014b
Synthetic	IAFMBR[d]/F	Sub	35	-	6	-	70[i,k,m]	52[m]	18[m]	2.8	Gao et al., 2014b
Aerobic MBRs											
Crude[b]	CSTR	Sub	16-22	∞	13.3	5.2-10.5	25.5-79.8[i]	20.4-64.5	3.4-34.0	2.3	Bella et al., 2011
Crude[b]	CSTR	Sub	-	40-45	16	10-31.2	34-157[i]	-	-	-	Holba et al., 2012
Crude[b]	CSTR	Sub	-	30-75	42	2.2-5.6	38-114[i]	-	-	-	Holba et al., 2012
Crude[b]	CSTR	Sub	11-23.8	5-12	6	10-11.2	90-140[h]	-	-	-	Fan et al., 2006
Crude[b]	CSTR	Sub	13-26	10	10	3.8-4.2	162.7[i]	58.7	42.9	1.4	Liu et al., 2012b
Crude[b]	CSTR[e]	Sub	13-26	10	10	3.8-4.3	165.2[i]	58.6	41.8	1.4	Liu et al., 2012b
Crude[c]	CSTR	Sub	-	-	-	6.0	6.9[h]	3.5	3.4	1.0	Gabarrón et al., 2013
Settled	CSTR	Sub	-	10-30	-	12-18	81-115[i]	57-88	24-29	2.4-3.2	Trussell et al., 2007
Settled	CSTR	Sub	20	10	16	1.9	45-70[i]	-	-	2-4	Massé et al., 2006
Settled	CSTR	Sub	20	53	16	6.0	20-40[i]	-	-	2-4	Massé et al., 2006
Synthetic	CSTR	Sub	-	20,40,60	7.8	2.8-5.5[g]	63-70[i]	30-36	30-35	1.0	Lee et al., 2003
Synthetic	CSTR	Sub	-	10-80	-	1.7-3.7	-	<2	3-6	0.33-0.67	Duan et al., 2015

a. Crude: Pre-treatment including screening, degritter and grease removal; b. Crude- after screening; c. Data from full scale plant, Crude- after coarse screen, grit chamber, buffering and fine screen; d. With 40g GAC addition; e. With biofilm carrier; f. Not report SRT, but no sludge is wasted during the tests except sampling. SRT can be assumed the same as experiment duration time; g. Reported MLVSS; h. Reported as extracted EPS; i. Reported EPS; j. EPS of sludge on granules; k. EPS of sludge on membrane; l. EPS in the UASB effluent; m. No MLSS or MLVSS, data is reported with initial unit mg L^{-1}; n. Use MLVSS/MLSS ratio=0.63 to convert the unit from mg g SS^{-1} to mg g VSS^{-1}; o. Values in the bracket were calculated directly from the average value

Acronyms: CSTR- completely stirred tank reactor; F-flocculent sludge; G-granular sludge; GAC-granular activated carbon; IAFMBR- integrated anaerobic fluidised-bed membrane bioreactor; SAF-MBR- staged anaerobic fluidised membrane bioreactor; UASB-upflow anaerobic sludge blanket

Table 2-4. Concentration and composition of soluble microbial products in aerobic and anaerobic MBRs.

Source	Reactor type[a]/ Sludge	Config.	Temp °C	SRT d	HRT h	MLSS g L^{-1}	SMP_{COD}[b] mg L^{-1}	SMP_c mg L^{-1}	SMP_p mg L^{-1}	Ratio SMP_p/SMP_c	Ref.
Anaerobic MBRs											
Crude	UASB/F	Side	22	180	6	0.4	-	99.2	133.2	1.3	Herrera-Robledo et al., 2011
Crude[c]	IAFMBR[j]	Sub	35	-	6	-	-	3-5	14-15	3.5-3.8	Gao et al., 2014b
Black	UASB/F	Sub	37	-	12	-	327 (0.29)	81	70	0.9	van Voorthuizen et al., 2008
Black	CSTR/F	Sub	37	-	12	-	269 (0.24)	45	69	1.5	van Voorthuizen et al., 2008
Settled	UASB/G[k]	Sub	10-25	250[l]	16	0.1-0.6	198 (0.59)	18	50	2.8	Martin Garcia et al., 2013
Settled	CSTR/G	Sub	12-35	120[l]	6	5.9-6.8	180 (0.40)	8	59	7.4	Fawehinmi, 2006
Settled	CSTR/F	Sub	-	100	16	7.7	598 (1.77)	47	108	2.3	Martin Garcia et al., 2013
Settled	CSTR/F	Side	25	233	24	7.1	51 (0.61)[n]	-	-	-	Baek and Pagilla, 2006
Settled	CSTR/F	Sub	25-30	30-90	10	8.0-13.6	-	18-19	40-50	2.2-2.5	Huang et al., 2013
Synthetic	UASB/G	Sub	21-24	-	8	-	-	0.5-1.2	1.1-3.3	2.6	Cerón-Vivas et al., 2012
Synthetic	UASB/F	Sub	35	-	12	0.14	-	1.2-16.6	7.4-15.1	0.7-6.5	An et al., 2010
Synthetic	UASB/F	Side	25	-	6	0.5	122 (0.23)	25-40	60-80	2.1	Ozgun et al., 2015a
Synthetic	UASB/F	Side	-	-	4-12	-	40 (0.11)	-	-	-	Salazar-Peláez et al., 2011
Synthetic	CSTR/F	Sub	35	150	6	3.7[m]	180[o] (0.40)	31	58	1.9	Aquino et al., 2006
Synthetic	CSTR/F	Sub	35	250	15	12-16	1787 (0.45)	-	-	-	Akram and Stuckey, 2008
Synthetic	CSTR/F	Sub	35	250	6	6-19	228-360[o] (0.09)	-	-	-	Akram and Stuckey, 2008
Synthetic	CSTR/F	Sub	25-30	30,60, ∞	8-12	5.6-10.5	-	4.5-14	7-18	0.9-2.0	Huang et al., 2011
Synthetic	CSTR/F	Side	35	190[l]	48-120	15[m]	1200 (0.24)	80	400	5	Harada et al., 1994
Aerobic MBRs											
Crude[d]	CSTR	Sub	13-26	10	10	3.8-4.2	-	3.5 (1.8)[p]	3.6 (1.9)[p]	1.0 (1.1)[p]	Liu et al., 2012b
Crude[e,f]	CSTR	Sub	10-25	-	-	-	-	3.6	2.4	0.7	Lyko et al., 2007
Crude[g]	CSTR	Sub	11-12	5-12	6	9.7-11.9	-	17-38	10-58	1.2	Fan et al., 2006
Crude[e,h]	CSTR	Sub	-	14-38	12-41	2.2-13.5	-	3-18	<5	0.5-1.7	Shen et al., 2012
Crude[e,i]	CSTR	Sub	-	-	-	6.0	-	3.7	2.7	0.7	Gabarrón et al., 2013
Settled	CSTR	Sub	-	10-30	-	12-18	37-82 (0.11-0.24)	12-26	10-79	0.5-3.0	Trussell et al., 2007
Settled	CSTR	Sub	-	10-30	-	12-18	33-166 (0.10-0.48)	16-27	12-140	0.6-5.4	Trussell et al., 2007
Settled	CSTR	Sub	20	10-110	16	1.9-7.2	45-110 (0.12-0.30)	37.2	8.9	0.2-0.6	Massé et al., 2006
Settled	CSTR	Sub	-	100	16	8.7	99 (0.29)	18	18	1.0	Martin-Garcia et al., 2011
Synthetic	CSTR	Sub	28	10-40	10	3.1-7.8	-	8-12	5-9	1.4	Liang et al., 2007

a. Report SMP from UASB effluent, CSTR and IAFMBR from mixed liquor; b. Values in brackets correspond to normalised SMP_{COD} with respect to influent COD; c. Crude: from septic tank; d. Crude: after sand settler and screening; e. Data from full scale plant; f. Crude: after coarse screen, grit chamber, grease trap and fine screen; g. Crude: pre-treatment with screening; h. Crude: after screening; i. Crude: flow after coarse screen, grit chamber, buffering and fine screen; j. With 40g GAC addition; k. Reported SMP in the membrane tank; l. Not report SRT, but no sludge is wasted during the tests except sampling. SRT can be assumed as same as experiment duration time; m. Reported MLVSS; n. Normalised against influent soluble COD; o. With addition of PAC (powdered activated carbon); p. Values in bracket is with bio-carrier.
Acronyms: CSTR- completely stirred tank reactor; F-flocculent sludge; G-granular sludge; IAFMBR- integrated anaerobic fluidised-bed membrane bioreactor; UASB-upflow anaerobic sludge blanket

2.3 Fouling control strategies

Whilst much of the early research on AnMBR for industrial applications sought to pursue externally configured MBR, the development of AnMBR for municipal applications has been generally more focused on immersed MBR technology, which is presumably due to the lower energy penalty that this configuration can achieve (Judd, 2011).

2.3.1 Specific gas demand and operation flux

The operational costs related to membrane operation in immersed MBRs are mainly determined by the relationship between the specific gas demand (SGD_m) and operating flux, with the SGD_m being the gas flow rate per unit membrane area (the specific aeration demand, SAD_m, for aerobic systems). This reflects the relationship between the convective flow towards the membrane produced by permeate suction and the back transport induced by the gas sparging and tangential shear at the boundary layer (Liu et al., 2003).

In AeMBRs, sustainable or critical fluxes have been reported to increase by increasing gas intensity up to a certain threshold value beyond which no further increase in flux is observed for flat sheet (Guglielmi et al., 2008; Ueda and Hata, 1999), hollow fibre (Guglielmi et al., 2007) and multi-tubular membranes (Le-Clech et al., 2006). For instance, Yu et al. (2003) reported an increase in critical flux from 7.3 to 50.2 L m^{-2} h^{-1} as the specific gas demand increased from 0.08 to 0.68 m^3 m^{-2} h^{-1} in an AeMBR operated at a biomass concentration of 3 g MLSS L^{-1}. Chen et al. (2016) also reported an increase in critical flux from 23 to 47 L m^{-2} h^{-1} for an AeMBR when SAD_m increased from 4.5 to 9.0 m^3 m^{-2} h^{-1}. Analysis of full scale immersed AeMBRs indicated an operational SAD_m range of 0.21 to 0.88 m^3 m^{-2} h^{-1}, corresponding to fluxes between 24 and 31 L m^{-2} h^{-1} (Verrecht et al., 2008).

Increasing membrane flux, has been shown to increase fouling rates and decrease the duration of the slow fouling phase in AeMBRs under conditions of sub-critical flux operation, prior to the widely reported “TMP jump” (Le-Clech et al., 2006; Pollice et al., 2005). For example, Zhang et al. (2006) reported increased fouling rates from 0.0016 to 0.12 kPa h^{-1} and decreased filtration time prior to the TMP jump from 280 hours to 48 hours when the flux increased from 10 to 30 L m^{-2} h^{-1}. Under sub-critical conditions, a

decrease in flux from 10 to 2 L m^{-2} h^{-1} caused an exponential decrease in the fouling rate, from 19.8 to 0.46 kPa h^{-1} and prolonged the time before the TMP jump to up to 8 days (Brookes et al., 2006). Results from a pilot scale study suggest that the duration before the TMP jump decreases linearly at fluxes close to the critical flux and that an asymptote exists at a certain flux below which operation can be extended to long filtration cycles (Guglielmi et al., 2007).

Research into immersed AnMBR for municipal wastewater treatment (Table 2-1) has employed a wide range of SGD_m up to 7.2 m^3 m^{-2} h^{-1} (Smith et al., 2013). Similar to AeMBR, optimum hydrodynamic conditions have been identified by increasing gas sparging until a threshold is reached, or the sustainable or critical flux is identified (Martin-Garcia et al., 2011; Martin Garcia et al., 2013; Robles et al., 2012). Robles et al. (2012) observed a linear increase in critical flux from 12 to 19 L m^{-2} h^{-1} when SGD_m was increased from 0.17 to 0.50 m^3 m^{-2} h^{-1}. Martin Garcia et al. (2011) also demonstrated an improvement in critical flux from 3 to 14 L m^{-2} h^{-1} when SGD_m increased from 0.20-0.77 m^3 m^{-2} h^{-1} for a granular AnMBR treating temperate municipal wastewater.

Operational fluxes for AnMBR (Table 2-1) between 2.5 and 25 L m^{-2} h^{-1} have been reported with the higher fluxes achieved using synthetic wastewater (Gouveia et al., 2015a; Wu et al., 2009). Similar to AeMBRs, an increase in membrane flux, albeit below the critical flux, also leads to an increased fouling rate in AnMBRs (Vallero et al., 2005). An increase in gas sparging intensity appears to be effective in extending membrane operation in both AeMBRs and AnMBRs, but does not obviously enhance permeability. For instance, Weinrich and Grélot (2008) reported sustained permeability for an AeMBR of 600 L m^{-2} h^{-1} bar^{-1} for around 2 months at a flux of 25 L m^{-2} h^{-1} and SAD_m 0.20-0.35 m^3 m^{-2} h^{-1}. A SGD_m of 3 m^3 m^{-2} h^{-1} was introduced to sustain permeability of 20 L m^{-2} h^{-1} bar^{-1} (8 L m^{-2} h^{-1}) for an AnMBR over 90 days of operation (Hu and Stuckey, 2006). Robles et al. (2013b) reported sustained permeability above 100 L m^{-2} h^{-1} bar^{-1} in an AnMBR for over 30 days whilst operating at a sub-critical flux of 13.3 L m^{-2} h^{-1} and a SGD_m of 0.33 m^3 m^2 h^{-1}. Three years of AnMBR operation has been reported, by adopting an operating flux of 12 to 14 L m^{-2} h^{-1}, which sustained TMP between 0.35 and 0.6 bar, without extra physical and chemical cleaning required (Gouveia et al., 2015b). Overall the permeability

is still lower than for AeMBRs which for full scale municipal wastewater treatment plants is between 150 and 250 L m^{-2} h^{-1} bar^{-1} (Judd, 2006) even when the quantity of gas provided to the membrane is up 4 times higher and fluxes between 2 and 3 times lower.

2.3.2 Physical and chemical cleaning: Reversible, irreversible and irrecoverable fouling

Membrane fouling can be generally classified as external fouling (cake and gel formation) and internal fouling (pore clogging) (Judd, 2011; Wang et al., 2014). In AeMBRs, cake and gel layer fouling are generally considered to govern membrane fouling (Liu et al., 2012b; Wang et al., 2011). Dominant cake layer resistance has similarly been reported by a number of authors in AnMBR for municipal wastewater (Liu et al., 2012a; Martinez-Sosa et al., 2012; Ozgun et al., 2015b), which is therefore comparable to the general trend for AeMBR. Chu et al. (2005) reported that 90 % of total resistance for an AnMBR corresponded to cake resistance while only 9 % was internal fouling. Choo and Lee (1996) observed substantive accumulation of biosolids at the membrane wall and a notable decline in reactor biomass concentration from 7 to less than 1 g MLSS L^{-1} in 20 days, with a consequent decline in flux of over 90 %. Although the reduction in biomass concentration was attributed to cell lysis induced by shear stress, the major contributors to hydraulic resistance were concentration polarization and cake layer formation (82 and 16 % of total resistance, respectively). Ozgun et al. (2015b) reported that the relative contribution of cake layer resistance in their AnMBR study decreased with a decrease in operating temperature, which suggests transients in the bulk particulate and colloidal characteristics will influence cake deposition.

Resistance to filtration due to membrane fouling can also be classified as reversible, irreversible or irrecoverable depending on whether it can be removed physically during operation (by relaxation or backflushing), chemically or if it remains after chemical cleaning (Judd, 2011). In immersed AeMBRs, physical cleaning procedures like relaxation and backwashing have shown to be effective in extending membrane operation compared to continuous filtration reducing the chemical cleaning frequency (Zhang et al., 2005). By applying physical cleaning procedures, it is possible to apply fluxes that result in an increase of resistance to filtration as long as the cake layer deposited onto the membrane surface can be removed by relaxation or backflushing. For instance,

operational cycles of 10 minutes of filtration followed by one minute relaxation at fluxes between 22.3 and 28.5 L m^{-2} h^{-1}, resulted in fouling rates during filtration cycles of 1.39 and 1.8 mbar min^{-1} respectively, while the irreversible fouling rates were two orders of magnitude lower (Guglielmi et al., 2007). Similarly, in AnMBRs, relaxation and backwashing have also been applied and proved to be effective for membrane fouling mitigation (Table 2-5, Table 2-6). Jeison and van Lier (2006) reported that a 30 s backwash limited hysteresis indicating that cake layer deposition was mostly reversible in both mesophilic and thermophilic conditions. Smith et al. (2013) also showed that a 4 min backwash every 4 h reduced membrane fouling from 0.045 to below 0.001 mbar min^{-1}, with similar observations made for side-stream AnMBR (An et al., 2009). A four times decrease in fouling rate was observed following implementation of backwash at double the permeate flux, which indicates backwash flux specification is also important. Zsirai et al. (2012) reported that backwash was efficient to sustain irreversible fouling below 0.08 mbar min^{-1} in AeMBR. This implies that physical cleaning (relaxation or backwash) can be used to remove the loosely bound cake layer (reversible fraction) but also prevent further increase of strongly bound cake layer (irreversible fraction). van Voorthuizen et al. (2008) also showed that the irreversible fouling rate was sustained by completing the filtration cycle with 1 min relaxation followed by 1 min backflushing at 30 L m^{-2} h^{-1}.

Once a tenacious cake layer is formed, it is hard to remove just with physical cleaning which is evidenced by cake layer growth on membranes exposed to high shear flow (Imasaka et al., 1993) or high shear in combination with relaxation and depressurization (Choo and Lee, 1996). Permeability recovery can be variable following chemical cleaning in both aerobic and anaerobic MBRs, which is illustrative of irrecoverable fouling. Gouveia et al. (2015a) reported a chemical cleaning protocol for an AnMBR comprising 1000 mg L^{-1} sodium hypochlorite (NaClO), which achieved recovery of only 61 % of initial permeability. However, more typically only around 7 to 20 % of the total resistance is regarded irrecoverable following incorporation of chemical cleaning policies in AnMBR (Chu et al., 2005; Dong et al., 2016a; Ozgun et al., 2015b).

Table 2-5. Hydrodynamic conditions and specific energy demand of immersed anaerobic MBRs treating municipal wastewater (real and synthetic).

Source	Reactor type/ Sludge	Material/ Geo./ Pore size	Temp	MLSS	Flux	Filtration cycle			Others	SGD	U_g	Gas sparging cycle			Energy consump.	Ref.
						FI	R	BW				Gas	On	Off		
		µm	°C	g. L^{-1}	L m^{-2} h^{-1}	min	min	min		m^3 m^{-2} h^{-1}	m h^{-1}		min	min	kWh m^{-3}	
Crude[a]	CSTR/F	PVDF/HF/0.05	33	23	12-19	250s	50s	30s[h]	40s V+30s D[j]	0.17-0.5	-	B	Con.		0.10-0.46	Robles et al., 2012
Crude[a]	CSTR/F	PVDF/HF/0.05	20-33	23	10-13.3	250s	50s	30s[h]	40s V+30s D[j]	0.23	-	B	Con.		0.19-0.26	Robles et al., 2013a
Crude[a]	CSTR/F	PVDF/HF/0.05	17-29	10-25	7-11	250s	50s	30s[h]	40s V+40s D[j]	0.23	-	B	Con.		0.23-0.37	Giménez et al., 2014
Crude[b]	CSTR/F	PVDF/HF/0.04	18.9	21.3	10	Con.	-	-	-	1.3	-	B	Con.		2.10[m]	Ruigómez et al., 2016b
Crude[b]	CSTR/F	PVDF/HF/0.04	18.9	21.3	10	Con.	-	-	-	0	-	-	-		2.30[m]	Ruigómez et al., 2016b
Crude[b]	CSTR/F	PVDF/HF/0.04	23	-	17	8	2	4[i]	-	0.146	-	B	Con.		0.10	Dong et al., 2016a
Crude[b]	CSTR/F	PVDF/FS/140[d]	30	6.4-9.3	11	9	1	-	-	0.11	-	B	Con.		0.10	Lin et al., 2011
Crude[c]	IAFMBR	-/HF/0.4	15-35	-	11.3	Con.	-	-	-	0	-	-	-		-	Gao et al., 2014a, 2014b
Crude (GA)	CSTR/F	PES/FS/0.038	20	9.5-14.7	7	10	0.5	1	-	-	62	B	Con.		-	Martinez-Sosa et al., 2012
Black	UASB/G	PVDF/Tub/250[d]	37	-	10[f]	8	1	1	-	-	8-16	-	Con.		-	van Voorthuizen et al., 2008
Black	CSTR	PVDF/Tub/250[d]	37	-	8[f]	8	1	1	-	-	40	-	Con.		-	van Voorthuizen et al., 2008
Settled	UASB/G	PVDF/HF/0.04	10-25	0.1-0.6	6[f]	10	-	1	-	1.17	148	N	10s	10s	0.88	Martin Garcia et al., 2013
Settled	UASB/G	PVDF/HF/0.04	10-25	0.1-0.6	6[f]	10	-	1	-	1.17	148	N	1	10	0.16	Martin Garcia et al., 2013
Settled	UASB/F	PVDF/HF/0.045	18	5.95[e]	10-14	7.5	5s	15s	5s R	0.32-0.48[k]	40-60	B	Con.		0.26-0.39	Gouveia et al., 2015a
Settled	UASB/G	PVDF/HF/0.045	18	2[e]	8	15	10s	1	10s R	0.07[k]	9	B	Con.		0.09	Gouveia et al., 2015b
Settled	CSTR/F	PVDF/HF/0.08	10-25	7.7	6[f]	10	-	1	-	0.39	277	N	10s	10s	0.29	Martin Garcia et al., 2013
Settled	SAF-MBR/F	PVDF/HF/0.03	8-30	-	5.1-6.2[f]	30	5	-	-	0	-	-	-		0.23[m]	Shin et al., 2014
Synthetic	UASB/G	PVDF/Tub/100[d]	21-24	-	4.2	10	1	-	-	5.29	-	N	1	10	1.13	Cerón-Vivas et al., 2012
Synthetic	UASB/G	PVDF/Tub/100[d]	21-24	-	5.2	4	1	-	-	5.29	-	N	1	4	2.27	Cerón-Vivas et al., 2012
Synthetic	CSTR/F	PS/Tub/0.2	55	25-50	16-23	10	-	0.5	-	0.29-1.02[l]	12-42	B	Con.		0.12-0.63	Jeison and van Lier, 2006
Synthetic	CSTR/F	PS/Tub/0.2	30	25-50	5-21	10	-	0.5	-	0.85-1.70[l]	35-70	B	Con.		0.40-3.35	Jeison and van Lier, 2006
Synthetic	CSTR/F	PE/FS/0.4	35	-	5-8	Con.	-	-	-	3	-	B	10	5	2.2-3.6	Vyrides and Stuckey, 2009
Synthetic	CSTR/F	PE/FS/0.4	35	-	5-8	Con.	-	-	-	3	-	B	Con.		3.4-5.4	Vyrides and Stuckey, 2009
Synthetic	CSTR/F	PE/FS/0.4	-	-	7.2	Con.	-	-	-	2.4	-	B	Con.		3.0	Fox and Stuckey, 2015
Synthetic	CSTR/F	PES/FS/0.2	15	-	7	30 (240)[g]	-	0.5 (4)[g]	-	7.24	14	B	Con.		9.6	Smith et al., 2013
Synthetic	CSTR/F	PES/FS/0.2	3-15	-	1.2-12	5	-	1	-	5.8	-	B	Con.		6.5-64.8	Smith et al., 2015
Synthetic	ARMBR	PE/FS/0.2	30	5.5	11	8	2	-	-	0	-	-	-		0.10[m]	Kim et al., 2014
Synthetic	ABR+AFMR	PVDF/HF/0.1	35	-	7-10	Con.	-	-	-	0	-	-	-		0.058[m]	Kim et al., 2011

a. Crude: pre-treatment including screening, degritter and grease removal; b. Crude: after screening; c. Crude- from septic tank; d MWCO (kDa); e. Reported MLVSS; f.Net flux; g. values in the bracket are the second filtration conditions; h. backwash 30s every 50min; i. backwash weekly with chemicals; j. 40s Ventilation every 50min, 30s degasification every 250min; k. ZW-10 module, use membrane cross-sectional area of 74cm^2 (Martin-Garcia et al., 2013); l. Assume 50% of the membrane package ratio and membrane mount area is double size of the membrane fibre cross-sectional area; m. Energy demand provided in the paper.

Acronyms: ABR+AFMBR- anaerobic baffle reactor + anaerobic fluidised bed membrane bioreactor; ARMBR- anaerobic rotate disk membrane bioreactor; AT-ambient temperature; B-biogas; BW-backwash; CSTR- completely stirred tank reactor; F-flocculent sludge; FI-filtration; FS-flat sheet; G-granular sludge; GA-glucose addition; HF-hollow fibre; IAFMBR- integrated anaerobic fluidised-bed; MWCO-molecular weight cut off; N- Nitrogen; PE- Polyethylene; PVDF-Polyvinylidene fluoride; R-relaxation; SAF-MBR-staged anaerobic fluidised membrane bioreactor; Tub-tubular; UASB-upflow anaerobic sludge blanket

Table 2-6. Overview of operating conditions and membrane performance in side-stream anaerobic MBRs.

Source	Reactor type/ Sludge	Temp	Material/Geo./ Pore size	Mode	MLSS	CFV[a]	U_g[b]	J_c	Flux	TMP	Fouling rate			T_{OP}	Filtration cycle			Ref.
		°C	µm		g L^{-1}	m s^{-1}	m s^{-1}	L $m^{-2}h^{-1}$	L $m^{-2}h^{-1}$	kPa	mbar min^{-1} [c]	kPa h^{-1} [c]	L $m^{-2}h^{-1}$ d^{-1} [d]	h	FI (min)	R (min)	BW (min)	
Industrial [e]	CSTR	53-55	-/-/20[i]	Pumped	0.3-3.0[j]	0.2-1.0	-	-	10-70	100-200	-	-	-	4800		Dep +relax [k]		[1]
Crude	UASB/F	4	PAN/Tub/-	Pumped	-	0.4	-	-	10.5	<50	0.067	0.400	-	<125	Con.	-	-	[2]
Crude	UASB/F	4	PAN/Tub/-	Pumped	-	0.4	-	-	10.5	<50	0.040	0.238	-	<210	10	20s	-	[2]
Crude	UASB/F	4	PAN/Tub/-	Pumped	-	0.4	-	-	10.5	<15	<0.001	0.007	-	2150	10	-	20s	[2]
Crude	UASB	22	PVDF/Tub/100[i]	Pumped	-	2.25	-	-	45-50	-	-	-	-	-	Con.	-	-	[3]
Crude	CSTR	37	-/-/100[i]	Pumped	0.5-10[j]	3	-	-	9-13	100-200	-	-	0.056	4080	Con.	-	-	[4]
Settled	UASB/G	-	PVDF/Tub/0.03	Pumped	-	0.4-2.0	-	4-41	-	-	-	-	-	-	Con.	-	-	[5]
Settled	UASB/G	-	PVDF/Tub/0.03	Gas-lift	-	-	0.02-0.14	4	11-12	-	1-2	6-12	-	-	Con.	-	-	[5]
Settled	CSTR/F	-	PVDF/Tub/0.03	Pumped	-	0.4-2.0	-	4-19	-	-	-	-	-	-	Con.	-	-	[5]
Settled	CSTR/F	-	PVDF/Tub/0.03	Gas-lift	-	-	0.02-0.14	4	11-12	-	8-25	48-150	-	-	Con.	-	-	[5]
Settled	CSTR/G	12-35	PE/Tub/0.1	Pumped	5	0.7	-	-	9-20	-	0.001-0.002	0.004-0.011		-	Con.	-	-	[6]
Synthetic	UASB/F	-	PVDF/Tub/100[i]	Pumped	-	2	-	-	-	103.4	-	-		<6.7	Con.	-	-	[7]
Synthetic [f]	UASB	-	PVDF/-/0.22	Pumped	0.3-0.55	0.93	-	50	30	<40	0.008-0.042	0.05-0.25	-	>400	Con.	-	-	[8]
Synthetic	UASB/F	25	PES/Tub/0.03	Pumped	0.5	1	-	-	12.3	8.7	-	-	-	-	Con.	-	-	[9]
Synthetic	UASB/F	25	PES/Tub/0.03	Pumped	0.3-0.5	1	-	41-70	12.3	<150	0.001-0.003	0.008-0.021	-	720	3	-	20s	[10]
Synthetic	UASB/F	15	PES/Tub/0.03	Pumped	0.3-0.5	1	-	34-41	12.3	<450	0.003-0.009	0.017-0.055	-	720	3	-	20s	[10]
Synthetic [g]	CSTR	55	Ceramic/Tub/0.2	Pumped	-	1-1.5	0.1	-	20	-	-	-	-	-	5	-	20s	[11]
Synthetic [h]	CSTR	35	Ceramic/Tub/0.2	Pumped	-	2	-	-	14-19	40-50	-	-	-	1680	Con.	-	-	[12]
Synthetic	CSTR/F	35	PS/PF/3000[i]	Pumped	15[j]	0.8	-	-	21-75	49	-	-	1.9-9.2	168-240	Con.	-	-	[13]
Synthetic	CSTR	35	Ceramic/0.2	Pumped	1.6-22	2	-	-	25-65	35	-	-	-	120	Con.	-	-	[14]
Synthetic	CSTR/F	25	PTFE/Tub/1	Pumped	6-12	0.1-0.2	-	-	5	7-55	-	-	-	-	Con.	-	-	[15]
Synthetic	CSTR/F	35	PVDF/HF/0.03	Pumped	6	0.1-0.3	-	10-12.5	6	<5	0.200	1.2	-	2160	9	1	-	[16]

a. Liquid cross flow velocity; b. Gas scouring rate; c. Fouling rate under constant flux; d. Permeate drop down (fouling rate under constant transmembrane pressure); e. Alcohol-distillery wastewater; f. Not mention synthetic, but assume according to the influent characteristics; g. VFA mixed; h. Synthetic wastewater containing starch; i. MWCO (kDa); j. Reported MLVSS; k. Depressurisation (down to about 0.3bar) + relaxation (flow stopping)

Acronyms: BW-backwash; CSTR- completely stirred tank reactor; F-flocculent sludge; FI-filtration; G-granular sludge; MWCO-molecular weight cut off; Tub-Tubular; PAN- polyacrylonitrile; PE- polyethylene; PF-flat and plate; PES-polyethersulphone; PTFE-poly-tetrafluoroethylene; PVDF-Polyvinylidene fluoride; R-relaxation; UASB-upflow anaerobic sludge blanket

Reference:

[1] Choo and Lee, 1996; [2] An et al., 2009; [3] Herrera-Robledo et al., 2011; [4] Saddoud et al., 2007 [5] Martin-Garcia et al., 2011; [6] Fawehinmi, 2006; [7] Salazar-Peláez et al., 2011; [8] Cho and Fane, 2002; [9] Ozgun et al., 2015a; [10]Ozgun et al., 2015b; [11] Jeison et al., 2009; [12] Cadi et al., 1994; [13] Harada et al., 1994;[14] Beaubien et al., 1996; [15] Ho and Sung, 2009; [16] Wei et al., 2014.

2.4 Establishing the energy profile of AnMBR for municipal application

2.4.1 Towards energy neutral wastewater treatment

The key facet that drives commercial interest for AnMBR is in the potential to achieve energy neutral wastewater treatment through a reduction in net energy demand for treatment, coupled with an increase in total biogas production, without having to rely on sludge imports (McAdam et al., 2011). Several flowsheets have been proposed for how to incorporate AnMBR technology. In the upstream, the decision must be made as to whether primary sedimentation is introduced to divert particulate COD toward anaerobic digestion, leaving only settled wastewater to be processed by AnMBR (McAdam et al., 2011) or whether the full organic load (crude wastewater) is to be treated within the AnMBR (Giménez et al., 2011; Robles et al., 2013a, 2013b). Downstream of the AnMBR, the decision to have biological (Eusebi et al., 2013) or physical separation processes for polishing and nutrient removal is a further consideration (McAdam et al., 2011; Sutton et al., 2011). The merit of these various approaches is beyond the scope of this review. Nevertheless, it is implicit in each of these cases that the AnMBR itself needs to be energy neutral, or better, energy positive (to provide residual energy for the ancillary processes), if overall energy-neutrality is to be achieved.

Typical headspace methane yield from the literature is between 0.02 and 0.27 L $CH_4 \cdot g\ COD^{-1}$ for both settled and crude wastewater (Table 2-7). This is below the expected stoichiometric conversion of 0.35 L $CH_4 \cdot g\ COD^{-1}$. The difference between measured and expected values can be explained by: (i) the fact that yield does not take into consideration the solids which are retained (and accumulate) within the bioreactor (Lester et al., 2013; Uemura and Harada, 2000); (ii) differences in HRT or organic loading rate (OLR) between literature studies which can influence specific yield, and (iii) the dissolved methane fraction which is released with the AnMBR effluent. Several studies have now demonstrated this dissolved fraction can comprise over 50 % of the methane balance (Cookney et al., 2012; Hartley and Lant, 2006), with losses exacerbated at lower temperature (Cookney et al., 2016). Downstream membrane technology has been demonstrated that can recover this fraction (Bandara et al., 2011; Cookney et al., 2016) in sufficient concentration for reuse in power generation (McLeod et al., 2016).

Collectively the average dissolved and headspace methane yield from the literature provides around 0.34 kWh m^{-3} of permeate produced (0.80 kWh m^{-3} maximum), which is comparable to the typical energy consumption of membrane operation in full-scale AeMBR (0.19-0.70 kWh m^{-3}) (Itokawa et al., 2014; Judd, 2011; Krzeminski et al., 2012). Consequently, the specific energy demand for AnMBR membrane operation must be towards the low energy demand range of conventional AeMBR to achieve 'energy-neutral' conditions. Comparison of specific energy production with membrane energy demand estimated from published AnMBR literature (Figure 2-1) demonstrates that several AnMBR studies can achieve membrane operation within 'energy-neutral' conditions (Figure 2-2). Since the shear promoted at laboratory scale is generally a conservative estimate of that attained at scale (Delgado et al., 2004), such evidence is encouraging. Whilst many studies have sought to optimise hydrodynamics to lower energy (Cerón-Vivas et al., 2012; Martin-Garcia et al., 2011; Martin Garcia et al., 2013; Seib et al., 2016), an explicit focus on achieving energy neutral membrane operation would facilitate further improvements toward this goal.

Table 2-7. Biogas production from anaerobic MBRs treating municipal wastewater (real and synthetic).

Source	Volume		Inf. COD (BOD/ COD)	SO_4^{2-}		COD[a]	OLR[b]	Temp	HRT[c]		CH_4	CH_4 production (Normalised to STP)			Dissolved CH_4 (Normalised to STP)		Total CH_4[e]	Ref.
	RE.	FI.		Inf.	Eff.				RE.	FI.								
	L		mg L^{-1}	mg L^{-1}		%	kg COD $m^{-3}d^{-1}$	°C	h		%	L CH_4 $gCOD_{rem}^{-1}$[d]	L CH_4 m^{-3}	kWh m^{-3}	L CH_4 m^{-3}	kWh m^{-3}	kWh m^{-3}	
Crude[f]	17.7[n]		98-2600	-	-	97	0.5-12.5	14-25	4-6		53-66	0.02-0.06	25-82	0.10-0.33	20.0[x]	0.080	0.18-0.41	Wen et al., 1999
Crude	34		58-348	-	-	(77-81)	0.3-0.9	4	5.5-10	-	59-64	0.04-0.07[s]	5.5-10.8	0.02-0.04	27.9[x]	0.111	0.13-0.15	An et al., 2009
Crude[g]	1300	800	445	297	5	87	0.9-3.0	33	6-21		55	0.06[s]	22.8	0.10	17.2[w]	0.069	0.160	Giménez et al., 2011
Crude[g]	1300	800	445	297	5	87	0.9-3.0	33	6-21		55	0.26[s,t]	-	-	17.2[w]	0.069	>0.160	Giménez et al., 2011
Crude[g]	1300	800	468-598	300-343[o]	-	90-94	0.6-1.9	17-29	12.1-28.4		-	0.001-0.05	0.7-22.1	0.003-0.088	7.1-10.2[w]	0.03-0.04	0.03-0.12	Giménez et al., 2014
Crude[g]	1300	800	650	315	-	-	-	17-33	-	-	-	-	1.3-23.6[s]	0.005-0.095	6.7-13.0[w]	0.03-0.05	0.03-0.15	Pretel et al., 2014
Crude[f]	550	80	304-388	50-55	-	88-92	1.1	23	8.5		35	0.04-0.07	14-19	0.06-0.08	13.3[w]	0.053	0.11-0.13	Dong et al., 2016b
Crude[f]	60		342-527	-	-	90	1.0	30	10		75-85	0.22[s]	83	0.331	22.3[x]	0.089	0.420	Lin et al., 2011
Crude[h]	5.8		247-449	-	-	51-74	1.2-1.4	15-35	6		-	0.13-0.17[s]	23.6-43.4	0.09-0.17	-	-	>0.09-0.17	Gao et al., 2014a
Crude[i]	350	-	630 (0.63)	-	-	82,90	0.6-1.1	20,35	14.3		88,80	0.23-0.27[s]	127-149	0.506-0.594	29,21[x]	0.12,0.08	0.62-0.68	Martinez-Sosa et al.,2011
Set[j]	160	150	892 (0.64)	47	-	74-90	0.8-2.6	18	13-17	-	80-83	0.14-0.26	57-285	0.23-1.14	28.6[x]	0.114	0.31-1.25	Gouveia et al., 2015a
Set[j]	326	175	978 (0.48)	47	-	75-90	0.6-3.2	18	10-15	-	81-83	0.11-0.19	25-191	0.16-0.76	28.6[w]	0.114	0.21-0.88	Gouveia et al., 2015b
Set	42.5	30	265	-	-	93	0.2-0.6	14	12		-	0.004	1.0	0.004	13.0[w]	0.052	0.056	Cookney et al., 2016
Set	5	1	427	-	-	84-86	1.0	25-30	10		-	0.04-0.10	14-38	0.06-0.15	-	-	>0.06-0.15	Huang et al., 2013
Set[l,m]	0.25	0.25	154 (0.57)	-	-	84	4-6 (1.3)[q]	25	1	1.3	-	-	-	0.03[v]	-	0.05-0.06[v]	0.08-0.10[v]	Bae et al., 2013
Set[l]	0.25	0.25	154 (0.57)	63	0	84	3.5 (1.2)[q]	25	1	1.3	40 (54)[r]	0.05	9.1	0.04	15.8[w]	0.063	0.099	Yoo et al., 2012
Set	990	770	233 (0.50)	41	7	91-93	2.5-3.0	9-25	2	2.6	-	0.09-0.13	17-31	0.07-0.12	12-27[w]	0.05-0.11	0.17-0.18	Shin et al., 2014
Syn	4.7[n]		383-849	-	-	85-96	1.6-4.5	11-25	3.5-5.7		63-72	0.06-0.12	32-66	0.13-0.27	23.5[x]	0.09-0.10	0.22-0.35	Chu et al., 2005
Syn	30[n]		390	-	-	89[p]	0.78	35	12		81.2	-	26.3	0.105	20.8[x]	0.083	0.189	An et al., 2010
Syn	5[n]		440	-	-	92	0.7	15	16		-	0.05-0.13	20-53	0.08-0.21	29.1[w]	0.09-0.14	0.20-0.33	Smith et al., 2013
Syn	3[n]		460	-	-	90-95	0.2-3.7	35	3-48		60-70	0.20-0.29[s]	83-125	0.33-0.50	16.7[x]	0.067	0.40-0.57	Hu et al., 2006
Syn	2	-	400	-	-	98	0.8-1.6	35	6-12		80-90	0.08-0.12[s]	30-47	0.12-0.19	-	0.055	0.18-0.24	Wei et al., 2014
Syn	4	-	500	60-90	-	>90	1.0-2.0	25	6-12		70-75	0.19-0.20[s]	89-93	0.35-0.37	21[w]	0.084	>0.44-0.46	Ho and Sung, 2009
Syn	3.93	2	513	-	-	99 (88)	4-6	-	35	2-3	-	86	0.18	92[u]	0.368	40[w]	0.159	0.527	Kim et al., 2011
Syn	4[n]		342	-	-	96	-	30	-		68	0.14[s]	-	0.144[v]	19.0[x]	0.076	0.220	Kim et al., 2014

a. The values in bracket means the biological reactor removal; b. Organic loading rate of anaerobic reactor; c. Split tables showed the HRT of biological reactor and membrane tank, combined tables showed the HRT of whole AnMBR; d. LCH_4 $gCOD^{-1}$ removed based on CODt influent and CODt permeate; e. Assume 1 m^3 CH_4 can generate 10 kWh of energy and combined heat and power (CHP) engine efficiency is 40 % CH_4; f. Crude: after screening; g. Crude: pre-treatment including screening, degritter and grease removal; h. Crude: from septic tank; i. Crude wastewater with glucose addition; j. With recirculation; l. Settled sewage go through 10 μm cartridge filter; m. Settled sewage go through 1 mm screen; n. Membrane submerged in the anaerobic reactor; o. Reported as SO_4^{2-}-S; p. TOC removal; q. OLR for AFBF (OLR of AFMBR); r. CH_4 composition in SAF (membrane tank); s. Directly reported from literature; t. Calculate the methane yield on CODt used for methanogenesis bacterium by subtracting the CODt removed for sulphate reduction bacterium (Giménez et al., 2012; Lens et al., 1998); u. Only consider the methane from AFBR; v. Directly reported the energy production; w. Literature reported the dissolved CH_4 (directly test or estimate from Henry's law); x. Use Henry's law to for dissolved CH_4 calculation (assume saturation index is 1.00) (Giménez et al., 2012)

Acronyms: Eff- Effluent; FI- filtration section; Inf-Influent; RE. Anaerobic reactor; Set-settled; STP, standard temperature and pressure, 0°C and 1bar; Syn-Synthetic

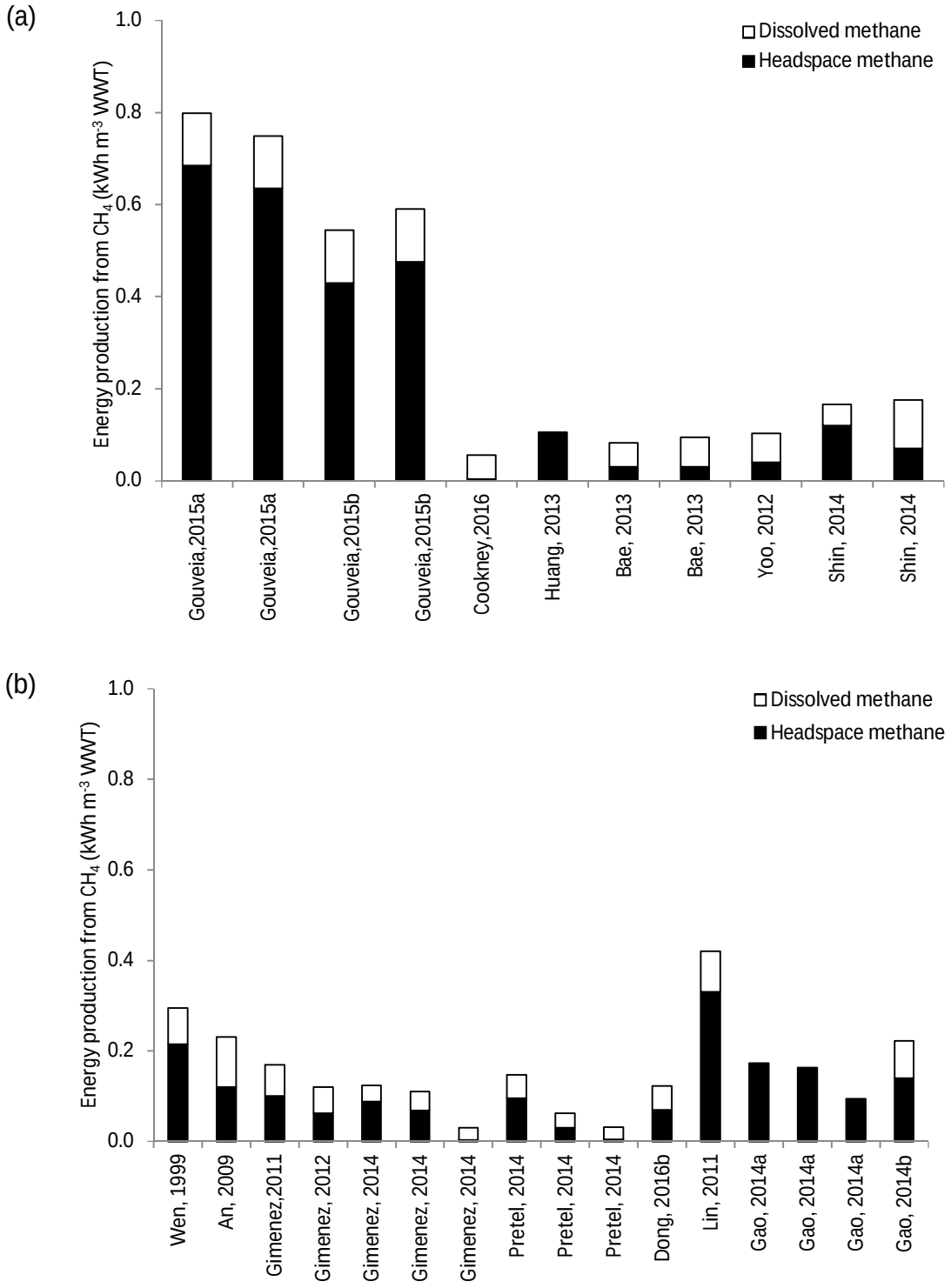

Figure 2-1. Combined headspace and dissolved methane production rates from anaerobic MBR treating: (a) settled sewage; and (b) crude sewage. Where dissolved methane data was not provided, the dissolved fraction was estimated using Henry's law. Energy data was normalised assuming 40 % CHP conversion efficiency.

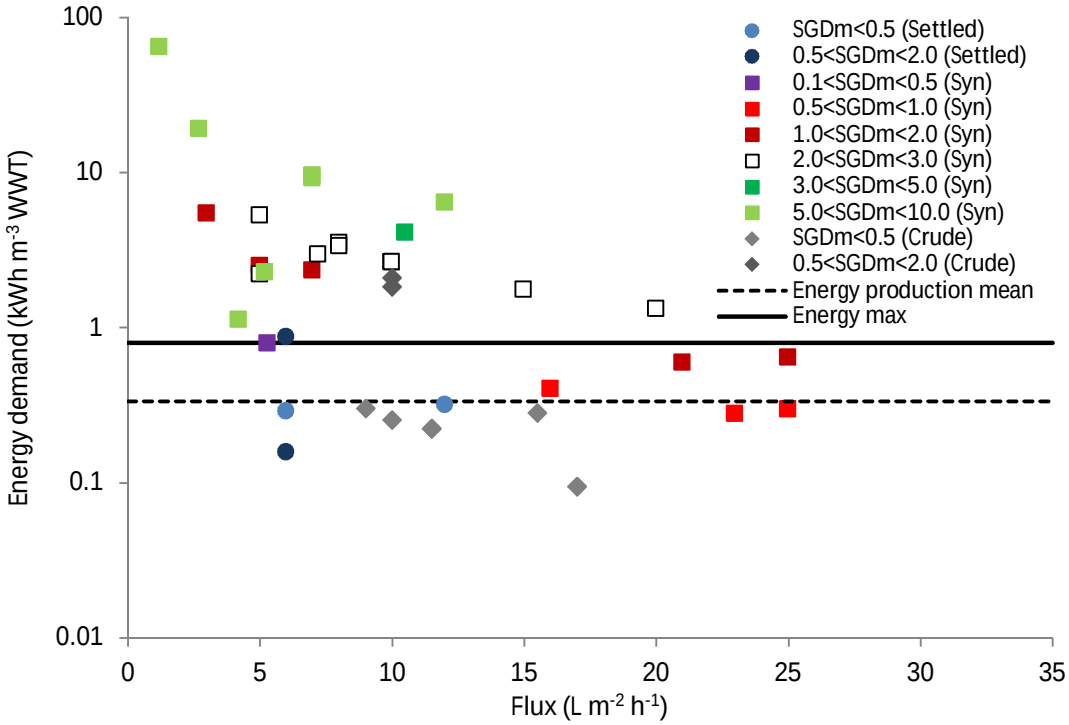

Figure 2-2. Comparison of membrane energy demand to the average (0.34 kWh m^{-3}, dashed line) and maximum (0.80 kWh m^{-3}, continuous line) energy production reported in the literature to date for anaerobic MBR treating settled wastewater.

2.4.2 Emerging engineered solutions to constrain energy demand within AnMBR

Several authors have now directly compared different AnMBR reactor configurations, and have identified that when configured as an UASB, membrane fouling and energy demand is constrained (Martin-Garcia et al., 2011; van Voorthuizen et al., 2008). The authors ascribed the enhanced performance to the lower particle concentration within the downstream membrane tank (Martin-Garcia et al., 2011). Martin-Garcia et al. (2011) also screened a host of membrane geometries and were able to demonstrate a specific gas demand of 0.3 kWh m^{-3} for immersed hollow fibre membranes compared to 3.7 kWh m^{-3} for externally configured membranes. It has been shown that further reduction in specific energy demand can be attained for immersed membranes through inclusion of novel gas sparging strategies (Cerón-Vivas et al., 2012; Martin Garcia et al., 2013; McAdam et al., 2011).

Shin et al. (2016) introduced the anaerobic fluidised bed MBR which incorporates granular activated carbon (GAC) into the reactor to scour the membrane. Significantly, the authors demonstrated that sustainable fluxes could be achieved with an immersed

membrane without the need for gas sparging, provided a critical upflow velocity could be achieved to sufficiently fluidise the GAC (Wang et al., 2017). Kim et al. (2011) reported a specific energy demand of 0.028 kWh m^{-3} for this configuration, which evidences a substantial energy reduction when compared to classically commercially configured aerobic MBR technology. One of the future challenges with GAC is to identify a compatible membrane that can withstand the abrasion introduced by the GAC (Shin et al., 2016; Wang et al., 2017). Ruigómez et al. (2016a, 2016b) integrated rotating membrane technology into a CSTR configuration, as an alternative method of shear (Zsirai et al., 2016). The authors demonstrated an improvement in critical flux with membrane rotation when compared to conventional gas sparging; specific energy demand for disk rotation is around 0.104 kWh m^{-3} (Kim et al., 2014).

Within the context of scaling-up AnMBR, membrane cost must also be considered as the sustainable fluxes identified at present of around 10 L m^{-2} h^{-1} (Table 2-1), are markedly below those nominally achieved in commercial AeMBR. For large scale installations, investment decisions are strongly influenced by initial capital investment. As such, there is a need to establish new paradigms that can access cost efficient water productivities whilst still delivering to the energy neutral objective. One innovative example is anaerobic dynamic membrane bioreactors (Alibardi et al., 2014; Ersahin et al., 2016) which employ woven and non-woven filter substrates as a low cost alternative (less than 13 € m^{-2} (Ersahin et al., 2016)) to conventional polymeric membranes. Mesh sizes of 10 to 200 µm have been tested which provide substantial clean water permeability. The developed cake provides the rejection (Alibardi et al., 2014) with >99 % COD rejection noted for several prospective applications, coupled with sustainable fluxes, which evidences their considerable potential to making AnMBR both capitally and energetically efficient (Alibardi et al., 2014; Ersahin et al., 2016).

2.5 Conclusions

The present literature review reveals significant differences with respect to biomass characteristics and fouling behavior between aerobic and anaerobic MBRs which can be summarized as follows:

- The ratio of proteins to carbohydrates in eEPS is higher in AnMBRs than in AeMBRs.

However, the total eEPS appears slightly higher in AeMBR. There is a general lack of knowledge regarding the relationship between eEPS concentration and composition and surface properties such as charge and hydrophobicity for AnMBR.

- Although similar median particle sizes have been reported in aerobic and anaerobic MBRs, the presence of a population of fine solids with particle sizes ranging from 1 to 10-15 microns have been widely reported in the latter and associated to biomass of high fouling propensity.
- The SMP_{COD} concentration contained within bulk sludge is an order of magnitude higher in AnMBR than in AeMBR. The main operational parameters that have shown to enhance SMP production in AnMBRs are low temperature and extended SRT.
- The effect of turbulent gas sparging on membrane performance in immersed AnMBRs seems to be limited as compared to aerobic systems, indicating that fouling is more determined by sludge properties than by membrane operational conditions.
- AnMBR fluxes are between one-third and one-half of those reported in AeMBRs. Reported permeabilities in AnMBR are around 50 % below those of AeMBR and employ specific gas demands between 50 % and 300 % higher.
- Although as with aerobic systems the predominant fouling mechanism in AnMBRs has been reported to be cake filtration, contradictory results with respect to the effectiveness of membrane backwashing at reducing membrane fouling and permeability recovery after chemical cleaning have been reported and would require further research.
- Whilst membrane fouling remains a critical challenge, several research groups have already demonstrated the potential to achieve energy self-sustained conditions at pilot scale. Whilst AeMBR is comparatively mature, continued investment in commercial module and aeration (gas scouring) engineering, is still enabling radical reductions in specific energy demand to be realised at scale. Consequently, the potential to achieve energy neutral wastewater treatment at a commercial scale appears inherently viable.

This literature review indicates a more challenging bulk sludge matrix in AnMBR than AeMBR, leading to high operational cost of energy demand for fouling control and high capital cost of membrane investments due to low attainable flux in AnMBR. Therefore, more research is warranted in order to overcome these limitations of the full-scale AnMBR application for municipal wastewater treatment and ultimately achieve the energy neutral sewage treatment as the main ambitious of AnMBR technology: (i) low energy demand membrane fouling control strategies to increase attainable flux and reduce energy demand of AnMBR, therefore reduce both the capital and operational costs of AnMBR; (ii) cost-effective membrane such as anaerobic dynamic membrane to reduce the membrane capital investment; and (iii) low energy demand dissolved methane recovery technologies from the permeate of AnMBR to enhance the energy recovery.

2.6 Acknowledgements

The authors would also like to thank our industrial sponsors Severn Trent Water, Yorkshire Water, Thames Water, Anglian Water and Scottish Water for their financial and technical support. Dr. Martin-Garcia was supported by a Marie Curie Early Stage Research Training Fellowship of the European Community's Sixth Framework Programme under contract number MEST-CT-2005-021050.

2.7 References

Achilli, A., Marchand, E.A. and Childress, A.E. (2011) 'A performance evaluation of three membrane bioreactor systems: aerobic, anaerobic, and attached-growth', *Water Science & Technology*, 63, pp. 2999–3005.

Akram, A. and Stuckey, D.C. (2008) 'Flux and performance improvement in a submerged anaerobic membrane bioreactor (SAMBR) using powdered activated carbon (PAC)', *Process Biochemistry*, 43, pp. 93–102.

Alibardi, L., Cossu, R., Saleem, M. and Spagni, A. (2014) 'Development and permeability of a dynamic membrane for anaerobic wastewater treatment', *Bioresource Technology*, 161, pp. 236–244.

An, Y., Wu, B., Wong, F.S. and Yang, F. (2010) 'Post-treatment of upflow anaerobic sludge blanket effluent by combining the membrane filtration process: Fouling control by intermittent permeation and air sparging', *Water and Environment Journal*, 24, pp. 32–38.

An, Y., Yang, F., Bucciali, B. and Wong, F. (2009) 'Municipal wastewater treatment using a UASB coupled with cross-flow membrane filtration', *Journal of Environmental Engineering*, 135, pp. 86–91.

Aquino, S.F., Hu, A.Y., Akram, A. and Stuckey, D. (2006) 'Characterization of dissolved compounds in submerged anaerobic membrane bioreactors (SAMBSs)', *Journal of Chemical Technology and Biotechnology*, 81, pp. 1894–1904.

Bae, J., Shin, C., Lee, E., Kim, J. and McCarty, P.L. (2014) 'Anaerobic treatment of low-strength wastewater: A comparison between single and staged anaerobic fluidized bed membrane bioreactors', *Bioresource Technology*, 165, pp. 75–80.

Bae, J., Yoo, R., Lee, E. and McCarty, P.L. (2013) 'Two-stage anaerobic fluidized-bed membrane bioreactor treatment of settled domestic wastewater', *Water Science & Technology*, 68, pp. 394–399.

Baek, S. and Pagilla, K.R. (2006) 'Aerobic and anaerobic membrane bioreactors for municipal wastewater treatment', *Water Environment Research*, 78, pp. 133–140.

Bailey, A.D., Hansford, G.S. and Dold, P.L. (1994) 'The enhancement of upflow anaerobic sludge bed reactor performance using crossflow microfiltration', *Water Research*, 28, pp. 291–295.

Bandara, W.M.K.R.T.W., Satoh, H., Sasakawa, M., Nakahara, Y., Takahashi, M. and Okabe, S. (2011) 'Removal of residual dissolved methane gas in an upflow anaerobic sludge blanket reactor treating low-strength wastewater at low temperature with degassing membrane', *Water Research*, 45, pp. 3533–3540.

Barker, D.J. and Stuckey, D.C. (1999) 'A review of soluble microbial products (SMP) in wastewater treatment systems', *Water Research*, 33, pp. 3063–3082.

Batstone, D.J. (2006) 'Mathematical modelling of anaerobic reactors treating domestic wastewater: Rational criteria for model use', *Reviews in Environmental Science and Biotechnology*, 5, pp. 57–71.

Beaubien, A., Bâty, M., Jeannot, F., Francoeur, E. and Manem, J. (1996) 'Design and operation of anaerobic membrane bioreactors: development of a filtration testing strategy', *Journal of Membrane Science*, 109, pp. 173–184.

Bella, G.D., Torregrossa, M. and Viviani, G. (2011) 'The role of EPS concentration in MBR foaming: Analysis of a submerged pilot plant', *Bioresource Technology*, 102, pp. 1628–1635.

Brockmann, M. and Seyfried, C.F. (1997) 'Sludge activity under the conditions of crossflow microfiltration', *Water Science & Technology*, 35, pp. 173–181.

Brookes, A., Jefferson, B., Guglielmi, G. and Judd, S.J. (2006) 'Sustainable flux fouling in a membrane bioreactor: impact of flux and MLSS', *Separation Science and Technology*, 41, pp. 1279–1291.

Cadi, Z., Huyard, H., Manem, J. and Moletta, R. (1994) 'Anaerobic digestion of a synthetic wastewater containing starch by a membrane reactor', *Environmental Technology*, 15, pp. 1029–1039.

Cerón-Vivas, A., Morgan-Sagastume, J.M. and Noyola, A. (2012) 'Intermittent filtration and gas bubbling for fouling reduction in anaerobic membrane bioreactors', *Journal of Membrane Science*, 423–424, pp. 136–142.

Chang, I.S., Le Clech, P., Jefferson, B. and Judd, S. (2002) 'Membrane fouling in membrane bioreactors for wastewater treatment', *Journal of Environmental Engineering*, 128, pp. 1018–1029.

Chen, W., Liu, Y. and Liu, J. (2016) 'Selecting aeration in a PVDF flat-sheet membrane bioreactor for municipal wastewater treatment', *Desalination and Water Treatment*, 57, pp. 6193–6201.

Cho, B.D. and Fane, A.G. (2002) 'Fouling transients in nominally sub-critical flux operation of a membrane bioreactor', *Journal of Membrane Science*, 209, pp. 391–403.

Choo, K.H. and Lee, C.H. (1998) 'Hydrodynamic behavior of anaerobic biosolids during crossflow filtration in the membrane anaerobic bioreactor', *Water Research*, 32, pp. 3387–3397.

Choo, K.H. and Lee, C.H. (1996) 'Membrane fouling mechanisms in the membrane-coupled anaerobic bioreactor', *Water Research*, 30, pp. 1771–1780.

Chu, L.B., Yang, F.L. and Zhang, X.W. (2005) 'Anaerobic treatment of domestic wastewater in a membrane-coupled expended granular sludge bed (EGSB) reactor under moderate to low temperature', *Process Biochemistry*, 40, pp. 1063–1070.

Cookney, J., Cartmell, E., Jefferson, B. and McAdam, E.J. (2012) 'Recovery of methane from anaerobic process effluent using poly-di-methyl-siloxane membrane contactors', *Water Science & Technology*, 65, pp. 604–610.

Cookney, J., Mcleod, A., Mathioudakis, V., Ncube, P., Soares, A., Jefferson, B. and McAdam, E.J. (2016) 'Dissolved methane recovery from anaerobic effluents using hollow fibre membrane contactors', *Journal of Membrane Science*, 502, pp. 141–150.

Defrance, L., Jaffrin, M.Y., Gupta, B., Paullier, P. and Geaugey, V. (2000) 'Contribution of various constituents of activated sludge to membrane bioreactor fouling', *Bioresource Technology*, 73, pp. 105–112.

Delgado, S., Díaz, F., Vera, L., Díaz, R. and Elmaleh, S. (2004) 'Modelling hollow-fibre ultrafiltration of biologically treated wastewater with and without gas sparging', *Journal of Membrane Science*, 228, pp. 55–63.

Dong, Q., Parker, W. and Dagnew, M. (2015) 'Impact of FeCl3 dosing on AnMBR treatment of municipal wastewater.', *Water Research*, 80, pp. 281–293.

Dong, Q., Parker, W. and Dagnew, M. (2016a) 'Long term performance of membranes in an anaerobic membrane bioreactor treating municipal wastewater', *Chemosphere*, 144, pp. 249–256.

Dong, Q., Parker, W. and Dagnew, M. (2016b) 'Influence of SRT and HRT on bioprocess performance in anaerobic membrane bioreactors treating municipal wastewater', *Water Environment Research*, 88, pp. 158–167.

Drews, A., Lee, C.H. and Kraume, M. (2006) 'Membrane fouling - a review on the role of EPS', *Desalination*, 200, pp. 186–188.

Duan, L., Tian, Z., Song, Y., Jiang, W., Tian, Y. and Li, S. (2015) 'Influence of solids retention time on membrane fouling: characterization of extracellular polymeric substances and soluble microbial products', *Biofouling*, 31, pp. 181–191.

Dvořák, L., Marcel, G., Dolina, J. and Černín, A. (2016) 'Anaerobic membrane bioreactors—a mini review with emphasis on industrial wastewater treatment: applications, limitations and perspectives', *Desalination and Water Treatment*, 57, pp. 19062–19076.

Elmaleh, S. and Abdelmoumni, L. (1997) 'Cross-flow filtration of an anaerobic methanogenic suspension', *Journal of Membrane Science*, 131, pp. 261–274.

Elmitwalli, T.A., Soellner, J., De Keizer, A., Bruning, H., Zeeman, G. and Lettinga, G. (2001) 'Biodegradability and change of physical characteristics of particles during anaerobic digestion of domestic sewage', *Water Research*, 35, pp. 1311–1317.

Ersahin, M.E., Tao, Y., Ozgun, H., Spanjers, H. and van Lier, J.B. (2016) 'Characteristics and role of dynamic membrane layer in anaerobic membrane bioreactors', *Biotechnology and Bioengineering*, 113, pp. 761–771.

Eusebi, A.L., Martin-Garcia, N., Mcadam, E.J., Jefferson, B., Lester, J.N. and Cartmell, E. (2013) 'Nitrogen removal from temperate anaerobic-aerobic two-stage biological systems: Impact of reactor type and wastewater strength', *Journal of Chemical Technology and Biotechnology*, 88, pp. 2107–2114.

Fan, F., Zhou, H. and Husain, H. (2006) 'Identification of wastewater sludge characteristics to predict critical flux for membrane bioreactor processes', *Water Research*, 40, pp. 205–212.

Fawehinmi, F. (2006) *Anaerobic membrane bioreactor for municipal wastewater treatment*. Cranfield University.

Fawehinmi, F., Lens, P., Stephenson, T., Rogalla, F. and Jefferson, B. (2004) 'The influent of operation conditions of EPS, SMP and bio-fouling in anaerobic MBR', *Water Environment-Membrane Technology Conference*. Seoul, Korea.

Fox, R.A. and Stuckey, D.C. (2015) 'The effect of sparging rate on transmembrane pressure and critical flux in an AnMBR.', *Journal of Environmental Management*, 151, pp. 280–285.

Gabarrón, S., Gómez, M., Monclús, H., Rodríguez-Roda, I. and Comas, J. (2013) 'Ragging phenomenon characterisation and impact in a full-scale MBR', *Water Science & Technology*, 67, pp. 810–816.

Gao, D., Hu, Q., Yao, C. and Ren, N. (2014a) 'Treatment of domestic wastewater by an integrated anaerobic fluidized-bed membrane bioreactor under moderate to low temperature conditions', *Bioresource Technology*, 159, pp. 193–198.

Gao, D., Hu, Q., Yao, C., Ren, N. and Wu, W. (2014b) 'Integrated anaerobic fluidized-bed membrane bioreactor for domestic wastewater treatment', *Chemical Engineering Journal*, 240, pp. 362–368.

Ghyoot, W.R. and Verstraete, W.H. (1997) 'Coupling membrane filtration to anaerobic primary sludge digestion', *Environmental Technology*, 18, pp. 569–580.

Giménez, J.B., Carretero, L., Gatti, M.N., Martí, N., Borrás, L., Ribes, J. and Seco, A. (2012) 'Reliable method for assessing the COD mass balance of a submerged anaerobic membrane bioreactor (SAMBR) treating sulphate-rich municipal wastewater', *Water Science & Technology*, 66, pp. 494–502.

Giménez, J.B., Martí, N., Robles, A., Ferrer, J. and Seco, A. (2014) 'Anaerobic treatment of urban wastewater in membrane bioreactors: evaluation of seasonal temperature variations', *Water Science & Technology*, 69, pp. 1581–1588.

Giménez, J.B., Robles, A., Carretero, L., Durán, F., Ruano, M.V., Gatti, M.N., Ribes, J., Ferrer, J. and Seco, A. (2011) 'Experimental study of the anaerobic urban wastewater treatment in a submerged hollow-fibre membrane bioreactor at pilot scale', *Bioresource Technology*, 102, pp. 8799–8806.

Gouveia, J., Plaza, F., Garralon, G., Fdz-Polanco, F. and Peña, M. (2015a) 'Long-term operation of a pilot scale anaerobic membrane bioreactor (AnMBR) for the treatment of municipal wastewater under psychrophilic conditions', *Bioresource Technology*, 185, pp. 225–233.

Gouveia, J., Plaza, F., Garralon, G., Fdz-Polanco, F. and Peña, M. (2015b) 'A novel configuration for an anaerobic submerged membrane bioreactor (AnSMBR)', *Bioresource Technology*, 198, pp. 510–519.

Guglielmi, G., Chiarani, D., Judd, S.J. and Andreottola, G. (2007) 'Flux criticality and sustainability in a hollow fibre submerged membrane bioreactor for municipal wastewater treatment', *Journal of Membrane Science*, 289, pp. 241–248.

Guglielmi, G., Chiarani, D., Saroj, D.P. and Andreottola, G. (2008) 'Impact of chemical cleaning and air-sparging on the critical and sustainable flux in a flat sheet membrane bioreactor for municipal wastewater treatment', *Water Science & Technology*, 57, pp. 1873–1879.

Harada, H., Momonoi, K., Yamazaki, S. and Takizawa, S. (1994) 'Application of anaerobic-UF membrane reactor for treatment of a waste-water containing high-strength particulate organics', *Water Science & Technology*, 30, pp. 307–319.

Hartley, K. and Lant, P. (2006) 'Eliminating non-renewable CO2 emissions from sewage treatment: An anaerobic migrating bed reactor pilot plant study', *Biotechnology and Bioengineering*, 95, pp. 384–398.

Herrera-Robledo, M., Cid-León, D.M., Morgan-Sagastume, J.M. and Noyola, A. (2011) 'Biofouling in an anaerobic membrane bioreactor treating municipal sewage', *Separation and Purification Technology*, 81, pp. 49–55.

Ho, J. and Sung, S. (2009) 'Anaerobic membrane bioreactor treatment of synthetic municipal wastewater at ambient temperature', *Water Environment Research*, 81, pp. 922–928.

Ho, J. and Sung, S. (2010) 'Methanogenic activities in anaerobic membrane bioreactors (AnMBR) treating synthetic municipal wastewater', *Bioresource Technology*, 101, pp. 2191–2196.

Holba, M., Plotěný, K., Dvořák, L., Gómez, M. and Růžičková, I. (2012) 'Full-scale Applications of membrane filtration in municipal wastewater treatment plants', *Clean - Soil, Air, Water*, 40, pp. 479–486.

Hu, A.Y. and Stuckey, D.C. (2007) 'Activated carbon addition to a submerged anaerobic membrane bioreactor: effect on performance, transmembrane pressure, and flux', *Journal of Environmental Engineering*, 133, pp. 73–80.

Hu, A.Y. and Stuckey, D.C. (2006) 'Treatment of dilute wastewaters using a novel submerged anaerobic membrane bioreactor', *Journal of Environmental Engineering*, 132, pp. 190–198.

Huang, X., Gui, P. and Qian, Y. (2001) 'Effect of sludge retention time on microbial behavior in a submerged membrane bioreactor', *Process Biochemistry*, 36, pp. 1001–1006.

Huang, Z., Ong, S.L. and Ng, H.Y. (2013) 'Performance of submerged anaerobic membrane bioreactor at different SRTs for domestic wastewater treatment', *Journal of Biotechnology*, 164, pp. 82–90.

Huang, Z., Ong, S.L. and Ng, H.Y. (2011) 'Submerged anaerobic membrane bioreactor for low-strength wastewater treatment: effect of HRT and SRT on treatment performance and membrane fouling', *Water Research*, 45, pp. 705–713.

Imasaka, T., Kanekuni, N., So, H. and Yoshino, S. (1989) 'Cross-flow filtration of membrane fermentation broth by ceramic membranes', *Journal of Fermentation and Bioengineering*, 68, pp. 200–206.

Imasaka, T., So, H., Matsushita, K., Furukawa, T. and Kanekuni, N. (1993) 'Application of gas-liquid two-phase cross-flow filtration to pilot-scale methane fermentation', *Drying Technology*, 11, pp. 769–785.

Ince, B.K., Ince, O., Sallis, P.J. and Anderson, G.K. (2000) 'Inert COD production in a membrane anaerobic reactor treating brewery wastewater', *Water Research*, 34, pp. 3943–3948.

Itokawa, H., Tsuji, K., Yamashita, K. and Hashimoto, T. (2014) 'Design and operating experiences of full-scale municipal membrane bioreactors in Japan', *Water Science & Technology*, 69, pp. 1088–1093.

Jeison, D. and van Lier, J.B. (2006) 'Cake layer formation in anaerobic submerged membrane bioreactors (AnSMBR) for wastewater treatment', *Journal of Membrane Science*, 284, pp. 227–236.

Jeison, D., Telkamp, P. and van Lier, J.B. (2009) 'Thermophilic sidestream anaerobic membrane bioreactors: the shear rate dilemma', *Water Environment Research*, 81, pp. 2372–2380.

Judd, S.J. (2011) *Principles and Applications of Membrane Bioreactors in Water and Wastewater Treatment*. 2nd edn. London,UK: Elsevier.

Judd, S.J. (2006) *Principles and Applications of Membrane Bioreactors in Water and Wastewater Treatment*. 1st edn. London,UK: Elsevier.

Kim, J., Kim, K., Ye, H., Lee, E., Shin, C., McCarty, P.L. and Bae, J.H. (2011) 'Anaerobic fluidized bed membrane bioreactor for wastewater treatment', *Environmental Science & Technology*, 45, pp. 576–581.

Kim, J., Shin, J., Kim, H., Lee, J., Yoon, M., Won, S., Lee, B. and Song, K.G. (2014) 'Membrane fouling control using a rotary disk in a submerged anaerobic membrane sponge bioreactor', *Bioresource Technology*, 172, pp. 321–327.

Krzeminski, P., Van Der Graaf, J.H.J.M. and van Lier, J.B. (2012) 'Specific energy consumption of membrane bioreactor (MBR) for sewage treatment', *Water Science & Technology*, 65, pp. 380–392.

Lant, P. and Hartley, K. (2007) 'Solids characterisation in an anaerobic migrating bed reactor (AMBR) sewage treatment system', *Water Research*, 41, pp. 2437–2448.

Laspidou, C.S. and Rittmann, B.E. (2002) 'Non-steady state modeling of extracellular polymeric substances, soluble microbial products, and active and inert biomass', *Water Research*, 36, pp. 1983–1992.

Le-Clech, P., Chen, V. and Fane, T.A.G. (2006) 'Fouling in membrane bioreactors used in wastewater treatment', *Journal of Membrane Science*, 284, pp. 17–53.

Le-Clech, P., Jefferson, B. and Judd, S.J. (2003) 'Impact of aeration, solids concentration and membrane characteristics on the hydraulic performance of a membrane bioreactor', *Journal of Membrane Science*, 218, pp. 117–129.

Lee, D., Li, Y., Noike, T. and Cha, G. (2008) 'Behavior of extracellular polymers and bio-fouling during hydrogen fermentation with a membrane bioreactor', *Journal of Membrane Science*, 322, pp. 13–18.

Lee, W., Kang, S. and Shin, H. (2003) 'Sludge characteristics and their contribution to microfiltration in submerged membrane bioreactors', *Journal of Membrane Science*, 216, pp. 217–227.

Lens, P.N.L., Visser, A., Janssen, A.J.H., Pol, L.W.H. and Lettinga, G. (1998) 'Biotechnological treatment of sulfate-rich wastewaters', *Critical Reviews in Environmental Science and Technology*, 28, pp. 41–88.

Lesjean, B., Rosenberger, S., Laabs, C., Jekel, M., Gnirss, R. and Amy, G. (2005) 'Correlation between membrane fouling and soluble/colloidal organic substances in membrane bioreactors for municipal wastewater treatment', *Water Science & Technology*, 51, pp. 1–8.

Lester, J., Jefferson, B., Eusebi, A.L., Mcadam, E. and Cartmell, E. (2013) 'Anaerobic treatment of fortified municipal wastewater in temperate climates', *Journal of Chemical Technology and Biotechnology*, 88, pp. 1280–1288.

Lettinga, G., Rebac, S. and Zeeman, G. (2001) 'Challenge of psychrophilic anaerobic wastewater treatment', *Trends in Biotechnology*, 19, pp. 363–370.

Liang, S., Liu, C. and Song, L. (2007) 'Soluble microbial products in membrane bioreactor operation: Behaviors, characteristics, and fouling potential', *Water Research*, 41, pp. 95–101.

Liao, B.Q., Allen, D.G., Droppo, I.G., Leppard, G.G. and Liss, S.N. (2001) 'Surface properties of sludge and their role in bioflocculation and settleability', *Water Research*, 35, pp. 339–350.

Liao, B.Q., Kraemer, J.T. and Bagley, D.M. (2006) 'Anaerobic membrane bioreactors: applications and research directions', *Critical Reviews in Environmental Science and Technology*, 36, pp. 489–530.

Lin, H., Chen, J., Wang, F., Ding, L. and Hong, H. (2011) 'Feasibility evaluation of submerged anaerobic membrane bioreactor for municipal secondary wastewater treatment', *Desalination*, 280, pp. 120–126.

Lin, H., Peng, W., Zhang, M., Chen, J., Hong, H. and Zhang, Y. (2013) 'A review on anaerobic membrane bioreactors: Applications, membrane fouling and future perspectives', *Desalination*, 314, pp. 169–188.

Lin, H.J., Xie, K., Mahendran, B., Bagley, D.M., Leung, K.T., Liss, S.N. and Liao, B.Q. (2009) 'Sludge properties and their effects on membrane fouling in submerged

anaerobic membrane bioreactors (SAnMBRs)', *Water Research*, 43, pp. 3827–3837.

Liu, R., Huang, X., Sun, Y.F. and Qian, Y. (2003) 'Hydrodynamic effect on sludge accumulation over membrane surfaces in a submerged membrane bioreactor', *Process Biochemistry*, 39, pp. 157–163.

Liu, Y., Liu, H., Cui, L. and Zhang, K. (2012a) 'The ratio of food-to-microorganism (F/M) on membrane fouling of anaerobic membrane bioreactors treating low-strength wastewater', *Desalination*, 297, pp. 97–103.

Liu, Y., Liu, Z., Zhang, A., Chen, Y. and Wang, X. (2012b) 'The role of EPS concentration on membrane fouling control: Comparison analysis of hybrid membrane bioreactor and conventional membrane bioreactor', *Desalination*, 305, pp. 38–43.

Lousada-Ferreira, M., van Lier, J.B. and van der Graaf, J.H.J.M. (2015) 'Impact of suspended solids concentration on sludge filterability in full-scale membrane bioreactors', *Journal of Membrane Science*, 476, pp. 68–75.

Lyko, S., Al-Halbouni, D., Wintgens, T., Janot, A., Hollender, J., Dott, W. and Melin, T. (2007) 'Polymeric compounds in activated sludge supernatant - Characterisation and retention mechanisms at a full-scale municipal membrane bioreactor', *Water Research*, 41, pp. 3894–3902.

Martin-Garcia, I., Monsalvo, V., Pidou, M., Le-Clech, P., Judd, S.J., McAdam, E.J. and Jefferson, B. (2011) 'Impact of membrane configuration on fouling in anaerobic membrane bioreactors', *Journal of Membrane Science*, 382, pp. 41–49.

Martin Garcia, I., Mokosch, M., Soares, A., Pidou, M. and Jefferson, B. (2013) 'Impact on reactor configuration on the performance of anaerobic MBRs: Treatment of settled sewage in temperate climates', *Water Research*, 47, pp. 4853–4860.

Martinez-Sosa, D., Helmreich, B. and Horn, H. (2012) 'Anaerobic submerged membrane bioreactor (AnSMBR) treating low-strength wastewater under psychrophilic temperature conditions', *Process Biochemistry*, 47, pp. 792–798.

Martinez-Sosa, D., Helmreich, B., Netter, T., Paris, S., Bischof, F. and Horn, H. (2011) 'Anaerobic submerged membrane bioreactor (AnSMBR) for municipal wastewater

treatment under mesophilic and psychrophilic temperature conditions', *Bioresource Technology*, 102, pp. 10377–10385.

Massé, A., Spérandio, M. and Cabassud, C. (2006) 'Comparison of sludge characteristics and performance of a submerged membrane bioreactor and an activated sludge process at high solids retention time', *Water Research*, 40, pp. 2405–2415.

Mathioudakis, V.L., Soares, A., Briers, H., Martin-Garcia, I., Pidou, M. and Jefferson, B. (2012) 'Treatment and energy efficiency of a granular sludge anaerobic membrane reactor handling domestic sewage', *Procedia Engineering*, 44, pp. 1977–1979.

McAdam, E.J., Cartmell, E. and Judd, S.J. (2011) 'Comparison of dead-end and continuous filtration conditions in a denitrification membrane bioreactor', *Journal of Membrane Science*, 369, pp. 167–173.

McAdam, E.J., Luffler, D., Martin-Garcia, N., Eusebi, A.L., Lester, J.N., Jefferson, B. and Cartmell, E. (2011) 'Integrating anaerobic processes into wastewater treatment', *Water Science & Technology*, 63, pp. 1459–1466.

McLeod, A., Jefferson, B. and McAdam, E.J. (2016) 'Toward gas-phase controlled mass transfer in micro-porous membrane contactors for recovery and concentration of dissolved methane in the gas phase', *Journal of Membrane Science*, 510, pp. 466–471.

Meng, F., Chae, S.R., Drews, A., Kraume, M., Shin, H.S. and Yang, F. (2009) 'Recent advances in membrane bioreactors (MBRs): membrane fouling and membrane material', *Water Research*, 43, pp. 1489–1512.

Morgan, J.W., Forster, C.F. and Evison, L. (1990) 'A comparative study of the nature of biopolymers extracted from anaerobic and activated sludges', *Water Research*, 24, pp. 743–750.

Ozgun, H., Dereli, R.K., Ersahin, M.E., Kinaci, C., Spanjers, H. and van Lier, J.B. (2013) 'A review of anaerobic membrane bioreactors for municipal wastewater treatment: Integration options, limitations and expectations', *Separation and Purification Technology*, 118, pp. 89–104.

Ozgun, H., Gimenez, J.B., Evren, M., Tao, Y., Spanjers, H. and van Lier, J.B. (2015a) 'Impact of membrane addition for effluent extraction on the performance and sludge characteristics of upflow anaerobic sludge blanket reactors treating municipal wastewater', *Journal of Membrane Science*, 479, pp. 95–104.

Ozgun, H., Tao, Y., Ersahin, M.E., Zhou, Z., Gimenez, J.B., Spanjers, H. and van Lier, J.B. (2015b) 'Impact of temperature on feed-flow characteristics and filtration performance of an upflow anaerobic sludge blanket coupled ultrafiltration membrane treating municipal wastewater', *Water Research*, 83, pp. 71–83.

Pollice, A., Brookes, A., Jefferson, B. and Judd, S. (2005) 'Sub-critical flux fouling in membrane bioreactors - A review of recent literature', *Desalination*, 174, pp. 221–230.

Pretel, R., Robles, A., Ruano, M.V., Seco, A. and Ferrer, J. (2014) 'The operating cost of an anaerobic membrane bioreactor (AnMBR) treating sulphate-rich urban wastewater', *Separation and Purification Technology*, 126, pp. 30–38.

Robles, A., Ruano, M.V., García-Usach, F. and Ferrer, J. (2012) 'Sub-critical filtration conditions of commercial hollow-fibre membranes in a submerged anaerobic MBR (HF-SAnMBR) system: the effect of gas sparging intensity', *Bioresource Technology*, 114, pp. 247–254.

Robles, A., Ruano, M.V., Ribes, J. and Ferrer, J. (2013a) 'Performance of industrial scale hollow-fibre membranes in a submerged anaerobic MBR (HF-SAnMBR) system at mesophilic and psychrophilic conditions', *Separation and Purification Technology*, 104, pp. 290–296.

Robles, A., Ruano, M.V., Ribes, J. and Ferrer, J. (2013b) 'Factors that affect the permeability of commercial hollow-fibre membranes in a submerged anaerobic MBR (HF-SAnMBR) system', *Water Research*, 47, pp. 1277–1288.

Rosenberger, S., Laabs, C., Lesjean, B., Gnirss, R., Amy, G., Jekel, M. and Schrotter, J.C. (2006) 'Impact of colloidal and soluble organic material on membrane performance in membrane bioreactors for municipal wastewater treatment', *Water Research*, 40, pp. 710–720.

Ruigómez, I., Vera, L., González, E., González, G. and Rodríguez-Sevilla, J. (2016a) 'A novel rotating HF membrane to control fouling on anaerobic membrane bioreactors treating wastewater', *Journal of Membrane Science*, 501, pp. 45–52.

Ruigómez, I., Vera, L., González, E. and Rodríguez-Sevilla, J. (2016b) 'Pilot plant study of a new rotating hollow fibre membrane module for improved performance of an anaerobic submerged MBR', *Journal of Membrane Science*, 514, pp. 105–113.

Saddoud, A., Ellouze, M., Dhouib, A. and Sayadi, S. (2007) 'Anaerobic membrane bioreactor treatment of domestic wastewater in Tunisia', *Desalination*, 207, pp. 205–215.

Salazar-Peláez, M.L., Morgan-Sagastume, J.M. and Noyola, A. (2011) 'Influence of hydraulic retention time on fouling in a UASB coupled with an external ultrafiltration membrane treating synthetic municipal wastewater', *Desalination*, 277, pp. 164–170.

Sanders, W.T.M., Geerink, M., Zeeman, G. and Lettinga, G. (2000) 'Anaerobic hydrolysis kinetics of particulate substrates', *Water Science & Technology*, 41, pp. 17–24.

Seib, M.D., Berg, K.J. and Zitomer, D.H. (2016) 'Low energy anaerobic membrane bioreactor for municipal wastewater treatment', *Journal of Membrane Science*, 514, pp. 450–457.

Shen, Y.X., Xiao, K., Liang, P., Sun, J.Y., Sai, S.J. and Huang, X. (2012) 'Characterization of soluble microbial products in 10 large-scale membrane bioreactors for municipal wastewater treatment in China', *Journal of Membrane Science*, 415–416, pp. 336–345.

Shin, C., Kim, K., McCarty, P.L., Kim, J. and Bae, J. (2016) 'Integrity of hollow-fiber membranes in a pilot-scale anaerobic fluidized membrane bioreactor (AFMBR) after two-years of operation', *Separation and Purification Technology*, 162, pp. 101–105.

Shin, C., McCarty, P.L., Kim, J. and Bae, J. (2014) 'Pilot-scale temperate-climate treatment of domestic wastewater with a staged anaerobic fluidized membrane bioreactor (SAF-MBR)', *Bioresource Technology*, 159, pp. 95–103.

Skouteris, G., Hermosilla, D., López, P., Negro, C. and Blanco, Á. (2012) 'Anaerobic membrane bioreactors for wastewater treatment: A review', *Chemical Engineering Journal*, 198–199, pp. 138–148.

Smith, A.L., Skerlos, S.J. and Raskin, L. (2013) 'Psychrophilic anaerobic membrane bioreactor treatment of domestic wastewater', *Water Research*, 47, pp. 1655–1665.

Smith, A.L., Skerlos, S.J. and Raskin, L. (2015) 'Anaerobic membrane bioreactor treatment of domestic wastewater at psychrophilic temperatures ranging from 15 °C to 3 °C', *Environmental Science: Water Research & Technology*, 1, pp. 56–64.

Smith, A.L., Stadler, L.B., Love, N.G., Skerlos, S.J. and Raskin, L. (2012) 'Perspectives on anaerobic membrane bioreactor treatment of domestic wastewater: a critical review', *Bioresource Technology*, 122, pp. 149–159.

Soto, M., Méndez, R. and Lema, J.M. (1993) 'Methanogenic and non-methanogenic activity tests. Theoretical basis and experimental set up', *Water Research*, 27, pp. 1361–1376.

Stuckey, D.C. (2012) 'Recent developments in anaerobic membrane reactors', *Bioresource Technology*, 122, pp. 137–148.

Sun, J., Rong, J., Dai, L., Liu, B. and Zhu, W. (2011) 'Control of membrane fouling during hypersaline municipal wastewater treatment using a pilot-scale anoxic/aerobic-membrane bioreactor system', *Journal of Environmental Sciences*, 23, pp. 1619–1625.

Sutton, P.M., Rittmann, B.E., Schraa, O.J., Banaszak, J.E. and Togna, A.P. (2011) 'Wastewater as a resource: A unique approach to achieving energy sustainability', *Water Science & Technology*, 63, pp. 2004–2009.

Trussell, R.S., Merlo, R.P., Hermanowicz, S.W. and Jenkins, D. (2007) 'Influence of mixed liquor properties and aeration intensity on membrane fouling in a submerged membrane bioreactor at high mixed liquor suspended solids concentrations', *Water Research*, 41, pp. 947–958.

Ueda, T. and Hata, K. (1999) 'Domestic wastewater treatment by a submerged membrane bioreactor with gravitational filtration', *Water Research*, 33, pp. 2888–2892.

Uemura, S. and Harada, H. (2000) 'Treatment of sewage by a UASB reactor under moderate to low temperature conditions', *Bioresource Technology*, 72, pp. 275–282.

Vallero, M.V.G., Lettinga, G. and Lens, P.N.L. (2005) 'High rate sulfate reduction in a submerged anaerobic membrane bioreactor (SAMBaR) at high salinity', *Journal of Membrane Science*, 253, pp. 217–232.

Vavilin, V.A., Fernandez, B., Palatsi, J. and Flotats, X. (2008) 'Hydrolysis kinetics in anaerobic degradation of particulate organic material: An overview', *Waste Management*, 28, pp. 939–951.

Verrecht, B., Judd, S., Guglielmi, G., Brepols, C. and Mulder, J.W. (2008) 'An aeration energy model for an immersed membrane bioreactor', *Water Research*, 42, pp. 4761–4770.

van Voorthuizen, E., Zwijnenburg, A., van der Meer, W. and Temmink, H. (2008) 'Biological black water treatment combined with membrane separation', *Water Research*, 42, pp. 4334–4340.

Vyrides, I. and Stuckey, D.C. (2009) 'Saline sewage treatment using a submerged anaerobic membrane reactor (SAMBR): Effects of activated carbon addition and biogas-sparging time', *Water Research*, 43, pp. 933–942.

Wang, J., Wu, B., Liu, Y., Fane, A.G. and Chew, J.W. (2017) 'Effect of fluidized granular activated carbon (GAC) on critical flux in the microfiltration of particulate foulants', *Journal of Membrane Science*, 523, pp. 409–417.

Wang, P., Wang, Z., Wu, Z. and Mai, S. (2011) 'Fouling behaviours of two membranes in a submerged membrane bioreactor for municipal wastewater treatment', *Journal of Membrane Science*, 382, pp. 60–69.

Wang, Z., Ma, J., Tang, C.Y., Kimura, K., Wang, Q. and Han, X. (2014) 'Membrane cleaning in membrane bioreactors: A review', *Journal of Membrane Science*, 468, pp. 276–307.

Wei, C.H., Harb, M., Amy, G., Hong, P.Y. and Leiknes, T. (2014) 'Sustainable organic loading rate and energy recovery potential of mesophilic anaerobic membrane bioreactor for municipal wastewater treatment', *Bioresource Technology*, 166, pp. 326–334.

Weinrich, L. and Grélot, A. (2008) 'Evaluation of innovative operation concept for fiat sheet MBR filtration system', *Water Science & Technology*, 57, pp. 613–620.

Wen, C., Huang, X. and Qian, Y. (1999) 'Domestic wastewater treatment using an anaerobic bioreactor coupled with membrane filtration', *Process Biochemistry*, 35, pp. 335–340.

Wu, B., An, Y., Li, Y. and Wong, F.S. (2009) 'Effect of adsorption/coagulation on membrane fouling in microfiltration process post-treating anaerobic digestion effluent', *Desalination*, 242, pp. 183–192.

Yoo, R., Kim, J., McCarty, P.L. and Bae, J. (2012) 'Anaerobic treatment of municipal wastewater with a staged anaerobic fluidized membrane bioreactor (SAF-MBR) system', *Bioresource Technology*, 120, pp. 133–139.

Yoo, R.H., Kim, J.H., McCarty, P.L. and Bae, J.H. (2014) 'Effect of temperature on the treatment of domestic wastewater with a staged anaerobic fluidized membrane bioreactor', *Water Science & Technology*, 69, pp. 1145–1150.

Yu, K., Wen, X., Bu, Q.J. and Xia, H. (2003) 'Critical flux enhancements with air sparging in axial hollow fibers cross-flow microfiltration of biologically treated wastewater', *Journal of Membrane Science*, 224, pp. 69–79.

Zhang, J., Chua, H.C., Zhou, J. and Fane, A.G. (2006) 'Factors affecting the membrane performance in submerged membrane bioreactors', *Journal of Membrane Science*, 284, pp. 54–66.

Zhang, S., Qu, Y., Liu, Y., Yang, F., Zhang, X., Furukawa, K. and Yamada, Y. (2005) 'Experimental study of domestic sewage treatment with a metal membrane bioreactor', *Desalination*, 177, pp. 83–93.

Zhou, L., Zhang, Z., Jiang, W., Guo, W., Ngo, H., Meng, X., Fan, J., Zhao, J. and Xia, S. (2014) 'Effects of low-concentration Cr(VI) on the performance and the

membrane fouling of a submerged membrane bioreactor in the treatment of municipal wastewater', *Biofouling*, 30, pp. 105–114.

Zsirai, T., Buzatu, P., Aerts, P. and Judd, S. (2012) 'Efficacy of relaxation, backflushing, chemical cleaning and clogging removal for an immersed hollow fibre membrane bioreactor', *Water Research*, 46, pp. 4499–4507.

Zsirai, T., Qiblawey, H., A-Marri, M.J. and Judd, S. (2016) 'The impact of mechanical shear on membrane flux and energy demand', *Journal of Membrane Science*, 516, pp. 56–63.

CHAPTER 3

Evaluation of the impact of solids accumulation in granular and flocculent upflow anaerobic sludge blanket (UASB) reactors for settled municipal wastewater treatment under temperate conditions

3 Evaluation of the impact of solids accumulation in granular and flocculent upflow anaerobic sludge blanket (UASB) reactors for settled municipal wastewater treatment under temperate conditions

K. M. Wang[a], Y. Aguilera[a], A. Soares[a], B. Jefferson[a], E. J. McAdam[a*]
[a]Cranfield Water Science Institute, Vincent Building, Cranfield University, Bedfordshire, MK43 0AL, UK

Abstract

In this study, the impact of solids accumulation in upflow anaerobic sludge blanket (UASB) reactors is evaluated during low temperature municipal wastewater treatment. Three stages of operation were determined for both the granular and flocculent UASB: (i) sludge blanket development, (ii) steady-state operation, and (iii) breakthrough. During the steady-state operation, solids accumulation in the sludge blanket enhanced treatment efficiency, which was explained by the filtration capability of the sludge blanket formed either within the flocculent UASB (F-UASB) sludge bed or above the granular matrix in the granular UASB (G-UASB). Once a critical solids concentration was reached, solids breakthrough was observed in the effluent. This was exacerbated by higher biogas production, which was introduced through partial hydrolysis of the entrapped particulate matter at an extended solids retention time. Soluble COD also increased, which we suggest is a product of hydrolysis following extended solids storage. An optimum solids concentration (or blanket height), was therefore determined to protect effluent quality, but this was dependent upon temperature. At low temperatures, the F-UASB was less stable which was attributed to the increased fluid viscosity, which decreased settling velocity. Whilst for the G-UASB, the higher inertial force of the granular sludge coupled with a lower gas production rate, enhanced reactor stability. Therefore, whilst higher upflow velocity is needed in G-UASB to promote stratification of particular and granular material, a lower upflow velocity is required for F-UASB to sustain operation at lower temperatures. Importantly, we propose both solids management (control the sludge blanket at a threshold between the sludge blanket development and steady-state period) and boundary condition selection (adjust the upflow velocity according to temperatures) to enable a more resilient operation of low temperature UASB for municipal wastewater treatment.

Keywords: sludge bed, stability, solids washout, upflow velocity, domestic wastewater

3.1 Introduction

Upflow anaerobic sludge blanket (UASB) reactors are high-rate anaerobic reactors that have been widely applied to municipal wastewater treatment. In UASB, the upflow velocity (V_{up}) introduces a hydraulic selection pressure to extend the solids retention time (SRT) and to allow the retention of large amounts of highly active biomass (Chong et al., 2012). Currently, there are hundreds of full-scale UASB plants in tropical and sub-tropical countries, notably in Latin America, India and the Middle East, treating crude municipal wastewater (Chernicharo et al., 2015), where their capabilities are well accepted for chemical oxygen demand (COD) removal of around 60-80 % (Nada et al., 2011; Oliveira and von Sperling, 2011).

There are currently no full-scale UASB treating municipal wastewater in temperate regions such as Northern America and Northern Europe, as low temperature and low substrate concentrations coupled with typically high half saturation kinetics (Ks), reduces the anaerobic organic biodegradation rate (Elmitwalli et al., 2002; Lester et al., 2013; McAdam et al., 2011). Mckeown et al. (2009) demonstrated sound methanogenesis activities from a granular UASB treating soluble industrial wastewater at temperatures between 4 and 15 °C, suggesting that reasonable conversion at similar temperatures is possible for municipal wastewater treatment. However, the quality of carbon in municipal wastewater is variable and distributed across soluble, colloidal and particulate fractions. Lester et al. (2013) demonstrated that good methane production was achievable from municipal wastewater, at a low temperature of <10 °C, but this was primarily dependent upon the partial hydrolysis of entrapped particulate matter. It is generally proposed that particulate matter is first removed by physical processes including settling, adsorption and entrapment in the sludge bed (Lettinga et al., 2001; Mahmoud et al., 2003). However, the reduced hydrolysis rate of entrapped particulate matter at low temperatures is generally regarded as the rate-limiting step (Lettinga et al., 2001), with the accumulation of sludge inevitably having a negative influence on both effluent quality and process stability (Cavalcanti et al., 1999; Sayed and Fergala, 1995). Therefore, the challenge of UASB applications for low temperature municipal wastewater treatment is how best to manage solids accumulation in order to achieve good effluent quality, whilst simultaneously enabling energy recovery.

Granular biomass has been shown to possess superior settling characteristics (Liu et al., 2002; Sabry, 2008) and higher specific activity (Lim and Kim, 2014) compared with flocculent inoculum biomass, subsequently providing improved treatment performance versus flocculent UASB reactors. However, there are only a few studies that directly compared the UASB treatment efficiencies with granular and flocculent inoculum biomass. Most of the experience was from soluble industrial wastewater or synthetic municipal wastewater (Rajeshwari et al., 2000; Sabry, 2008; van Lier et al., 2015) without solids accumulation challenges rather than real municipal wastewater (Lettinga et al., 1983). It is of importance to ascertain whether the proposed benefits of granular inoculum over flocculent inoculum treating municipal wastewater at low temperatures can outweigh the limited sources (Liu and Tay, 2004) and high cost between 500 and 1000 USD per ton wet weight (Liu et al., 2002). Previous studies demonstrated that solids accumulation at low temperatures led to the washout of active biomass and decrease of SRT (Elmitwalli et al., 2001; Syutsubo et al., 2011). This phenomenon resulted in the deterioration of the methanogenesis bacteria activities and overall reactor performance in flocculent UASB (F-UASB) (Elmitwalli et al., 2001; Syutsubo et al., 2011). In granular UASB (G-UASB), solids accumulation (particulate matter entrapment) led to a higher total COD removal of 70 % than expected at low temperate conditions treating crude municipal wastewater (Uemura and Harada, 2000). However, due to the relatively low V_{up} of 0.5-0.6 m h^{-1}, the solids accumulation mainly occurred within the granule bed, which also led to the deterioration of the methanogenesis bacteria activity (Uemura and Harada, 2000; Zeeman and Lettinga, 1999). Whilst Lester et al. (2013) applied a higher V_{up} of 1.0 m h^{-1}, by applying an external recycle to supplement the V_{up} set by the incoming flow, which yielded sufficient fluidisation of the granular sludge to avoid solids accumulation and instead developed a stratified solids layer above the granular interface, due to the difference in density between the two suspensions.

Numerous previous studies demonstrated that pre-removal of solids such as feeding pre-settled sewage instead of crude sewage to the anaerobic treatment at low temperatures can be beneficial (Elimitwalli et al., 1999; Lew et al., 2004; Seghezzo et al., 2002). This can improve the treatment performance due to low solids loading and better

colloidal and dissolved COD removals (Elimitwalli et al., 1999; Lew et al., 2004; Seghezzo et al., 2002) and simultaneously increase the energy recovery in anaerobic digester (AD) through more solids settlement as primary sludge (McAdam et al., 2011). However, there have been no previous studies that have explicitly sought to understand the impact of solids accumulation and how to manage the sludge blanket stability in the UASB reactor to sustain treatment performance treating settled municipal wastewater in temperate climates. The aim of this study is therefore to evaluate the impact of solids accumulation in both granular and flocculent UASB reactors, in order to ascertain whether sludge blanket stability can be sustained during low temperature treatment of settled municipal wastewater. The specific objectives were: (i) to evaluate impacts of the solids accumulation on UASB treatment performance in temperate climates; (ii) to investigate the impact of temperature and upflow velocity on sludge blanket stability and reactor treatment performance, and propose the engineering solutions to maintain stable sludge blanket; and (iii) to compare the treatment efficiency of granular and flocculent UASB reactor treating settled municipal wastewater at low temperatures.

3.2 Materials and methods

3.2.1 UASB pilot plants

Two 70 L cylindrical UASB (0.2 m diameter x 1.8 m height) were operated in parallel (Model products, Wootton, UK) with a solid/liquid/gas separation (0.4 m diameter x 0.2 height) at the top of the column, resulting in the effluent being located at about 2.0 m of the reactor (Figure 3-1). Three lamella settlers were utilised and the lowest separator reached at a column height of 1.5 m. The UASB columns had a total of five sampling points placed every 30 cm. The G-UASB and F-UASB were inoculated with 15 L of granular and flocculent sludge from a mesophilic UASB used for pulp and paper industry and an anaerobic digester treating a mixture of municipal primary and secondary sludges with 3.6 % total solids (78 % volatile solids (VS)) respectively. Settled wastewater from Cranfield University's sewage treatment works was fed via the bottom of the two UASB reactors through peristaltic pumps (520U, Watson Marlow, Falmouth, UK). Both the G-UASB and F-UASB were operated at a HRT of 8 h for 360 days to acclimatise before this experiment. The internal recirculation was operated by peristaltic pumps (620S,

Watson Marlow, Falmouth, UK) to keep the V_{up} of 0.8-0.9 m h^{-1} (Tchobanoglous et al., 2003). The mixed gas and liquid velocity (V_{mix}) can be calculated (Massey and Ward-Smith, 2006; Vera et al., 2000; Verberk et al., 2001):

$$V_{mix} = \frac{\dot{m}}{\rho_{mix} \cdot A} \tag{3-1}$$

$$\dot{m} = \rho_g Q_g + \rho_l Q_l \tag{3-2}$$

$$\rho_{mix} = \frac{\rho_g Q_g + \rho_l Q_l}{Q_g + Q_l} \tag{3-3}$$

where $\dot{m}$ is mass flow rate (kg s^{-1}), ρ_{mix} is the mixed fluid density (kg m^{-3}), A is the reactor cross-sectional area (m^2), ρ_g is the gas density (kg m^{-3}), ρ_l is the liquid density (kg m^{-3}), Q_g is the gas flow rate (m^3 s^{-1}), Q_l is the liquid flow rate (m^3 s^{-1}).

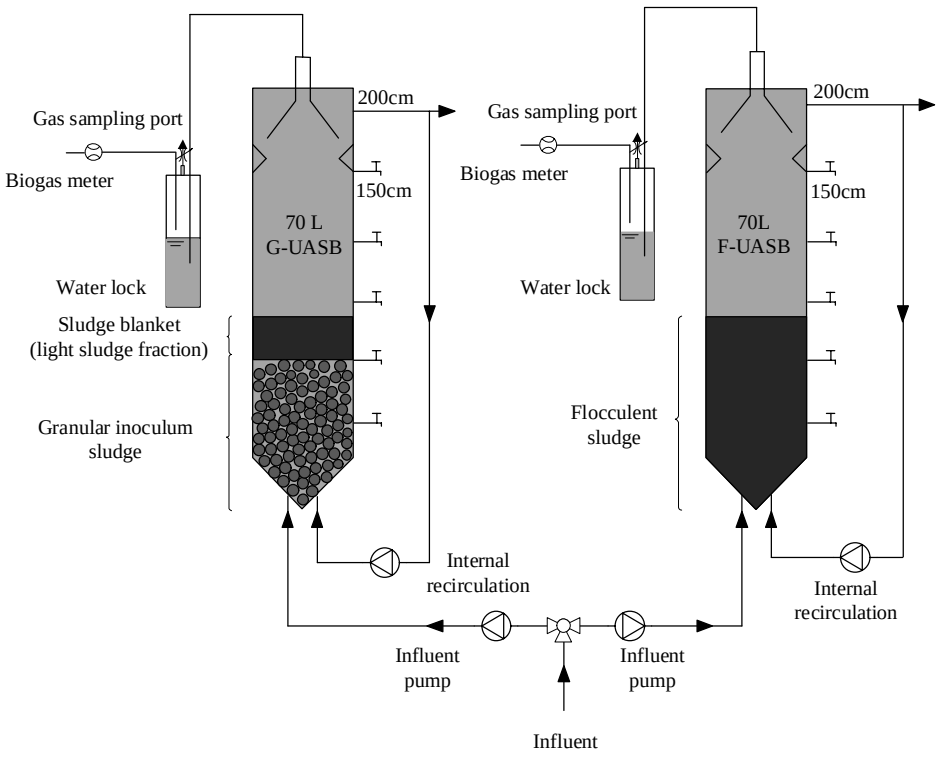

Figure 3-1. Schematics of pilot scale G-UASB and F-UASB.

In the G-UASB, the granular sludge bed expanded to about 30 % of the total column height with the light sludge fraction formed a sludge blanket layer above the granular sludge bed, which was constituted of dispersed growth flocs from the influent (Aiyuk et al., 2006; Chong et al., 2012). The sludge blanket height in the G-UASB was measured as the total height of sludge blanket and inoculum granular matrix. Whilst for the F-UASB,

there is no obvious differentiation between accumulated solids and inoculum flocculent sludge bed. The sludge blanket works as a cake filter, in which the proportion of volume of filtrate/volume of sludge bed (K_H) can be determined by (Figure S3-1):

$$k_H = \frac{V_{filter}}{A \cdot X} \quad (3\text{-}4)$$

where V_{filter} is the volume of wastewater filtered (m^3), A is reactor cross-sectional area (m^2), X is the sludge blanket height (m). The light flocculent sludge blanket in the G-UASB and flocculent sludge bed in the F-UASB were withdrawn once solids washout into the UASB effluent was noted by an increase of suspended solids concentration.

The settling velocities of sludge particle (flocculent sludge above granules in the G-UASB and flocculent sludge in the F-UASB) were tested in a temperature controlled water bath at 10 and 20 °C. Based on the data at a water temperature of 10 °C, particle settling velocities at a water temperature of 20 °C were predicted by applying Stoke's law (Reynolds number< 1.0) (Tchobanoglous et al., 2003):

$$v_p = \frac{g(\rho_p - \rho_w)d_p^2}{18\mu} \quad (3\text{-}5)$$

where V_p is particle settling velocity (m s^{-1}), ρ_p is particle density (kg m^{-3}), ρ_w is liquid density (kg m^{-3}), d_p is particle diameter (m), μ is the liquid viscosity (Pa. s). The confidence interval of 95 % for prediction values were calculated following the method as reported previously (Altman and Gardner, 1988; Zaiontz, 2018). In order to evaluate the impact of temperature on system resilience, both G-UASB and F-UASB reactors were operated in a period of high and low seasonal temperature (19.5±2.1 and 10.2±1.5 °C). Whilst for the investigation of the impact of V_{up} on reactor stability, the tests were conducted at a similar temperature of 15.0-15.4 °C.

3.2.2 Statistical analysis

A Chow test is applied to determine whether a set of experimental points is better correlated in multiple regressions or in a pooled regression. The data points were divided into two subgroups starting with the first two points as first group and regarded the rest of the data points as the second group. Linear regression was then applied to both groups and the sum of the square residuals (SSR) between the predicted and experimental data were calculated. This was done for an increasing number of data for

the first group with the second group containing the rest of data points. The sum of the SSR for each pair of linear regressions was calculated and the minimum was determined as the optimum separation between the data points. The F test was subsequently utilised to test the statistical significance:

$$F = \frac{(SSR_p - SSR_1 - SSR_2)/2}{(SSR_1 + SSR_2)/(N-4)} \quad (3\text{-}6)$$

where SSR_p, SSR_1 and SSR_2 are SSR of pooled regression, first group and second group respectively, N is the number of data points. Statistical analysis was completed with the software IBM SPSS Statistics 23. The data sets were first analysed for normal distribution through Shapiro-Wilk tests to determine the application of parametric and non-parametric statistical tools. Parametric data were examined with ANOVA tests whilst non-parametric data were examined with Mann-Whitney U test for independent data. All the statistically significant differences were based on 95 % of the confidence level ($p<0.05$).

3.2.3 Analytical methods

Suspended solids (SS) and biochemical oxygen demand (BOD_5) were measured according to Standard Methods (APHA, 2005). Total and soluble chemical oxygen demand (COD) were analysed with Merck test kits (Merck KGaA, Darmstadt, Germany). Soluble COD was measured after filtering with 1.2 μm filter paper (70 mm Glass Fibre Filter Paper Grade GF/C, Whatman, GE Healthcare Life Sciences, Little Chalfont, UK). Biogas flow rate was measured with a gas meter (TG0.5, Ritter, Bochum, Germany). Methane (CH_4) composition was analysed by a gas analyser (Servomex 1440, Crowborough, UK).

Sludge blanket height was observed and measured daily. The mixed sludge samples (from 90 cm, 120 cm and 150 cm) were used for the particle settling experiment. The settling column apparatus consisted of a central settling column with deionised water enclosed by a water bath to control the temperature at 10 and 20 °C. The sludge particles were introduced into the settling column via a taped entry port with a wide-mouthed pipet to ensure that the particles settle in the centre of the column. Particle images were captured by a Sony ICX674 sensor (Infinity 3-3UR, Lumenera Corporation,

Ottawa, Canada). An image analysis software (Image-Pro Premier 9) was used to analyse the particle size and settling velocity. Biochemical methane potential (BMP) tests of primary sludge and sludge blanket from both G-UASB and F-UASB reactors (after UASB operation for 70 and 140 days) were measured with 1 L bottles connected with gas meters (Milligas Counter MGC-1 PMMA, Ritter, Bochum, Germany), lasting for 28 days. The VS ratio between inoculum and substrate was kept at 2:1. The bottles were purged with nitrogen-enriched air (BOC Ltd, Guildford, UK). The bottles were placed in a water bath at 37±1 °C with continuous magnetic stirring. Blank samples were tested with only inoculum to show the background methanogenic production.

Both granular and flocculent inoculum biomass were taken from the tap at reactor height of 30 cm for microbial diversity analyses. 25 mL of the sludge samples preserved in a 1:1 (v/v) ethanol (>99 %, Fisher Scientific, UK) and stored under -20 °C until deoxyribonucleic acid (DNA) extraction and microbial analyses performed at Prokarya limited (Sunderland, UK). The DNA was extracted using the MPBio FastDNA® SPIN Kit for Soil (Q-Biogene, MP Biomedicals, Cambridge, UK). Universal polymerase chain reaction primers 515F and 926R were used to target the V4 and V5 regions of the 16S ribosomal ribonucleic acid (rRNA) (Quince et al., 2011). The amplified 16S rRNA was sequenced and analysed by Ion Torrent Personal Genome Machine with 400 bp HiQ chemistry (Life Technologies, Carlsbad, USA). The sequences results were analysed using QIIME pipeline version 1.9 (Caporaso et al., 2010).

Granular inoculum biomass was further analysed by fluorescence in situ hybridisation (FISH) technique to identify the spatial distribution of microbes within the granules. The granules were washed and fixed according to Sekiguchi et al. (1999), followed by dehydration by serial immersion in 50, 70, 96 (two times) and 100 % (three times) ethanol, eucalyptol, 100 % xylene (two times) and embedded in melted paraffin wax. Serial sections about 8 μm thick were cut with microtome and mounted on gelatin-coated glass slides. The sections were dewaxed through 100 % xylene (two times) and 100 % ethanol (two times). In situ hybridisation was conducted according to the method using by Manz et al. (1992) with the 16S rRNA-targeted oligonucleotide sequences specific for fluorescein (FITC) labeled domain bacteria (EUB338-I, EUB338-II, EUB338-III)

(Amann et al., 1990; Daims et al., 1999), cyanine (cy3) labeled domain archaea (ARCH915) (Stahl and Amann, 1991) and cy5 labeled domain methanosaeta (MX825) (Stahl and Amann, 1991). Images of the slides were viewed with a confocal laser scanning microscope (CLSM) (Nikon CS-1, Nikon, Tokyo, Japan). All analysis was conducted in triplicate.

3.3 Results

3.3.1 Impact of sludge blanket stability on solid and organic separation

During the 120-day trial, Chow tests were applied based on the data of sludge blanket/effluent height ratios (X/XT) to identify the optimum separations between the data points, followed by F tests to determine the statistical significance and stage separations. As a result, the operation of the G-UASB and F-UASB reactors can be divided into three stages namely sludge blanket development, steady-state operation and breakthrough (Figure 3-2a). However, the steady-state operation period of the G-UASB (41-86 days, 46 days) was twice as long as that in the F-UASB (43-65 days, 23 days) (Figure 3-2). The stage separation was corroborated with particulate COD (PCOD) removals, as the lowest C/C_0 ratios of 23±12 % and 23±11 % (with low coefficient variations <20 %) were obtained during the steady-state operation period for the G-UASB and F-UASB reactors respectively (Figure 3-2b), indicating effective PCOD entrapments with average PCOD removals of 77 %.

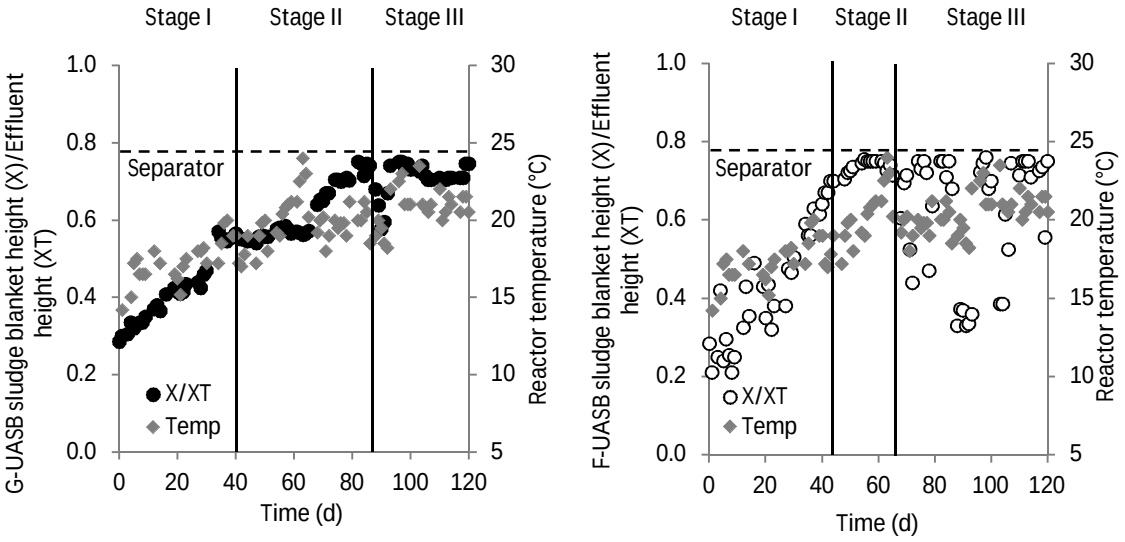

(a)

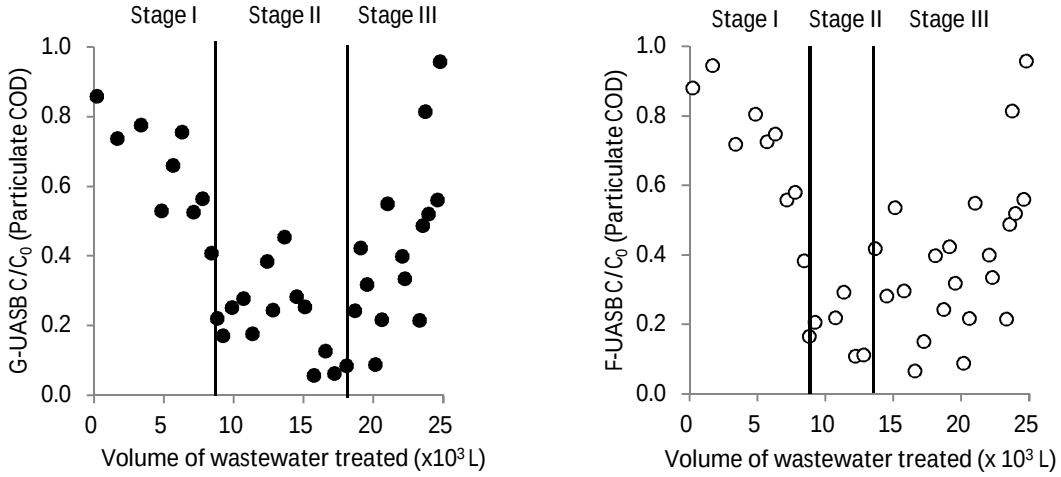

(b)

Figure 3-2. (a) Temporal variation of UASB sludge blanket height (X)/Effluent height (XT) ratio and reactor temperature. (b) Impact of sludge blanket on particulate COD separation. Stage I, sludge blanket development (0-40 d for G-UASB, 0-42 d for F-UASB); Stage II, steady-state operation (41-86 d for G-UASB, 43-65 d for F-UASB); Stage III, breakthrough (87-120 d for G-UASB, 66-120 d for F-UASB).

3.3.2 Impact of sludge blanket stability on biogas production

During the steady-state operation (between 41-86 days for the G-UASB and 43-65 days for the F-UASB), higher average headspace CH_4 productions were observed with maximum values of 6.7 and 8.1 L d^{-1} for the G-UASB and F-UASB respectively at reactor temperature of 21 °C (Figure 3-3a). Higher effluent SCOD concentrations were also observed for both the G-UASB and F-UASB during this steady-state operation (Figure 3-3b). The residual energy production of primary sludge and mixed sludge blanket after 70 and 140 days inside the UASB reactors were measured through BMP tests (Figure 3-4). Noticeable reductions of residual energy by 54-60 % were observed from primary sludge (0.263 L CH_4 g^{-1}VS fed) to solids accumulated for 70 days in the G-UASB and F-UASB reactors. Longer solids accumulation period (140-days) resulted in further decrease of the residual energy production to only 0.057 L CH_4 g^{-1}VS fed for both the G-UASB and F-UASB, leading to about 80 % of the residual energy reduction from primary sludge.

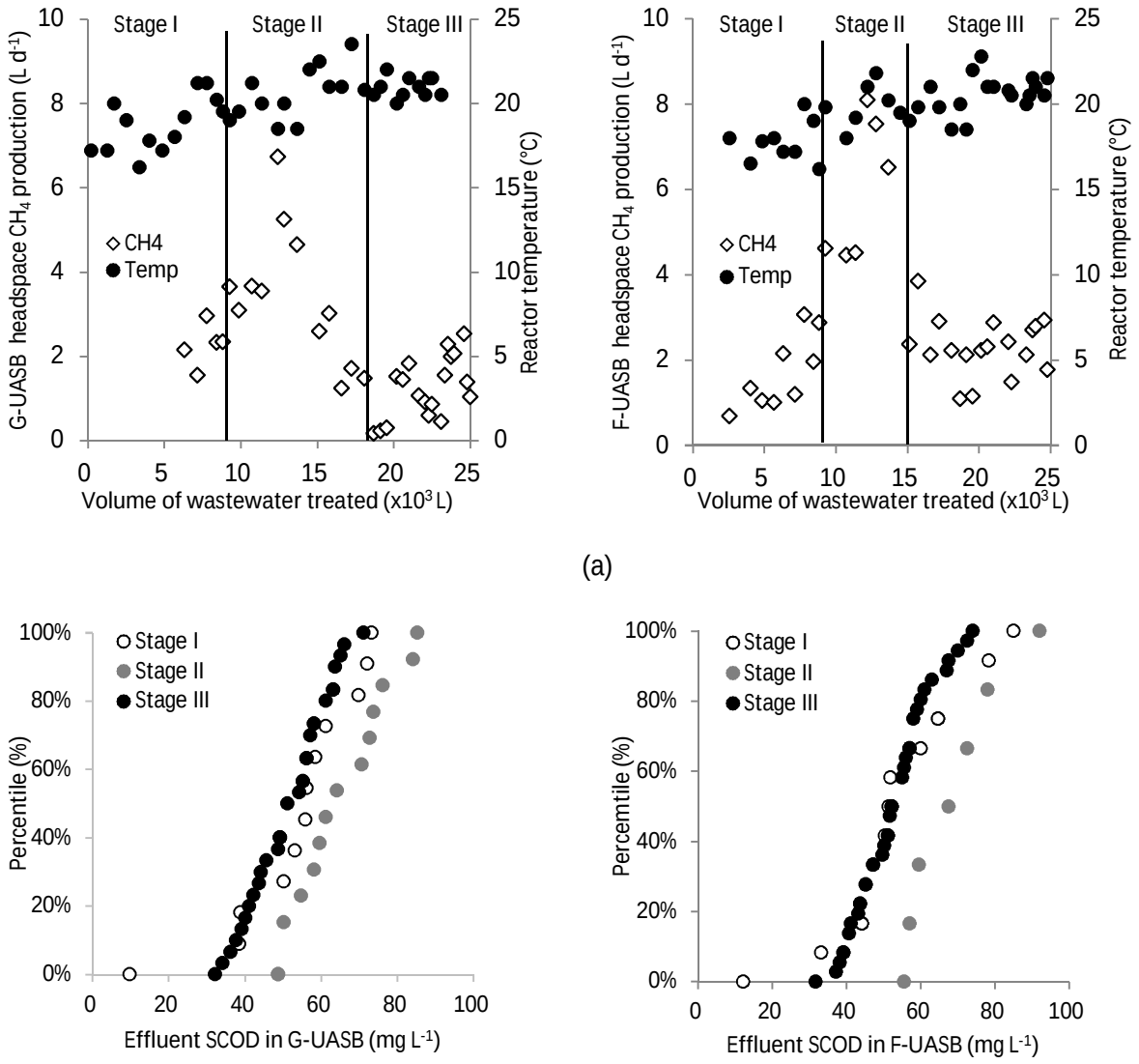

Figure 3-3. (a) Headspace CH_4 production from G-UASB and F-UASB and reactor temperatures. (b) Effluent SCOD concentrations in G-UASB and F-UASB. Stage I, sludge blanket development (0-40 d for G-UASB, 0-42 d for F-UASB); Stage II, steady-state operation (41-86 d for G-UASB, 43-65 d for F-UASB); Stage III, breakthrough (87-120 d for G-UASB, 66-120 d for F-UASB).

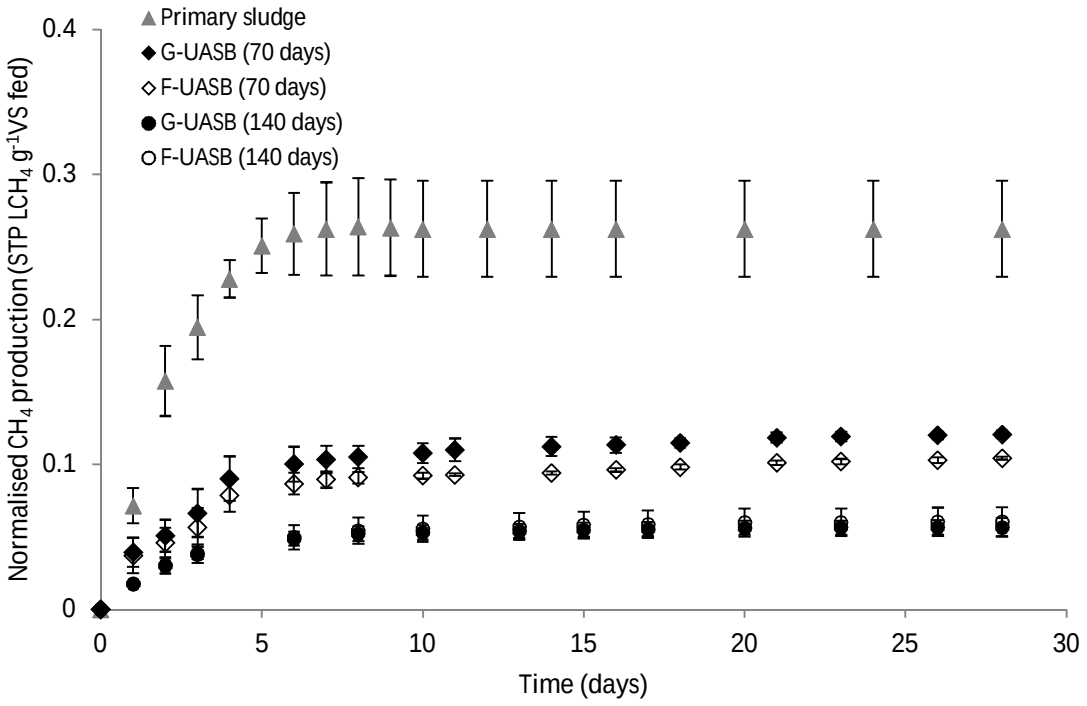

Figure 3-4. Residual energy production through BMP tests from primary sludge and the sludge blanket under different desludge strategy (for 70 days, because the low sludge blanket height, samples were only taken from 90 cm port; for 140 days, the mixed sludge samples were from three sampling ports: 90 cm, 120 cm and 150 cm from the bottom of the UASB reactor).

3.3.3 Impact of temperature on sludge blanket stability

The impact of temperature on sludge blanket stability was investigated at average temperatures of about 20 and 10 °C (Figure 3-5). The low average temperature led to the instability of the sludge blanket and solids washout for both the G-UASB and F-UASB, but was exacerbated in the F-UASB. To illustrate, the period before unstable operation in the G-UASB decreased from 86 days to about 50 days when the reactor temperature dropped from about 20 to 10 °C. Whilst for the F-UASB, the sludge blanket became unstable within only 19 days at a low average reactor temperature of 10 °C. Lower PCOD removal efficiencies were also obtained for both the G-UASB and F-UASB at a low average reactor temperature of 10 °C (Figure 3-5).

The impact of temperature on particle settling velocity was subsequently conducted in a temperature-controlled water bath with average temperatures of 10 and 20 °C (Figure 3-6). Higher settling velocity was observed at a higher water temperature

of 20 °C for both flocculent particles above the granules in the G-UASB and flocculent sludge particles in the F-UASB (Figure 3-6 a,b). The prediction data of settling velocities at a water temperature of 20 °C (calculated from the data for the particles at a water temperature of 10 °C through Stoke's law (Equation 3-5 and Figure 3-6a,b) fitted well with the experimental data (within 95 % of the confidence intervals). Comparison of the particle settling velocity of the flocculent sludge above the granules in the G-UASB and flocculent sludge in the F-UASB revealed that there was no difference at both wastewater temperatures of 10 and 20 °C (Figure 3-6c,d). The fixed liquid V_{up} of 0.8 m h^{-1} (222 µm s^{-1}) had already exceeded the settling velocity of some small particles with particle size <130-150 µm at a low average temperature of 10 °C (Figure 3-6c). Considering the mixed velocity of gas and liquid with V_{up} of 1.2 m h^{-1} (339 µm s^{-1}), more solids with particle size <150-170 µm cannot be settled (Figure 3-6c).

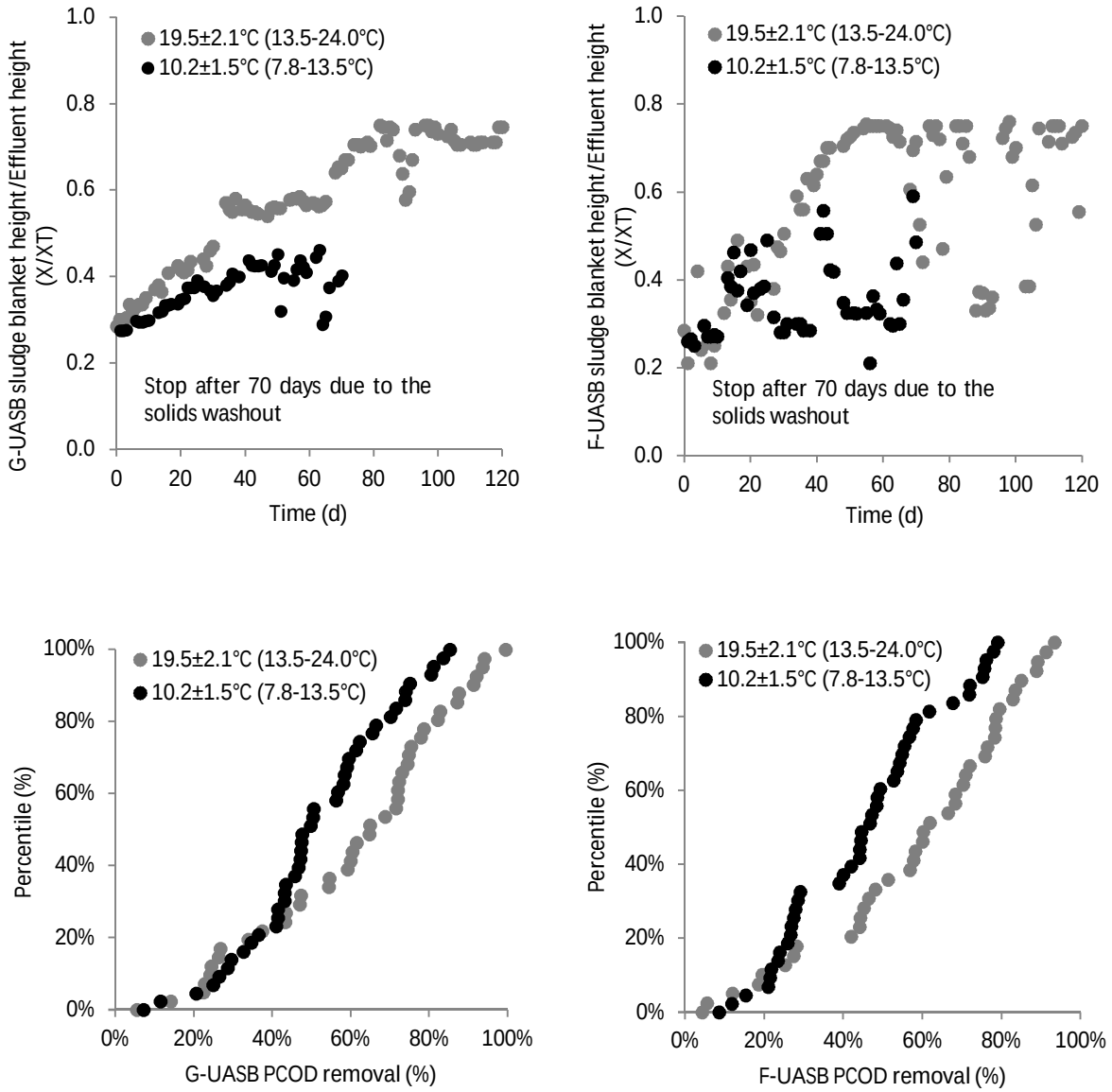

Figure 3-5. Impact of temperature on sludge blanket stability and particulate COD separation.

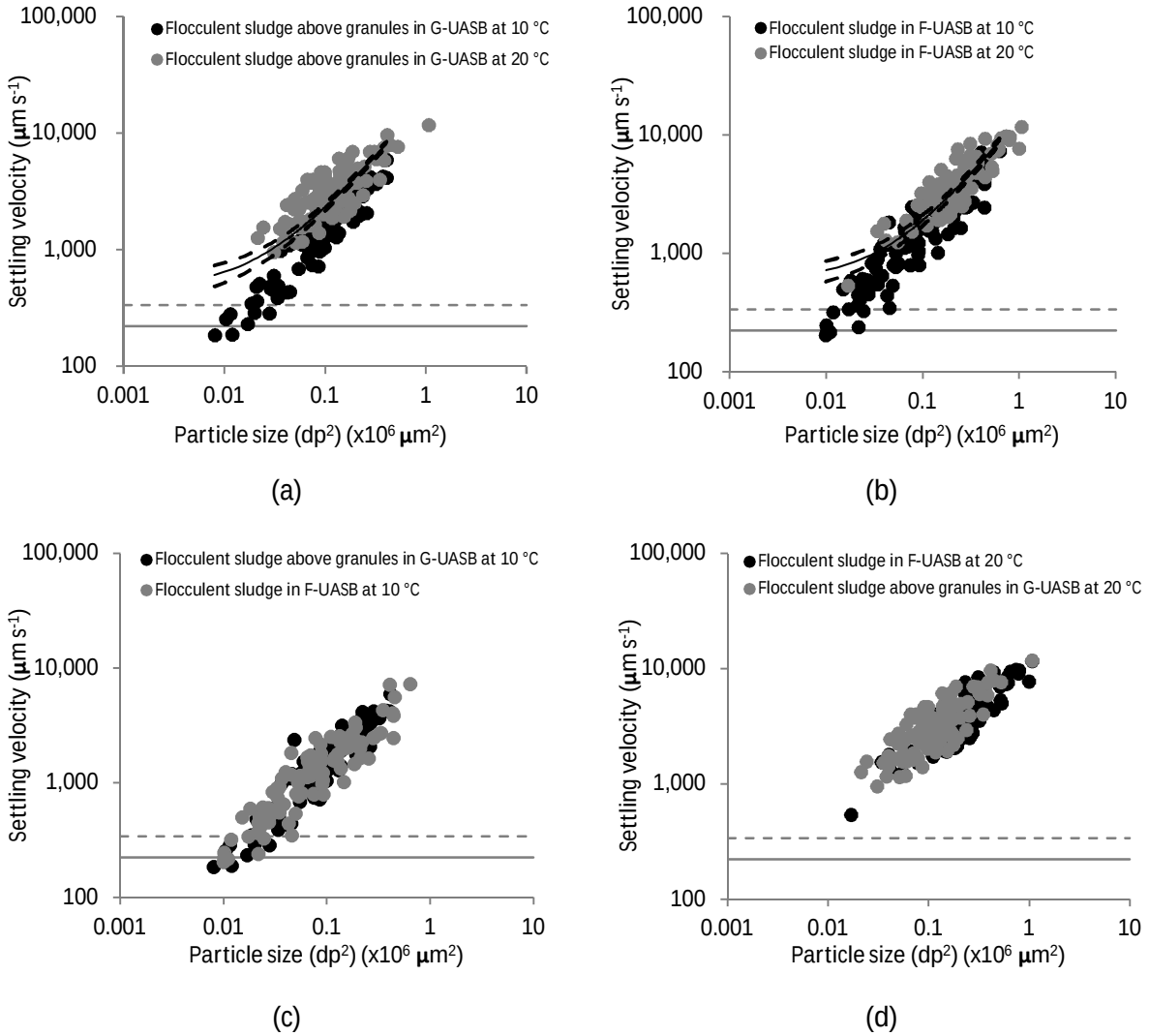

Figure 3-6. Impact of temperature on particle settling velocity in G-UASB and F-UASB (the average temperature when sampling particles from G-UASB and F-UASB reactors was 19.6±0.5 °C). Grey line represents V_{up} liquid (0.8 m h^{-1}, 222 μm s^{-1}), dashed grey line represents V_{up} mixed gas and liquid (1.22 m h^{-1}, 339 μm s^{-1}). Black line represents linear trend line of predicted settling velocity at 20 °C calculated from the particle settling velocity at 10 °C. Dashed black line represents confidence interval range (95 %). Impact of temperature on particle settling velocity for (a) flocculent sludge above granules in G-UASB and (b) flocculent sludge in F-UASB at water temperatures of 10 and 20 °C. Comparison of particle settling velocity between flocculent sludge above granules in G-UASB and flocculent sludge in F-UASB at a water temperature of (c) 10 °C and (d) 20 °C.

The treatment efficiencies also significantly deteriorated when the average reactor temperature reduced from 20 to 10 °C, which was more obvious in the F-UASB (Table 3-1). For example, the SS removal efficiencies decreased from 56-64 % to 36-42 % when the average temperature declined from 20 to 10 °C. At a moderate average temperature of 20 °C, slightly better solids treatment efficiency was observed in the G-UASB than the F-UASB, whilst lower COD_t, PCOD and SS removal efficiencies were obtained in the F-UASB than the G-UASB at average reactor temperature of 10 °C (Table 3-1). Similar CH_4 production was observed from the G-UASB and F-UASB at an average reactor temperature of 20 °C, whilst significantly higher CH_4 production ($p<0.05$) was obtained in the F-UASB at a low average temperature of 10 °C (Table 3-1).

Table 3-1. Impact of temperature on G-UASB and F-UASB treatment performance including sludge blanket development, steady-state operation and breakthrough.

			G-UASB		F-UASB	
			19.5±2.1 °C (13.5-24.0 °C)[a]	10.2±1.5 °C (7.8-13.5 °C)[a]	19.5±2.1 °C (13.5-24.0 °C)[a]	10.2±1.5 °C (7.8-13.5 °C)[a]
Effluent	SS	mg L^{-1}	45±14	69±11[#]	54±14*	75±9[#,*]
	COD_t	mg L^{-1}	113±36	129±19[#]	122±35	140±25[#,*]
	PCOD	mg L^{-1}	57±30	66±20[#]	67±32	80±17[#,*]
	SCOD	mg L^{-1}	55±12	64±13[#]	54±14	60±13[#]
	BOD_5	mg L^{-1}	61±15	84±8[#]	61±15	88±10[#]
	Particle size (d_{50})	µm	138±34	83±28[#]	237±53*	161±35[#,*]
Removal efficiency	SS	%	64±12	42±13[#]	56±14*	36±14[#,*]
	COD	%	51±18	41±14[#]	45±22	36±16[#,*]
	PCOD	%	60±24	52±18[#]	55±25	43±19[#,*]
	SCOD	%	38±16	18±12[#]	39±15	24±14[#]
	BOD_5	%	46±14	26±17[#]	45±16	19±11[#]
CH_4 production	Headspace	STP L d^{-1}	3.3±2.0	0.3±0.2[#]	3.7±2.3	0.8±0.3[#,*]
	Headspace + dissolved	STP L d^{-1}	6.7±1.7	2.9±1.2[#]	7.0±1.3*	6.6±0.8[#,*]

a. Show temperature range in the bracket
STP: standard temperature and pressure
* Statistical difference ($p<0.05$) between G-UASB and F-UASB at 20 °C, G-UASB and F-UASB at 10 °C
[#] Statistical difference ($p<0.05$) between G-UASB at 20 °C and G-UASB at 10 °C, F-UASB at 20 °C and F-UASB at 10 °C

In order to further compare the G-UASB and F-UASB, the microbial diversity of the granular and flocculent inoculum biomass were measured (Figure 3-7). The relative abundance of bacterial at phylum level demonstrated that *Firmicutes, Bacteroidetes and Proteobacteria* were the dominant bacteria, representing 24.9, 22.8, and 16.0 % in the G-UASB and 20.5, 18.6 and 19.0 % in the F-UASB respectively (Figure 3-7a). Analysing

the archaeal microbial communities of the granular and flocculent inoculum biomass indicated that *Methanosaeta* and *Methanospirillum* were the two dominant archaea *at* genus level despite the difference of the relative abundances (Figure 3-7b). The FISH analysis was further conducted to evaluate the microbial spatial distributions within granules (Figure 3-8). Two-layer structure in the granules was observed, with the bacterial cell layer on the surface and an inner layer of archaeal cell including *Methanosaeta*.

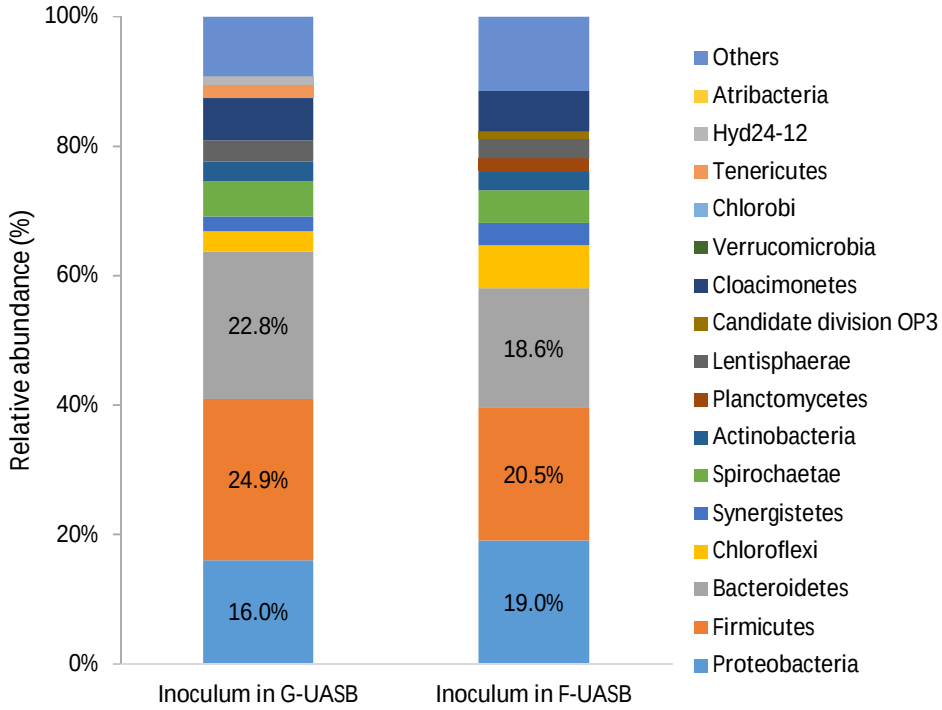

(a)

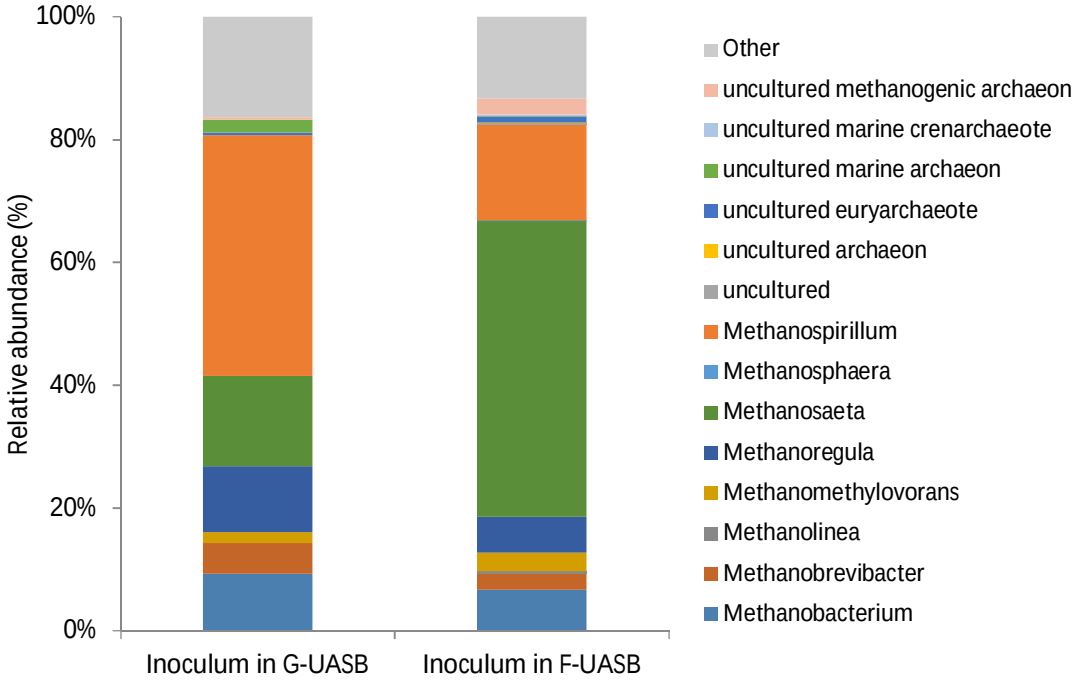

(b)

Figure 3-7. (a) Major bacterial phyla and their relative abundance of inoculum sludge in G-UASB and F-UASB (bacterial phyla with abundance over 1 %). (b) Relative abundance of all archaea at genus level.

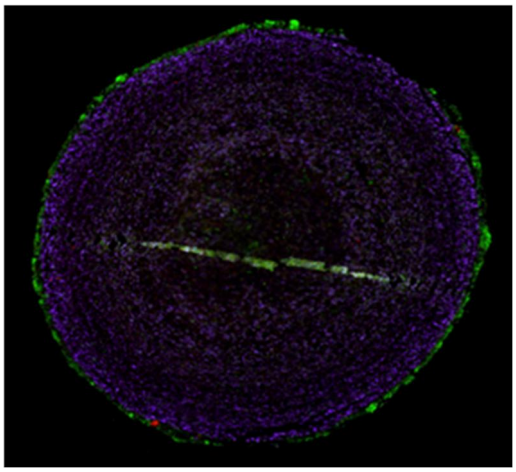

Figure 3-8. The spatial distribution of granules by fluorescence in situ hybridisation (FISH) analyses viewed by confocal laser scanning microscope (CLSM). Cells in green are bacteria hybridised by the Bacteria (EUB338-I, EUB338-II, EUB338-III) probe and cells in purple are methanosaeta co-hybridised by the Archaea (ARCH915) and the Methanosaeta (MX825) probes.

3.3.4 Adjustment of V_{up} to maintain sludge blanket stability

The impact of V_{up} on the sludge blanket stability and PCOD entrapment were investigated (Figure 3-9). With the V_{up} reduced from 0.8 to 0.4 m h^{-1}, the sludge blanket of the F-UASB became more stable, maintaining the X/XT below the separator during the 60-day trial. After about 20 days, the PCOD C/C_0 started to increase at the V_{up} of 0.8 m h^{-1}, whilst it still kept less than 20 % at a V_{up} of 0.4 m h^{-1}. For the G-UASB, although stable sludge blanket was observed for both V_{up} of 0.4 and 0.8 m h^{-1}, lower PCOD C/C_0 was obtained with a V_{up} of 0.4 m h^{-1}. The UASB treatment efficiencies were improved for both the G-UASB and F-UASB by reducing the V_{up} from 0.8 to 0.4 m h^{-1} (Table 3-2). For instance, the SS removal efficiencies increased from 59±9 to 70±15 % and from 50±12 to 65±14 % for the G-UASB and F-UASB respectively. Similar treatment efficiencies were obtained at the V_{up} of 0.4 m h^{-1} for the G-UASB and F-UASB.

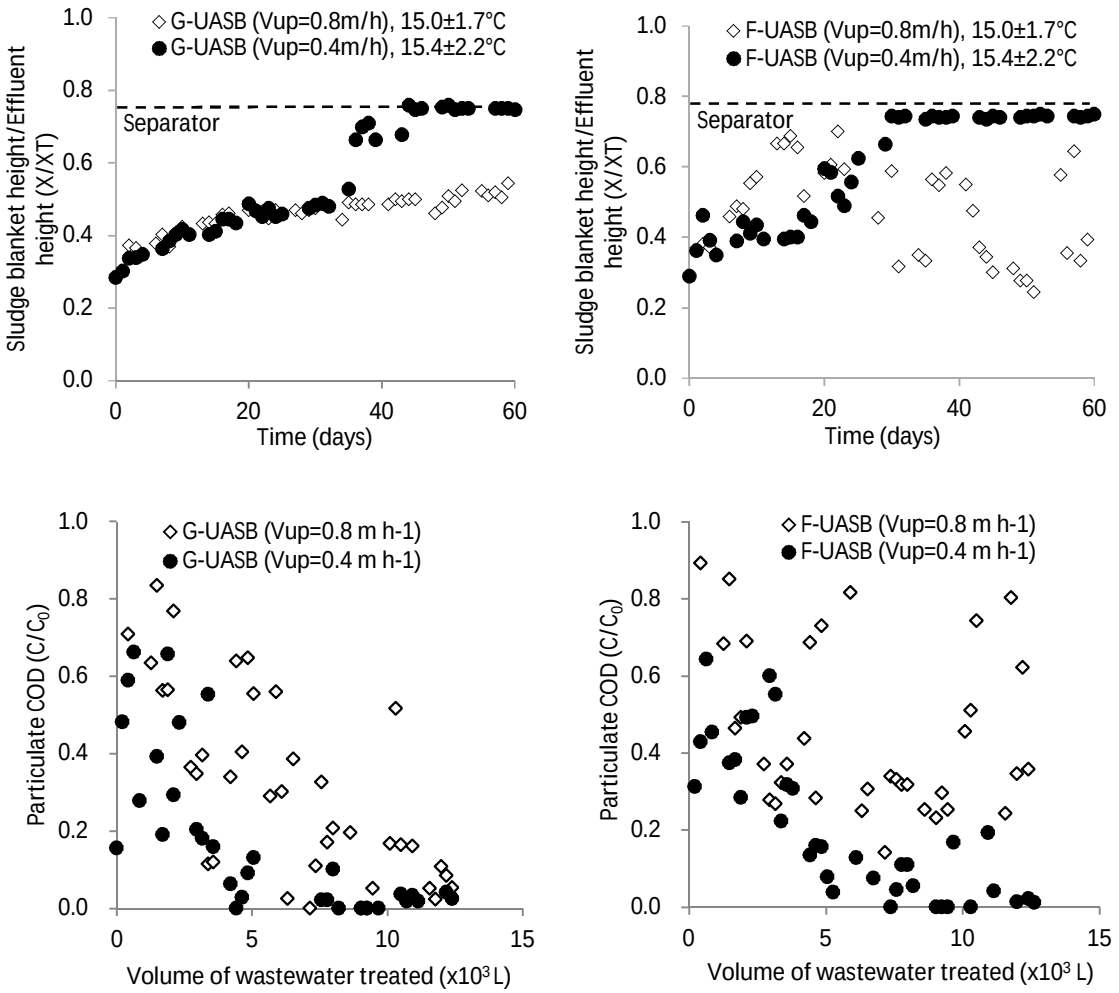

Figure 3-9. Impact of upflow velocity (0.8 and 0.4 m h^{-1}) on sludge blanket stability and particulate COD separation.

Table 3-2. UASB performance under different upflow velocity (0.8 and 0.4 m h^{-1}) including sludge blanket development, steady-state operation and breakthrough, average temperature of 15.0-15.4 °C.

			G-UASB		F-UASB	
			V_{up}=0.8 m h^{-1}	V_{up}=0.4 m h^{-1}	V_{up}=0.8 m h^{-1}	V_{up}=0.4 m h^{-1}
Effluent	SS	mg L^{-1}	59±13	45±21#	71±9*	52±17#
	COD	mg L^{-1}	122±43	94±39#	149±37*	76±32#
	PCOD	mg L^{-1}	54±42	28±26#	77±34*	27±26#
	SCOD	mg L^{-1}	69±8	66±7#	72±11	52±12*,#
	BOD_5	mg L^{-1}	77±16	63±12	81±13*	56±10#
Removal efficiency	SS	%	59±9	70±15#	50±12*	65±14#
	COD	%	54±15	57±18	43±16*	63±16#
	PCOD	%	69±24	81±20#	55±21*	81±19#
	SCOD	%	32±11	18±12#	29±12	32±18*
	BOD_5	%	43±14	33±16	40±10	41±14
CH_4 production	Headspace	STP L d^{-1}	1.3±0.6	1.3±0.8	1.9±0.6	1.9±1.2
	Headspace + dissolved	STP L d^{-1}	5.3±0.7	6.5±2.0#	7.1±0.9*	8.3±1.7*,#

a. Show temperature range in the bracket
STP: standard temperature and pressure
* Statistical difference ($p<0.05$) between G-UASB and F-UASB at V_{up}=0.8 m h^{-1}, G-UASB and F-UASB at V_{up}=0.4 m h^{-1}
# Statistical difference ($p<0.05$) between G-UASB at V_{up} of 0.4 and G-UASB at V_{up} of 0.8 m h^{-1}, F-UASB at V_{up} of 0.4 and G-UASB at V_{up} of 0.8 m h^{-1}

3.4 Discussion

This study demonstrated that solids accumulation in the UASB reactors enhanced the treatment efficiency and improved gas production during the steady-state operation. This can be explained by the filtration capacity of the sludge blanket formed either within the F-UASB sludge bed or above the granular matrix in the G-UASB. Three stages of operations (sludge blanket development, steady-state operation and breakthrough) were identified and determined for both G-UASB and F-UASB reactors. During the steady-state operation, effective PCOD entrapment with a high average removal of 77 % were obtained for both the G-UASB and F-UASB (Figure 3-2b). Similarly, Umeura and Harada (2000) also obtained a high PCOD removal of 80 %, a result obtained from a G-UASB treating crude municipal wastewater at 13-25 °C. With an increase of the solids accumulation, a critical solids concentration (sludge blanket height) was reached, leading to solids breakthrough in the effluent (Figure 3-2). Previous studies (Cavalcanti et al., 1999; Sayed and Fergala, 1995) also observed solids washout at a high sludge bed height. This was exacerbated by higher biogas production (Figure 3-3a), which was

introduced through partial hydrolysis of the entrapped particulate matter at an extended solids retention time. Soluble COD increase was also observed (Figure 3-3b), which we suggest is a product of hydrolysis following extended solids storage. The hydrolysis of the retained solids was also supported by about 80 % of residual energy reduction from the initial solids in the influent (primary sludge) to the solids accumulated in the reactor for 140 days (Figure 3-4). Several authors also observed the partial hydrolysis of the retained solids with crude municipal wastewater fortified with primary sludge or settled municipal wastewater (Lester et al., 2013; Lew et al., 2004).

At a moderate average temperature of 20 °C, similar treatment efficiencies were achieved in G-UASB and F-UASB with slightly better solids treatment efficiency in the G-UASB (Table 3-1). When both UASBs were operated at a lower average temperature of 10 °C, sludge blanket instability and solids washout were observed (Figure 3-5, Table 3-1). Previous studies also demonstrated reactor performance deteriorations at lower reactor temperatures due to solids washout treating municipal wastewater for both G-UASB and F-UASB (Lew et al., 2004; Syutsubo et al., 2011). This might be attributed to the reduced particle settling velocity due to the increased wastewater viscosity at low temperatures (Lettinga et al., 2001; Mahmoud et al., 2003) according to Stoke's law (Equation 3-5). This was corroborated by the noticeable settling velocity reductions for both flocculent sludge above granules in the G-UASB and flocculent sludge in the F-UASB, when the water temperature reduced from 20 to 10 °C (Figure 3-6). In this study, the settling velocity of some small particles (<130-150 µm) at a lower average temperature of 10 °C had already been insufficient to counteract the V_{up} from fixed liquid of 0.8-0.9 m h^{-1} (Figure 3-6). Despite the low daily average headspace methane productions of 0.3-0.8 L d^{-1} (0.01-0.03 L h^{-1}) (Table 3-1), a peak gas flow rate of 13 L h^{-1} was recorded in a previous study with this specific wastewater at similar temperatures. This provided an unsteady-state flow rate of mixed gas and liquid V_{up} of 1.2 m h^{-1} and led to more solids washout with particle size <150-170 µm (Figure 3-6). Compared with F-UASB, G-UASB was more resilient at the lower average temperature of 10 °C, evidenced by higher COD_t, PCOD and SS removal efficiencies in comparison to the F-UASB (Table 3-1). This can be attributed to the larger particle size and higher density of granules (0.5-3 mm),

compared with flocs (10 to 150 µm) (Nicolella et al., 2000), providing larger inertia to follow the liquid (Tsutsumi et al., 1999) and subsequently quicker energy dissipation and less mixing in the G-UASB system. Consequently, despite similar settling velocities being observed for flocculent sludge above granules in G-UASB and flocculent sludge in F-UASB (Figure 3-6), the former is less subject to mixing, resulting in a more stable sludge blanket with a lower tendency to be washed out. The lower headspace methane production in the G-UASB at low temperature may further limit the mixing (Table 3-1). The microbial diversity comparisons of granular and flocculent inoculum biomass indicated similar bacteria dominated by *Firmicutes, Bacteroidetes and Proteobacteria* at phyla level (Figure 3-7a) and archaea dominated by *Methanosaeta* and *Methanospirillum* at genus level (Figure 3-7b) although the relative abundances were different which warrants further research. Consequently, the lower methane production in the G-UASB at low temperatures might be attributed to the larger granule particle size (Nicolella et al., 2000) and two-layer granular structure (Figure 3-8) (Sekiguchi et al., 1999; Tsushima et al., 2010), thus limiting the substrate diffusion into the inner layer of the granules to be utilised to produce methane. This was exacerbated at low temperatures as the diffusion rate was more than 25 % lower at 10 °C than that at 20 °C (Lettinga et al., 2001). Nicolella et al. (2000) also demonstrated a slower diffusional transport in granular biomass than flocculent biomass due to the larger particle size and less porous structure.

In order to maintain the stable sludge blanket, it is suggested to control the solids accumulation at a threshold between the sludge blanket development and steady-state operation period. This will thus extend solids retention to improve the treatment efficiency, enhance biogas production and minimise solids washout. Due to the less stable sludge blanket in the F-UASB, especially at low temperatures, it is therefore suggested to reduce the V_{up} from 0.8 to 0.4 m h^{-1} for the F-UASB at lower temperatures. As a result, similar stable sludge blanket and overall reactor performance can be obtained for both the G-UASB and F-UASB (Figure 3-9, Table 3-2). Lew et al. (2004) also demonstrated a critical V_{up} of 0.35 m h^{-1} in order to limit solids washout for a G-UASB treating settled municipal wastewater. Whilst for the G-UASB, a higher V_{up} is still needed

to promote stratification of particular and granular material in order to obviate the solids accumulation within the granular matrix.

3.5 Conclusions

This study investigated the impact of solids accumulation in both granular and flocculent UASB reactors treating settled municipal wastewater and further proposed engineering solutions to maintain sludge blanket stability in order to sustain the UASB treatment performance in temperate climates. The following conclusions can be drawn:

- Three stages (sludge blanket development, steady-state operation and breakthrough) of operation were determined for both G-UASB and F-UASB.
- During the steady-state operation, solids accumulation in the sludge blanket enhanced treatment efficiency, which can be explained by the filtration capability of the sludge blanket formed either within the F-UASB sludge bed or above the granular matrix in the G-UASB.
- Solids accumulation should be controlled at a threshold between the sludge blanket development and steady-state period, in order to improve the treatment efficiency, enhance biogas production and minimise solids washout.
- At a modest temperature of temperature of 20 °C, similar treatment efficiencies were achieved in G-UASB and F-UASB, whilst at a lower average temperature of 10 °C, G-UASB demonstrated better treatment performance than F-UASB.
- Similar dominated bacteria (*Firmicutes, Bacteroidetes and Proteobacteria*) at phyla level and archaea (*Methanosaeta* and *Methanospirillum*) at genus level were observed in granular and flocculent inoculum biomass, despite the differences of relative abundances. More microbial diversity research with temporal sampling is warranted to further characterise granular and flocculent inoculum biomass.
- Granular inoculum biomass has better stability for solids accumulation than flocculent inoculum biomass especially at low temperatures, suggesting to keep a high V_{up} for the G-UASB whilst reducing the V_{up} for the F-UASB at low temperatures to minimise solids washout.

3.6 Acknowledgements

The authors would like to thank our industrial sponsors: Anglian Water, Scottish Water, Severn Trent Water and Thames Water for their financial and technical support. Dr. Aguilera was supported as part of the EU Framework 7 project "ATWARM" (Marie Curie ITN, No. 238273).

3.7 References

Aiyuk, S., Forrez, I., Lieven, D.K., van Haandel, A. and Verstraete, W. (2006) 'Anaerobic and complementary treatment of domestic sewage in regions with hot climates-A review', *Bioresource Technology*, 97, pp. 2225–2241.

Altman, D.G. and Gardner, M.J. (1988) 'Calculating confidence intervals for regression and correlation', *British Medical Journal*, 296, pp. 1238–1242.

Amann, R.I., Binder, B.J., Olson, R.J., Chisholm, S.W., Devereux, R. and Stahl, D.A. (1990) 'Combination of 16S rRNA-targeted oligonucleotide probes with flow cytometry for analyzing mixed microbial populations', *Applied and Environmental Microbiology*, 56, pp. 1919–1925.

APHA (2005) *Standard Methods for the Examination of Water and Wastewater*. 21st edn. Washington D.C: American Public Health Association.

Caporaso, J.G., Kuczynski, J., Stombaugh, J., Bittinger, K., Bushman, F.D., Costello, E.K., Fierer, N., Peña, A.G., Goodrich, J.K., Gordon, J.I., Huttley, G.A., Kelley, S.T., Knights, D., Koenig, J.E., Ley, R.E., Lozupone, C.A., Mcdonald, D., Muegge, B.D., Pirrung, M., Reeder, J., Sevinsky, J.R., Turnbaugh, P.J., Walters, W.A., Widmann, J., Yatsunenko, T., Zaneveld, J. and Knight, R. (2010) 'QIIME allows analysis of high-throughput community sequencing data', *Nature Methods*, 7, pp. 335–336.

Cavalcanti, P.F.F., Medeiros, E.J.S., Silva, J.K.M. and van Haandel, A. (1999) 'Excess sludge discharge frequency for UASB reactors', *Water Science & Technology*, 40, pp. 211–219.

Chernicharo, C.A.L., van Lier, J.B., Noyola, A. and Bressani Ribeiro, T. (2015) 'Anaerobic sewage treatment: state of the art, constraints and challenges', *Reviews in Environmental Science and Bio/Technology*, 14, pp. 649–679.

Chong, S., Sen, T.K., Kayaalp, A. and Ang, H.M. (2012) 'The performance enhancements of upflow anaerobic sludge blanket (UASB) reactors for domestic sludge treatment - A State-of-the-art review', *Water Research*, 46, pp. 3434–3470.

Daims, H., Brühl, A., Amann, R., Schleifer, K.H. and Wagner, M. (1999) 'The domain-specific probe EUB338 is insufficient for the detection of all bacteria: Development and evaluation of a more comprehensive probe set', *Systematic and Applied Microbiology*, 22, pp. 434–444.

Elimitwalli, T., Zandvoort, M., Zeeman, G., Bruning, H. and Lettinga, G. (1999) 'Low temperature treatment of domestic sewage in upflow anaerobic sludge blanket and anaerobic hybrid reactors', *Water Science & Technology*, 39, pp. 177–185.

Elmitwalli, T.A., Sklyar, V., Zeeman, G. and Lettinga, G. (2002) 'Low temperature pre-treatment of domestic sewage in an anaerobic hybrid or an anaerobic filter reactor', *Bioresource Technology*, 82, pp. 233–239.

Elmitwalli, T., Zeeman, G., Lettinga, G. and E., F. (2001) 'Anaerobic treatment of domestic sewage at low temperature', *Water Science & Technology*, 44, pp. 33–40.

Lester, J., Jefferson, B., Eusebi, A.L., Mcadam, E. and Cartmell, E. (2013) 'Anaerobic treatment of fortified municipal wastewater in temperate climates', *Journal of Chemical Technology and Biotechnology*, 88, pp. 1280–1288.

Lettinga, G., Rebac, S. and Zeeman, G. (2001) 'Challenge of psychrophilic anaerobic wastewater treatment', *Trends in Biotechnology*, 19, pp. 363–370.

Lettinga, G., Roersma, R. and Grin, P. (1983) 'Anaerobic treatment of raw domestic sewage at ambient temperatures using a granular bed UASB reactor', *Biotechnology and Bioengineering*, 25, pp. 1701–1723.

Lew, B., Tarre, S., Belavski, M. and Green, M. (2004) 'UASB reactor for domestic wastewater treatment at low temperatures: A comparison between a classical UASB and hybrid UASB-filter reactor', *Water Science & Technology*, 49, pp. 295–301.

van Lier, J.B., van der Zee, F.P., Frijters, C.T.M.J. and Ersahin, M.E. (2015) 'Celebrating 40 years anaerobic sludge bed reactors for industrial wastewater treatment', *Review Environmental Science Bio/Technology*, 14, pp. 681–702.

Lim, S.J. and Kim, T. (2014) 'Applicability and trends of anaerobic granular sludge treatment processes', *Biomass and Bioenergy*, 60, pp. 189–202.

Liu, Y. and Tay, J.H. (2004) 'State of the art of biogranulation technology for wastewater treatment', *Biotechnology Advances*, 22, pp. 533–563.

Liu, Y., Xu, H.L., Show, K.Y. and Tay, J.H. (2002) 'Anaerobic granulation technology for wastewater treatment', *World Journal of Microbiology and Biotechnology*, 18, pp. 99–113.

Mahmoud, N., Zeeman, G., Gijzen, H. and Lettinga, G. (2003) 'Solids removal in upflow anaerobic reactors, a review', *Bioresource Technology*, 90, pp. 1–9.

Manz, W., Amann, R., Ludwig, W., Wagner, M. and Schleifer, K.H. (1992) 'Phylogenetic oligodeoxynucleotide probes for the major subclasses of proteobacteria: problems and solutions', *Systematic and Applied Microbiology*, 15, pp. 593–600.

Massey, B.S. and Ward-Smith, A.J. (2006) *Mechanics of Fluids*. 8th edn. UK: Taylor & Francis.

McAdam, E.J., Luffler, D., Martin-Garcia, N., Eusebi, A.L., Lester, J.N., Jefferson, B. and Cartmell, E. (2011) 'Integrating anaerobic processes into wastewater treatment', *Water Science & Technology*, 63, pp. 1459–1466.

McKeown, R.M., Scully, C., Enright, A.M., Chinalia, F.A., Lee, C., Mahony, T., Collins, G. and O'Flaherty, V. (2009) 'Psychrophilic methanogenic community development during long-term cultivation of anaerobic granular biofilms', *ISME Journal*, 3, pp. 1231–1242.

Nada, T., Moawad, A., El-gohary, F.A. and Farid, M.N. (2011) 'Full-scale municipal wastewater treatment by up-flow anaerobic sludge blanket (UASB) in Egypt', *Desalination and Water Treatment*, 30, pp. 134–145.

Nicolella, C., Van Loosdrecht, M.C.M. and Heijnen, J.J. (2000) 'Wastewater treatment with particulate biofilm reactors', *Journal of Biotechnology*, 80, pp. 1–33.

Oliveira, S.C. and von Sperling, M. (2011) 'Performance evaluation of different wastewater treatment technologies operating in a developing country', *Journal of Water, Sanitation and Hygiene for Development*, 1, pp. 37–56.

Quince, C., Lanzen, A., Davenport, R.J. and Turnbaugh, P.J. (2011) 'Removing noise from pyrosequenced amplicons', *BMC Bioinformatics*, 12, pp. 1–18.

Rajeshwari, K.V., Balakrishnan, M., Kansal, A., Lata, K. and Kishore, V.V.N. (2000) 'State-of-the-art of anaerobic digestion technology for industrial wastewater treatment', *Renewable and Sustainable Energy Reviews*, 4, pp. 135–156.

Sabry, T. (2008) 'Application of the UASB inoculated with flocculent and granular sludge in treating sewage at different hydraulic shock loads', *Bioresource Technology*, 99, pp. 4073–4077.

Sayed, S.K.I. and Fergala, M.A.A. (1995) 'Two-stage UASB concept for treatment of domestic sewage including sludge stabilization process', *Water Science & Technology*, 32, pp. 55–63.

Seghezzo, L., Guerra, R.G., González, S.M., Trupiano, A.P., Figueroa, M.E., Cuevas, C.M., Zeeman, G. and Lettinga, G. (2002) 'Removal efficiency and methanogenic activity profiles in a pilot-scale UASB reactor treating settled sewage at moderate temperatures', *Water Science & Technology*, 45, pp. 243–248.

Sekiguchi, Y., Kamagata, Y., Nakamura, K., Ohashi, A. and Harada, H. (1999) 'Fluorescence in situ hybridization using 16S rRNA-targeted oligonucleotides reveals localization of methanogens and selected uncultured bacteria in mesophilic and thermophilic sludge granules', *Applied and Environmental Microbiology*, 65, pp. 1280–1288.

Stahl, D.A. and Amann, R. (1991) 'Development and application of nucleic acid probes', in Stackebrandt, E. and Goodfellow, M. (eds.) *Nucleic Acid Techniques in Bacterial Systematics*. Chichester, UK: John Wiley & Sons Ltd., pp. 205–248.

Syutsubo, K., Yoochatchaval, W., Tsushima, I., Araki, N., Kubota, K., Onodera, T., Takahashi, M., Yamaguchi, T. and Yoneyama, Y. (2011) 'Evaluation of sludge properties in a pilot-scale UASB reactor for sewage treatment in a temperate region', *Water Science & Technology*, 64, pp. 1959–1966.

Tchobanoglous, G., Burton, F.L. and Stensel, H.D. (2003) *Wastewater Engineering Treatment and Reuse*. 4th edn. New York: McGraw-Hill Companies.

Tsushima, I., Yoochatchaval, W., Yoshida, H., Araki, N. and Syutsubo, K. (2010) 'Microbial community structure and population dynamics of granules developed in expanded granular sludge bed (EGSB) reactors for the anaerobic treatment of low-strength wastewater at low temperature', *Journal of Environmental Science and Health - Part A Toxic/Hazardous Substances and Environmental Engineering*, 45, pp. 754–766.

Tsutsumi, A., Chen, W. and Kim, Y.H. (1999) 'Classification and characterization of hydrodynamic and transport behaviors of three-phase reactors', *Korean Journal of Chemical Engineering*, 16, pp. 709–720.

Uemura, S. and Harada, H. (2000) 'Treatment of sewage by a UASB reactor under moderate to low temperature conditions', *Bioresource Technology*, 72, pp. 275–282.

Vera, L., Delgado, S. and Elmaleh, S. (2000) 'Gas sparged cross-flow microfiltration of biologically treated wastewater', *Water Science & Technology*, 41, pp. 173–180.

Verberk, J.Q.J.C., Worm, G.I.M., Futselaar, H. and van Dijk, J.C. (2001) 'Combined air-water flush in dead-end ultrafiltration', *Water Science and Technology: Water Supply*, 1, pp. 393–402.

Zaiontz, C. (2018) *Real Statistics Using Excel*. [WWW Document]. URL www.real-statistics.com

Zeeman, G. and Lettinga, G. (1999) 'The role of anaerobic digestion of domestic sewage in closing the water and nutrient cycle at community level', *Water Science and Technology*, 39, pp. 187–194.

3.8 Supplementary data

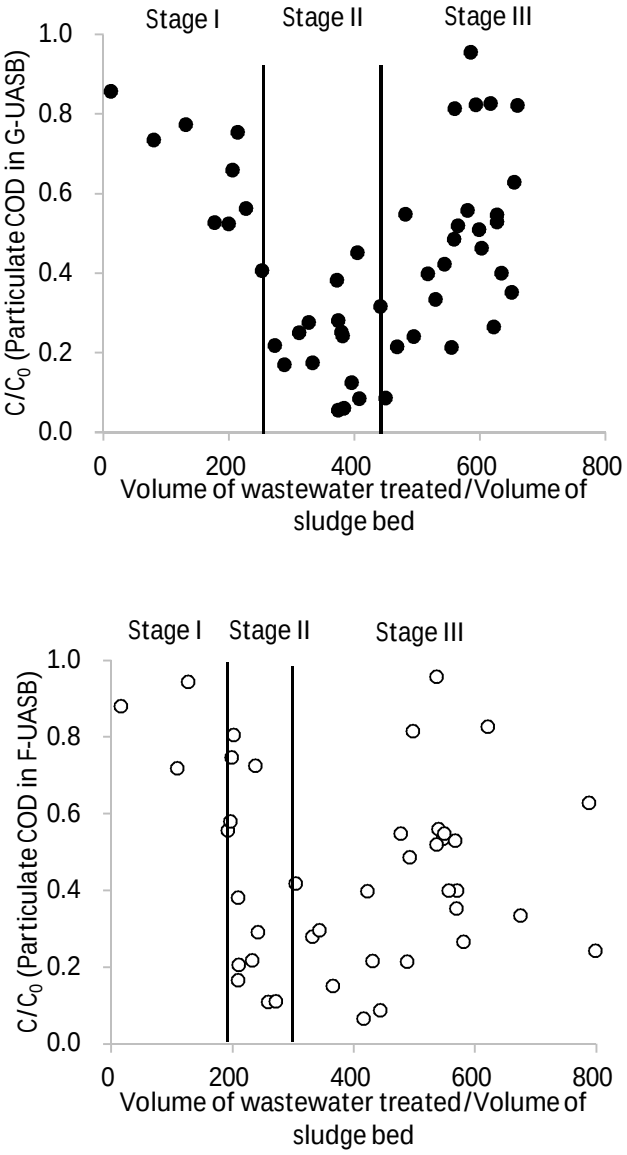

Figure S3-1. Impact of sludge blanket on particulate COD separation (Stage I, sludge blanket development (0-40 d for G-UASB, 0-42 d for F-UASB), Stage II, steady-state operation (41-86 d for G-UASB, 43-65 d for F-UASB), Stage III, breakthrough (87-120 d for G-UASB, 66-120 d for F-UASB). Volume of wastewater treated/volume of sludge bed can be calculated by Equation 3-4.

CHAPTER 4

Comparison of granular and flocculent upflow anaerobic sludge blanket configured anaerobic membrane bioreactors for municipal wastewater treatment

4 Comparison of granular and flocculent upflow anaerobic sludge blanket configured anaerobic membrane bioreactors for municipal wastewater treatment

K.M. Wang[a], A. Soares[a], B. Jefferson[a], E. J. McAdam[a*]
[a]Cranfield Water Science Institute, Vincent Building, Cranfield University, Bedfordshire, MK43 0AL, UK

Abstract

Anaerobic membrane bioreactor (AnMBR) in upflow anaerobic sludge blanket (UASB) configuration has been demonstrated to be advantageous to reduce energy demand for membrane fouling control. However, this is dependent upon the stability of the UASB reactor, as solids and organics separations in the UASB will affect the downstream membrane operation. Due to the superior settling characteristics, granular inoculum can be inferred to be conducive to AnMBR resilience compared with flocculent inoculum. However, few studies have applied granular inoculum in AnMBR, and further there is no direct comparison of granular and flocculent inoculums in UASB configured AnMBR. In this study, a comparison was conducted with two pilot scale UASB configured AnMBRs treating settled municipal wastewater, focusing on bulk sludge characteristics and membrane fouling propensity. The results showed that membrane inclusion provided similar permeate quality compliance to COD, BOD_5 and TSS International discharge standards for both granular and flocculent UASB configured AnMBRs. The membrane fouling comparison demonstrated lower fouling propensity with granular than flocculent AnMBR at low average temperatures, due to a more stable sludge blanket in the former. However, reducing upflow velocity was evidenced to be effective to sustain sludge blanket stability and minimise solids washout of flocculent AnMBR at low average temperatures. Importantly, the low energy demand pseudo dead-end gas sparging strategy can be applied to both granular and flocculent AnMBRs with sustained membrane operation by controlling the sludge blanket or possibly reducing the pseudo dead-end cycle length. These findings demonstrate that granular inoculum has good stability which exerts a positive influence on sustained permeability, whilst membrane inclusion can dissipate the disadvantages of flocculent biomass to deliver similar sustained membrane operation provided the sludge blanket is controlled.

Keywords: UASB, MBR, sewage, resilience, cost, energy, permeate quality

4.1 Introduction

Anaerobic processes are an attractive alternative to aerobic technologies for municipal wastewater treatment at ambient temperature, as they use less energy, produce less sludge and can increase the energy recovered from wastewater through biogas production (Gouveia et al., 2015a; Martin Garcia et al., 2013). The key challenge for anaerobic processes is to prevent biomass washout due to the slow growth rate of anaerobic bacteria. Such effects are exacerbated in municipal wastewater treatment as the low temperature and limited substrate availability further limit their growth. Upflow anaerobic sludge blanket (UASB) reactors are the most widely used high-rate anaerobic reactors for municipal wastewater treatment, where the upflow velocity (V_{up}) introduces a hydraulic selection pressure which extends the solids retention time (SRT) for sludge of high density, to yield a high biomass concentration (Chong et al., 2012).

Several authors have now investigated the integration of UASB reactors into anaerobic membrane bioreactor (AnMBR) technology. Inclusion of the membrane allows independent control of SRT, which obviates the risk of washout (Robles et al., 2012) and can produce solids-free permeate that is low in chemical oxygen demand (COD) (Martin Garcia et al., 2013; Smith et al., 2013). From the few studies that have compared AnMBR configurations, UASB configured AnMBR have also been indicated to promote lower irreversible fouling than AnMBR configured as completely stirred tank reactors (CSTR) (Martin-Garcia et al., 2011; van Voorthuizen et al., 2008). This was ascribed to the lower solids concentration in the membrane tank which limited fouling due to cake layer formation (Liao et al., 2006; Ozgun et al., 2015). Martin-Garcia et al. (2013) illustrated the nascent advantage of low solids membrane operation through application of a pseudo dead-end gas sparging strategy that required a gas sparging frequency of only 1 min for every 10 min to sustain permeability, therefore providing a considerable reduction in membrane energy demand. This is of importance since it provides the potential to move towards the energy neutral sewage treatment as one of the main motivations for AnMBR treating municipal wastewater (McAdam et al., 2011). However, the advantage that UASB configured AnMBR provides to membrane operation is strongly dependent upon the stability of the UASB reactor, as the solids and organics separations are directly associated with the downstream membrane tank characteristics. Both

suspended solids and COD removal have been noted to decline with temperature decrease in UASB reactors (Lew et al., 2004; Syutsubo et al., 2011; Uemura and Harada, 2000), which leads to solids washout sufficient to increase bulk sludge concentration in the downstream membrane tank, and may therefore influence the membrane permeability attained.

Start-up without the use of inoculum introduces a significant lag time before steady-state is reached (up to 6 months), which is not feasible at industrial scale (Chong et al., 2012; Seghezzo et al., 1998). Therefore granular or flocculent biomass is used for inoculation (Chong et al., 2012; Liu and Tay, 2004). Granular biomass has been shown to possess superior settling characteristics (Liu et al., 2002; Sabry, 2008) and higher specific activity (Lim and Kim, 2014), subsequently providing improved treatment performance versus flocculent UASB reactors. However, much of this knowledge is based on treatment of soluble industrial wastewater (van Lier et al., 2015; Rajeshwari et al., 2000) rather than municipal wastewater (Elimitwalli et al., 1999; Lettinga et al., 1983), the latter being inherently more complex due to the broad particle size distribution of the influent organic fraction (Martin-Garcia et al., 2011). With the membrane inclusion to form an AnMBR, this advantage over flocculent biomass may not be that distinct, which could eliminate the use of granular inoculum with limited sources (Liu and Tay, 2004) and high cost between 500 and 1000 USD per ton wet weight (Liu et al., 2002). During operation, granule disintegration has also been noted (Aiyuk and Verstraete, 2004), and as granulation has not been obviously identified in municipal wastewater (Abbasi and Abbasi, 2012; Aiyuk et al., 2006), there will be continued demand for granular inoculum, which poses economic and operational risks due to the current absence of a secure supply chain.

It can be inferred from the advanced settling characteristics of granular sludge (Liu et al., 2002) that granular biomass will be advantageous to AnMBR resilience. However, to date, few studies have applied granular inoculum in AnMBR (Chu et al., 2005; Gouveia et al., 2015b; Martin-Garcia et al., 2011; Martin Garcia et al., 2013) and limited studies compared granular and flocculent biomass in order to infer an advantage of one inoculum over another (Lettinga et al., 1983; Sabry, 2008) without direct comparison in

UASB configured AnMBR treating municipal wastewater. Martin et al. (2011, 2013) compared a granular UASB (G-UASB) configured AnMBR to a flocculent CSTR configured AnMBR and identified the G-UASB configured AnMBR to have lower fouling propensity. However, due to the different reactor configurations applied, the direct impact of granular and flocculent biomass on membrane fouling in UASB configured AnMBR is still not fully understood. This is critical to ascertain how dependent the inoculum selection is to achieving the low energy membrane operation with UASB configured AnMBR. The aim of this study is therefore to compare the impact of inoculum selection on membrane permeability in UASB configured AnMBR, in order to determine whether the proposed advantage of granular biomass outweighs the risks to cost and supply, and further to identify whether membrane inclusion can dissipate the apparent disadvantages associated with flocculent biomass. Specific objectives are: (i) to evaluate the transition from UASB to UASB configured AnMBR to determine the impact of membrane integration on separation and bulk sludge characteristics; (ii) to discern how inoculum selection influences the bulk sludge matrix and hence membrane fouling propensity; and (iii) to ascertain whether both granular and flocculent biomass can sustain membrane permeability using alternative membrane gas sparging strategies that can promote low energy membrane operation.

4.2 Material and methods

4.2.1 UASB and UASB configured AnMBR pilot plants

Two 70 L cylindrical UASB reactors (0.2 m diameter x 1.8 m height) were operated in parallel (Model products, Wootton, UK) with a solid/liquid/gas separator located at the top of the column to form a total reactor height of 2.0 m (Figure 4-1). Granular and flocculent biomass were imported as inoculum sludge. The G-UASB was initially inoculated with 15 L granular sludge from a mesophilic UASB used for pulp and paper industry. The flocculent UASB (F-UASB) was inoculated with 15 L municipal digested sludge treating a mixture of primary and secondary sludges with 3.6 % total solids (78 % volatile solids). Settled wastewater from Cranfield University's sewage treatment works was fed to the bottom of the two UASB reactors through peristaltic pumps (520U, Watson Marlow, Falmouth, UK). Both G-UASB and F-UASB were operated at a hydraulic

retention time (HRT) of 8 h for 360 days to acclimatise before this experiment. The internal recirculation was operated by peristaltic pumps (620S, Watson Marlow, Falmouth, UK) to keep the V_{up} of 0.8-0.9 m h^{-1} (Tchobanoglous et al., 2003). For the G-UASB, the granular sludge bed expanded to about 30 % of the total column height, the light sludge fraction comprised of dispersed growth flocs from the influent formed a sludge blanket layer above the granular sludge bed (Aiyuk et al., 2006; Chong et al., 2012). For the F-UASB reactor, there is no obvious differentiation between the sludge blanket and inoculum flocculent sludge bed.

Following conversion of the UASB reactor to an AnMBR, effluent from the G-UASB and F-UASB overflowed into a 30 L cylindrical membrane tank (0.17 m diameter x 1.25 m height) (Figure 4-1). The retentate was recycled back to the bottom of the UASB reactor through a peristaltic pump (620S, Watson Marlow, Falmouth, UK) to sustain the V_{up}. The membrane module (ZW-10) (SUEZ Water & Process Technologies, Oakville, Canada) comprised of four elements, each of which consisted of 76 polyvinylidene fluoride (PVDF) hollow fibres (0.52 m in length and 1.9 mm outer diameter). The membrane had a nominal pore size of 0.04 µm and total surface area of 0.93 m^2. Permeate was withdrawn from the membrane header by a peristaltic pump (520U, Watson Marlow, Falmouth, UK). The transmembrane pressure (TMP) was monitored by a pressure transducer (-1-1 bar, Gems sensor, Basingstoke, UK) in the permeate line recording by a data logger (ADC-2006, Pico Technology, St Neots, UK). Nitrogen-enriched air for gas sparging was produced by a nitrogen generator (NG6, Noblegen gas generator, Dunston, UK). In the standard gas sparging condition, intermittent filtration (10 min on/1 min off) with cyclic gas sparging (10 s on/10 s off) was deployed (Martin Garcia et al., 2013). Low energy demand pseudo dead-end (DE) gas sparging strategy was applied in which filtration was conducted without gas sparging followed by membrane relaxation coupled with gas sparging (Intermittent filtration, 10 min on/1 min off; intermittent gas sparging, 1 min on/10 min off). The intermittent gas sparging was controlled using a solenoid valve (Type 6014, Burkert, Ingelfingen, Germany) connected to a time relay (815E, Crouzet, Valence, France) and the intermittent filtration was controlled by another time relay (PL2R1, Crouzet, Valence, France). Specific gas demand per unit

membrane area (SGD_m) was set at 1.1 $m^3 m^{-2} h^{-1}$ and controlled by a needle valve (0-30 L min^{-1}, Key Instruments, Langhorne, US). In order to directly compare the transition from UASB to UASB configured AnMBR, the tests were conducted in the same season with a similar low average temperature range of 10-13 °C. The HRT was fixed to 8 h in the UASB which resulted in an initial permeate flux of 12 L $m^{-2} h^{-1}$, normalised to 20 °C according to Judd (2011):

$$J = J_{20} \cdot 1.025^{(T-20)} \quad (4\text{-}1)$$

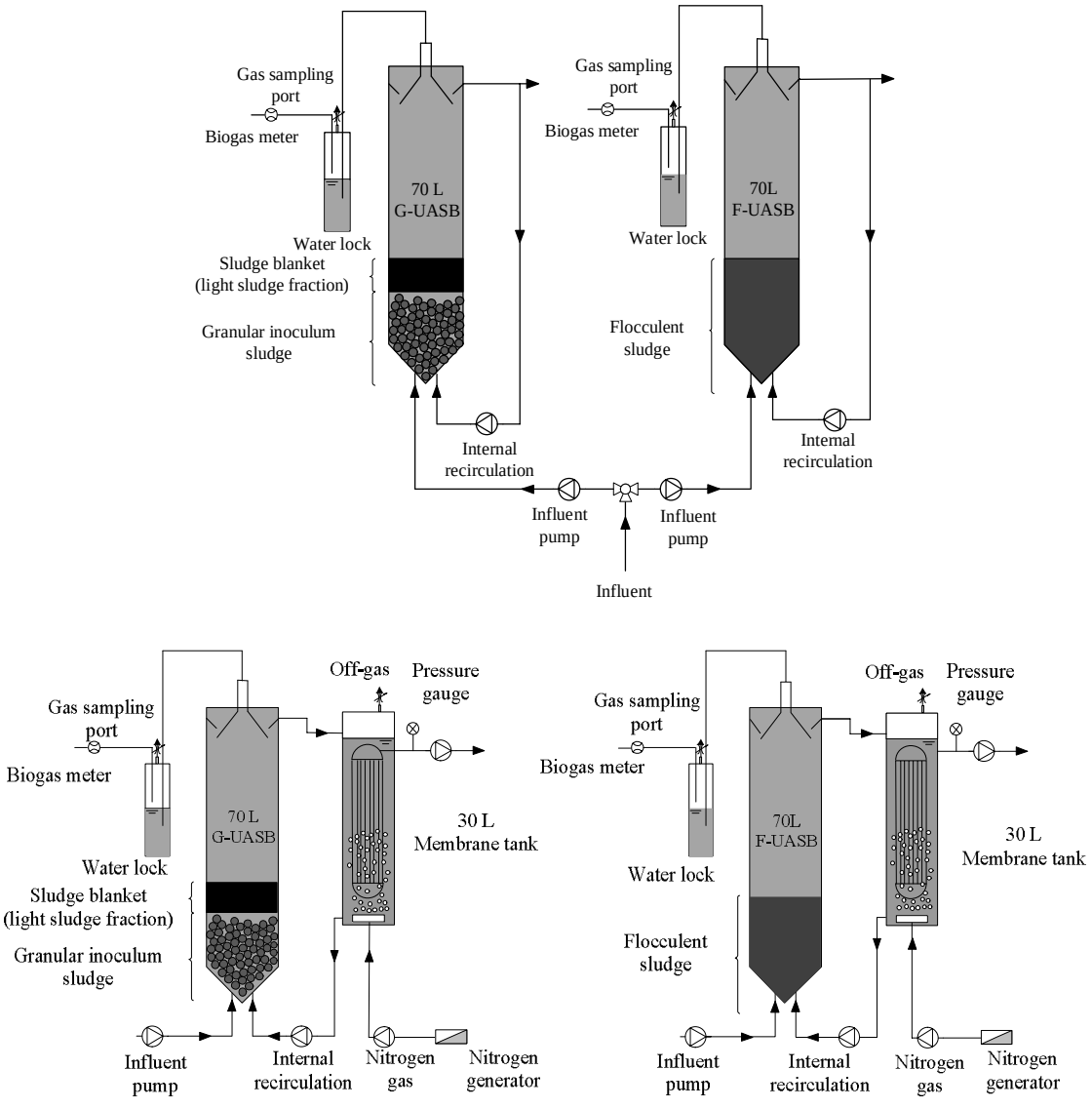

Figure 4-1. Schematics of G-UASB and F-UASB (top) and G-AnMBR and F-AnMBR (bottom).

Each test lasted for around 20 days to monitor the G-AnMBR and F-AnMBR performance during steady state. Another two normalised initial fluxes of 7.5 L m^{-2} h^{-1} and 16.5 L m^{-2} h^{-1} (equivalent to HRT of 12.8 and 5.8 h respectively) were also conducted for both the G-AnMBR and F-AnMBR, to compare membrane fouling. To evaluate the impact of temperature on the system resilience, both AnMBRs were also operated during a period of high seasonal temperature (21-23 °C, British summer time).

Membrane fouling cake fractionation was analysed according to the method using by Metzger et al. (2007). Darcy's law was used to calculate the membrane resistance (Equation 4-2). The intrinsic resistance of the membrane (R_m) was first determined by a tap water permeability test. After the long-term test around 200 h (equivalent to a total filtered volume of 1500 L), total resistance of fouled membrane was calculated (R_{total}). The fouled membrane from the G-AnMBR and F-AnMBR were cleaned by the following protocol: (1) rinsing with 45 L tap water; (2) backwash with 45 L tap water at 22.5 L m^{-2} h^{-1} (300 % of permeate); (3) chemical desorption with sodium hydroxide (pH=11-12) for 24 h. Tap water permeability tests were conducted to obtain hydraulic resistance after rinsing (R_{rinsed}) and backwash (R_{bw}). The hydraulic resistance of total fouling layer (R_{TF}), and hydraulic resistances caused by upper, intermediate and lower fraction (R_{UF}, R_{IF}, R_{LF}) were calculated according to the following Equations (4-3) to (4-6):

$$R = \frac{TMP}{\mu \cdot J} \quad (4\text{-}2)$$

$$R_{TF} = R_{total} - R_m \quad (4\text{-}3)$$

$$R_{UF} = R_{total} - R_{rinsed} \quad (4\text{-}4)$$

$$R_{IF} = R_{rinsed} - R_{bw} \quad (4\text{-}5)$$

$$R_{LF} = R_{bw} - R_m \quad (4\text{-}6)$$

The relationship between the total hydraulic resistances (R_{TF}) and total concentration of total biopolymer (TBP, D_p) in the fouling layer can be expressed as specific biopolymer resistance (α_{TBP}, m kg^{-1}) (McAdam and Judd, 2008; Metzger et al., 2007; Nagaoka et al. , 1996):

$$\alpha_{TBP} = \frac{R_{TF}}{D_p} \quad (4\text{-}7)$$

Pseudo DE filtration cycle analysis was conducted by using the three profile characteristics (Vera et al., 2015b). The initial transmembrane pressure (TMP_i) is related

to hydraulic resistance by the clean membrane (R_m) and the internal residual fouling resistance (R_{if}):

$$TMP_i = J \cdot \mu \cdot (R_m + R_{if}) \quad (4\text{-}8)$$

where J is the permeate flux (L m^{-2} h^{-1}) and μ is the permeate viscosity (Pa. s). Within the filtration cycle, fouling through cake formation can be characterised by a linear increase in TMP. The slope of the straight line can be defined as cake fouling rate (r_f):

$$TMP = TMP_i + r_f \cdot t \quad (4\text{-}9)$$

The TMP drop from cake layer formation (ΔTMP_c) can be described considering the suspension characteristics (Vera et al., 2015a):

$$\Delta TMP_c = TMP - TMP_i = \mu\alpha\varpi J^2 t \quad (4\text{-}10)$$

where α is specific cake resistance (m kg^{-1}), ω is the solids concentration in the cake per unit filtrate volume (assuming similar to MLSS concentration in the bulk sludge, kg m^{-3}).

4.2.2 Analytical methods

Biochemical oxygen demand (BOD_5) and mixed liquor suspended solids (MLSS) were measured according to Standard Methods (APHA, 2005). Chemical oxygen demand and soluble COD (filtered with 1.2 μm filter paper, 70 mm Glass Fibre Filter Paper Grade GF/C, Whatman, GE Healthcare Life Sciences, Little Chalfont, UK) were analysed with Merck vial test kit (Merck KGaA, Darmstadt, Germany). Bulk sludge particle size distribution and zeta potential were measured with Mastersizer 3000 and Zetasizer Nano ZS respectively (Malvern Instruments Ltd, Malvern, UK). Protein concentrations were measured using the modified Lowry method ($UV_{750\ nm}$) (Lowry et al., 1951) with bovine serum albumin (BSA) (Sigma-Aldrich, UK) as the standard while carbohydrate concentrations were measured using and Dubios phenol sulphuric acid method ($UV_{490\ nm}$) (Dubois et al., 1956) with glucose (Acros Organics, UK) as the standard reference. Biogas flow rate was measured with a gas meter (TG0.5, Ritter, Bochum, Germany). Methane (CH_4) composition was analysed by a gas analyser (Servomex 1440, Crowborough, UK).

Molecular weight fractionation experiments were conducted to determine the colloidal matter fractions using an Amicon 8400 series stirred cell (EMD Millipore HQ, Billerica, USA) at room temperature (20 °C) with 2 bars pressure of nitrogen-enriched

air (BOC Ltd, Guildford, UK). The samples were pre-filtered using 1.2 μm filter and subsequently filtered through polyethersulfone ultrafiltration membrane of 500, 100 and 10 kDa (EMD Millipore HQ, Billerica, USA). Concentration polarisation was limited by using a stirrer (100 rpm) and the adopted filtrate/retentate ratio of 0.4. A cross-flow membrane cell (CF-042, Sterlitech Corporation, Kent, USA) was used as a diagnostic tool with critical flux (J_c) as the surrogate measure (Figure 4-2). A PVDF flat sheet membrane was used (pore size, 0.08 μm; surface area, 42 cm^2); all experiments were conducted at 20 °C. The J_c tests were determined with the flux step method (Le Clech et al., 2003) in which successive filtration with flux steps of 2 L m^{-2} h^{-1} were maintained for 15 mins and average TMP monitored. During analysis of the arising cake, rinsing, backwash and desorption solutions were collected to measure TBP and soluble microbial products (SMP) (filtered samples with 1.2 μm filter paper) through protein and carbohydrate analyses. All analyses were conducted in triplicate. Statistical analysis was completed with the software IBM SPSS Statistics 23. Data sets normality was first analysed through Shapiro-Wilk tests. For the normal distributed data sets, ANOVA tests were applied otherwise non-parametric Mann-Whitney U tests for independent data were utilised. All the statistical differences were based on 95 % of the confidence level ($p<0.05$).

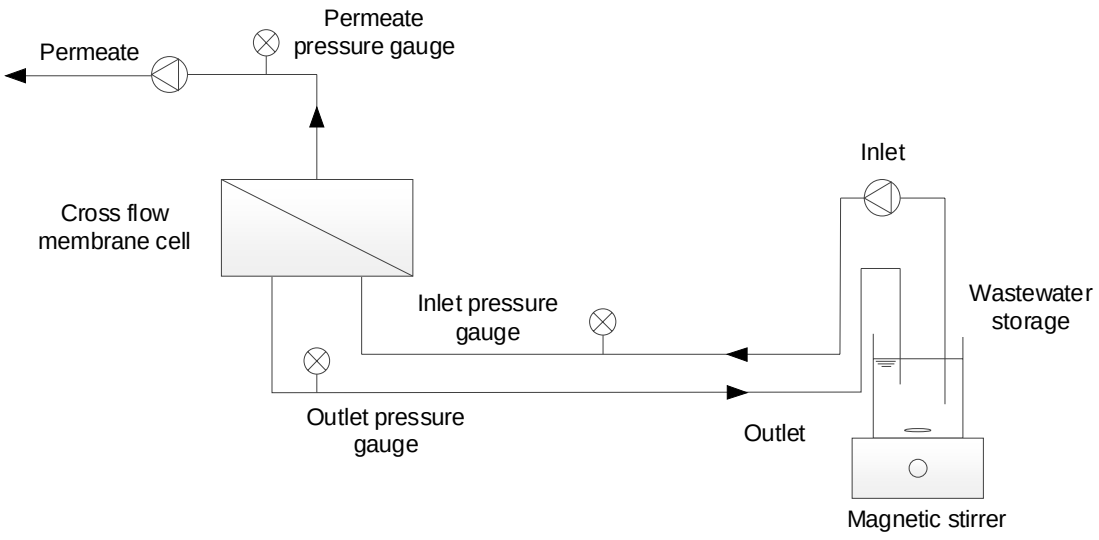

Figure 4-2. Schematics of membrane cell for critical flux test in the laboratory (ambient temperature around 20 °C).

4.3 Results

4.3.1 Comparison of granular and flocculent UASB and UASB configured AnMBR

For both the G-UASB and F-UASB, poor TSS, COD_t and BOD_5 removals of 39-42, 36-41 and 19-26 % respectively were observed, which was more obvious in the F-UASB at an average temperature of 10 °C (Table 4-1). After UASB coupled with membrane to form AnMBR, solids-free (not detected) permeate with consistently low COD_t of 34-39 mg L^{-1} and BOD_5 of 10-13 mg L^{-1} were achieved for both the G-AnMBR and F-AnMBR, indicating a stable performance during the study compliance to the International discharge standards. Higher headspace CH_4 production was observed in the flocculent than granular system under similar temperature variations (Table 4-1).

Table 4-1. Impact of membrane addition on the overall system performance.

			G-UASB	F-UASB	G-AnMBR	F-AnMBR
	Temperature	°C	10.2±1.5	10.2±1.5	12.5±1.8	13.1±1.8
TSS	Influent	mg L^{-1}	113±23	113±23	105±9	127±29*
	UASB effluent	mg L^{-1}	69±11	75±9*	168±49	325±72*
	Permeate	mg L^{-1}	-	-	<DL	<DL
	Removal	%	42±13	39±14*	>99	>99
COD_t	Influent	mg L^{-1}	213±62	213±62	168±28	208±83
	UASB effluent	mg L^{-1}	129±19	140±25*	304±84	560±153*
	Permeate	mg L^{-1}	-	-	39±2	34±3
	Removal	%	41±14	36±16*	76±4	89±4*
SCOD	Influent	mg L^{-1}	72±16	72±16	75±12	88±24
	UASB effluent	mg L^{-1}	64±13	60±13	97±16	166±52*
	Permeate	mg L^{-1}	-	-	39±2	34±3
	Removal	%	18±12	24±14	48±7	55±5
BOD_5	Influent	mg L^{-1}	107±22	107±22	88±9	138±4*
	UASB effluent	mg L^{-1}	84±8	88±10	142±69	249±61
	Permeate	mg L^{-1}	-	-	10±5	13±3
	Removal	%	26±17	19±11	89±5	91±2
Headspace CH_4 production (STP)		L d^{-1}	0.3±0.2	0.8±0.3*	0.2±0.1	0.8±0.5*

DL-detection limit; STP-standard temperature and pressure

* Statistical difference ($p<0.05$) between G-UASB and F-UASB, G-AnMBR and F-AnMBR

Similar soluble and colloidal matter concentration (measured as SMP_{COD}) of 60-64 mg L^{-1} ($p>0.05$) was observed in the G-UASB and F-UASB effluents (Table 4-2). The membrane integration increased the SMP_{COD} concentration in the bulk sludge by 2 and 4 times for the granular and flocculent system respectively (Table 4-2), mainly due to the increase of high molecular weight colloidal fraction between 500 kDa and 1.2 μm,

representing about 83 % and 62 % of the total SMP_{COD} in the G-AnMBR and F-AnMBR respectively (Table 4-3). The significantly higher SMP_{COD} in the F-AnMBR than the G-AnMBR ($p<0.05$) can be attributed to higher SMP_{COD} of molecular weight between 10 and 100 kDa (Table 4-3). Additionally, MLSS and particulate COD (PCOD) concentrations also increased after membrane integration, which was more obvious in the flocculent system, leading to higher MLSS and PCOD concentrations in the F-AnMBR (Table 4-2). To illustrate, MLSS concentration increased from 69±11 and 75±9 mg L^{-1} by 4 and 6 times for the granular and flocculent systems respectively, and MLSS concentration in the F-AnMBR was about 1.7 times higher than that in the G-AnMBR (Table 4-2). Particle size (d_{50}) reductions were observed after membrane integration for both the granular and flocculent systems, with significantly higher d_{50} in the flocculent system ($p<0.05$) (Table 4-2). During the J_c tests through external membrane cell as a diagnostic tool, a clear decline of the J_c from 10 to about 8 L m^{-2} h^{-1} can be obtained for both the granular and flocculent systems from UASB to UASB configured AnMBR (Figure 4-3). Although similar J_c were obtained for the G-AnMBR and F-AnMBR, a noticeable decrease of the permeate flux can be observed for the F-AnMBR when the flux exceeded J_c (Figure 4-3).

Table 4-2. Impact of membrane addition on bulk sludge characteristics.

		UASB effluent		Membrane tank	
		G-UASB	F-UASB	G-AnMBR	F-AnMBR
MLSS	mg L^{-1}	69±11	75±9*	273±33#	464±65*,#
PSD	µm				
d_{10}		1.6±0.1	3.4±0.4	0.9±0.1#	1.5±0.6#
d_{50}		85±7	119±21*	18±7#	68±6*,#
d_{90}		564±201	927±295	81±5#	345±65*,#
Zeta potential	mV	-13.3±1.4	-15.3±3.0	-12.4±1.5	-16.2±1.3*
pH		7.8±0.1	7.5±0.1*	8.1±0.1	7.7±0.1*
COD_t		129±19	140±25*	533±13#	971±216*,#
PCOD		66±20	80±17*	393±11#	750±228*,#
SMP COD	mg L^{-1}	64±13	60±13	140±22#	222±12*,#
SMP proteins	mg L^{-1}	13±1	14±3	54±8#	88±22*,#
SMP carbohydrates	mg L^{-1}	5±2	6±0	15±2#	22±5*,#
SMP P/C		2.8±0.7	2.5±0.3	3.7±0.5	3.7±0.9

* Statistical difference ($p<0.05$) between G-UASB and F-UASB, G-AnMBR and F-AnMBR
\# Statistical difference ($p<0.05$) between G-UASB and G-AnMBR, F-UASB and F-AnMBR

Table 4-3. Colloidal SMP fractionation in UASB effluent and membrane tank bulk sludge (n=3).

Fractionation X (kDa)	UASB effluent		Membrane tank bulk	
	G-UASB	F-UASB	G-AnMBR	F-AnMBR
Total	45.3±4.5	56.3±3.8	135.7±7.1#	174.3±2.5*,#
X>500	8.3±5.5 (18.4%)	10.0±5.2 (17.8%)	112.7±7.8 (83.1%)#	121.3±10.2 (62.0%)#
100<X<500	0.3±3.1 (0.7%)	2.0±4.0 (3.6%)	0.3±5.5 (0.3%)	0.0±2.0 (0.0%)
10<X<100	4.7±5.5 (10.3%)	16.7±1.5 (29.6%)*	4.7±2.1 (3.4%)	23.0±9.5 (13.2%)*
X<10	32.0±5.6 (70.6%)	27.7±1.5 (49.1%)	30.0±1.0 (22.1%)	30.0±1.0 (17.2%)

All units are in mg COD L^{-1}

* Statistical difference ($p<0.05$) between G-UASB and F-UASB, G-AnMBR and F-AnMBR

Statistical difference ($p<0.05$) between G-UASB and G-AnMBR, F-UASB and F-AnMBR

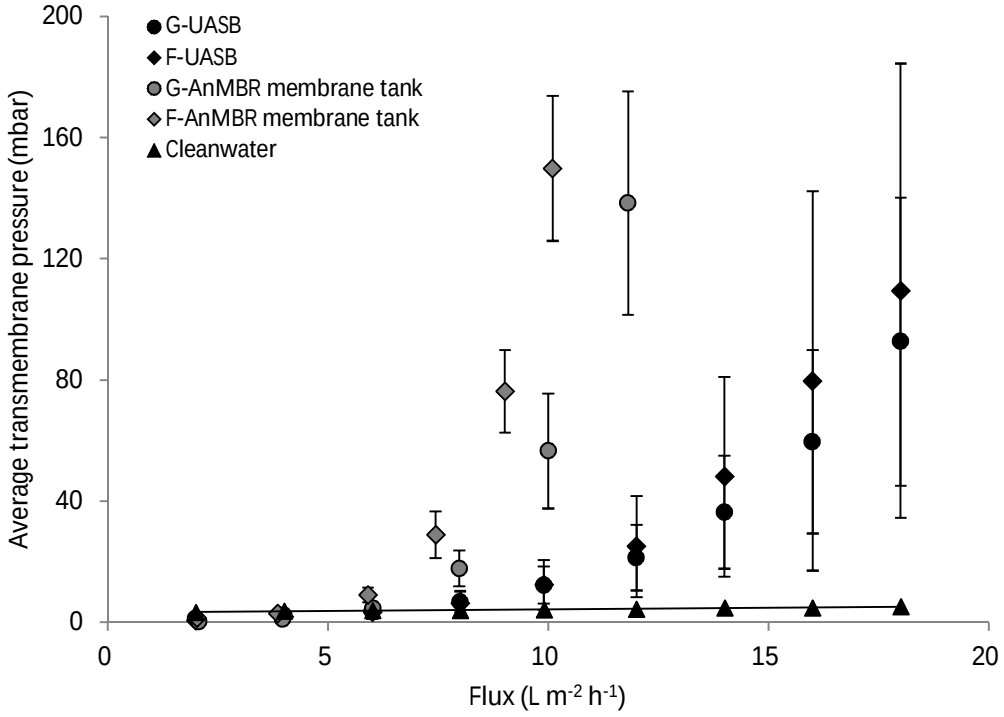

Figure 4-3. Critical flux tests of UASB effluent and membrane tank bulk sludge (2 L m^{-2} h^{-1} per step; 15 mins step), sampled at the wastewater average temperature of 10.2-13.1 °C.

4.3.2 Membrane operation comparison between G-AnMBR and F-AnMBR

Long term membrane operation comparisons between the G-AnMBR and F-AnMBR were conducted with net flux normalised to 20 °C at 7.5, 12.0 and 16.5 L m^{-2} h^{-1} and operated in a temperature range of 9.6-12.6 °C (Figure 4-4). As the imposed flux increased, TMP increased as expected for both the G-AnMBR and F-AnMBR. At all three fluxes, the G-AnMBR had lower fouling propensity compared with the F-AnMBR. For example, at net flux of 7.5 L m^{-2} h^{-1} during 200 h operation, sustainable membrane

operation with a fouling rate (d*P*/dt) of 1.8 mbar d^{-1} was achieved for the G-AnMBR compared with a higher d*P*/dt of 8.8 mbar d^{-1} for the F-AnMBR.

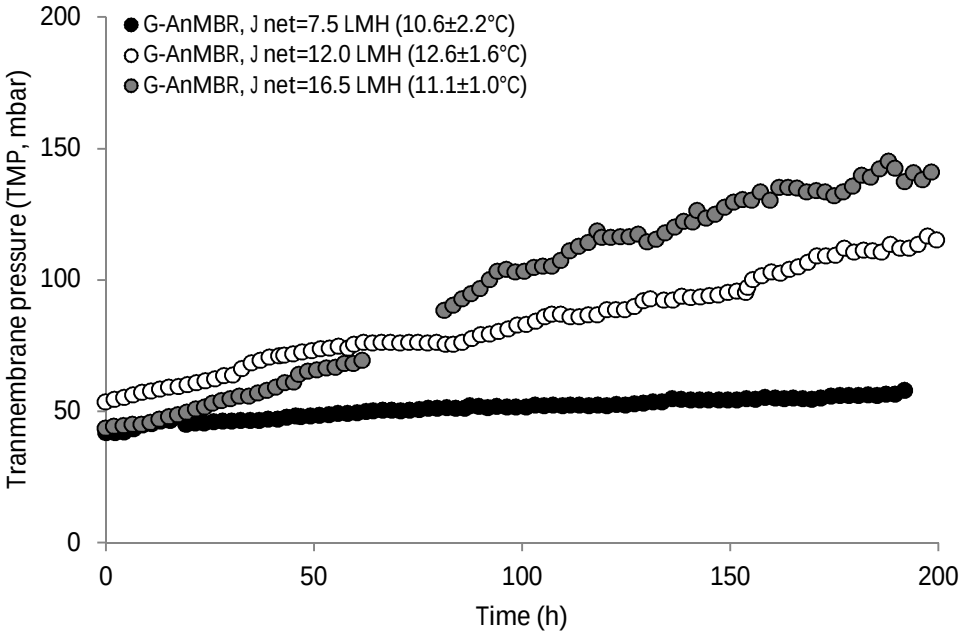

(a)

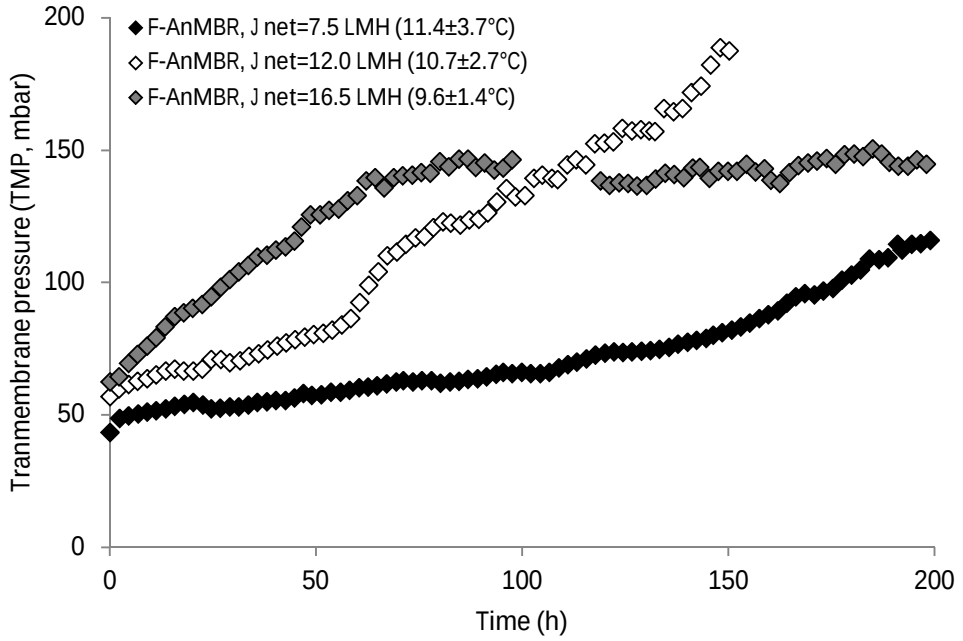

(b)

Figure 4-4. (a) G-AnMBR and (b) F-AnMBR membrane fouling curves using filtration/relaxation (10 min on/1 min off) and cyclic gas sparging (10 s on/10 s off, SGD_m=1.12 m^3 m^{-2} h^{-1} and SGD_{mnet}=0.56 m^3 m^{-2} h^{-1}). Flux has been normalised to 20 °C.

4.3.3 Impact of temperature on G-AnMBR and F-AnMBR system resilience

The impact of temperature on G-AnMBR and F-AnMBR system resilience was conducted in the first and second operational period with low and high average temperature range of 10-13 °C and 21-23 °C respectively (Figure 4-5, Table 4-4). Similar sustained membrane operation and bulk sludge characteristics were observed in the G-AnMBR at both low and high average temperatures (Figure 4-5, Table 4-4). For the F-AnMBR at an average temperature of 21 °C, sustainable membrane operation was also achieved, which is comparable with the G-AnMBR (Figure 4-5). However, at a low average temperature of 10.7 °C, a noticeable higher TMP profile was observed for the F-AnMBR associated to a significant increase of MLSS and PCOD concentrations in the bulk sludge (Table 4-4) ($p<0.05$). To illustrate, MLSS and PCOD concentrations in the F-AnMBR significantly increased from 253±48 to 465±65 mg L^{-1} and from 386±86 to 750±228 mg L^{-1} respectively ($p<0.05$), with the reactor average temperatures decline from 21.3 to 10.7 °C (Table 4-4). This was corroborated by the J_c tests of the F-AnMBR with an external membrane cell conducted in the laboratory (ambient temperature around 20 °C), demonstrating a d*P*/dt increase from <2.0 to 2.7 mbar h^{-1} when the reactor temperature reduced from 21.3 to 10.7 °C at a flux above the critical flux (J_c, 8 L m^{-2} h^{-1}, Figure 4-5 inset). This suggested that the higher TMP in the F-AnMBR at a low average temperature of 10.7 °C was attributed to bulk sludge with more solids and particulate matter rather than the increased permeate viscosity at a lower temperature. With the V_{up} reducing from 0.8-0.9 to 0.35 m h^{-1} at similar reactor temperature of 10.7-12.7 °C ($p>0.05$), the d*P*/dt in the F-AnMBR reduced from 0.86 mbar h^{-1} by over 2 times to a d*P*/dt as low as that in the G-AnMBR (Figure 4-6).

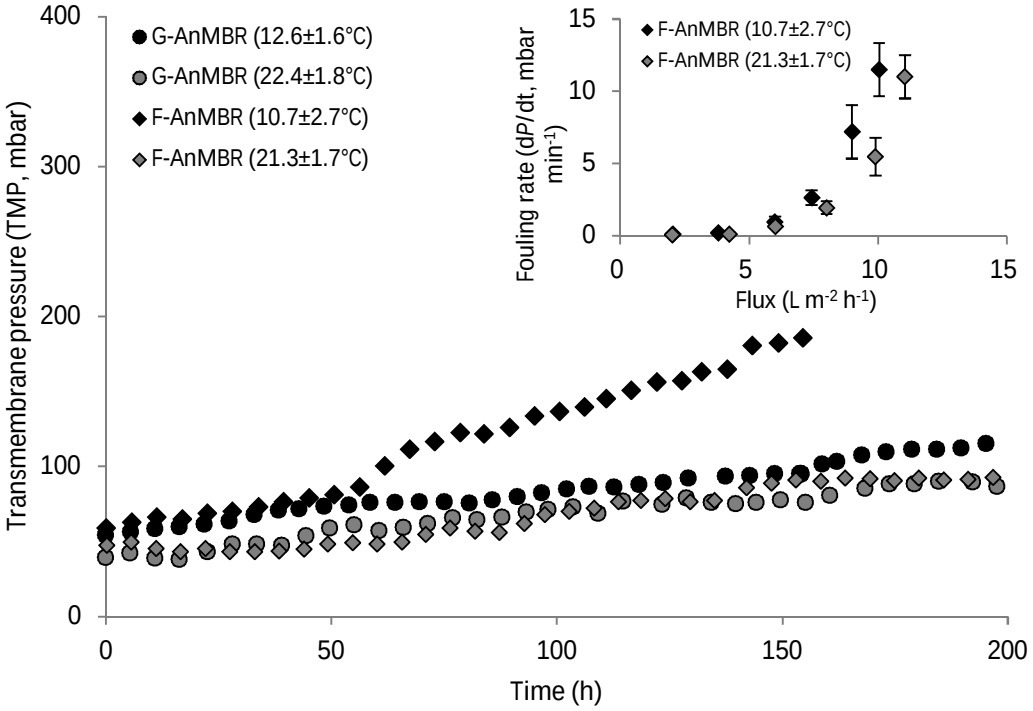

Figure 4-5. G-AnMBR and F-AnMBR membrane fouling curves. Filtration/relaxation (10 min on/1 min off), cyclic gas sparging (10 s on/10 s off) with same $J_{20\ net}$=12 L m^{-2} h^{-1}. Inset the critical flux tests of F-AnMBR (samples taken at different reactor temperatures). The tests were run in the laboratory (ambient temperature around 20 °C).

Table 4-4. Impact of temperature on G-AnMBR and F-AnMBR bulk sludge characteristics.

	Temp °C	MLSS mg L^{-1}	COD_t mg L^{-1}	PCOD mg L^{-1}	SMP_{COD}[a] mg L^{-1}	SMP_P mg L^{-1}	SMP_C mg L^{-1}	SMP P/C
G-AnMBR	12.6±1.6	273±33	533±13	398±11#	140±22	54±9	15±2	3.7±0.5#
	22.4±1.8	207±35	475±72	286±47	180±26	63±12	12±2	2.6±0.3
F-AnMBR	10.7±2.7	465±65#, *	971±216#, *	750±228#, *	222±12*	88±22	23±2*	3.7±0.9#
	21.3±1.7	253±48	589±85	368±86	221±21	83±19	28±4*	3.0±0.4

a. SCOD is equivalent to SMP_{COD}, samples were filtered through 1.2 μm filter paper

* Statistical difference ($p<0.05$) between G-AnMBR and F-AnMBR at an average temperature of 10.7-12.6 °C, G-AnMBR and F-AnMBR at average temperature of 21.3-22.4 °C.

Statistical difference ($p<0.05$) between G-AnMBR at 12.6±1.6 °C and G-AnMBR at 22.4±1.8°C, F-AnMBR at 10.7±2.7 °C and F-AnMBR at 21.3±1.7 °C.

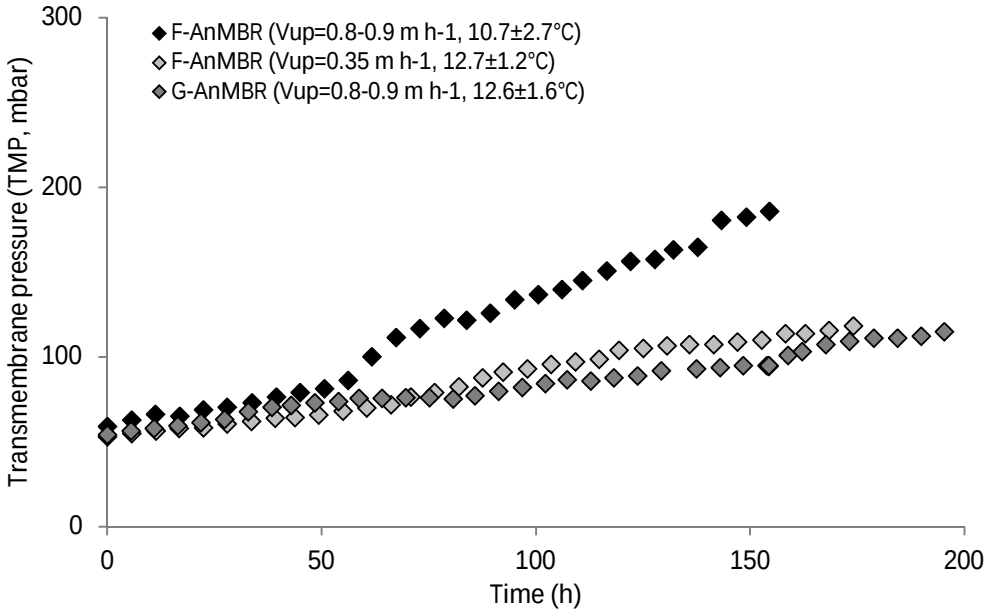

Figure 4-6. G-AnMBR and F-AnMBR membrane fouling curves under different upflow velocity (V_{up}). Filtration/relaxation (10 min on/1 min off), cyclic gas sparging (10 s on/10 s off) with same $J_{20\ net}$=12 L m^{-2} h^{-1}.

4.3.4 Alternative pseudo dead-end gas sparging strategy

An alternative hydrodynamic regime, in which pseudo dead-end operation is sustained through filtration without gas sparging followed by membrane relaxation coupled with gas sparging (Intermittent filtration, 10 min on/1 min off; intermittent gas sparging, 1 min on/10 min off), was tested as a method to reduce specific membrane energy demand (Figure 4-7) (Martin Garcia et al., 2013; McAdam et al., 2011). For the net flux adopted of 7.5 L m^{-2} h^{-1}, the TMP profile with pseudo DE gas sparging strategy slightly increased for both the G-AnMBR and F-AnMBR, whilst the energy demand of the gas sparging reduced by more than 80 %, compared with the standard gas sparging strategy (Figure 4-7). A higher d*P*/dt of 0.30 mbar h^{-1} within 200 h operation of the F-AnMBR was obtained at a low average temperature of 9.6 °C (Figure 4-8a), compared with the F-AnMBR at a high average temperature of 22.8 °C and the G-AnMBR at both high and low average temperatures (Figure 4-8a). Characterisation of individual pseudo DE filtration cycles also demonstrated a higher cake fouling rate (r_f) of the F-AnMBR at low average temperatures with d*P*/dt of 1.7 mbar min^{-1}, about two times higher than that at a high average temperature after 100 h operation (Figure 4-8b). Although slightly higher total

resistance and total TBP was observed in the F-AnMBR ($p>0.05$) (Figure 4-9), similar α_{TBP} between 10^{14} to 10^{15} m kg^{-1} was obtained for the G-AnMBR and F-AnMBR (Equation 4-7). The easier removed upper layers occupied more than 75 % of TBP and 85 % of total resistance for both the G-AnMBR and F-AnMBR (Figure 4-9). Although significantly higher SMP/TBP ratio was observed in the F-AnMBR than G-AnMBR at intermediate and lower layer ($p<0.05$), similar intermediate and lower layer hydraulic resistance were achieved ($p>0.05$).

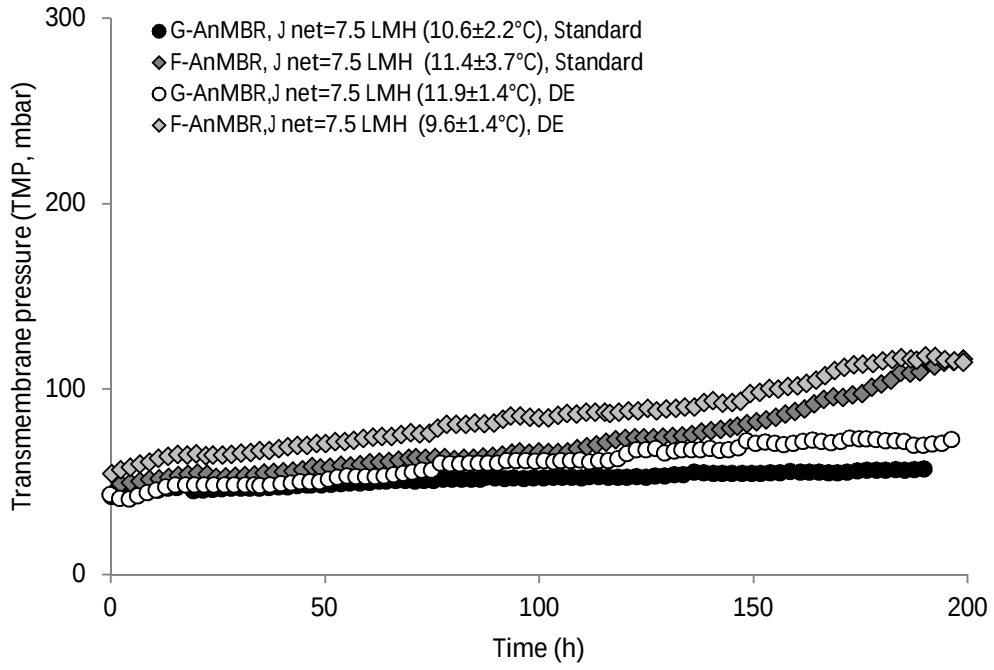

Figure 4-7. G-AnMBR and F-AnMBR membrane fouling curves using two hydrodynamic conditions with $J_{20\ net}$=7.5 L m^{-2} h^{-1}: (a) Standard, Filtration/relaxation (10 min on/1 min off) and gas sparging (10 s on/10 s off), SGD_m=1.12 m^3 m^{-2} h^{-1} and SGD_{mnet}=0.56 m^3 m^{-2} h^{-1}; (b) Pseudo dead-end (DE), Intermittent filtration (10 min on/1 min off) and intermittent gas sparging (1 min on/10 min off), SGD_m=1.12 m^3 m^{-2} h^{-1} and SGD_{mnet}=0.102 m^3 m^{-2} h^{-1}. Flux has been normalised to 20 °C.

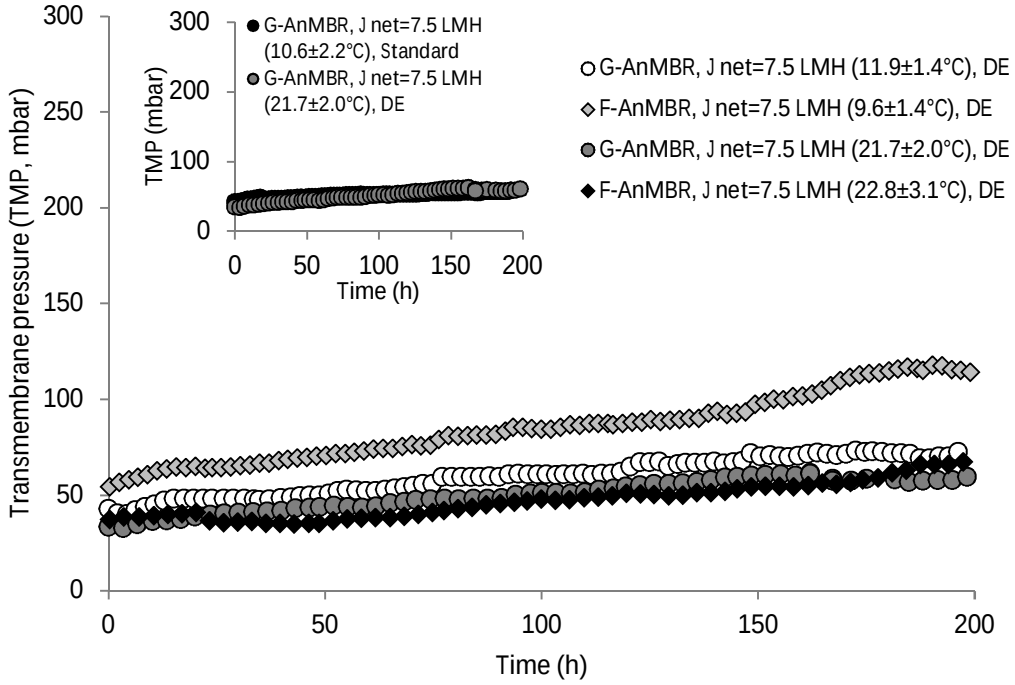

(a)

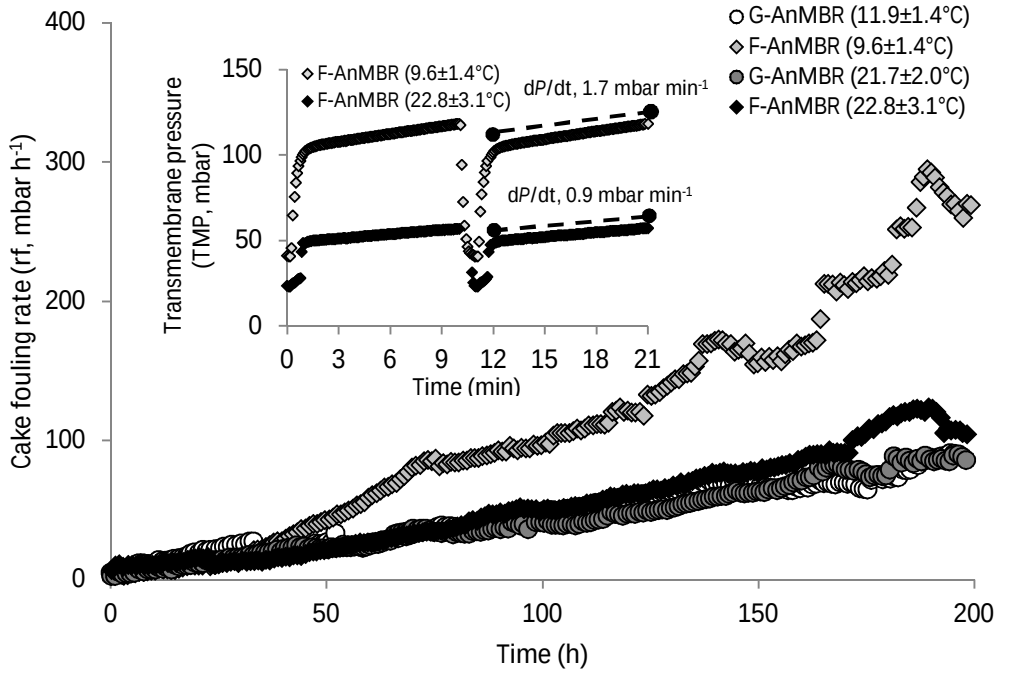

(b)

Figure 4-8. (a) Impact of temperature on G-AnMBR and F-AnMBR transmembrane pressure under pseudo dead-end gas sparging regime. (b) Cake fouling rate (r_f, dP/dt) analyses under pseudo dead-end gas sparging regime. Intermittent filtration (10 min on/1 min off) and intermittent gas sparging (1 min on/10 min off) with $J_{20\ net}$ = 7.5 L m^{-2} h^{-1}, SGD_m=1.12 m^3 m^{-2} h^{-1} and SGD_{mnet}=0.102 m^3 m^{-2} h^{-1}. The data of the inset is transmembrane pressure after 100 h. Flux has been normalised to 20 °C.

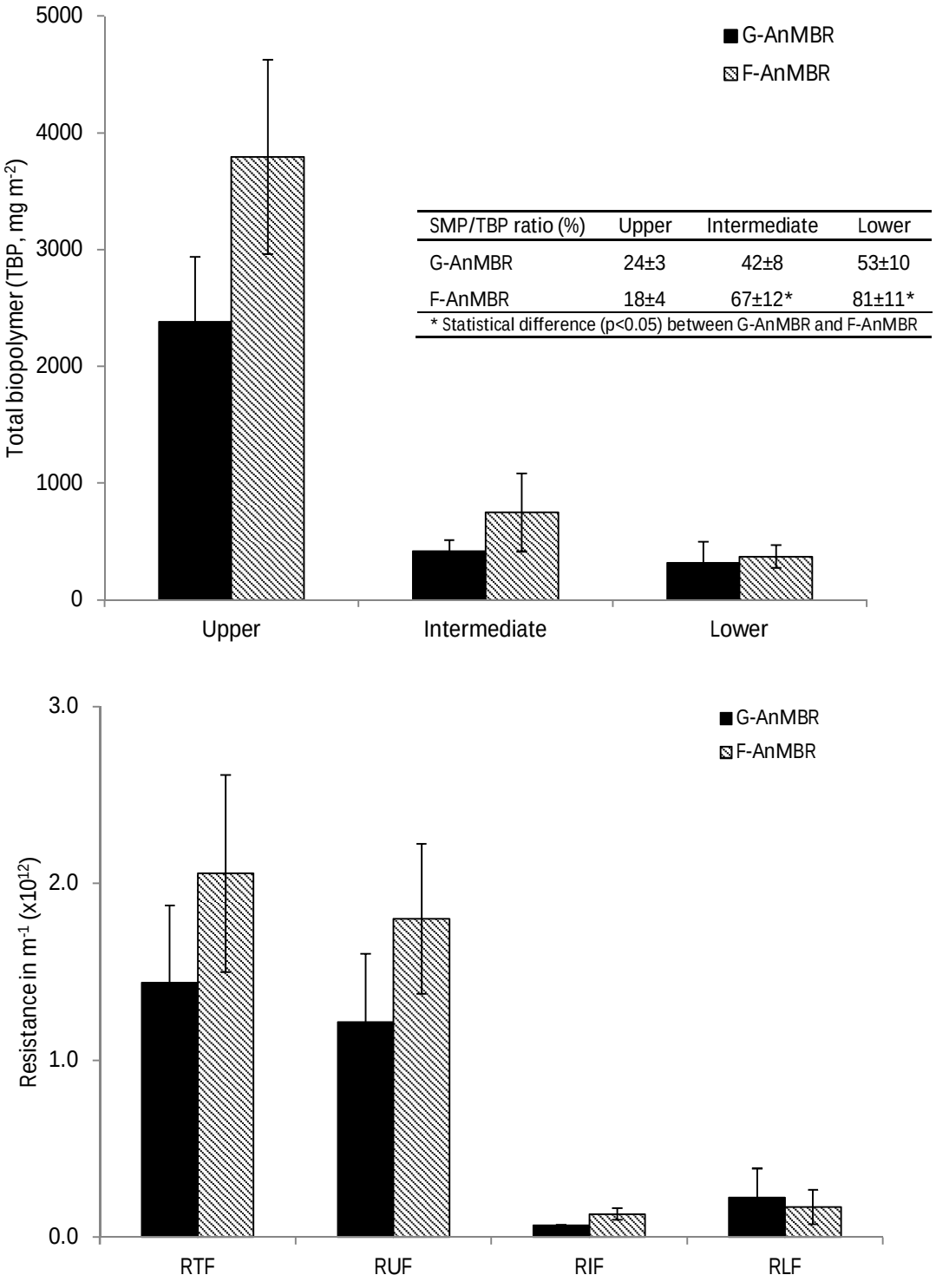

SMP/TBP ratio (%)	Upper	Intermediate	Lower
G-AnMBR	24±3	42±8	53±10
F-AnMBR	18±4	67±12*	81±11*

* Statistical difference ($p<0.05$) between G-AnMBR and F-AnMBR

Figure 4-9. Total biopolymer (TBP) (protein + carbohydrates in mg m^{-2}) and hydraulic resistances from three fouling layer fraction of G-AnMBR and F-AnMBR after long term run. Intermittent filtration (10 min on/1 min off, J_{20}=8.25 L m^{-2} h^{-1}, $J_{20\ net}$=7.5 L m^{-2} h^{-1}) and intermittent gas sparging (1 min on/10 min off, SGD_m=1.12 m^3 m^{-2} h^{-1}, SGD_{mnet}=0.102 m^3 m^{-2} h^{-1}). Each system filtered for 200 h with about 1500 L wastewater.

4.4 Discussion

This study has demonstrated that granular inoculum has good stability which exerts a positive influence on sustained permeability, whilst membrane inclusion can dissipate the disadvantages of flocculent biomass, to deliver similar membrane permeability provided the sludge blanket is controlled. The effluent instability of the G-UASB and F-UASB reactors at low temperatures of 10-13 °C can be overcome through membrane inclusion providing similar permeate quality compliance to COD, BOD_5 and TSS International discharge standards (Table 4-1). Similarly, Hejnic et al. (2016) demonstrated a COD_t removal efficiency increase from 64 % in a F-UASB to 85 % in a F-AnMBR treating raw municipal wastewater. Martin et al. (2013) also demonstrated similar low COD_t of 47-54 mg L^{-1} and BOD_5 of 10-11 mg L^{-1} for an UASB configured G-AnMBR and a CSTR configured F-AnMBR operated on the same sewage with this study. The treatment efficiency improvements after membrane inclusion and the similar permeate quality between the G-AnMBR and F-AnMBR can be attributed to the complete retention of solids and particulate matter, and retention of most colloidal matter by the membrane barrier, therefore only low molecular weight fraction can go through.

The membrane integration resulted in soluble and colloidal matter increases (measured as SMP_{COD}) by 2-4 times (Table 4-2), leading to a reduction in the critical flux of both suspensions (Figure 4-3). Ozgun et al. (2015) also reported a SMP increase from about 37 to 120 mg L^{-1} by more than 3 times after membrane integration. This is mainly due to the high molecular weight fraction retention evidenced by an increase of molecular weight fraction between 500 kDa and 1.2 μm by about 12-14 times (Table 4-3), which was reported to cause higher fouling propensity of a CSTR than an UASB configured AnMBR (van Voorthuizen et al., 2008). Total SMP was significantly higher in the F-AnMBR than G-AnMBR ($p<0.05$) due also to the accumulation of SMP with a molecular weight between 10 and 100 kDa (Table 4-2, Table 4-3). Martin et al. (2011, 2013) also demonstrated that the SMP_{COD} in a CSTR configured F-AnMBR was more than 3 times higher than that in an UASB configured G-AnMBR with higher SMP_{COD} fraction between 10 and 100 kDa. It is therefore suggested that the higher SMP_{COD} in the F-AnMBR might be due to either the floc erosion or poor flocculation under high SRT

(Wilén et al., 2003) and shear stress from gas sparging in the membrane tank, leading to the accumulation of high molecular weight degradation by-products (Martin-Garcia et al., 2011).

Similar membrane permeability can be sustained in the F-AnMBR compared with the G-AnMBR at an average temperature of 21-22 °C (Figure 4-5). However, a higher membrane fouling propensity was observed in the F-AnMBR compared with the G-AnMBR under similar low average temperatures of 9.6-12.6 °C (Figure 4-4). Evaluation of the matrix in the F-AnMBR revealed significantly higher particulate COD within the membrane tank at a lower temperature (Table 4-4). This can be explained by the particle settling velocity reduction according to Stoke's law as wastewater viscosity increased with the decrease of temperature (Lettinga et al., 2001; Mahmoud et al., 2003). In this study, a relatively high V_{up} of 0.8-0.9 m h^{-1} was applied, which might exceed the flocculent biomass settling velocity and cause solids washout in the F-AnMBR (Mahmoud et al., 2003). This is corroborated through a reduction in V_{up} from 0.8-0.9 to 0.35 m h^{-1} (Lew et al., 2004), in which the membrane permeability was similar to that of the G-AnMBR at 12.6°C (Figure 4-6). Ozgun et al. (2013) also illustrated a more stable sludge blanket when V_{up} reduced from 1.2 to 0.6 m h^{-1} in a flocculent UASB with TSS decreased from 230-270 to 90-110 mg L^{-1}. On the contrary, similar fouling profiles were observed for the G-AnMBR at 12.6 and 22.4°C (Figure 4-5). We suggest this might be due to the larger particle size and higher density of granular biomass (Nicolella et al., 2000), providing larger inertia for the granules (Tsutsumi et al., 1999) to follow the liquid, leading to quicker energy dissipation and less mixing in the G-AnMBR. This was supported by the lower particulate COD increase observed following temperature reduction, in comparison to the F-AnMBR (Table 4-4). The lower headspace methane production in G-AnMBR at low temperatures may further limit the mixing (Table 4-1), which might be ascribed to the limited diffusion induced by the internal structure of the granule especially at low temperatures (Gonzalez-Gil et al., 2001; Nicolella et al., 2000). These findings suggested that V_{up} should be reduced for the F-AnMBR at low temperatures to control the sludge blanket stability and minimise the solids washout,

thus similar sustained membrane operation can also be realised for both the G-AnMBR and F-AnMBR.

Characterisation of the fouling cake with pseudo dead-end gas sparging regime indicated similar α_{TBP} between 10^{14} to 10^{15} m kg^{-1} for the G-AnMBR and F-AnMBR, an order of magnitude lower than those in the previous studies with α_{TBP} value of 10^{15} to 10^{16} m kg^{-1} (Metzger et al., 2007). The distinction can be attributed to the different gas sparging regimes, as a more heterogeneous and reversible cake layer was formed in the absence of shear within the pseudo dead-end cycle (McAdam et al., 2011; McAdam and Judd, 2008), evidenced by the high proportions of easier removed upper layers with more than 75 % of TBP and 85 % of R_{TF} for both the G-AnMBR and F-AnMBR (Figure 4-9). Similar α of 10^{13}-10^{14} m kg^{-1} (Equation 4-10) for the G-AnMBR and F-AnMBR at both high and low average temperatures suggests that the higher r_f at low average temperatures in the F-AnMBR (Figure 4-8b) can be explained by the high solids loadings (Table 4-4). It is therefore proposed to reduce the solids loadings towards the membrane to maintain low r_f by controlling the sludge blanket or possibly shortening the pseudo dead-end cycle length. In this study, lower solids environment in the F-AnMBR at a higher temperature was effective to keep low r_f and mitigate membrane fouling as low as the G-AnMBR (Figure 4-8b, Table 4-4). This can be explained by the critical deposition mass concept, where the drag force within the first layer of the loose cake increased as layer number increased until a critical deposition value was achieved, leading to aggregation and collapse occurrence to form a compacted cake layer (Bessiere et al., 2005; Harmant and Aimar, 1996). In this study, higher SMP/TBP ratio was observed at intermediate and lower layer of the F-AnMBR than G-AnMBR, which might be due to higher SMP_{COD} in the F-AnMBR especially at low average temperatures (Table 4-4). However, the high SMP/TBP ratio did not result in high hydraulic resistance, which is consistent with Metzger et al. (2007) in an aerobic MBR treating synthetic wastewater. This might be due to the complete cover of the membrane surface by biopolymer and an equilibrium has been reached, in which further pore clogging due to higher SMP concentration occurred very slowly (Metzger et al., 2007). Accordingly, this alternative gas sparging strategy can be applied to both the G-AnMBR and F-AnMBR with sustained membrane

operation at a specific energy demand of 0.12 kWh m^{-3}, equivalent to less than 50 % of the energy recovered from AnMBR (Cookney et al., 2016). Importantly, AnMBR with more attractive option flocculent inoculum in terms of cost and supply chains, can deliver similar sustained membrane permeability of AnMBR with granular inoculum, to achieve an energy neutral sewage treatment provided the sludge blanket is controlled.

4.5 Conclusions

This study demonstrated granular biomass in an UASB configured AnMBR provides good stability and sustained membrane operation, whilst membrane inclusion can dissipate the disadvantages of flocculent biomass, to deliver similar membrane permeability provided the sludge blanket is controlled. Accordingly, flocculent biomass can be utilised as an alternative to granular biomass, which presents a more attractive option from the perspective of cost and supply chain, to deliver a low energy demand or even energy neutral UASB configured AnMBR for municipal wastewater treatment. The following conclusions can be drawn:

- Membrane inclusion overcame the poor performance of UASB by providing similar permeability with consistently low COD_t of 34-39 mg L^{-1} and BOD_5 of 10-13 mg L^{-1} for both the G-AnMBR and F-AnMBR, regardless of the bulk sludge characteristics.
- The membrane inclusion resulted in the soluble and colloidal matter increase by 2-4 times in the bulk sludge mainly due to high molecular weight fraction retention.
- Granular inoculum biomass provides a more stable sludge blanket in the AnMBR with a lower membrane fouling propensity compared with the F-AnMBR at lower average temperatures. Higher average temperatures led to increased solids settling velocity and less solids washout due to decreased wastewater viscosity. Consequently, similar low membrane fouling can be achieved for both the G-AnMBR and F-AnMBR.
- Reducing the upflow velocity in the F-AnMBR at low temperatures was evidenced to be effective to sustain sludge blanket stability and minimise the solids washout, thus similar low sustained membrane permeability can be achieved as that in the G-AnMBR. More sludge blanket stability strategies such as reducing the sludge bed

height to total column height ratio to increase the height for energy dissipation can also be applied.

- The alternative pseudo dead-end gas sparging strategy can be applied to both the G-AnMBR and F-AnMBR with sustained membrane operation by limiting the solids mass to the membrane through controlling the sludge blanket or possibly reducing the pseudo dead-end cycle length, achieving the energy neutral sewage treatment.

4.6 Acknowledgements

The authors would like to thank our industrial sponsors Anglian Water, Severn Trent Water, Scottish Water and Thames Water for their financial and technical support. The authors also want to thank Youngseck Hong from SUEZ Water & Process Technologies Canada to provide ZW-10 membrane for this work.

4.7 References

Abbasi, T. and Abbasi, S.A. (2012) 'Formation and impact of granules in fostering clean energy production and wastewater treatment in upflow anaerobic sludge blanket (UASB) reactors', *Renewable and Sustainable Energy Reviews*, 16, pp. 1696–1708.

Aiyuk, S., Forrez, I., Lieven, D.K., van Haandel, A. and Verstraete, W. (2006) 'Anaerobic and complementary treatment of domestic sewage in regions with hot climates-A review', *Bioresource Technology*, 97, pp. 2225–2241.

Aiyuk, S. and Verstraete, W. (2004) 'Sedimentological evolution in an UASB treating SYNTHES, a new representative synthetic sewage, at low loading rates', *Bioresource Technology*, 93, pp. 269–278.

APHA (2005) *Standard Methods for the Examination of Water and Wastewater*. 21st edn. Washington D.C: American Public Health Association.

Bessiere, Y., Abidine, N. and Bacchin, P. (2005) 'Low fouling conditions in dead-end filtration: Evidence for a critical filtered volume and interpretation using critical osmotic pressure', *Journal of Membrane Science*, 264, pp. 37–47.

Chong, S., Sen, T.K., Kayaalp, A. and Ang, H.M. (2012) 'The performance enhancements of upflow anaerobic sludge blanket (UASB) reactors for domestic sludge treatment - A State-of-the-art review', *Water Research*, 46, pp. 3434–3470.

Chu, L.B., Yang, F.L. and Zhang, X.W. (2005) 'Anaerobic treatment of domestic wastewater in a membrane-coupled expended granular sludge bed (EGSB) reactor under moderate to low temperature', *Process Biochemistry*, 40, pp. 1063–1070.

Cookney, J., Mcleod, A., Mathioudakis, V., Ncube, P., Soares, A., Jefferson, B. and McAdam, E.J. (2016) 'Dissolved methane recovery from anaerobic effluents using hollow fibre membrane contactors', *Journal of Membrane Science*, 502, pp. 141–150.

Dubois, M., Gilles, K.A., Hamilton, J.K., Rebers, P.A. and Smith, F. (1956) 'Colorimetric method for determination of sugars and related substances', *Analytical Chemistry*, 28, pp. 350–356.

Elimitwalli, T., Zandvoort, M., Zeeman, G., Bruning, H. and Lettinga, G. (1999) 'Low temperature treatment of domestic sewage in upflow anaerobic sludge blanket and anaerobic hybrid reactors', *Water Science & Technology*, 39, pp. 177–185.

Gonzalez-Gil, G., Seghezzo, L., Lettinga, G. and Kleerebezem, R. (2001) 'Kinetics and mass-transfer phenomena in anaerobic granular sludge', *Biotechnology and Bioengineering*, 73, pp. 125–134.

Gouveia, J., Plaza, F., Garralon, G., Fdz-Polanco, F. and Peña, M. (2015a) 'Long-term operation of a pilot scale anaerobic membrane bioreactor (AnMBR) for the treatment of municipal wastewater under psychrophilic conditions', *Bioresource Technology*, 185, pp. 225–233.

Gouveia, J., Plaza, F., Garralon, G., Fdz-Polanco, F. and Peña, M. (2015b) 'A novel configuration for an anaerobic submerged membrane bioreactor (AnSMBR)', *Bioresource Technology*, 198, pp. 510–519.

Harmant, P. and Aimar, P. (1996) 'Coagulation of colloids retained by porous wall', *AIChE Journal*, 42, pp. 3523–3532.

Hejnic, J., Dolejs, P., Kouba, V., Prudilova, A., Widiayuningrum, P. and Bartacek, J. (2016) 'Anaerobic treatment of wastewater in colder climates using UASB reactor and anaerobic membrane bioreactor', *Environmental Engineering Science*, 33, pp. 918–928.

Judd, S.J. (2011) *Principles and Applications of Membrane Bioreactors in Water and Wastewater Treatment*. 2nd edn. London,UK: Elsevier.

Le Clech, P., Jefferson, B., Chang, I.S. and Judd, S.J. (2003) 'Critical flux determination by the flux-step method in a submerged membrane bioreactor', *Journal of Membrane Science*, 227, pp. 81–93.

Lettinga, G., Rebac, S. and Zeeman, G. (2001) 'Challenge of psychrophilic anaerobic wastewater treatment', *Trends in Biotechnology*, 19, pp. 363–370.

Lettinga, G., Roersma, R. and Grin, P. (1983) 'Anaerobic treatment of raw domestic sewage at ambient temperatures using a granular bed UASB reactor', *Biotechnology and Bioengineering*, 25, pp. 1701–1723.

Lew, B., Tarre, S., Belavski, M. and Green, M. (2004) 'UASB reactor for domestic wastewater treatment at low temperatures: A comparison between a classical UASB and hybrid UASB-filter reactor', *Water Science & Technology*, 49, pp. 295–301.

Liao, B.Q., Kraemer, J.T. and Bagley, D.M. (2006) 'Anaerobic membrane bioreactors: applications and research directions', *Critical Reviews in Environmental Science and Technology*, 36, pp. 489–530.

van Lier, J.B., van der Zee, F.P., Frijters, C.T.M.J. and Ersahin, M.E. (2015) 'Celebrating 40 years anaerobic sludge bed reactors for industrial wastewater treatment', *Review Environmental Science Bio/Technology*, 14, pp. 681–702.

Lim, S.J. and Kim, T. (2014) 'Applicability and trends of anaerobic granular sludge treatment processes', *Biomass and Bioenergy*, 60, pp. 189–202.

Liu, Y. and Tay, J.H. (2004) 'State of the art of biogranulation technology for wastewater treatment', *Biotechnology Advances*, 22, pp. 533–563.

Liu, Y., Xu, H.L., Show, K.Y. and Tay, J.H. (2002) 'Anaerobic granulation technology for wastewater treatment', *World Journal of Microbiology and Biotechnology*, 18, pp. 99–113.

Lowry, O.H., Rosebrough, N.J., Farr, A.L. and Randall, R.J. (1951) 'Protein measurement with the folin phenol reagent', *Journal of Biological Chemistry*, 193, pp. 265–275.

Mahmoud, N., Zeeman, G., Gijzen, H. and Lettinga, G. (2003) 'Solids removal in upflow anaerobic reactors, a review', *Bioresource Technology*, 90, pp. 1–9.

Martin-Garcia, I., Monsalvo, V., Pidou, M., Le-Clech, P., Judd, S.J., McAdam, E.J. and Jefferson, B. (2011) 'Impact of membrane configuration on fouling in anaerobic membrane bioreactors', *Journal of Membrane Science*, 382, pp. 41–49.

Martin Garcia, I., Mokosch, M., Soares, A., Pidou, M. and Jefferson, B. (2013) 'Impact on reactor configuration on the performance of anaerobic MBRs: Treatment of settled sewage in temperate climates', *Water Research*, 47, pp. 4853–4860.

McAdam, E.J., Cartmell, E. and Judd, S.J. (2011) 'Comparison of dead-end and continuous filtration conditions in a denitrification membrane bioreactor', *Journal of Membrane Science*, 369, pp. 167–173.

McAdam, E.J. and Judd, S.J. (2008) 'Optimisation of dead-end filtration conditions for an immersed anoxic membrane bioreactor', *Journal of Membrane Science*, 325, pp. 940–946.

McAdam, E.J., Luffler, D., Martin-Garcia, N., Eusebi, A.L., Lester, J.N., Jefferson, B. and Cartmell, E. (2011) 'Integrating anaerobic processes into wastewater treatment', *Water Science & Technology*, 63, pp. 1459–1466.

Metzger, U., Le-Clech, P., Stuetz, R.M., Frimmel, F.H. and Chen, V. (2007) 'Characterisation of polymeric fouling in membrane bioreactors and the effect of different filtration modes', *Journal of Membrane Science*, 301, pp. 180–189.

Nagaoka, H., Ueda, S. and Miya, A. (1996) 'Influence of bacterial extracellular polymers on the membrane separation activated sludge process', *Water Science & Technology*, 34, pp. 165–172.

Nicolella, C., Van Loosdrecht, M.C.M. and Heijnen, J.J. (2000) 'Wastewater treatment with particulate biofilm reactors', *Journal of Biotechnology*, 80, pp. 1–33.

Ozgun, H., Ersahin, M.E., Tao, Y., Spanjers, H. and van Lier, J.B. (2013) 'Effect of upflow velocity on the effluent membrane fouling potential in membrane coupled upflow anaerobic sludge blanket reactors', *Bioresource Technology*, 147, pp. 285–292.

Ozgun, H., Gimenez, J.B., Evren, M., Tao, Y., Spanjers, H. and van Lier, J.B. (2015) 'Impact of membrane addition for effluent extraction on the performance and

sludge characteristics of upflow anaerobic sludge blanket reactors treating municipal wastewater', *Journal of Membrane Science*, 479, pp. 95–104.

Rajeshwari, K.V., Balakrishnan, M., Kansal, A., Lata, K. and Kishore, V.V.N. (2000) 'State-of-the-art of anaerobic digestion technology for industrial wastewater treatment', *Renewable and Sustainable Energy Reviews*, 4, pp. 135–156.

Robles, A., Ruano, M.V., García-Usach, F. and Ferrer, J. (2012) 'Sub-critical filtration conditions of commercial hollow-fibre membranes in a submerged anaerobic MBR (HF-SAnMBR) system: the effect of gas sparging intensity', *Bioresource Technology*, 114, pp. 247–254.

Sabry, T. (2008) 'Application of the UASB inoculated with flocculent and granular sludge in treating sewage at different hydraulic shock loads', *Bioresource Technology*, 99, pp. 4073–4077.

Seghezzo, L., Zeeman, G., van Lier, J.B., Hamelers, H.V.M. and Lettinga, G. (1998) 'A review: The anaerobic treatment of sewage in UASB and EGSB reactors', *Bioresource Technology*, 65, pp. 175–190.

Smith, A.L., Skerlos, S.J. and Raskin, L. (2013) 'Psychrophilic anaerobic membrane bioreactor treatment of domestic wastewater', *Water Research*, 47, pp. 1655–1665.

Syutsubo, K., Yoochatchaval, W., Tsushima, I., Araki, N., Kubota, K., Onodera, T., Takahashi, M., Yamaguchi, T. and Yoneyama, Y. (2011) 'Evaluation of sludge properties in a pilot-scale UASB reactor for sewage treatment in a temperate region', *Water Science & Technology*, 64, pp. 1959–1966.

Tchobanoglous, G., Burton, F.L. and Stensel, H.D. (2003) *Wastewater Engineering Treatment and Reuse*. 4th edn. New York: McGraw-Hill Companies.

Tsutsumi, A., Chen, W. and Kim, Y.H. (1999) 'Classification and characterization of hydrodynamic and transport behaviors of three-phase reactors', *Korean Journal of Chemical Engineering*, 16, pp. 709–720.

Uemura, S. and Harada, H. (2000) 'Treatment of sewage by a UASB reactor under moderate to low temperature conditions', *Bioresource Technology*, 72, pp. 275–282.

Vera, L., Gonzalez, E., Diaz, O., Sanchez, R., Bohorque, R. and Rodriguez-Sevilla, J. (2015a) 'Fouling analysis of a tertiary submerged membrane bioreactor operated in dead-end mode at high-fluxes', *Journal of Membrane Science*, 493, pp. 8–18.

Vera, L., González, E., Ruigómez, I., Gómez, J. and Delgado, S. (2015b) 'Analysis of backwashing efficiency in dead-end hollow-fibre ultrafiltration of anaerobic suspensions', *Environmental Science and Pollution Research*, 22, pp. 16600–16609.

van Voorthuizen, E., Zwijnenburg, A., van der Meer, W. and Temmink, H. (2008) 'Biological black water treatment combined with membrane separation', *Water Research*, 42, pp. 4334–4340.

Wilén, B.M., Jin, B. and Lant, P. (2003) 'The influence of key chemical constituents in activated sludge on surface and flocculating properties', *Water Research*, 37, pp. 2127–2139.

CHAPTER 5

Identification of gas sparging regimes for granular anaerobic membrane bioreactor to enable energy neutral municipal wastewater treatment

5 Identification of gas sparging regimes for granular anaerobic membrane bioreactor to enable energy neutral municipal wastewater treatment

K.M. Wang[a], D. Cingolani[b], A.L. Eusebi[b], A. Soares[a], B. Jefferson[a], E.J. McAdam[a*]
[a]Cranfield Water Science Institute, Vincent Building, Cranfield University, Bedfordshire, MK43 0AL, UK
[b]Department of Materials, Environmental Sciences and Urban Planning (SIMAU), Università Politecnica delle Marche, 60131, Ancona, Italy

Abstract

In this study, conventional and novel gas sparging regimes have been evaluated for a municipal wastewater granular anaerobic MBR to identify how best to achieve high sustainable fluxes whilst simultaneously conserving energy demand. Using continuous gas sparging in combination with continuous filtration, flux was strongly dependent upon shear rate, which imposed a considerable energy demand. Intermittent gas sparging was subsequently evaluated to reduce energy demand whilst delivering an analogous shear rate. For a flux of 5 L m^{-2} h^{-1}, a fouling rate below 1 mbar h^{-1} was sustained with low gas sparging frequency and gas sparging rates. However, to sustain low fouling rates for fluxes above 10 L m^{-2} h^{-1}, a gas sparging frequency of 50 % (i.e. gas sparging 10 s on/10 s off) and an increase in gas sparging rate is needed, indicating the importance of shear rate and gas sparging frequency. An alternative gas sparging regime was subsequently tested in which filtration was conducted without gas sparging, followed by membrane relaxation for a short period coupled with gas sparging, to create a pseudo dead-end filtration cycle. Fouling characterisation evidenced considerable cake fouling rates of 200-250 mbar h^{-1} within each filtration cycle. However, long term fouling transient analysis demonstrated low residual fouling resistance, suggesting the cake formed during filtration was almost completely reversible, despite operating at a flux of 15 L m^{-2} h^{-1}, which was equivalent or higher than the critical flux of the suspension. It is therefore asserted that by operating filtration in the absence of shear, fouling is less dependent upon the preferential migration of the sub-micron particle fraction and is instead governed by the compressibility of the heterogeneous cake formed, which enables higher operational fluxes to be achieved. Comparison of energy demand for the three gas sparging regimes to the energy recovered from municipal wastewater AnMBR demonstrated that only by using pseudo dead-end filtration can energy neutral wastewater treatment be realised which is the ultimate ambition for the technology.

Keywords: MBR, gas bubbling, hydrodynamics, energy neutral, domestic, sewage

5.1 Introduction

Electricity demand in the water industry accounts for 2-3 % of national power production (Water UK, 2006). More than half of this demand is for aeration in activated sludge (Krzeminski et al., 2012; Tchobanoglous et al., 2003). Anaerobic processes therefore present an attractive alternative to conventional aerobic domestic wastewater treatment since there is no aeration, less sludge production and energy can be recovered from the biogas formed (Martin Garcia et al., 2013; Robles et al., 2012). The energy saved through aeration coupled with the potential for energy production, offers the prospect of energy neutral sewage treatment, which is the ultimate ambition for many advocates of this technology (McCarty et al., 2011).

For municipal application, the main challenge for conventional anaerobic technology is preventing biomass washout (Robles et al., 2012); an effect which is exacerbated at low temperature (Lettinga et al., 2001). In anaerobic membrane bioreactors (AnMBRs), the membrane enables complete biomass retention, thereby facilitating the separation of hydraulic retention time (HRT) from solids retention time (SRT) (Gouveia et al., 2015a; Liao et al., 2006; Smith et al., 2013). Furthermore, membrane integration can deliver permeate compliant for chemical oxygen demand (COD) and suspended solids (Smith et al., 2013) in addition to a reduced biochemical oxygen demand (BOD_5). Whilst the membrane enables process intensification, the AnMBR matrix is concentrated, and considerably more heterogeneous than conventional aerobic MBR which increases fouling propensity and reduces the attainable flux (Martin-Garcia et al., 2011). As such fouling mitigation contributes over two-thirds of the overall energy demand for immersed AnMBR (Pretel et al., 2014), which emphasises the need for fouling control strategies that limit AnMBR membrane fouling whilst conserving energy (Martin Garcia et al., 2013; Vera et al., 2016). Our previous anaerobic research on municipal wastewater with an average temperature of 18 °C (Cookney et al., 2016), demonstrated that 0.28 kWh m^{-3} energy is recoverable from biogas and dissolved methane, which is comparable to the average energy production of 0.34 kWh m^{-3} cited for AnMBR treating settled municipal wastewater in the literature (Cookney et al., 2016; Gouveia et al., 2015a, 2015b; Shin et al., 2014). For comparison, the specific energy demand for membrane operation of full-scale aerobic MBR is

typically between 0.19 and 0.70 kWh m^{-3} (Judd, 2011). Consequently, the specific energy demand for AnMBR membrane operation must be towards the low energy demand range of conventional aerobic MBR, to achieve energy self-sufficiency, despite operating in a more challenging matrix (Martin-Garcia et al., 2011) (Figure 5-1).

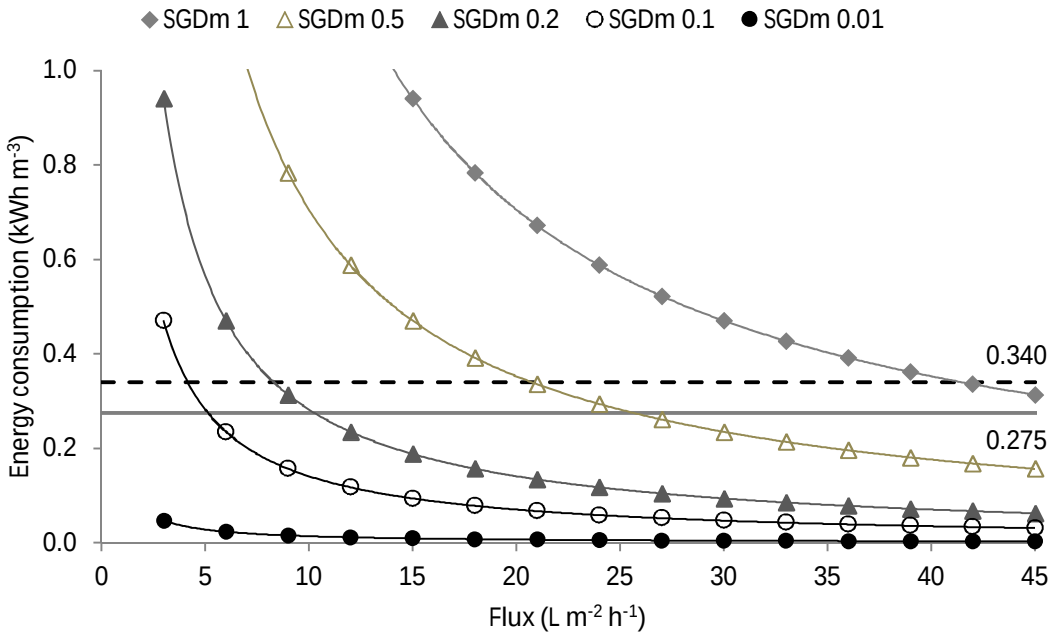

Figure 5-1. Energy consumption of AnMBR for different fluxes and specific gas demand per unit membrane area (SGD_m). Data compared to energy recovered from this sewage using AnMBR (0.275 kWh m^{-3}, biogas from UASB and dissolved CH_4) (Cookney et al., 2016). Black break line illustrates average energy recovery from municipal AnMBR literature (0.34 kWh m^{-3}) (Cookney et al., 2016; Gouveia et al., 2015a, 2015b; Shin et al., 2014).

Immersed membranes are predominantly studied for inclusion within AnMBR due to their lower specific energy demand, with gas sparging employed for fouling mitigation (Liao et al., 2006; Vera et al., 2016; Wibisono et al., 2014). Analogous gas sparging regimes to those of aerobic MBR are commonly employed in AnMBR studies, comprising of either continuous gas sparging (CGS) or intermittent gas sparging (IGS, 10 s on/10 s off) in which cycling enables analogous shear stress at the membrane wall, whilst enabling a 50 % reduction in energy demand (Dong et al., 2015; Gouveia et al., 2015a, 2015b; Martin Garcia et al., 2013; Martinez-Sosa et al., 2011; Robles et al., 2012). Several AnMBR studies have now evidenced that integrating immersed membranes within upflow anaerobic sludge blanket (UASB) configured AnMBR (Martin-Garcia et al., 2011;

Martin Garcia et al., 2013; Ozgun et al., 2015; van Voorthuizen et al., 2008) develop less tenacious fouling than within completely stirred tank reactor (CSTR) configured AnMBR. The authors accounted for this by the considerably lower solids concentration developed within the membrane tank, which evidently limited cake layer growth at the membrane surface (Cho and Fane, 2002; Liao et al., 2006; Ozgun et al., 2015). Using an UASB configured AnMBR, Martin-Garcia et al. (2013) undertook a preliminary investigation of an alternative gas sparging regime which comprised sequential filtration cycles without gas sparging, followed by a combination of backwash and gas sparging, to create a low energy pseudo dead-end (DE) filtration cycle (McAdam and Judd, 2008). The authors determined reasonable sustainable flux of 7 L m^{-2} h^{-1} despite undertaking filtration in the absence of shear, which considerably reduced the gas sparging requirement and corroborates findings of earlier investigation into pseudo dead-end (DE) filtration for MBR with low solids concentration (McAdam et al., 2011; McAdam and Judd, 2008).

To the best of our knowledge, there have been no previous studies that have explicitly sought to establish whether the gas sparging regimes employed in MBR literature can sustain flux using less energy than produced by an AnMBR treating domestic wastewater. Such investigation is critical to establishing whether the transition to energy neutral wastewater treatment is achievable. The aim of this study is therefore to critically evaluate conventional (continuous and intermittent) and non-conventional gas sparging regimes (pseudo dead-end) within UASB configured AnMBR, to identify controlling parameters that govern sustained permeability within each gas sparging regime whilst simultaneously identifying their capacity to deliver energy neutral operation. Specific objectives are to: (i) identify which parameters govern sustained operation for each gas sparging regime; (ii) compare fouling behaviours under different gas sparging regimes; and (iii) identify the most feasible gas sparging regime for delivering sustained membrane operation with minimum energy demand.

5.2 Material and methods

5.2.1 Anaerobic MBR pilot plant

The AnMBR consisted of a granular UASB (G-UASB) followed by a separate membrane tank. The 42.5 L cylindrical UASB was constructed of Perspex and fitted with a lamella

plate clarifier for solid/liquid/gas separation (Paques, Balk, The Netherlands) (Figure 5-2). The UASB was seeded with 16 L of granular sludge sourced from a mesophilic UASB used for the pulp and paper industry. Settled sewage from Cranfield University's sewage works was fed to the base of the UASB with a peristaltic pump (520S, Watson Marlow, Falmouth, UK). The average sewage temperature was 16.3±3.7 °C. The UASB was operated at a HRT of 8 h and allowed to acclimate for 360 days prior to this experiment. The upflow velocity was maintained at 0.8-0.9 m h^{-1}, which provided bed expansion to around 40 % of total column height. Due to the bed expansion, the light sludge fraction (dispersed growth from influent) accumulated in a layer above the granular bed (Aiyuk et al., 2006; Chong et al., 2012), and was withdrawn on occasion once washout into the downstream membrane tank was noted by an increase in suspended solids concentration. No granular biomass was withdrawn from the G-UASB during the 400-day trial.

Effluent from the UASB overflowed into a 30 L cylindrical membrane tank (0.17 m diameter x 1.25 m height) (Figure 5-2). The retentate was recycled from the membrane tank to the bottom of the UASB which helped sustain the upflow velocity. The membrane module (ZW-10) (SUEZ Water & Process Technologies, Trevose, USA) comprised four elements each of which consisted of 54 polyvinylidene fluoride (PVDF) hollow fibres (0.72 m in length and 1.9 mm outer diameter) with a nominal pore size of 0.04 µm, providing a total surface area of 0.93 m^2. Fibre looseness was around 5 % in accordance with manufacturer specification. Permeate was extracted by a peristaltic pump (520U, Watson Marlow, Falmouth, UK). Pressure transducers were sited on the permeate line (-1 to 1 bar, PMC 131, Endress + Hauser, Manchester, UK) and at the base of the membrane tank (0-2.5 bar, 060G2418, Danfoss, Nordborg, Denmark) to measure transmembrane pressure (TMP) and liquid level height respectively. Nitrogen-enriched air was produced by a nitrogen generator (NG6, Noblegen gas generator, Gateshead, UK) for gas sparging. During pseudo DE operation, filtration was conducted without gas sparging, followed by membrane relaxation for a short period coupled with gas sparging. The introduction of gas sparging between filtration cycles was controlled using a solenoid valve (Type 6014, Burkert, Ingelfingen, Germany) connected to a multifunction

timer relay (PL2R1, Crouzet, Valence, France). Specific gas demand per unit membrane area (SGD_m) was controlled by needle valve (Key Instruments, Langhorne, US). At a SGD_m of 2.0 m^3 m^{-2} h^{-1}, the shear stress intensity imparted through gas sparging bubbling corresponds to a gas velocity gradient of around 460 s^{-1} (Delgado et al., 2008; McAdam et al., 2011):

$$G = (\frac{Q_a g h}{V_T \nu_a})^{0.5} \quad (5\text{-}1)$$

where Q_a is gas flow-rate (m^3 s^{-1}), g is gravity constant (m s^{-2}), h is fluid height (m), V_T is reactor volume (m^3) and ν_a is the apparent kinetics viscosity (m^2 s^{-1}). ν_a can be calculated from dynamic viscosity (μ, Pa s) by $\nu_a = \mu/\rho$, where ρ is density (kg m^{-3}).

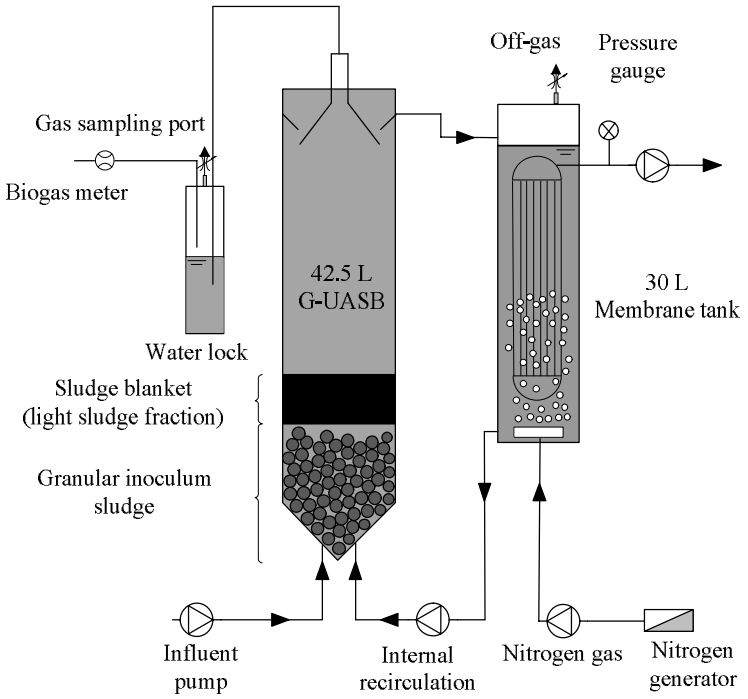

Figure 5-2. Schematic of the anaerobic membrane bioreactor (AnMBR).

Critical flux (J_C) analysis was conducted with the flux step method (Le-Clech et al., 2003) using flux steps of 3 L m^{-2} h^{-1}, with a step duration of 10 minutes. The trials were conducted in batch and permeate recycled back to the membrane tank. To establish reproducibility, critical flux trials were conducted in triplicate at a SGD_m of 2.0 m^3 m^{-2} h^{-1}. At 15 L m^{-2} h^{-1} during J_c test, a relative standard deviation for TMP of 3.6 % was

recorded. Gas sparging regimes were compared through trials conducted on 24 h of filtration, or where TMP reached a maximum of 550 mbar. Test fluxes were normalised to 20 °C (J_{20}) according to (Judd, 2011), as expressed in Equation (5-2):

$$J_T = J_{20} \cdot 1.025^{(T-20)} \quad (5\text{-}2)$$

where J_T is permeate at T °C, J_{20} is the permeate normalised to 20 °C, T is the temperature (°C). Analysis was undertaken in triplicate at fixed conditions to ascertain reproducibility after 24 h (CGS, J_{20}= 13.5 L m^{-2} h^{-1}, SGD_m= 2.0 m^3 m^{-2} h^{-1}), and a relative standard deviation for TMP of 7.6 % identified. The threshold for sustainable membrane operation was fixed to fouling rate (d*P*/dt) of <1 mbar h^{-1} over 24 h which corresponds to the d*P*/dt determined for sub-critical flux operation within full-scale municipal aerobic MBR (Guglielmi et al., 2007) and is coincident with the d*P*/dt observed in this study for TMP trends characterised by a 'flat' temporal profile. Pseudo dead-end filtration cycle analysis was undertaken using three profile characteristics (Vera et al., 2015b). The initial TMP for each filtration cycle (TMP_i) is related to the resistance provided by the clean membrane (R_m) and the internal residual fouling resistance (R_{if}) which is not removed by physical cleaning:

$$TMP_i = J.\mu.(R_m + R_{if}) \quad (5\text{-}3)$$

where J is the permeate flux (L m^{-2} h^{-1}). Within the filtration cycle, fouling originates from cake formation which can generally be characterised by a linear increase in TMP, with the slope defined as the cake fouling rate (r_f):

$$TMP = r_f.t + TMP_i \quad (5\text{-}4)$$

According to the cake model, the TMP can also be describe by Equation (5-5) (Vera et al., 2015a):

$$TMP = TMP_i + \Delta TMP_c = TMP_i + \mu\alpha\varpi J^2 t \quad (5\text{-}5)$$

where ΔTMP_c is the pressure drop of cake layer (Pa), α is specific cake resistance (m kg^{-1}), ω is the solids concentration in the cake per unit filtrate volume (assuming similar to MLSS concentration in the bulk sludge, kg m^{-3}). The cake compressibility can be described when filtering microbial suspensions (McCarty et al., 1999):

$$\alpha = \alpha_0(1 + \frac{\Delta TMP_c}{P_a}) \quad (5\text{-}6)$$

where α_0 is the specific cake resistance at zero pressure, P_a is the pressure required to obtain a specific cake resistance twice as high as α_0. The critical mass ($M_{critical}$) during the pseudo dead-end cycle is related to the critical filtered volume (V_{crit}) and MLSS concentration in the bulk sludge:

$$M_{critical} = V_{crit} \cdot C_b \quad (5\text{-}7)$$

After each test, the membrane was rinsed with tap water and chemically cleaned in 500 mg L^{-1} sodium hypochlorite for 3 h. During this period, a spare module was introduced to maintain constant AnMBR operation. After chemical cleaning, the module was rinsed with tap water and the clean water permeability assessed to assure recovery before reuse.

For the specific energy demand, only the blower for the gas sparging was considered and calculated by applying Equation (5-8) to (5-10) (Tchobanoglous et al., 2003):

$$P_{power} = \frac{w \cdot R \cdot T_1}{29.7 \cdot n \cdot e}\left[\left(\frac{P_2}{P_1}\right)^{0.283} - 1\right] \quad (5\text{-}8)$$

$$w = \frac{SGD_m \cdot a \cdot \rho_g}{3600} \quad (5\text{-}9)$$

$$W = \frac{P_{power} \cdot 1000}{J_{20} \cdot a} \quad (5\text{-}10)$$

where P_{power} is power requirement (kW); w is weight of flow of gas (kg s^{-1}); P_1 is inlet pressure (1.0×10^5 Pa); P_2 is outlet pressure (assuming 3 m hydraulic head, 1.3×10^5 Pa); T_1 is inlet temperature (K, assuming 293 K); n = (k-1)/k; k=1.4 for nitrogen in this case; e is compressor efficiency (0.70-0.90); a is membrane surface area (m^2); ρ_g is the gas density (1.165 kg m^{-3} for nitrogen); W is the specific energy demand (kWh m^{-3}).

5.2.2 Analytical methods

Mixed liquor suspended solids (MLSS) and biochemical oxygen demand (BOD_5) were measured according to Standard Methods (APHA, 2005). Total and soluble COD were analysed with Merck test kits (Merck KGaA, Darmstadt, Germany). Soluble COD was measured after filtering with 1.2 µm filter paper (70mm Glass Fibre Filter Paper Grade GF/C, Whatman, GE Healthcare Life Sciences, Little Chalfont, UK). Particle size was

measured by integrated laser diffractor (Mastersizer 3000, Malvern Instruments Ltd, Malvern, UK). Volatile fatty acid (VFA) as acetate concentration was carried out using high performance liquid chromatography (HPLC) (Shimadzu HPLC Class VP series, Kyoto, Japan) with a Rezex ROA/Organic Acid 7.80 mm x 300 mm column (Phenomenex, Macclesfield, UK) (Parawira et al., 2004). Protein and carbohydrate concentrations were measured using the modified Lowry method ($UV_{750\ nm}$) (Lowry et al., 1951) and Dubios phenol sulphuric acid method ($UV_{490\ nm}$) (Dubois et al., 1956) respectively. Bovine serum albumin (BSA) (Sigma-Aldrich, UK) and D-glucose (Acros Organics, UK) were used as the standard reference for protein and carbohydrates respectively. Samples were taken from the membrane tank for analyses. All analyses were undertaken in triplicate.

5.3 Results

5.3.1 Anaerobic MBR characterisation and critical flux determination

Consistently low effluent total COD (COD_t) and BOD_5 of 41±16 and 11±7 mg L^{-1} were achieved during 400 days operation (Table 5-1), which is comparable to an earlier study of AnMBR operated on the same sewage (Martin Garcia et al., 2013), demonstrating stable process performance throughout the study. Acetate was not detected in the permeate (<2.0 mg L^{-1}), which illustrates good utilisation of the soluble substrate. The membrane tank was characterised by an average MLSS of 384±190 mg MLSS L^{-1} and a soluble microbial products (SMP) concentration as COD of 149±65 mg COD L^{-1} (Table 5-1). The SMP concentration expressed as a sum of protein and carbohydrate was 78±28 mg L^{-1}, and was characterised by a protein/carbohydrate ratio (SMP P/C) of 3.8. Median particle size (d_{50}) of 62±45 µm was observed in the membrane tank. For SGD_m of 0.2 to 2.0 $m^3\ m^{-2}\ h^{-1}$, the fouling rate (d*P*/dt) was similar across the initial flux steps up to 9 L $m^{-2}\ h^{-1}$ applied during critical flux (J_c) analysis (Figure 5-3). However, following a progressive increase in flux, d*P*/dt began to increase which indicated the weak form of the J_c to lie between 12 and 15 L $m^{-2}\ h^{-1}$ for the AnMBR suspension at a SGD_m of 2.0 $m^3\ m^{-2}\ h^{-1}$. For comparison, J_c for a SGD_m of 0.5 $m^3\ m^{-2}\ h^{-1}$ was between 9 and 12 L $m^{-2}\ h^{-1}$.

Table 5-1. Influent characteristics, G-AnMBR treatment performance and bulk sludge characteristics.

Parameter	Unit	Influent	Membrane tank	Permeate	Removal %
pH	-	7.8±0.3 (n=181)	7.9±0.3 (n=165)	8.2±0.2 (n=80)	-
MLSS	mg L^{-1}	131±38 (n=181)	384±190 (n=156)	<DL	>99
COD_t	mg L^{-1}	221±78 (n=175)	663±333 (n=151)	41±16 (n=74)	83±7
BOD_5	mg L^{-1}	106±39 (n=39)	-	11±7 (n=42)	90±6
SCOD	mg L^{-1}	88±30 (n=174)	149±65 (n=153)	41±16 (n=74)	-
SMP_P	mg L^{-1}	39±9 (n=117)	59±19 (n=129)	-	-
SMP_C	mg L^{-1}	7±3 (n=117)	19±11 (n=137)	-	-
SMP P/C	-	6.1±2.7 (n=116)	3.8±1.7 (n=136)	-	-
Particle size (d_{50})	µm	64±24 (n=96)	62±45 (n=112)	-	-
VFA	mg CH_3COOH L^{-1}	22.8±14.8 (n=26)	-	<2.0[a] (n=18)	-

a. limit of detection (LOD), 2.0 mg L^{-1}
DL- detection limit

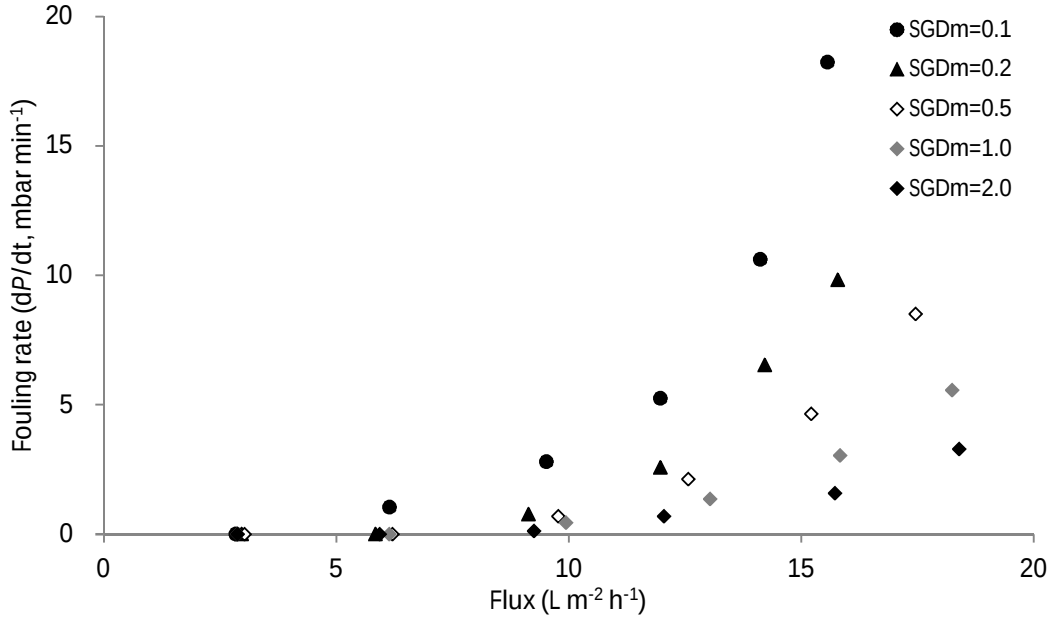

Figure 5-3. Critical flux determination under different specific gas demand per unit membrane area (SGD_m) (3 L m^{-2} h^{-1} per step; 10 mins step).

5.3.2 Continuous filtration and continuous gas sparging

The impact of flux on fouling rate was assessed using a fixed SGD_m of 0.2 m^3 m^{-2} h^{-1} (Figure 5-4). At a J_{20} *of* 5 L m^{-2} h^{-1}, d*P*/dt was below 1 mbar h^{-1}. However, with an increase in flux, d*P*/dt increased considerably, and for J_{20} exceeding 10 L m^{-2} h^{-1}, the TMP reached the maximum TMP (TMP_{max}, 550 mbar) in less than 24 h. The impact of SGD_m was subsequently evaluated at J_{20} of 13.5 L m^{-2} h^{-1}. When SGD_m increased from 0.1 to 1.0 m^3 m^{-2} h^{-1}, d*P*/dt decreased from 224 to less than 1 mbar h^{-1}. Upon increasing SGD_m further

from 1.0 to 2.0 m^3 m^{-2} h^{-1}, a decrease in d*P*/dt was not noted, indicating a plateau had been reached.

5.3.3 Continuous filtration and intermittent gas sparging

To reduce net energy demand, gas sparging frequency ($\Theta_{gs,f}$) was evaluated for J_{20} *of* 5, 10 and 13.5 L m^{-2} h^{-1} (Figure 5-5):

$$\Theta_{gs,f} = \frac{\theta_{gs,on}}{(\theta_{gs,on+}\theta_{gs,off})} \quad (5\text{-}11)$$

For this analysis, gas sparging on time ($\theta_{gs,on}$) was fixed at 10 s and gas sparging off time ($\theta_{gs,off}$) varied from 10 to 90 s. At the lowest J_{20} of 5 L m^{-2} h^{-1}, d*P*/dt of less than 1 mbar h^{-1} was achieved for all conditions except when SGD_m and $\Theta_{gs,f}$ were reduced to 0.2 m^3 m^{-2} h^{-1} and 10 % respectively. For J_{20} of 10 and 13.5 L m^{-2} h^{-1}, a d*P*/dt of less than 1 mbar h^{-1} was only achieved when $\Theta_{gs,f}$ was fixed at 50% and SGD_m was at least 1.0 m^3 m^{-2} h^{-1}. The impact of extending $\theta_{gs,on}$ was subsequently evaluated (Figure 5-6). Whilst increasing gas sparging frequency ($\Theta_{gs,f}$) reduced d*P*/dt with an applied $\theta_{gs,on}$ of 30 s, d*P*/dt remained higher than when operating with a $\theta_{gs,on}$ of 10 s. Under the same $\Theta_{gs,f}$ of 50 %, higher $\theta_{gs,on}$ with gas sparging 30 s on/30 s off had higher d*P*/dt than gas sparging 10 s on/10 s off.

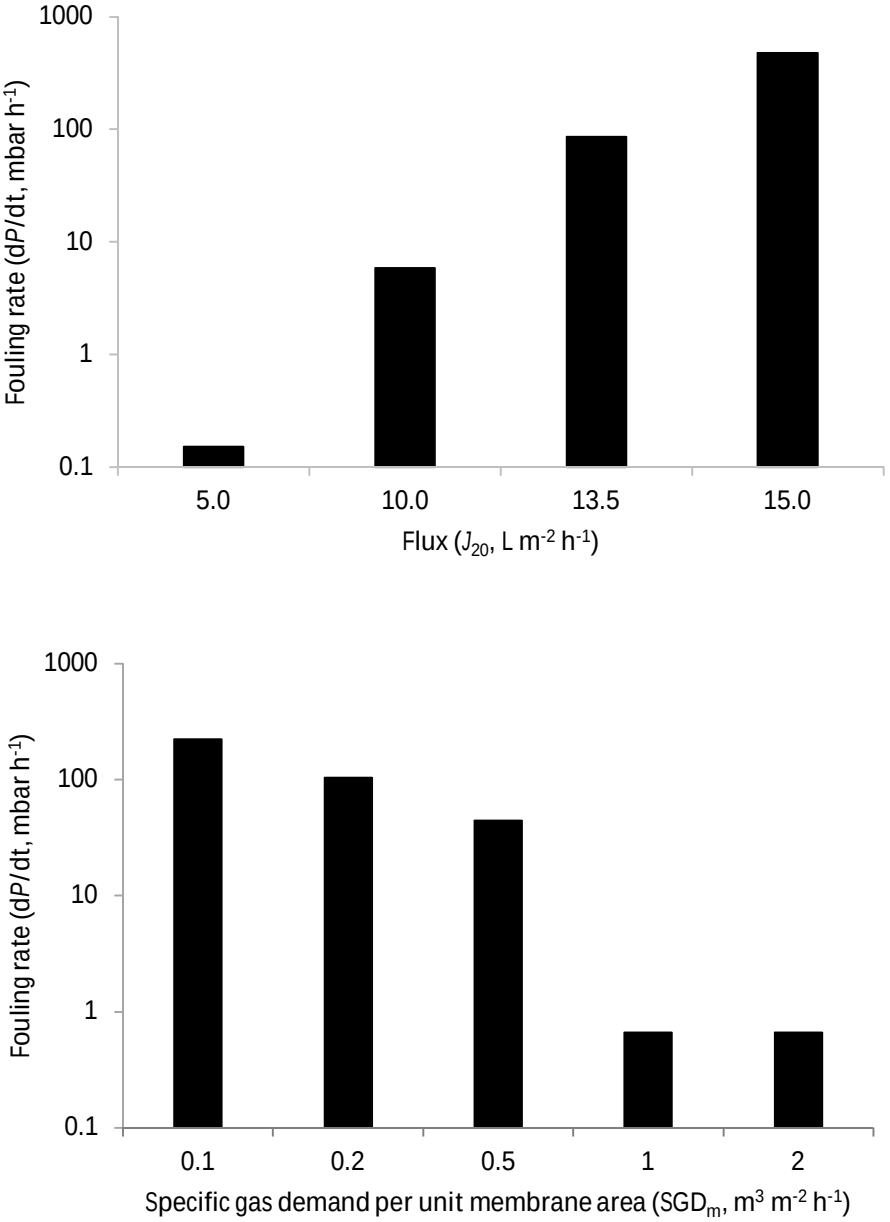

Figure 5-4. Impact of flux (specific gas demand per unit membrane area (SGD_m), 0.2 m^3 m^{-2} h^{-1}) and SGD_m (fixed flux, J_{20} =13.5 L m^{-2} h^{-1}) on membrane fouling rate using continuous filtration and continuous gas sparging. Filtration to 24 h or TMP_{max} (550 mbar).

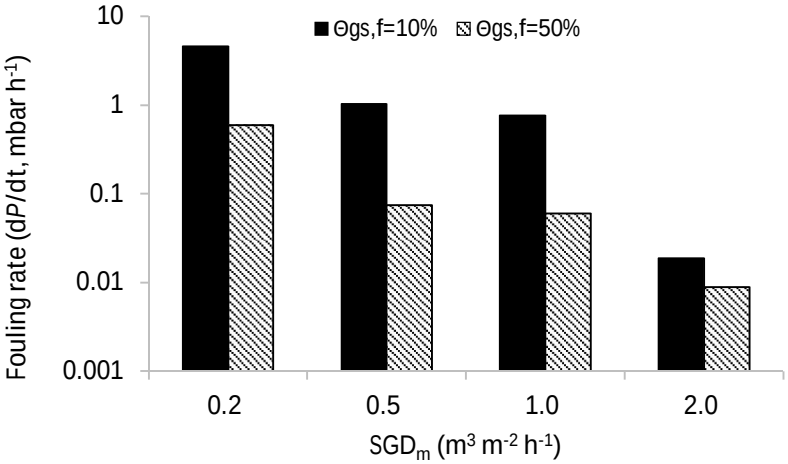

(a)

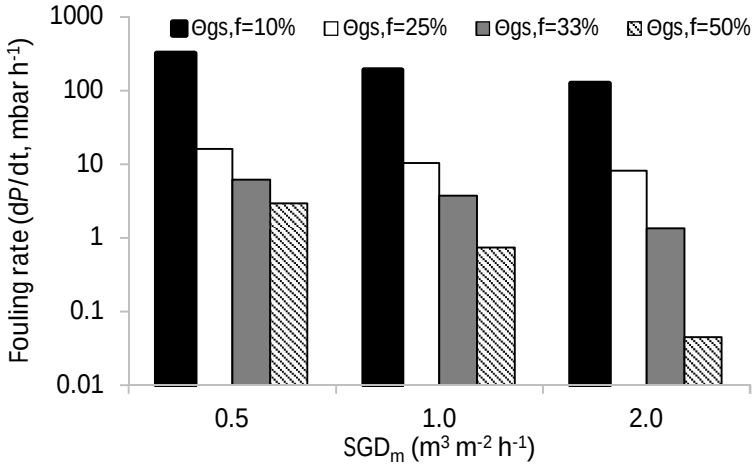

(b)

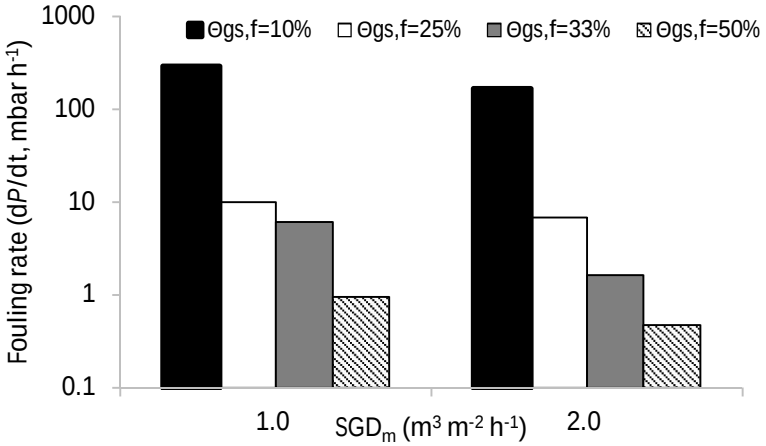

(c)

Figure 5-5. Impact of specific gas demand per unit membrane area (SGD_m) and gas sparging frequency ($\boldsymbol{\Theta}_{gs,f}$) (10 s on time fixed) on membrane fouling rate using continuous filtration and intermittent gas sparging: (a) J_{20}= 5 L m^{-2} h^{-1}; (b) 10 L m^{-2} h^{-1}; (c) 13.5 L m^{-2} h^{-1}. Filtration to 24 h or TMP_{max} (550 mbar).

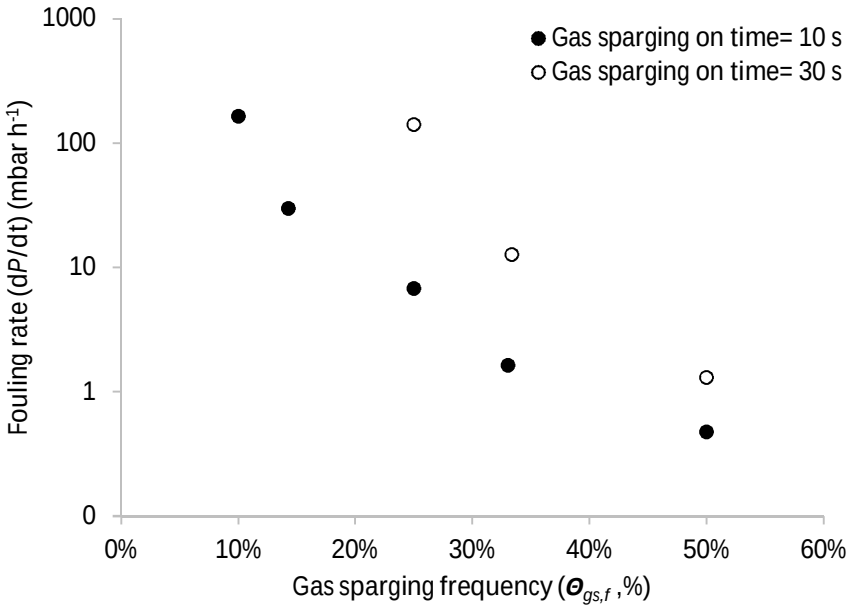

Figure 5-6. Impact of gas sparging frequency ($\Theta_{gs,f}$) and gas sparging on time ($\theta_{gs,on}$) on membrane fouling rate using continuous filtration and intermittent gas sparging at fixed flux (J_{20}=13.5 L m^{-2} h^{-1}, SGD_m=2.0 m^3 m^{-2} h^{-1}). Filtration to 24 h or TMP_{max} (550 mbar).

5.3.4 Pseudo dead-end filtration using intermittent filtration and intermittent gas sparging

The impact of SGD_m and flux were investigated using pseudo DE filtration (Figure 5-7). Each filtration cycle (9 min) was conducted without gas sparging, and was then followed by a combination of membrane relaxation and gas sparging for one minute. To compensate for the lost productivity introduced by membrane relaxation, the actual flux was increased to provide a net flux comparable to the other gas sparging regimes. For example, a J_{20} of 15 L m^{-2} h^{-1} was used to achieve a net flux ($J_{20\ net}$) of 13.5 L m^{-2} h^{-1}. Low dP/dt below 1 mbar h^{-1} can be achieved at $J_{20\ net}$ of 5 L m^{-2} h^{-1} with SGD_m above 0.5 m^3 m^{-2} h^{-1} and at $J_{20\ net}$ of 10 L m^{-2} h^{-1} with SGD_m above 1.0 m^3 m^{-2} h^{-1}. Interestingly, a fouling rate of less than 1 mbar h^{-1} was also recorded at 13.5 L m^{-2} h^{-1} when a SGD_m of 2.0 m^3 m^{-2} h^{-1} was used. Since gas sparging was introduced for only one minute in a ten minute cycle, a SGD_m of 2.0 m^3 m^{-2} h^{-1}, corresponded to a net SGD_m ($SGD_{m,net}$) of 0.2 m^3 m^{-2} h^{-1}. The impact of gas sparging time was subsequently evaluated which is analogous to the membrane relaxation period (Figure 5-8a). Provided gas sparging was at least one minute in length, dP/dt was limited to less than 1 mbar h^{-1}. Filtration cycle length was

also studied (Figure 5-8b). Increasing filtration cycle length greater than 9 min appeared detrimental to membrane performance. Further diagnostic investigation evidenced that the cake fouling rate (r_f) was around 200-250 mbar h^{-1} when filtration cycle length was at four and nine minutes (Figure 5-9). However, despite this considerable 'in-cycle' fouling rate, provided filtration cycle length was below 9 min, negligible increase in residual fouling resistance (R_{if}) was noted. In contrast, for a 14 min filtration cycle length, both r_f and R_{if} increased to 400 mbar h^{-1} and 3 x 10^{12} m^{-1} respectively.

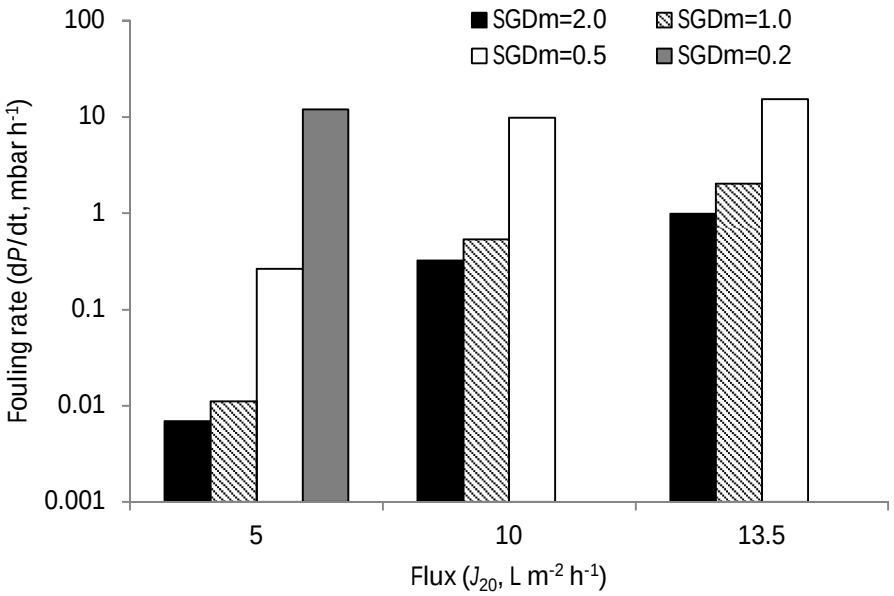

Figure 5-7. Impact of specific gas demand per unit membrane area (SGD_m) on membrane fouling rate using pseudo dead-end gas sparging regime: 9 min on/1 min off; $J_{20\,net}$= 5, 10, 13.5 L m^{-2} h^{-1}. Gas sparging introduced once filtration has stopped. Filtration to 24 h or TMP_{max} (550 mbar).

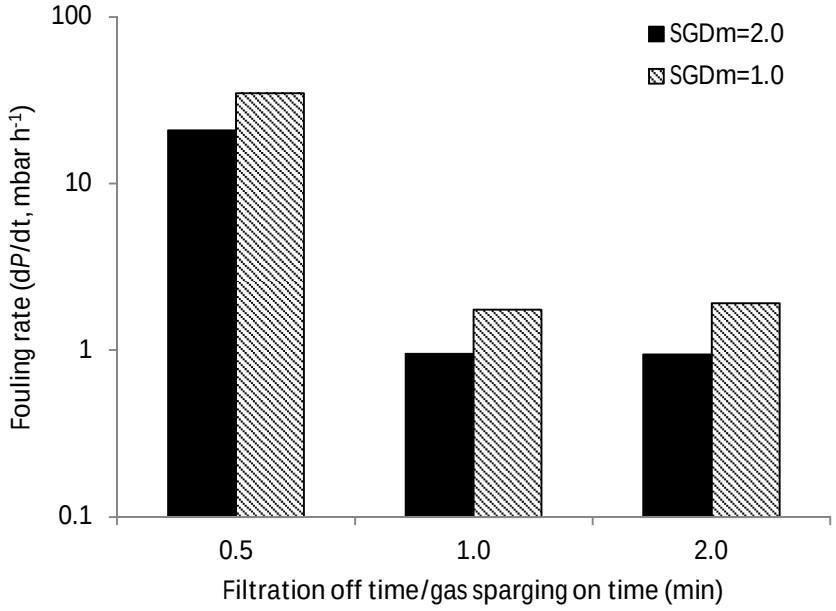

(a)

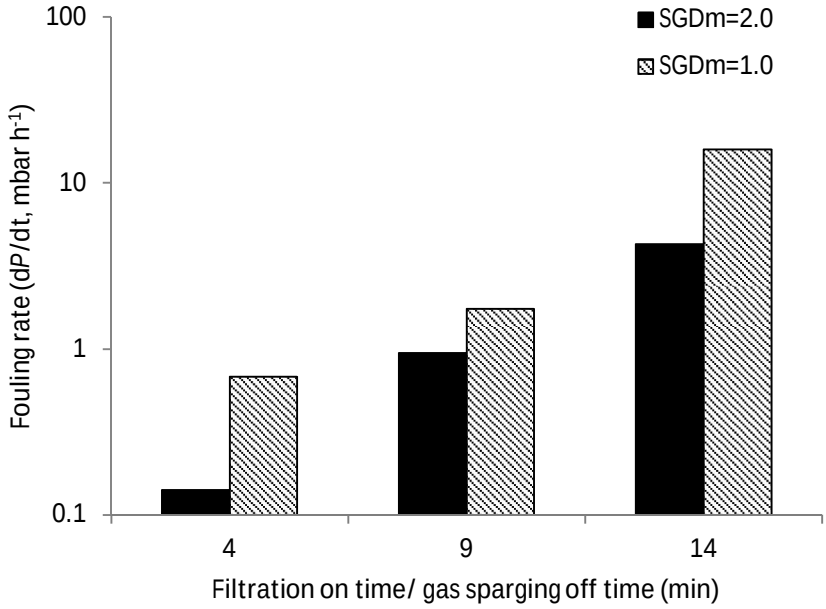

(b)

Figure 5-8. Impact of filtration off time (gas sparging on time) and filtration on time (gas sparging off time) on membrane fouling rate using pseudo dead-end gas sparging regime (J_{20}=13.5 L m^{-2} h^{-1}, $J_{20\ net}$ varied): (a) fixed filtration on time (9 min); (b) fixed filtration off time (1 min). Filtration to 24 h or TMP_{max} (550 mbar).

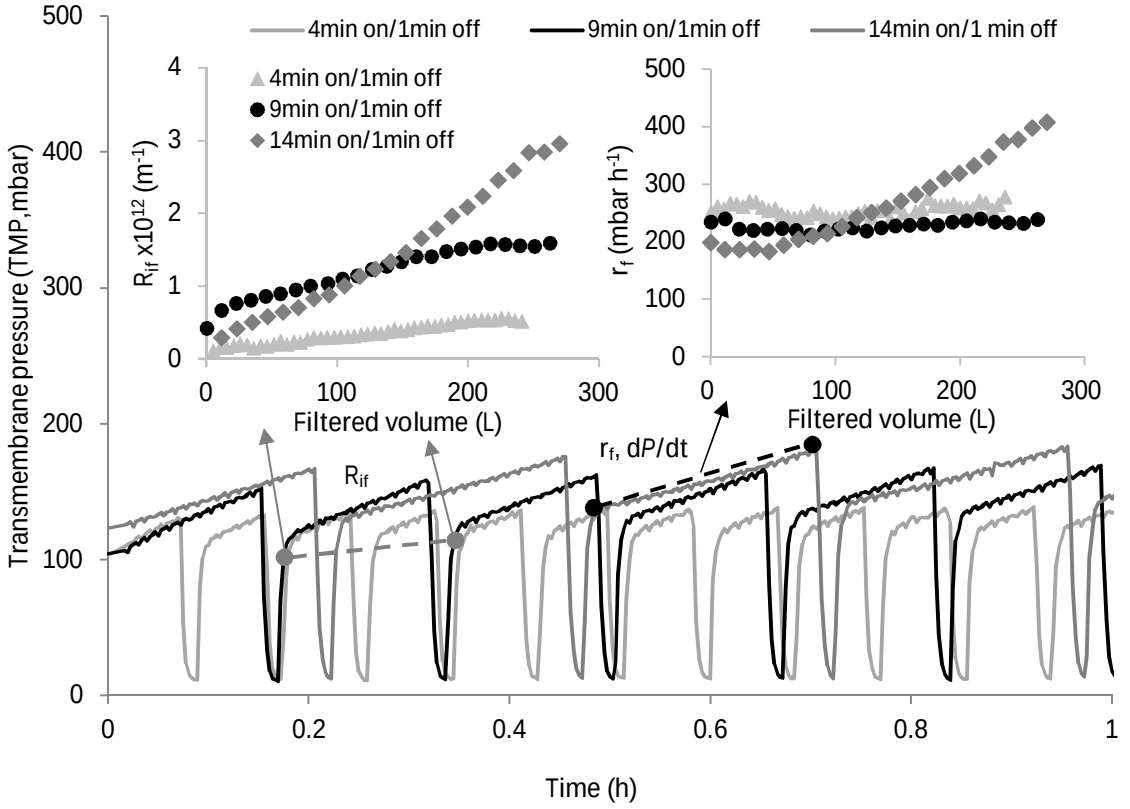

Figure 5-9. Internal residual fouling resistance (R_{if}, calculated from pressure at onset of filtration) and cake fouling rate (r_f, dP/dt) analyses under pseudo dead-end gas sparging regime. J_{20}, 13.5 L m^{-2} h^{-1}; filtration 4 min on/1 min off, 9 min on/1 min off, 14 min on/1 min off. Gas sparging introduced once filtration has stopped: SGD_m, 2.0 m^3 m^{-2} h^{-1}.

5.4 Discussion

In this study, a pseudo dead-end gas sparging regime has been identified that can deliver sustained membrane operation using a fraction of the energy demanded for conventional gas sparging strategies. Comparison of the various gas sparging strategies employing the same net energy demand (0.13 kWh m^{-3}, Figure 5-10) evidences that: (i) shear stress (G=460 s^{-1}) is critical to sustaining permeability during continuous gas sparging, such that equivalent low energy operation cannot be achieved; (ii) intermittent gas sparging (10s on/10s off) cannot sustain permeability when gas sparging rate is reduced to normalise energy use; and (iii) filtration without shear stress, as used in pseudo dead-end operation, enables sustained operation (no. 3,Table 5-2) analogous to that observed with continuous gas sparging, but using only a fraction of

the energy (McAdam et al., 2011). During continuous gas sparging (CGS), fouling rate (dP/dt) increased when flux increased at a fixed SGD_m and decreased when SGD_m was increased at a fixed flux (Figure 5-4). This is analogous to the J_c analysis (Figure 5-3), and demonstrates the importance of shear stress under CGS. At a J_{20} of 13.5 L m^{-2} h^{-1}, a plateau in fouling rate was achieved above a SGD_m of 1.0 m^3 m^{-2} h^{-1}, from which an optimum operating condition can be inferred (Figure 5-4). This is similar to earlier studies of CGS in both aerobic and anaerobic MBR (Guglielmi et al., 2007; Robles et al., 2012); although the SGD_m required to achieve a plateau, is specific to the suspension characteristics. In a study of particle deposition within model binary dispersions, Krompcamp et al. (2006) identified that only the small particles deposited at the membrane surface as they had a lower J_c. In this study, the considerable specific gas demand required to achieve this plateau at modest fluxes, relative to conventional aerobic MBR, can be ascribed to the matrix composition in AnMBR which comprises of concentrated biopolymers with a more disperse particle distribution, fostering a lower J_c for the suspension (Table 5-1). McAdam et al. (2011) reported that continuous gas sparging was sufficient to reduce d_{50} from 182 μm, observed during pseudo DE gas sparging, to 52 μm. Consequently, the additional shear stress introduced with high SGD_m could lead to the propagation of more fine particles (McAdam et al., 2011), with a lower J_c. Whilst sustaining continuous gas sparging at the membrane wall limits deposition of coarse particles, preferential deposition of soluble and colloidal biopolymers then occurs since their back-transport is mainly governed by Brownian rather than shear-induced diffusive effects (McAdam et al., 2011; McAdam and Judd, 2008; Tardieu et al., 1998). We assert that the modest fluxes achieved for AnMBR in CGS mode are due to the preferential deposition of SMP (McAdam et al., 2011), an effect which is exacerbated in AnMBR since SMP_{COD} is at least 1.5 times higher than conventional aerobic MBR (Table 5-1) (Martin-Garcia et al., 2011).

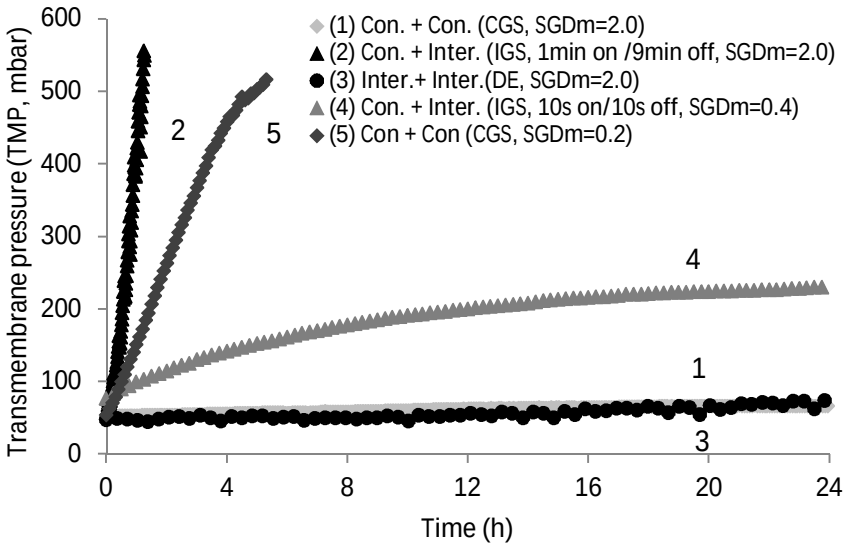

Figure 5-10. Comparison of membrane fouling under same specific gas demand per membrane area (SGD_m) and same net SGD_m ($SGD_{m\ net}$) with different gas sparging regimes ($J_{20\ net}$= 13.5 L m^{-2} h^{-1}). Con. (Continuous), Inter. (Intermittent); CGS (continuous gas sparging), IGS (intermittent gas sparging), DE (pseudo dead-end gas sparging). Detailed test parameters can be referred to Table 5-2.

Table 5-2. Comparison of different gas sparging regimes under same specific gas demand per membrane area (SGD_m) and same net SGD_m ($SGD_{m\ net}$).

Filtration	Gas sparging	Filtration On/Off	Gas sparing On/Off	J_{20}[a]	$J_{20\ net}$[b]	SGD_m	$SGD_{m\ net}$	Energy demand
		min	min	L m^{-2} h^{-1}	L m^{-2} h^{-1}	m^3 m^{-2} h^{-1}	m^3 m^{-2} h^{-1}	kWh m^{-3}
(1) Con.	Con. (CGS)	-	-	13.5	13.5	2	2	1.325
(2) Con.	Inter.(IGS)	-	1min/9min	13.5	13.5	2	0.2	0.133
(3) Inter.	Inter. (DE)	9min/1min	1min/9min	15	13.5	2	0.2	0.133
(4) Con.	Inter. (IGS)	-	10s/10s	13.5	13.5	0.4	0.2	0.133
(5) Con.	Con. (CGS)	-	-	13.5	13.5	0.2	0.2	0.133

J_{20}, flux at 20°C; b. $J_{20\ net}$, net flux at 20°C
Con. (Continuous), Inter. (Intermittent); CGS (continuous gas sparging), IGS (intermittent gas sparging), DE (pseudo dead-end gas sparging)

During intermittent gas sparging (IGS), a SGD_m greater than 1.0 m^3 m^{-2} h^{-1}, and a gas sparging frequency ($\Theta_{gs,f}$) of 50 % (i.e. gas sparging 10 s on/10 s off) was sufficient to achieve the threshold fouling rate of < 1 mbar h^{-1} at 13.5 L m^{-2} h^{-1} (Figure 5-5). This would indicate that particle deposition within the gas sparging 'off' period is reversible during the subsequent gas sparging 'on' period, provided sufficient shear-rate is applied (Yoon, 2015). In comparison to CGS, IGS with a 10 s on/10 s off sparging cycle, provides a 50 % energy saving whilst enabling similarly sustainable fluxes (Fan and Zhou, 2007);

such methodologies have been commercially realised in aerobic MBR for municipal wastewater treatment (Buer and Cumin, 2010). A lower $\Theta_{gs,f}$, indicating a longer gas sparging off time ($\theta_{gs,off}$) led to d*P*/dt greater than 1 mbar h^{-1} (Figure 5-5, Figure 5-6), which has been similarly demonstrated elsewhere (Vera et al., 2016). When adopting the same $\Theta_{gs,f}$ of 50 %, the longer gas sparging period ($\theta_{gs,on}$, 30 s on) provided higher d*P*/dt when compared with $\theta_{gs,on}$ of 10 s (Figure 5-6). Similarly, Guibert et al. (2002) also demonstrated higher d*P*/dt when applying a 60 s on/60 s off air sparging cycle compared with 15 s on/15 s off in an aerobic MBR. The authors proposed that the permeability decline was due to prolonged filtration periods without shear, that was no longer restorative following gas sparge inclusion. Consequently, IGS is limited to a 10 s on/ 10 s off cycle ($\Theta_{gs,f}$, 50%) to yield a maximum energy saving of 50 % at 13.5 L m^{-2} h^{-1} versus CGS.

Characterisation of individual filtration cycles within the pseudo dead-end regime, demonstrated significant cake fouling rates (r_f) of 200-250 mbar h^{-1} (Figure 5-9). However, provided the filtration cycle was fixed to below 9 mins., low fouling rate (<1 mbar h^{-1}) (Figure 5-8) and negligible internal residual fouling resistance (R_{if}) (Figure 5-9) were observed, which suggests that the cake developed during filtration can be reversed by the simultaneous use of gas sparging and relaxation introduced at the end of each filtration cycle. This is ostensibly similar to an earlier investigation of pseudo dead-end filtration for an application in low solids concentration MBR for groundwater denitrification which was comprised of dispersed growth biomass (0.5 to 1.1 g L^{-1}) (McAdam et al., 2011; McAdam and Judd, 2008). Although similar in solids concentration to this study (0.4 gMLSS L^{-1}) (Table 5-1), the AnMBR has a more complex bulk sludge matrix than denitrification and aerobic MBR, comprising of more high molecular weight colloidal matter. The authors proposed that deposit reversibility could be accounted for through the critical mass concept first proposed by Harmant and Aimar (1996) in which the permeation drag force within the first layer of the loose cake increased as layer number increased, thereby increasing deposit mass until a critical value was reached which induced aggregation and collapse into a compacted cake layer (McAdam et al., 2011; McAdam and Judd, 2008). In their study, a mono-disperse colloidal suspension

was employed, with a narrow size distribution within a controlled ionic environment, which then enabled the 'critical mass' that induced collapse to be described through discrete surface force interactions (Bessiere et al., 2005; Harmant and Aimar, 1996). Whilst the particle matrix within heterogeneous MBR systems, is regarded as too complex to be only described by discrete surface forces, a transition from limited to significant irreversible fouling was observed when the cycle length increased from 9 to 14 mins, which corresponded to a critical mass (Equation 5-7) between 0.7 and 1.1 g MLSS m^{-2} at J_{20} of 13.5 L m^{-2} h^{-1}. Vera et al. (2015a) described reversibility of the deposit formed within the pseudo dead-end filtration cycle of a MBR to be also governed by cake compressibility, which we propose to be dependent upon the matrix composition and character. To illustrate, in this study, the critical mass was considerably lower than previously identified for MBR (4.6-4.8 g MLSS m^{-2}, J= 24 L m^{-2} h^{-1}). This can be explained by the higher colloidal fraction within the AnMBR suspension as the SMP concentration (sum of protein and carbohydrate) (Table 5-1), which was around 5-7 times that in denitrification MBR (McAdam et al., 2011; McAdam and Judd, 2008). A high SMP P/C ratio of 3.8 was also obtained in this study compared with 0.6-2.1 in denitrification MBR (McAdam et al., 2011; McAdam and Judd, 2008); a higher P/C ratio having been linked to greater fouling propensity due to the greater probability for adhesion by the protein-rich fraction, which is generally regarded as more hydrophobic than carbohydrate (Meng et al., 2006). Specific cake resistance (α) of 10^{13-14} m kg^{-1} was estimated from filtration cycle analysis (Equation 5-5, 5-6). For illustration, this is higher than that has been previously reported for cake formed by microbial floc (10^{12}-10^{13} m kg^{-1}) and similar to that of a cohesive gel layer (10^{14} m kg^{-1}) (Hong et al., 2014). McAdam and Judd (2008) demonstrated a less clear transition from non-fouling to fouling conditions when evaluating pseudo dead-end cycle length at increasing SRTs, which was ascribed to the lower colloidal contribution in the matrix; although it was also recognised that this transition would be dependent upon both suspension characteristics (such as size, charge (Harmant and Aimar, 1996) and shape (Bessiere et al., 2005)) as well as particle-particle and particle-membrane interactions. Whilst this conceptually supports the development of a more cohesive cake when applying pseudo dead-end filtration to

AnMBR, it is important to recognise that the cake formed was almost completely reversible when cycle time was limited to around 9 mins at $J_{20\ net}$ of 13.5 L m^{-2} h^{-1}.

To achieve a net productivity with $J_{20\ net}$ of 13.5 L m^{-2} h^{-1}, an actual J_{20} of 15 L m^{-2} h^{-1} was used for the pseudo dead-end regime (Table 5-2). This is higher than compared with typical fluxes of 5-12 L m^{-2} h^{-1} reported in the AnMBR literature (Martin Garcia et al., 2013; Vera et al., 2015b) and is equivalent to or higher than the critical flux recorded for the suspension (Figure 5-3). This is consistent with earlier studies of pseudo dead-end gas sparging for MBR where sustained operation was demonstrated at fluxes exceeding the critical flux (Vera et al., 2015a, 2015b). Using continuous gas sparging, colloids undergo preferential migration towards the membrane due to particle size segregation introduced by shear induced diffusion, whereas when pseudo dead-end filtration is undertaken, simultaneous deposition of soluble, colloidal and particulate material occurs which results in the formation of a more heterogeneous cake (McAdam et al., 2011). Consequently, pseudo dead-end filtration is apparently independent of critical flux, which suggests that higher fluxes can be achieved with considerably less energy than conventional gas sparging strategies. However, it is asserted that this strategy is only possible within low solids concentration MBR, to limit cake deposition within specific filtration cycle time (e.g. 9 mins.) (Figure 5-8) (McAdam and Judd, 2008), since both the filtration time and TMP will also influence the compressibility of the cake (McAdam and Judd, 2008; Vera et al., 2015a).

For $J_{20\ net}$ of 13.5 L m^{-2} h^{-1}, the specific gas demand per unit permeate (SGD_p) was 14.8 m^3 m^{-3} (Figure 5-10). Verrecht et al. (2010) identified critical SGD_p of 15 and 19 m^3 m^{-3} corresponding to fluxes of 15 and 30 L m^{-2} h^{-1}, as the limit at which gas sparging energy was deployed efficiently to sustain permeability during modelling of full-scale hollow-fibre aerobic MBR. This closely corresponds to full scale municipal aerobic MBR, reportedly ranging 14 to 30 m^3 m^{-3} (Yoon, 2015). Consequently, the proposed pseudo dead-end gas sparging regime is comparable to the lower SGD_p threshold for aerobic MBR, despite operation within a more challenging matrix (Martin-Garcia et al., 2011). Experimental data was evaluated to identify hydrodynamic conditions capable of achieving sustained operation (dP/dt, <1 mbar h^{-1}) and benchmarked against average

data for energy production from this specific wastewater (0.28 kWh m^{-3}) (Cookney et al., 2016) and from the literature (0.34 kWh m^{-3}) (Cookney et al., 2016; Gouveia et al., 2015a, 2015b; Shin et al., 2014) (Figure 5-11). In this study, it was difficult to ascertain classical gas sparging conditions that could deliver to the energy neutral proposition, whereas the pseudo dead-end gas sparging regime produced permeate at around 0.14 kWh m^{-3}, equivalent to around 50 % of the energy recovered from AnMBR. Several authors have also identified that the pseudo dead-end gas sparging regime proposed can reduce the energy demand of membrane operation for niche aerobic and anoxic MBR applications (McAdam et al., 2011; Vera et al., 2015a). However, the membrane bulk sludge matrix in AnMBR is considerably more complex than aerobic MBR for groundwater and municipal final effluent tertiary treatment. This study compared different gas sparging regimes in the AnMBR system and applied this pseudo dead-end gas sparging regime in UASB configured AnMBR. Importantly, this study demonstrates that energy neutral wastewater can be achieved with AnMBR through adoption of an appropriate gas sparging regime. An analogy can be made to LEAPmbr and MEMPULSE^{TM} innovations in aerobic MBR which sought to extend the intermittent period for gas sparging. In addition to reducing energy demand, extending intermittency reduced capital cost in aeration equipment by up to 50 % (Yoon, 2015). Due to the increased length of the filtration cycle illustrated in this study between gas sparging cycles (around 9 min), it is suggested that pseudo dead-end gas sparging could therefore provide further indirect cost benefits through capital savings versus conventional MBR operation.

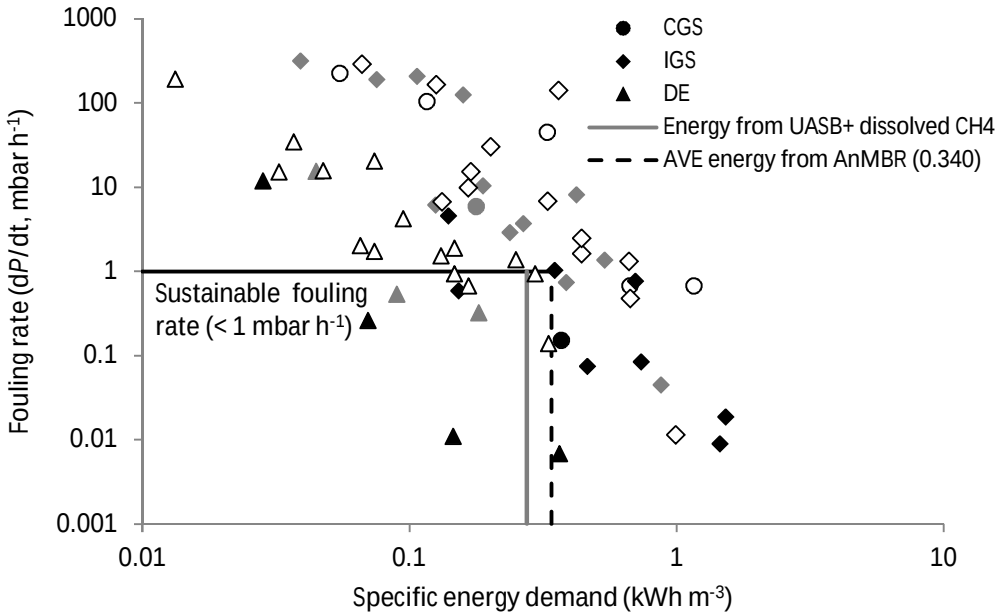

Figure 5-11. Impact of specific energy demand on membrane fouling (based on 3 m hydraulic head). CGS, continuous gas sparging; IGS, intermittent gas sparging; DE, pseudo dead-end. Black, grey and white data represent fluxes (J_{20}) of: 5, 10 and 13.5 L m^{-2} h^{-1}. Lines represent energy recovered from biogas and dissolved CH_4 using: sewage from the present study (grey solid line) (Cookney et al., 2016); average from the municipal AnMBR literature (black broken line) (Cookney et al., 2016; Gouveia et al., 2015a, 2015b; Shin et al., 2014).

5.5 Conclusions

The UASB configured AnMBR used in this study promoted a low solids concentration local to the membrane which made the application of non-conventional hydrodynamic conditions possible. In the pseudo dead-end filtration mode, reversibility was illustrated through critical mass which is a product of solids concentration, flux and time. It is suggested that reversibility will also be dependent upon transmembrane pressure and compressibility, which will be specific to the matrix. It is important to observe that pseudo dead-end operation has now been successfully applied to three different low solids MBR applications (potable, tertiary and anaerobic municipal wastewater). Consequently, whilst the matrix will exert an influence on the practicable filtration cycle length at a prescribed flux, there is increasing evidence of the viability of this filtration mode to enable sustainable fluxes with a conservative energy demand. In this study, the highest flux tested was 15 L m^{-2} h^{-1} at which a nine-minute pseudo dead-end filtration cycle was sustainable. Based on the mechanism proposed, it is suggested that higher

sustainable fluxes can be achieved by reducing the filtration cycle length which warrants further study. Importantly, pseudo dead-end filtration has been shown to provide low energy membrane operation in AnMBR sufficient to achieve the aspiration of energy neutral wastewater treatment.

5.6 Acknowledgements

The authors would like to thank our industrial sponsors: Anglian Water, Scottish Water, Severn Trent Water and Thames Water for their financial and technical support.

5.7 References

Aiyuk, S., Forrez, I., Lieven, D.K., van Haandel, A. and Verstraete, W. (2006) 'Anaerobic and complementary treatment of domestic sewage in regions with hot climates-A review', *Bioresource Technology*, 97, pp. 2225–2241.

APHA (2005) *Standard Methods for the Examination of Water and Wastewater*. 21st edn. Washington D.C: American Public Health Association.

Bessiere, Y., Abidine, N. and Bacchin, P. (2005) 'Low fouling conditions in dead-end filtration: Evidence for a critical filtered volume and interpretation using critical osmotic pressure', *Journal of Membrane Science*, 264, pp. 37–47.

Buer, T. and Cumin, J. (2010) 'MBR module design and operation', *Desalination*, 250, pp. 1073–1077.

Cho, B.D. and Fane, A.G. (2002) 'Fouling transients in nominally sub-critical flux operation of a membrane bioreactor', *Journal of Membrane Science*, 209, pp. 391–403.

Chong, S., Sen, T.K., Kayaalp, A. and Ang, H.M. (2012) 'The performance enhancements of upflow anaerobic sludge blanket (UASB) reactors for domestic sludge treatment - A State-of-the-art review', *Water Research*, 46, pp. 3434–3470.

Cookney, J., Mcleod, A., Mathioudakis, V., Ncube, P., Soares, A., Jefferson, B. and McAdam, E.J. (2016) 'Dissolved methane recovery from anaerobic effluents using hollow fibre membrane contactors', *Journal of Membrane Science*, 502, pp. 141–150.

Delgado, S., Villarroel, R. and González, E. (2008) 'Effect of the shear intensity on fouling in submerged membrane bioreactor for wastewater treatment', *Journal of Membrane Science*, 311, pp. 173–181.

Dong, Q., Parker, W. and Dagnew, M. (2015) 'Impact of FeCl3 dosing on AnMBR treatment of municipal wastewater', *Water Research*, 80, pp. 281–293.

Dubois, M., Gilles, K.A., Hamilton, J.K., Rebers, P.A. and Smith, F. (1956) 'Colorimetric method for determination of sugars and related substances', *Analytical Chemistry*, 28, pp. 350–356.

Fan, F. and Zhou, H. (2007) 'Interrelated effects of aeration and mixed liquor fractions on membrane fouling for submerged membrane bioreactor processes in wastewater treatment', *Environmental Science & Technology*, 41, pp. 2523–2528.

Gouveia, J., Plaza, F., Garralon, G., Fdz-Polanco, F. and Peña, M. (2015a) 'Long-term operation of a pilot scale anaerobic membrane bioreactor (AnMBR) for the treatment of municipal wastewater under psychrophilic conditions', *Bioresource Technology*, 185, pp. 225–233.

Gouveia, J., Plaza, F., Garralon, G., Fdz-Polanco, F. and Peña, M. (2015b) 'A novel configuration for an anaerobic submerged membrane bioreactor (AnSMBR)', *Bioresource Technology*, 198, pp. 510–519.

Guglielmi, G., Chiarani, D., Judd, S.J. and Andreottola, G. (2007) 'Flux criticality and sustainability in a hollow fibre submerged membrane bioreactor for municipal wastewater treatment', *Journal of Membrane Science*, 289, pp. 241–248.

Guibert, D., Aim, R.B., Rabie, H. and Côté, P. (2002) 'Aeration performance of immersed hollow-fiber membranes in a bentonite suspension', *Desalination*, 148, pp. 395–400.

Harmant, P. and Aimar, P. (1996) 'Coagulation of colloids retained by porous wall', *AIChE Journal*, 42, pp. 3523–3532.

Hong, H., Zhang, M., He, Y., Chen, J. and Lin, H. (2014) 'Fouling mechanisms of gel layer in a submerged membrane bioreactor', *Bioresource Technology*, 166, pp. 295–302.

Judd, S.J. (2011) *Principles and Applications of Membrane Bioreactors in Water and Wastewater Treatment*. 2nd edn. London,UK: Elsevier.

Krompcamp, J., Faber, F., Schroen, K. and Boom, R. (2006) 'Effects of particle size segregation on crossflow microfiltration performance: Control mechanism for concentration polarisation and particle fractionation', *Journal of Membrane Science*, 268, pp. 189–197.

Krzeminski, P., Van Der Graaf, J.H.J.M. and van Lier, J.B. (2012) 'Specific energy consumption of membrane bioreactor (MBR) for sewage treatment', *Water Science & Technology*, 65, pp. 380–392.

Le Clech, P., Jefferson, B., Chang, I.S. and Judd, S.J. (2003) 'Critical flux determination by the flux-step method in a submerged membrane bioreactor', *Journal of Membrane Science*, 227, pp. 81–93.

Lettinga, G., Rebac, S. and Zeeman, G. (2001) 'Challenge of psychrophilic anaerobic wastewater treatment', *Trends in Biotechnology*, 19, pp. 363–370.

Liao, B.Q., Kraemer, J.T. and Bagley, D.M. (2006) 'Anaerobic membrane bioreactors: applications and research directions', *Critical Reviews in Environmental Science and Technology*, 36, pp. 489–530.

Lowry, O.H., Rosebrough, N.J., Farr, A.L. and Randall, R.J. (1951) 'Protein measurement with the folin phenol reagent', *Journal of Biological Chemistry*, 193, pp. 265–275.

Martin-Garcia, I., Monsalvo, V., Pidou, M., Le-Clech, P., Judd, S.J., McAdam, E.J. and Jefferson, B. (2011) 'Impact of membrane configuration on fouling in anaerobic membrane bioreactors', *Journal of Membrane Science*, 382, pp. 41–49.

Martin Garcia, I., Mokosch, M., Soares, A., Pidou, M. and Jefferson, B. (2013) 'Impact on reactor configuration on the performance of anaerobic MBRs: Treatment of settled sewage in temperate climates', *Water Research*, 47, pp. 4853–4860.

Martinez-Sosa, D., Helmreich, B., Netter, T., Paris, S., Bischof, F. and Horn, H. (2011) 'Anaerobic submerged membrane bioreactor (AnSMBR) for municipal wastewater treatment under mesophilic and psychrophilic temperature conditions', *Bioresource Technology*, 102, pp. 10377–10385.

McAdam, E.J., Cartmell, E. and Judd, S.J. (2011) 'Comparison of dead-end and continuous filtration conditions in a denitrification membrane bioreactor', *Journal of Membrane Science*, 369, pp. 167–173.

McAdam, E.J. and Judd, S.J. (2008) 'Optimisation of dead-end filtration conditions for an immersed anoxic membrane bioreactor', *Journal of Membrane Science*, 325, pp. 940–946.

McCarty, A.A., Gilboy, P., Walsh, P.K. and Foley, G. (1999) 'Characterisation of cake compressibility in dead-end microfiltration of microbial suspensions', *Chemical Engineering Communications*, 173, pp. 79–90.

McCarty, P.L., Kim, J. and Bae, J. (2011) 'Domestic wastewater treatment as a net energy producer – Can this be achieved?', *Environmental Science & Technology*, 45, pp. 7100–7106.

Meng, F., Zhang, H., Yang, F., Li, Y., Xiao, J. and Zhang, X. (2006) 'Effect of filamentous bacteria on membrane fouling in submerged membrane bioreactor', *Journal of Membrane Science*, 272, pp. 161–168.

Ozgun, H., Tao, Y., Ersahin, M.E., Zhou, Z., Gimenez, J.B., Spanjers, H. and van Lier, J.B. (2015) 'Impact of temperature on feed-flow characteristics and filtration performance of an upflow anaerobic sludge blanket coupled ultrafiltration membrane treating municipal wastewater', *Water Research*, 83, pp. 71–83.

Parawira, W., Murto, M., Read, J.S. and Mattiasson, B. (2004) 'Volatile fatty acid production during anaerobic mesophilic digestion of solid potato waste', *Journal of Chemical Technology and Biotechnology*, 79, pp. 673–677.

Pretel, R., Robles, A., Ruano, M.V., Seco, A. and Ferrer, J. (2014) 'The operating cost of an anaerobic membrane bioreactor (AnMBR) treating sulphate-rich urban wastewater', *Separation and Purification Technology*, 126, pp. 30–38.

Robles, A., Ruano, M.V., García-Usach, F. and Ferrer, J. (2012) 'Sub-critical filtration conditions of commercial hollow-fibre membranes in a submerged anaerobic MBR (HF-SAnMBR) system: the effect of gas sparging intensity', *Bioresource Technology*, 114, pp. 247–254.

Shin, C., McCarty, P.L., Kim, J. and Bae, J. (2014) 'Pilot-scale temperate-climate treatment of domestic wastewater with a staged anaerobic fluidized membrane bioreactor (SAF-MBR)', *Bioresource Technology*, 159, pp. 95–103.

Smith, A.L., Skerlos, S.J. and Raskin, L. (2013) 'Psychrophilic anaerobic membrane bioreactor treatment of domestic wastewater', *Water Research*, 47, pp. 1655–1665.

Tardieu, E., Grasmick, A., Geaugey, V. and Manem, J. (1998) 'Hydrodynamic control of bioparticle deposition in a MBR applied to wastewater treatment', *Journal of Membrane Science*, 147, pp. 1–12.

Tchobanoglous, G., Burton, F.L. and Stensel, H.D. (2003) *Wastewater Engineering Treatment and Reuse*. 4th edn. New York: McGraw-Hill Companies.

Vera, L., Gonzalez, E., Diaz, O., Sanchez, R., Bohorque, R. and Rodriguez-Sevilla, J. (2015a) 'Fouling analysis of a tertiary submerged membrane bioreactor operated in dead-end mode at high-fluxes', *Journal of Membrane Science*, 493, pp. 8–18.

Vera, L., González, E., Ruigómez, I., Gómez, J. and Delgado, S. (2015b) 'Analysis of backwashing efficiency in dead-end hollow-fibre ultrafiltration of anaerobic suspensions', *Environmental Science and Pollution Research*, 22, pp. 16600–16609.

Vera, L., González, E., Ruigómez, I., Gómez, J. and Delgado, S. (2016) 'Influence of gas sparging intermittence on ultrafiltration performance of anaerobic suspensions', *Industrial and Engineering Chemistry Research*, 55, pp. 4668–4675.

Verrecht, B., Maere, T., Nopens, I., Brepols, C. and Judd, S. (2010) 'The cost of a large-scale hollow fibre MBR', *Water Research*, 44, pp. 5274–5283.

van Voorthuizen, E., Zwijnenburg, A., van der Meer, W. and Temmink, H. (2008) 'Biological black water treatment combined with membrane separation', *Water Research*, 42, pp. 4334–4340.

Water UK (2006) *Wastewater Treatment and Recycling*. London, UK.

Wibisono, Y., Cornelissen, E.R., Kemperman, A.J.B., Van Der Meer, W.G.J. and Nijmeijer, K. (2014) 'Two-phase flow in membrane processes: A technology with a future', *Journal of Membrane Science*, 453, pp. 566–602.

Yoon, S.H. (2015) *Membrane Bioreactor Processes: Principles and Applications*. CRC press.

CHAPTER 6

Sustaining membrane permeability during unsteady-state operation of anaerobic membrane bioreactors for municipal wastewater treatment following peak-flow

6 Sustaining membrane permeability during unsteady-state operation of anaerobic membrane bioreactors for municipal wastewater treatment following peak-flow

K. M. Wang[a], B. Jefferson[a], A. Soares[a], E. J. McAdam[a*]
[a]Cranfield Water Science Institute, Vincent Building, Cranfield University, Bedfordshire, MK43 0AL, UK

Abstract

In this study, the impact of peak flow on anaerobic membrane bioreactor operation is investigated to establish how system perturbation induced by diurnal peaks and storm water flows will influence membrane permeability. Good permeability recovery was attained through increasing gas sparging during peak flow, which was explained by the transition in critical flux of the suspension at higher shear rates. However, supra-critical fluxes could also be sustained, provided peak flow was for a short duration. We suggest longer durations of supra-critical operation could be sustained through introduction of reactive fouling control strategies (e.g. TMP set-point control). An initial flux below the critical flux, prior to the introduction of peak flow, was advantageous to permeability recovery, suggesting membrane 'conditioning' is important in governing recoverability following peak flow. The importance of conditioning was confirmed through analysis of multiple peak flow events in which the loss of permeability following each peak-flow event was increasingly negligible, and can be ascribed to the arrival of a steady-state in membrane surface deposition. Whilst responding to peak flow with increased gas sparging has been shown effective, the energy demand is considerable, and as such a pseudo dead-end filtration strategy was also evaluated, which required only 0.04 kWh m^{-3} of energy for gas sparging. Comparison of both filtration modes identified comparable fouling rates, and the feasibility of a low energy gas sparging method for peak flow management that has successfully enabled supra-critical fluxes to be achieved over long-periods in other MBR applications. Importantly, membrane area provides the highest contribution toward capital cost of AnMBR. The potential to turn-up flux in response to peak-flow has been identified in this study, which suggests membrane area can be specified based on average flow rather than peak flow, providing substantial reduction in the capital cost of AnMBR for municipal wastewater treatment.

Keywords: unsteady-state, diurnal flow, capital cost, membrane design

6.1 Introduction

Anaerobic membrane bioreactors (AnMBRs) are a promising alternative to conventional aerobic biotechnology for municipal wastewater treatment, as the combination of organic degradation without the demand for aeration, coupled with energy recovery from biogas production, offers the potential to realise energy neutral wastewater treatment (Martin Garcia et al., 2013). The key challenges limiting full-scale application of AnMBR for municipal wastewater treatment, are the membrane investment cost and energy demand associated with membrane fouling control (Ruigómez et al., 2016). Numerous previous studies have focussed on sustaining membrane operation through application of various hydrodynamic conditions (for example, gas sparging regime, physical cleaning frequency and duration). In each of these studies, a steady-state influent flow rate is assumed, with the membrane fixed at constant flux (Martin Garcia et al., 2013; Robles et al., 2013). However, at full-scale, MBR must be designed to manage diurnal peaks and storm water flows (Hirani et al., 2010). Installation of equalisation tanks can serve to ameliorate peak flow and improve flow regulation (Yoon, 2015). Nevertheless, in a survey of 17 full-scale municipal aerobic MBR plants in Europe (Itokawa et al., 2008), half were reported to have peak ratios (peak flow to average flow) between 2 and 3, due to the diurnal flow pattern and connection to combined sewer systems. The membrane must therefore be designed to cope with an increased flow without incurring substantial long-term fouling. This can be facilitated by sustaining an average flux at peak flow, through an increase in membrane surface area, or by temporarily increasing flux during periods of peak flow. This latter option will constrain capital investment in membrane surface area by up to three times, but its viability is impingent upon permeability not being compromised in the long-term from the short-term turn-up in flux.

A peak ratio of 1.4 to 1.5 is recommended for full-scale aerobic MBR which assumes that a maximum sustainable flux (defined as the flux required to limit fouling and avoid or limit the demand for reactive chemical cleaning) can be achieved during peak flow that is 40 to 50 % higher than the average flux (Judd, 2011; Metcalf, 2017; Verrecht et al., 2010). Some full-scale aerobic MBR plants have adopted more conservative design, instead specifying the membrane surface area to match peak flow,

which ensures a considerably lower operating flux during flow variation (Lesjean et al., 2009; Verrecht et al., 2010), but introduces a tremendous penalty in capital cost. This is significant since it is estimated that membrane area will comprise the largest proportion of capital cost (72 %) for a full-scale municipal wastewater AnMBR (Lin et al., 2011). Furthermore, by specifying membrane surface area based on peak flow, severe membrane under-utilisation has been reported (Verrecht et al., 2010). To illustrate, in several surveys of full-scale municipal aerobic MBRs (Barillon et al., 2013; Veltmann et al., 2011), the average flow was typically less than 50 % of the peak flow used for design. This also incurred an increased operational cost of around 54 %, due to the excess specific aeration demand per unit membrane area (SAD_m) required (Verrecht et al., 2010). In the context of AnMBR for municipal wastewater treatment, this increase in energy demand and operational cost may reduce the attractiveness of investment, since the core aspiration is to facilitate energy neutral wastewater treatment (McAdam et al., 2011).

Whilst the implications of peak flow on AnMBR design and operation are yet to be reported, laboratory and pilot scale evaluation of aerobic MBR have been conducted, in which the capacity for the membrane to withstand an increase in flux, in response to peak flow, has been determined using a constant SAD_m (Lebegue et al., 2008; Syed et al., 2009; Yoon, 2015). Lebegue et al. (2008) identified no significant difference in transmembrane pressure (TMP) before and after a 2 hour peak flow event in a lab-scale aerobic MBR treating synthetic municipal wastewater, which increased flux from 10 to 30 L m^{-2} h^{-1} for two hours on a daily basis. However, Metcalf (2017) observed a significant membrane permeability decline in a pilot scale aerobic MBR treating settled municipal wastewater, when the flux returned to the average flux of 20 L m^{-2} h^{-1}, from a peak flux of 25 L m^{-2} h^{-1} that was sustained for 24 h. The authors attributed the increased fouling to the operating flux exceeding the critical flux during peak flow. In recognition of such behaviour, several studies sought to identify fouling control strategies that could be deployed during peak flow, such as increasing SAD_m, shortening filtration cycle time, or increasing backwash flux (Hirani et al., 2010; Veltmann et al., 2011). Following evaluation of a laboratory scale aerobic MBR treating

synthetic settled municipal wastewater, Howell et al. (2004) concluded that membrane fouling introduced by a temporary increase in flux could be controlled by an increase in SAD_m, with the residual foulant removed following flux restoration to a sub-critical level. Hirani et al. (2010) tested five different pilot-scale submerged aerobic MBRs treating settled municipal wastewater, and demonstrated that a reduction in membrane permeability of 22-32 % following the introduction of a peak flux ratio 1.6-3.2, was reversible, indicating that the reactive implementation of physical cleaning strategies during peak flow, were effective to cope with peak flow (Hirani et al., 2010). Importantly, such observations suggest that membrane surface area can be specified based on average flow rather than peak flow, which would help constrain membrane capital investment.

In AnMBR, the bulk sludge matrix is considerably more complex than in conventional aerobic MBR, leading to significantly higher membrane fouling (Judd, 2011; Martin-Garcia et al., 2011). As such, the reported flux for AnMBR is ordinarily between 5-12 L m^{-2} h^{-1} (Martin Garcia et al., 2013; Vera et al., 2015b), which is considerably below the flux of 20-30 L m^{-2} h^{-1} typically specified for full-scale aerobic MBR (Judd, 2011). The membrane area required for AnMBR will therefore be greater than for aerobic MBR, with the membrane cost inevitably increasing, where membrane area is specified to sustain average flux at peak flow. The aim of this paper is therefore to evaluate the impact of a temporary increase in AnMBR flux, in response to peak flow, to ascertain whether AnMBR membrane surface area can be specified based on average flow rather than peak flow in order to diminish capital investment. The specific objectives were to: (i) evaluate the parameters governing permeability recovery (initial flux, peak flux to initial flux ratio, peak length); (ii) investigate the impacts of peak flow and strategies of increased gas sparging during the peak to enhance permeability recovery; and (iii) compare the conventional and alternative hydrodynamic conditions, to sustain permeability recovery whilst minimising energy demand.

6.2 Material and methods

6.2.1 Anaerobic MBR pilot plant

The AnMBR pilot plant was configured as a granular upflow anaerobic sludge blanket (G-UASB) reactor with a submerged hollow fibre membrane cited downstream (Figure 6-1). The UASB was 42.5 L in volume, and was fitted with a lamella plate clarifier for solid/liquid/gas separation (Paques, Balk, The Netherlands). Granular sludge (16 L) from a mesophilic UASB designed for the pulp and paper industry, was used for inoculum, and was left to acclimate for 360 days before experimentation commenced. Settled sewage from Cranfield University's sewage works was fed into the AnMBR with a peristaltic pump (520S, Watson Marlow, Falmouth, UK), to fix HRT at 8 hours for normal flow conditions. The resultant upflow velocity in the G-UASB was 0.8-0.9 m h^{-1} (Tchobanoglous et al., 2003), which provided granule bed expansion of around 40 % of total column height. A dispersed-growth sludge fraction accumulated above the granular bed (Chong et al., 2012), and was withdrawn occasionally once washout occurred into the downstream membrane tank. No granular biomass was withdrawn from the G-UASB during the 120-day trial. Average sewage temperature during experimentation was 19.5±3.4 °C.

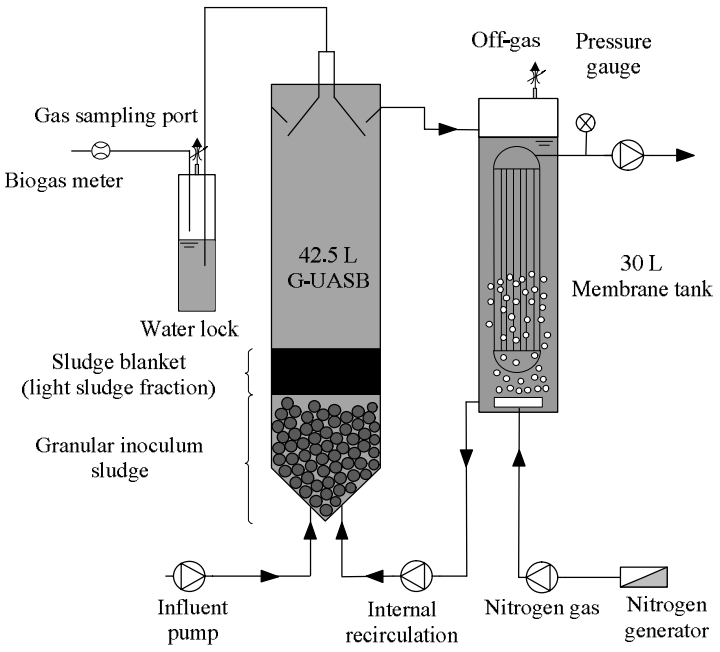

Figure 6-1. Schematic of the pilot granular anaerobic membrane bioreactor (G-AnMBR).

The 30 L membrane tank was fed with G-UASB effluent and a recycle from the membrane tank to the base of the G-UASB was employed to sustain the upflow velocity. The hollow-fibre membrane module (ZW-10) (SUEZ Water & Process Technologies, Oakville, Ontario, Canada) comprised four elements, each with 54 polyvinylidene fluoride (PVDF) hollow fibres (0.72 m in length and 1.9 mm outer diameter), providing a total surface area of 0.93 m^2. The hollow-fibres had a nominal pore size of 0.04 µm. Permeate was removed using a peristaltic pump (520U, Watson Marlow, Falmouth, UK). Pressure transducers on the permeate line (-1 to 1 bar, PMC 131, Endress + Hauser, Manchester, UK) and at the bottom of the membrane tank (0-2.5 bar, 060G2418, Danfoss, Nordborg, Denmark) were used to monitor TMP and liquid level height respectively. Nitrogen-enriched air, produced by a nitrogen generator (NG6, Noblegen gas generator, Gateshead, UK), was used for gas sparging. The membrane was operated under continuous filtration and continuous gas sparging (CGS), with several gas sparging strategies to manage peak flow (Figure 6-2). To benchmark performance, a 'control' was undertaken in which peak flow did not occur, and gas sparging was not increased (Figure 6-2). A typical single peak event was conducted over a 24 h cycle without repeated peak flows on a daily basis, where peak flow lasting 2 h was scheduled after 8 h operation at average flux (Figure 6-2). A novel pseudo dead-end (DE) gas sparging regime was compared to CGS operation, in which filtration was conducted for 9 minutes without gas sparging, after which filtration was stopped for 1 minute and gas sparging introduced. During the gas sparging cycle, the specific gas demand per unit area (SGD_m) was 0.5 or 2.0 $m^3\ m^{-2}\ h^{-1}$, which is equivalent to a $SGD_{m\ net}$ of between 0.05 and 0.2 $m^3\ m^{-2}\ h^{-1}$, when normalised to operational time (Figure 6-3). The introduction of gas sparging between filtration cycles was controlled using a solenoid valve (Type 6014, Burkert, Ingelfingen, Germany) connected to a multifunction timer relay (PL2R1, Crouzet, Valence, France). Specific gas demand per membrane surface area (SGD_m) of 0.5 and 2.0 $m^3\ m^{-2}\ h^{-1}$ were controlled by needle valves (0-10 and 0-50 L min^{-1}, Key Instruments, Langhorne, US). The normalised initial permeate flux at 20°C (J_{20}) was set at 6, 10 and 13 L $m^{-2}\ h^{-1}$:

$$J_T = J_{20} \cdot 1.025^{(T-20)} \quad (6\text{-}1)$$

At a SGD_m of 2.0 $m^3\ m^{-2}\ h^{-1}$, the shear stress intensity imparted through gas sparging bubbling corresponds to a gas velocity gradient of around 460 s^{-1} (McAdam et al., 2011):

$$G = (\frac{Q_a g h}{V_T \nu_a})^{0.5} \quad (6\text{-}2)$$

where Q_a is gas flow-rate ($m^3\ s^{-1}$), g is gravity constant ($m\ s^{-2}$), h is fluid height (m), V_T is reactor volume (m^3) and ν_a is the apparent kinetics viscosity ($m^2\ s^{-1}$). ν_a can be calculated from dynamic viscosity (μ, Pa s) by $\nu_a = \mu/\rho$, where ρ is density ($kg\ m^{-3}$). In order to sustain upflow velocity in the G-UASB at 0.8-0.9 m h^{-1}, the maximum attainable flux was around 27 L $m^{-2}\ h^{-1}$. Critical flux (J_C) analysis was conducted with the flux step method (Le Clech et al., 2003) using flux steps of 3 L $m^{-2}\ h^{-1}$ lasting for 10 minutes. The trials were conducted in batch with permeate recycled back to the membrane tank to sustain initial conditions. In order to demonstrate reproducibility, triplicate trials were conducted, and a relative standard deviation of 3.6 % recorded for TMP (J_{20}, 15 L $m^{-2}\ h^{-1}$; SGD_m, 2.0 $m^3\ m^{-2}\ h^{-1}$). Membrane permeability was calculated according to:

$$Permeability\ (K_{20}) = \frac{J_{20}}{TMP} \quad (6\text{-}3)$$

To discern total permeability recovery ($K_{20,tpr}$) following peak flow, a ratio of the average permeability within the initial 2 h (0-2 h) of experimentation (before peak flow), and the last 2 h (22-24 h) of experimentation (after peak flow) was used:

$$Total\ permeability\ recovery\ (K_{20,tpr}, \%) = \frac{K_{20,22-24h}}{K_{20,initial\ 2h}} \quad (6\text{-}4)$$

Similarly, peak permeability recovery ($K_{20,ppr}$) was calculated as a ratio of the average permeability within the 2 h after peak flow, and the 2 h before peak flow:

$$Peak\ permeability\ recovery\ (K_{20,ppr}, \%) = \frac{K_{20,2h\ after\ peak\ flow}}{K_{20,2h\ before\ peak\ flow}} \quad (6\text{-}5)$$

After each test, the membrane module was rinsed with tap water and chemically cleaned in 500 mg L^{-1} sodium hypochlorite for at least 8 h. A spare module was inserted to maintain constant AnMBR operation during this period. Before the membrane was reused, a clean water permeability test was undertaken, which evidenced less than 10 % deviation in membrane resistance throughout the trial.

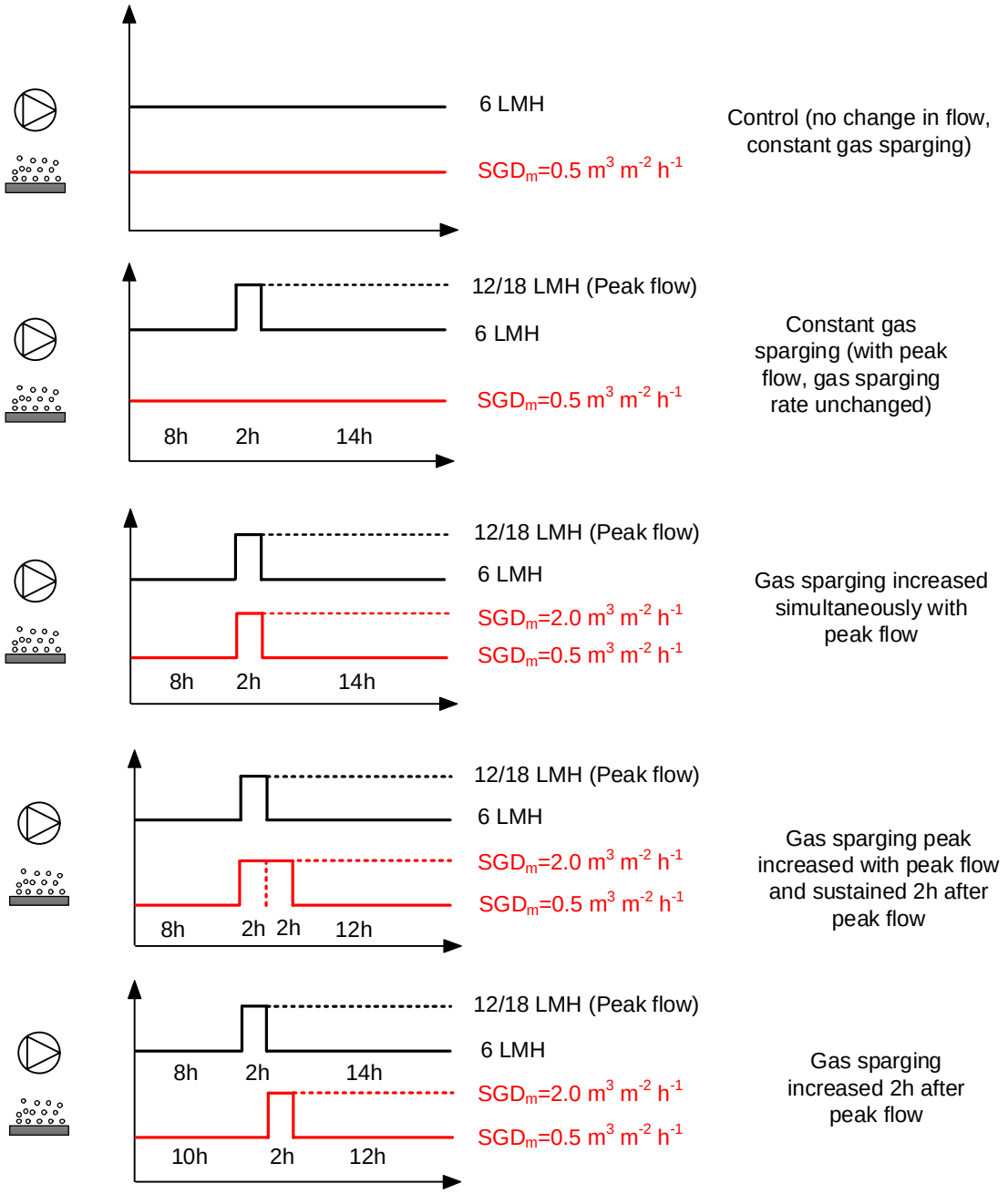

Figure 6-2. Gas sparging strategies tested to manage peak flow during continuous filtration.

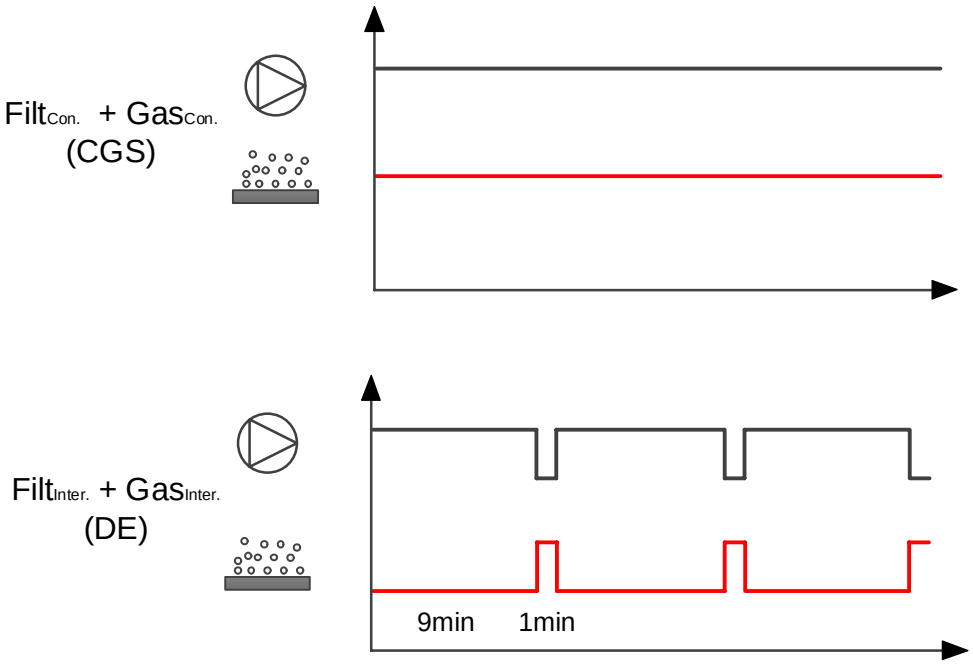

Figure 6-3. Comparison of continuous filtration and continuous gas sparging (Filt$_{Cont.}$ + Gas$_{Cont.}$, CGS) with pseudo dead-end (DE) operation, comprising intermittent filtration (9 min on/1 min off) and intermittent gas sparging (1 min on/9 min off) (Filt$_{Inter.}$ + Gas$_{Inter.}$).

6.2.2 Analytical methods

Mixed liquor suspended solids (MLSS) and biochemical oxygen demand (BOD_5) were measured according to Standard Methods (APHA, 2005). Total and soluble chemical oxygen demand (COD) were analysed with Merck test kits (Merck KGaA, Darmstadt, Germany). Soluble COD was determined following filtration through a 1.2 µm filter (Whatman 70mm GF/C, GE Healthcare Life Sciences, Little Chalfont, UK). Particle size was measured by a laser particle size analysis system (Mastersizer 3000, Malvern Instruments Ltd, Malvern, UK). Protein was measured using the modified Lowry method ($UV_{750\ nm}$) (Lowry et al., 1951) using bovine serum albumin (BSA) (Sigma-Aldrich, UK) as standard reference. Carbohydrate concentrations were measured using the Dubios method ($UV_{490\ nm}$) (Dubois et al., 1956) with D-glucose (Acros Organics, UK) used as the standard. All analyses were undertaken in triplicate.

6.3 Results

6.3.1 Characterisation of AnMBR bulk sludge, treatment and critical flux determination

Over the experimental period, the AnMBR produced effluent characterised by average COD_t and BOD_5 concentrations of 41±14 and 10±5 mg L^{-1} respectively, which corresponded to mean COD_t and BOD_5 removal efficiencies of 85±7 % and 92±5 % (Table 6-1). The bulk sludge within the membrane tank comprised TSS and soluble microbial product (SMP) concentrations of 123±38 mgSS L^{-1} and 90±19 mgCOD L^{-1} respectively (Table 6-1). Median particle size of the bulk suspension (d_{50}) was 72±37 µm. The critical flux (J_c) of the suspension was identified at two specific gas flow rates (Figure 6-4). At a SGD_m of 0.5 m^3 m^{-2} h^{-1}, the J_c was between 9 and 12 L m^{-2} h^{-1} and increased to between 12 and 15 L m^{-2} h^{-1}, when SGD_m was increased to 2.0 m^3 m^{-2} h^{-1}.

Table 6-1. AnMBR removal efficiency, wastewater and membrane bulk sludge characterisation.

Parameter	Unit	Influent	Membrane tank	Permeate	Removal %
pH	-	7.7±0.3 (n=50)	8.3±0.2 (n=50)	8.3±0.3 (n=15)	-
TSS	mg L^{-1}	157±66 (n=50)	123±38 (n=50)	<DL	>99
BOD_5	mg L^{-1}	143±43 (n=15)	-	10±5 (n=15)	92±5 (n=15)
COD_t	mg L^{-1}	320±124 (n=50)	225±74 (n=50)	41±14 (n=15)	85±7 (n=15)
COD_s	mg L^{-1}	109±31 (n=50)	90±19 (n=50)	41±14 (n=15)	64±12 (n=15)
SMP_p	mg L^{-1}	42±9 (n=50)	37±7 (n=50)	-	-
SMP_c	mg L^{-1}	11±2 (n=50)	13±4 (n=50)	-	-
SMP P/C	-	3.9±0.9 (n=50)	2.9±0.5 (n=50)	-	-
Particle size (d_{50})	µm	76±39 (n=33)	72±37 (n=33)	-	-

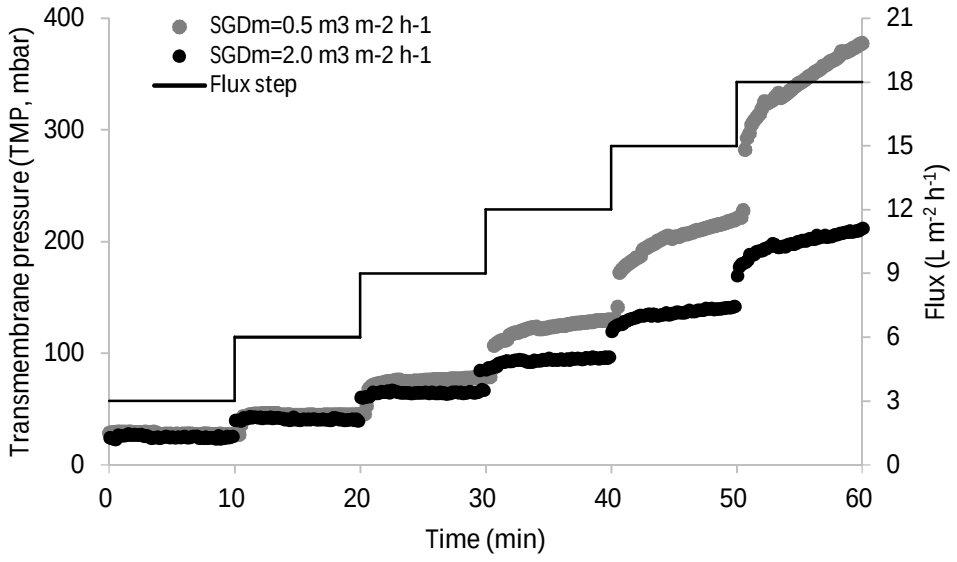

Figure 6-4. Critical flux determined using specific gas demand per unit membrane area (SGD_m) of 0.5 and 2 m^3 m^{-2} h^{-1} (flux step, 3 L m^{-2} h^{-1} per step; step length, 10 mins.).

6.3.2 Impact of gas sparging on AnMBR membrane permeability following peak flow

The impact of peak flow (Q_{peak}, 2Q) on membrane permeability was evaluated for three initial fluxes (6, 10, 13 L m^{-2} h^{-1}) with gas sparging fixed to a SGD_m of 0.5 m^3 m^{-2} h^{-1} (Figure 6-5). Total permeability recovery ($K_{20,tpr}$) of 86, 62 and 61 % were observed following peak flow induction for the initial fluxes of 6, 10 and 13 L m^{-2} h^{-1}, respectively. Within the peak flow period, TMP increased to 175, 514 and 591 mbar for 6, 10 and 13 L m^{-2} h^{-1} respectively, representing relative increases in TMP from before peak flow of 3.2, 4.4 and 2.9 times respectively. An increase in shear intensity from 0.5 to 2.0 m^3 m^{-2} h^{-1} during peak flow, seemingly improved permeability recovery for each initial flux studied (Figure 6-6). For example, at an initial flux of 6 L m^{-2} h^{-1}, $K_{20,tpr}$ increased from 86 % with constant SGD_m of 0.5 m^3 m^{-2} h^{-1} to 96 % when gas sparging was simultaneously increased to 2.0 m^3 m^{-2} h^{-1} with peak flow. In the initial stages of filtration, d*P*/dt was higher when a higher initial flux was specified (Table 6-2). At 6 L m^{-2} h^{-1}, the d*P*/dt recorded after peak flow was equivalent to that achieved before peak flow. At higher fluxes of 10 and 13 L m^{-2} h^{-1}, the fouling rate was generally below that achieved in the initial phase of filtration prior to peak flow. During the tests with different gas sparging strategies to manage peak flows, negligible permeability loss was identified in 'control' and for each of the other induction strategies a permeability decline of 50 to 70 % was observed during peak flow (Figure 6-7). However, permeability recovered to about >85 % for all gas sparging strategies. The rate of permeability recovery was improved by continuation of gas sparging for 2 h following peak flow, for investigation of both two and three times peak flow (Figure 6-7, Figure S6-1).

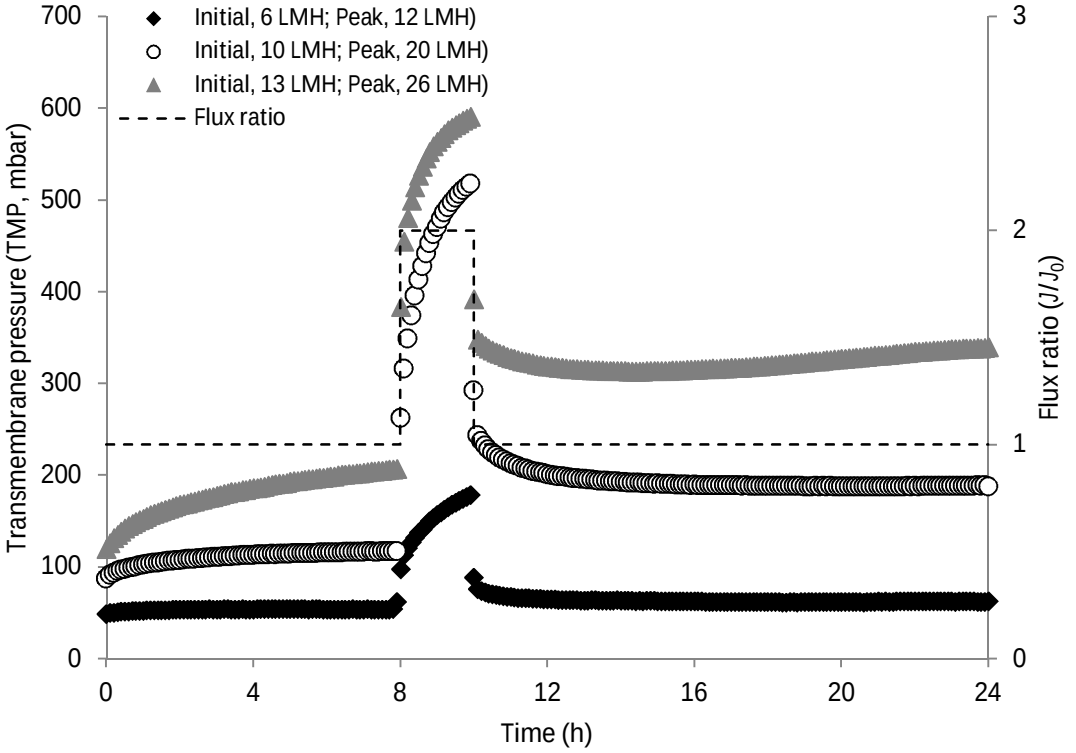

Figure 6-5. Impact of doubling flow (peak, 2Q) on transmembrane pressure at different initial fluxes using a fixed specific gas demand per unit membrane area (SGD_m) of 0.5 m^3 m^{-2} h^{-1} throughout.

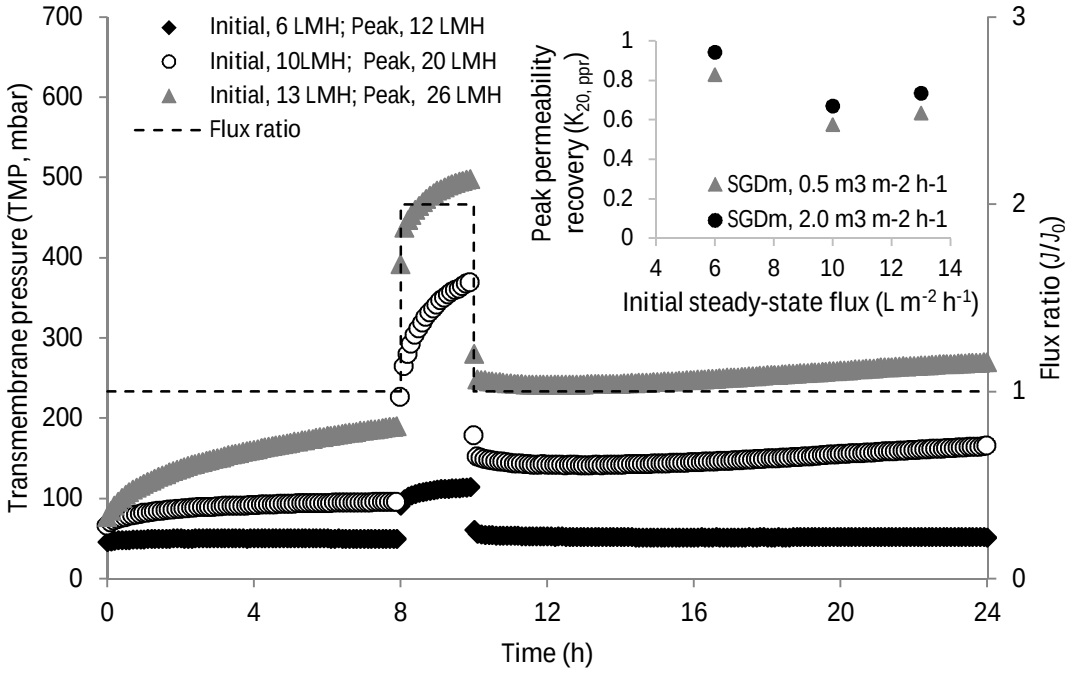

Figure 6-6. Impact of doubling flow (peak, 2Q) on transmembrane pressure at different initial fluxes. Specific gas demand per unit membrane area (SGD_m) increased from 0.5 to 2.0 m^3 m^{-2} h^{-1} during peak flow.

Table 6-2. Comparison of fouling rate before and after peak flow when SGD_m was either fixed to 0.5 m^3 m^{-2} h^{-1} or increased from 0.5 to 2.0 m^3 m^{-2} h^{-1} during peak flow (two hour peak).

Initial flux, J (L m^{-2} h^{-1})	Peak flux, J (L m^{-2} h^{-1})	Initial SGD_m (m^3 m^{-2} h^{-1})	Peak SGD_m (m^3 m^{-2} h^{-1})	Fouling rate (d*P*/dt) (mbar h^{-1})	
				Pre-peak (2-8h)	Post-peak (18-24h)
6	12 (2Q)	0.5	0.5	0.17	0.17
10	20 (2Q)	0.5	0.5	1.50	0.17
13	26 (2Q)	0.5	0.5	6.33	3.17
6	12 (2Q)	0.5	2.0	0.17	0.17
10	20 (2Q)	0.5	2.0	1.43	2.67
13	26 (2Q)	0.5	2.0	8.10	2.67

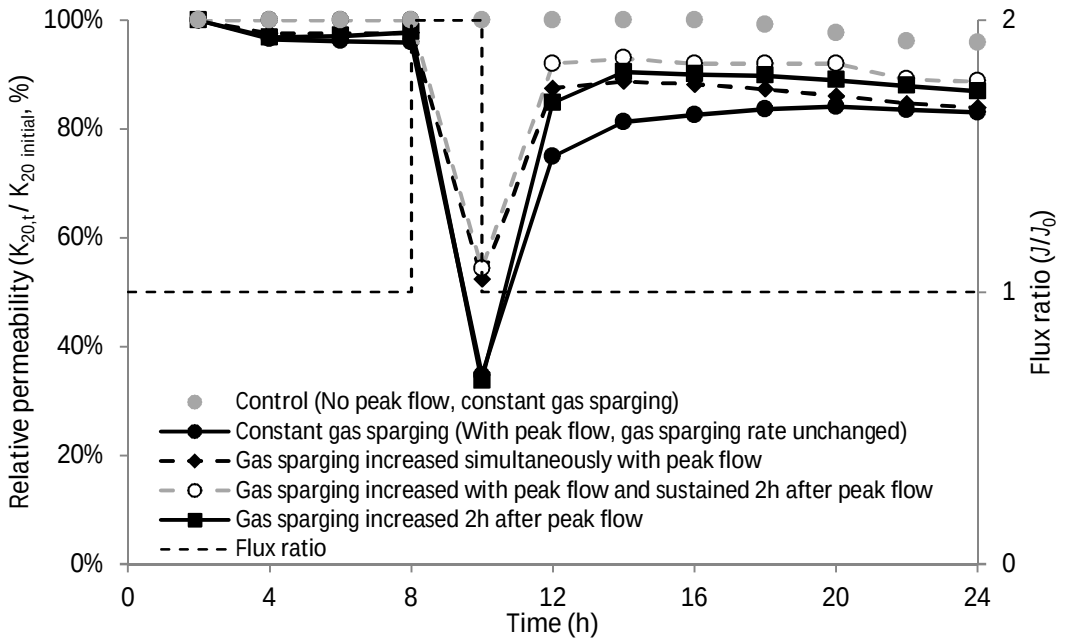

Figure 6-7. Impact of different gas sparging strategies on relative membrane permeability after flow was doubled (peak, 2Q). Initial flux, 6 L m^{-2} h^{-1}; Peak flux, 12 L m^{-2} h^{-1}. Constant specific gas demand per unit membrane area (SGD_m) of 0.5 m^3 m^{-2} h^{-1} during steady-state, and increased from 0.5 to 2.0 m^3 m^{-2} h^{-1} for set periods during specific trials (see Figure 6-2).

6.3.3 Impact of peak flux on AnMBR permeability

The impact of initial flux and peak flow to initial flow ratio were investigated at an initial flux of 6 and 10 L m^{-2} h^{-1}. As expected, with the increase of the peak flow from 2Q to 4Q for the initial flux of 6 L m^{-2} h^{-1} and 1.5Q to 2.5Q for the initial flux of 10 L m^{-2} h^{-1}, TMP increased during and after peak flow indicating permeability recovery reduction (Figure 6-8). For instance, at the initial flux of 6 L m^{-2} h^{-1} and peak flows of 2Q, 3Q and 4Q, the maximum TMP during peak flow were 128, 224 and 523 mbar respectively,

whilst the TMP after peak flow were 51, 52 and 64 mbar respectively, corresponding to total permeability recovery of 80 %, 79 % and 64 %. At similar peak fluxes of 18 and 20 L m^{-2} h^{-1}, higher total permeability recovery of approximately 80 % were observed for the initial flux of 6 L m^{-2} h^{-1} with 3Q peak flow, compared with about 53 % total permeability recovery at the initial flux of 10 L m^{-2} h^{-1} with 2Q peak flow. For both initial flux of 6 and 10 L m^{-2} h^{-1} with different peak flows, the d*P*/dt after peak flow were also generally equivalent or lower than that prior to peak flow (Table 6-3).

Table 6-3. Fouling rate determined before and after peak flow for initial fluxes of 6 and 10 L m^{-2} h^{-1}. SGD_m was increased from 0.5 to 2.0 m^3 m^{-2} h^{-1} during peak flow (two hour peak).

Initial flux, J (L m^{-2} h^{-1})	Peak flux, J (L m^{-2} h^{-1})	Fouling rate (d*P*/dt) (mbar h^{-1})	
		Pre-peak (2-8h)	Post-peak (18-24h)
6	12 (2Q)	0.17	0.17
	18 (3Q)	0.17	0.17
	24 (4Q)	0.17	0.17
10	15 (1.5Q)	1.55	2.00
	20 (2Q)	1.43	2.67
	25 (2.5Q)	1.58	0.69

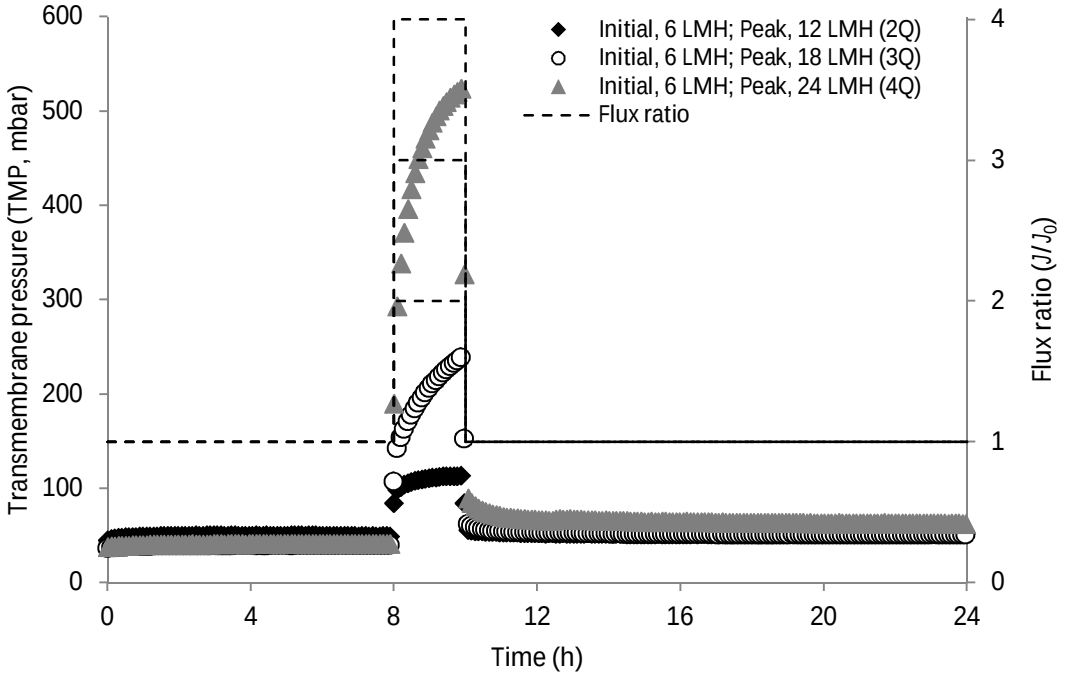

(a)

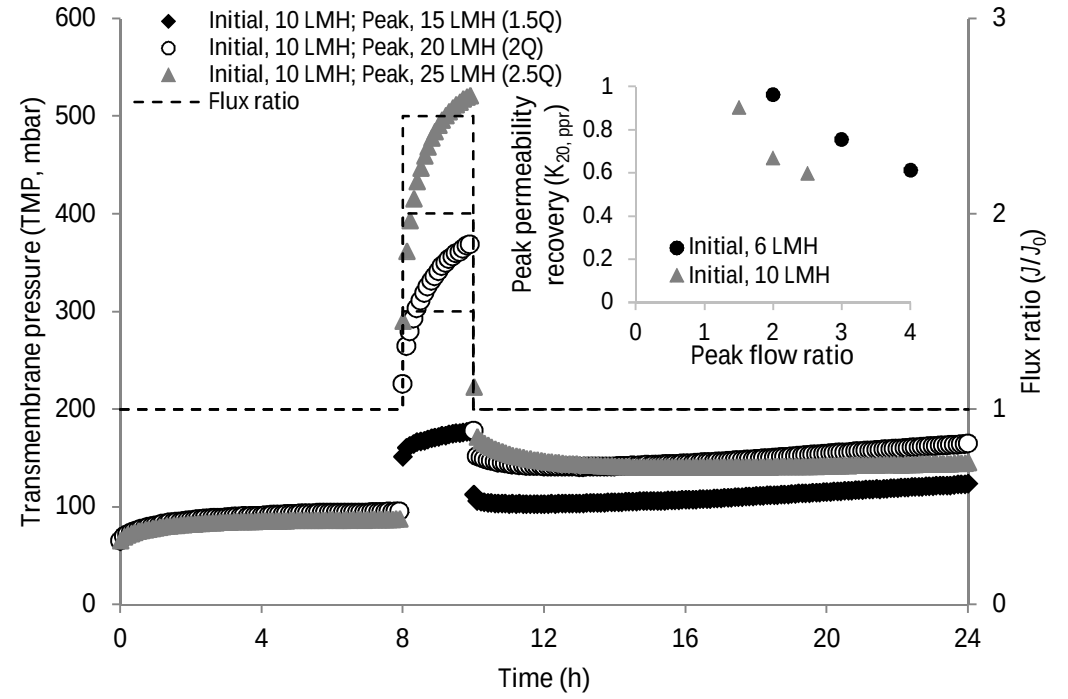

(b)

Figure 6-8. Impact of peak flow ratio on transmembrane pressure when: (a) Initial flux, 6 L m^{-2} h^{-1}; (b) Initial flux, 10 L m^{-2} h^{-1}. Specific gas demand per unit membrane area (SGD_m) increased from 0.5 to 2.0 m^3 m^{-2} h^{-1} during peak flow.

6.3.4 Impact of peak length and multiple peak events on AnMBR permeability

To establish the impact of peak length on permeability recovery, peak length was varied between 0.5 and 8 h at peak fluxes of two and three times the initial flux (Figure 6-9, Figure 6-10). For a short peak flow of 0.5 h, similar total permeability recovery (92-94 %) was observed at peak flows of 2Q and 3Q. For 2Q, the reduction in total permeability recovery over longer peak flow events was negligible, whereas at 3Q, a progressive decline in membrane permeability was observed (Figure 6-10). Multiple peak event analysis was undertaken using 2 h peak flow events equivalent to 3Q, and introduced every 8 h (Figure 6-11). During each peak flow event, a maximum TMP of between 370 and 420 mbar was achieved. Following the initial peak flow event, post peak permeability recovery ($K_{20, ppr}$) was between 60 and 70 %. However, the relative permeability decline following sequential peaks was markedly less, with $K_{20, ppr}$ of >90 % recorded following the third and fourth peak flow events (Figure 6-11, inset).

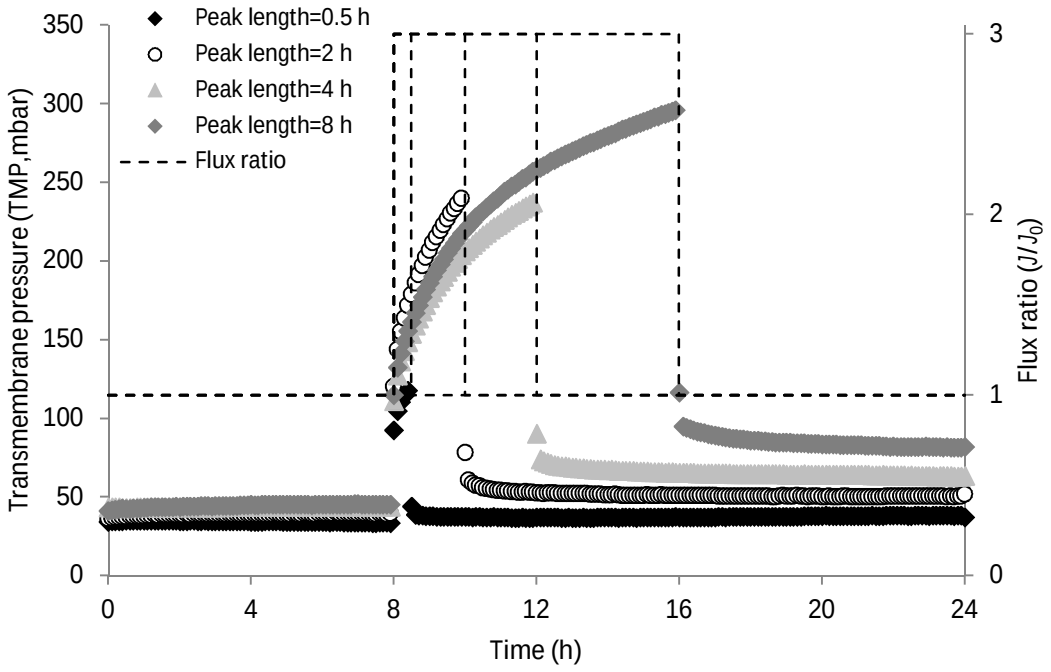

Figure 6-9. Impact of peak length on membrane permeability recovery. Initial flux, 6 L m^{-2} h^{-1}; Peak flux, 18 L m^{-2} h^{-1} (Peak, 3Q). Specific gas demand per unit membrane area (SGD_m) increased from 0.5 to 2.0 m^3 m^{-2} h^{-1} during peak flow.

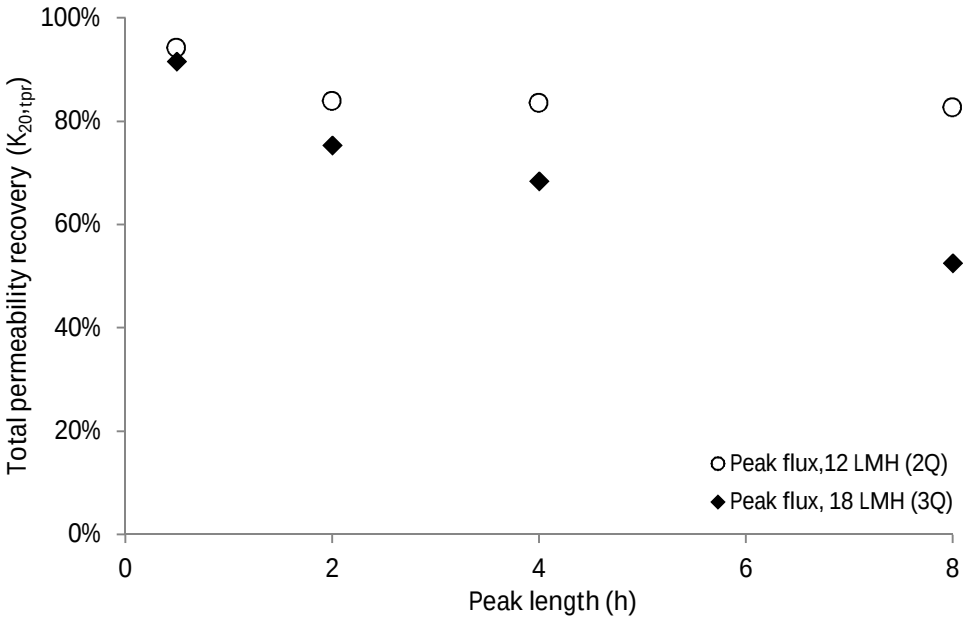

Figure 6-10. Impact of peak length on membrane permeability recovery for two different peak flow ratios. Initial flux, 6 L m^{-2} h^{-1}; Peak flux, 12 L m^{-2} h^{-1} (2Q) or 18 L m^{-2} h^{-1} (3Q). Specific gas demand per unit membrane area (SGD_m) increased from 0.5 to 2.0 m^3 m^{-2} h^{-1} during peak flow.

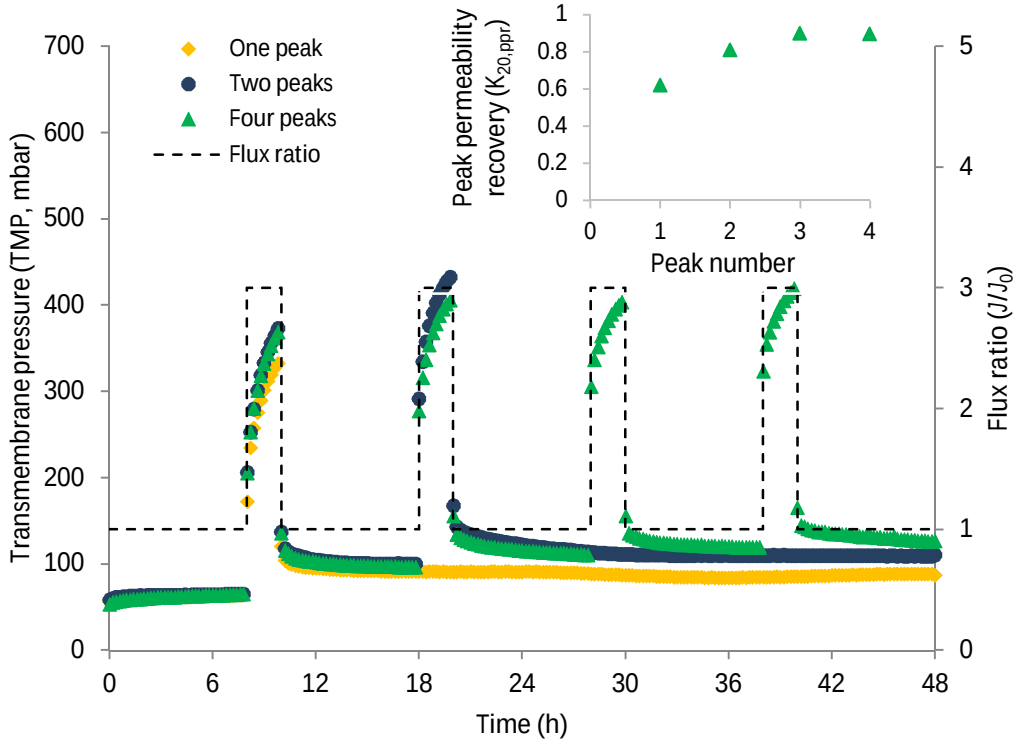

Figure 6-11. Impact of multiple peak flow events on transmembrane pressure. Initial flux, 6 L m^{-2} h^{-1}; Peak flux, 18 L m^{-2} h^{-1} (3Q). Specific gas demand per unit membrane area (SGD_m) increased from 0.5 to 2.0 m^3 m^{-2} h^{-1} during peak flow.

6.3.5 Alternative hydrodynamic conditions

Continuous gas sparging was compared to an alternative hydrodynamic regime, in which filtration was conducted without gas sparging (Figure 6-3). Following a period of filtration (9 minutes), gas sparging was introduced for 1 minute together with membrane relaxation to create a pseudo dead-end filtration cycle (McAdam and Judd, 2008). Initial fluxes of 6 and 10 L m^{-2} h^{-1} were evaluated, with fluxes doubled in response to peak flow (Figure 6-12). For both fluxes, the TMP trend developed in response to peak flow were comparable. Specifically, at 10 L m^{-2} h^{-1}, d*P*/dt of 1.43 and 0.17 mbar min^{-1} were recorded during the initial stage of filtration and for filtration following peak flow respectively for both hydrodynamic conditions.

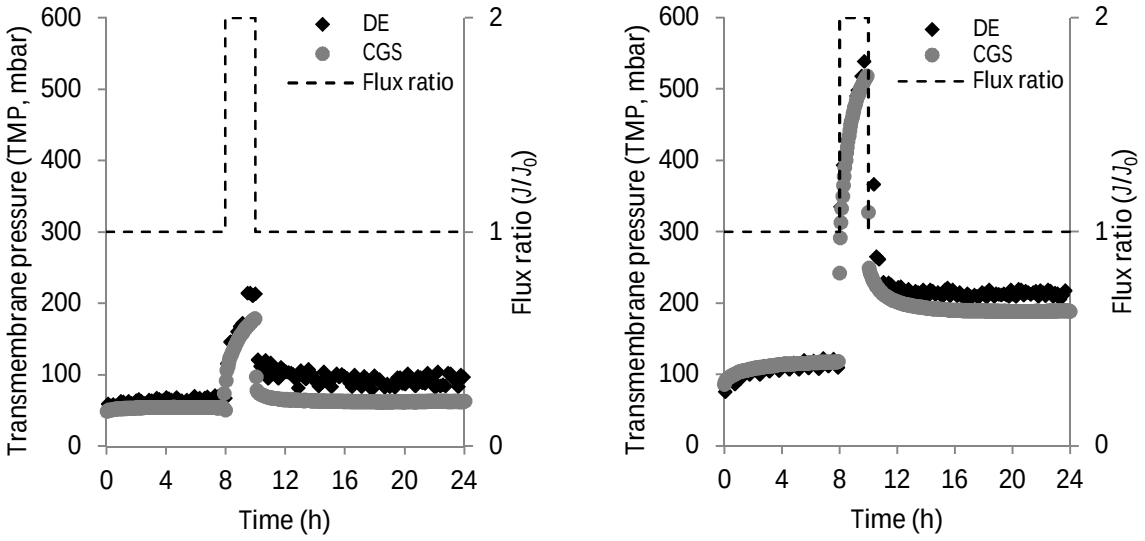

Figure 6-12. Comparison of two hydrodynamic conditions subject to peak flow: continuous filtration and continuous gas sparging (CGS); pseudo dead-end (DE) comprising intermittent filtration (9 min on/1 min off) and intermittent gas sparging (9 min off/ 1 min on). (a) Initial flux, 6 L m^{-2} h^{-1}; Peak flux, 12 L m^{-2} h^{-1} (2Q); (b) Initial flux, 10 L m^{-2} h^{-1}; Peak flux, 20 L m^{-2} h^{-1} (2Q). Constant specific gas demand per unit membrane area (SGD_m) of 0.5 m^3 m^{-2} h^{-1} applied throughout trial. See Figure 6-3.

6.4 Discussion

In this study, the potential to restore permeability following peak flow has been evidenced in AnMBR treating municipal wastewater. Although future complementary research focussed on longer-term impacts of peak flow to permeability would be beneficial, data from this study suggests that the membrane area requirement for AnMBR can be potentially specified based on average flow instead of peak flow, manifesting in a considerable reduction in capital cost by about 67 % compared with the design based on peak flows (3 times of average flow), sufficient to make AnMBR a more economically viable proposition. Total permeability recovery of 86 % ($K_{20,\,tpr}$) was recorded when peak flow doubled from an initial flux of 6 L m^{-2} h^{-1} and gas sparging was sustained at a SGD_m of 0.5 m^3 m^{-2} h^{-1} before and during peak flow (Figure 6-5). However, increasing gas sparging rate from 0.5 to 2.0 m^3 m^{-2} h^{-1}, during peak flow, improved $K_{20,\,tpr}$ to 96 % (Figure 6-6), which is similar to the observation of Howell et al. (2004) who studied peak flow in aerobic MBR. During peak flow, the flux (J, 12 L m^{-2} h^{-1}) was equivalent to the J_c of the suspension, when gas sparging was fixed to a SGD_m of 0.5 m^3 m^{-2} h^{-1}. The improved permeability recovery provided by the increase in SGD_m to 2.0 m^3 m^{-2} h^{-1} during peak flow can therefore be accounted for by the increase in the suspension J_c from 12 to 15 L m^{-2} h^{-1} (J_c>J) (Figure 6-4), which then limited particle deposition during peak flow (Guglielmi et al., 2007; Martin Garcia et al., 2013; Robles et al., 2012). Whilst similar total permeability recoveries were identified over the 24 h filtration period for the various methods of gas sparging induction trialled ($K_{20,tpr}$, 84-89 %), the rate of permeability recovery was improved by around 8 % when gas sparging rate was increased from 0.5 to 2.0 m^3 m^{-2} h^{-1} during peak flow and sustained for 2 h after peak flow (Figure 6-7). In a study of a model suspension, Lewis et al. (2012) illustrated how the cake formed during crossflow microfiltration could be completely eroded through an increase in shear stress. In this study, we suggest sustaining shear stress (SGD_m, 2.0 m^3 m^{-2} h^{-1}; G, 460 s^{-1}) whilst reducing flux to match average flow, provides analogous behaviour, in which faster permeability recovery (through cake erosion) can be obtained, thereby presenting value to sewage works exposed to frequent flow variations (Itokawa et al., 2008).

For a short peak flow period of 0.5 h, similar total permeability recoveries of 92 to 94 % were identified independent of whether the peak flux was two or three times higher than the initial flux (Figure 6-9, Figure 6-10). The performance observed following 0.5 h filtration at three times peak flow is noteworthy since despite $J>J_c$ for the duration of peak flow, total permeability recovery was higher than observed at lower peak flux (2Q) for longer duration. This is supported by the modeling approach of Giraldo and LeChevallier (2008) who illustrated that sustaining high peak flux for short durations was less challenging for membrane operation in aerobic MBR than low peak flux for longer duration. Whilst there is no definitive classification of peak flow duration, a typical duration for morning peak flow is around 2 to 3 h (Butler, 1993). At the higher peak flow (J, 18 L m^{-2} h^{-1}), permeability recovery diminished with an increase in peak length, whereas for the lower peak flow examined, permeability recovery was seemingly independent of peak length above 2 h (Figure 6-10). On face value, the data suggests that whilst fluxes above the critical flux can be managed for short durations of 0.5 h, the prescribed flux at peak flow should be below the J_c in order to sustain membrane permeability over extended peak flow durations. However, it is important to recognise that the maximum TMP reached increased with peak length, reaching a maximum of around 300 mbar following operation for 8 h at peak flow (Figure 6-9), which is above the operating TMP ordinarily adopted at full-scale. Several authors have adopted reactive maintenance philosophies where a TMP set-point initiates automated backwash/relaxation, rather than temporal cycling (Smith et al., 2006; Vera et al., 2015b). For example, Hirani et al. (2010) applied shorter filtration cycles, longer backwash durations or higher backwash fluxes during peak flow and evidenced only modest permeability reduction after several days of peak-flow assessment for aerobic MBR. Consequently, it is proposed that the introduction of TMP set-point control can potentially complement the permeability recovery already observed for supra-critical fluxes over short durations in this study, to extend supra-critical operation over considerably longer peak flow durations, without incurring substantial permeability loss.

Adoption of an initial flux well below the critical flux appears to limit fouling following peak flow. To illustrate, when flux was increased from an initial flux of 6 and 10 L m^{-2} h^{-1} to supra-critical fluxes of 24 L m^{-2} h^{-1} (4Q) and 25 L m^{-2} h^{-1} (2.5Q) respectively during peak flow, similar relative permeability losses ($K_{20,ppr}$) were obtained (Figure 6-8). However, the loss in absolute permeability following peak flow was markedly higher for an initial flux of 10 L m^{-2} h^{-1}, despite the similarity in peak flux (Figure 6-8). When initial flux was close or equivalent to the critical flux of the suspension, deposition was noted in the early stage of filtration, before the initiation of peak flow. Enhanced surface deposition was confirmed by the d*P*/dt observed for the higher fluxes (10 and 13 L m^{-2} h^{-1}) before peak flow (Table 6-2, Table 6-3); the increased resistance will have been exacerbated by the colloidal composition in the matrix (around 50 mgSMPp+c L^{-1}) (Yoon, 2015), which is approximately 1.5 times higher than in conventional aerobic MBR systems (Martin-Garcia et al., 2011). It is this deposition which is regarded to augment bacterial attachment and cake layer formation during peak flow under supra-critical flux (Chu and Li, 2005; Metzger et al., 2007). However, the fouling rate obtained following peak flow, was generally either the same or lower than before peak flow, which is the antithesis of the hysteresis profile ordinarily observed in critical flux analysis, following the 'step-down' in flux from a supra-critical state, where a higher d*P*/dt is commonly observed during step-down at an equivalent flux (McAdam et al., 2007). We therefore suggest that the fouling observed before and after peak flow in this study is analogous that of 'conditioning' (stage 1 fouling) and 'stage 2' fouling respectively (Le-Clech et al., 2006; Yoon, 2015), where the properties of the initial deposit formed are a function of how close initial flux is specified relative to the critical flux and directly affect to post-peak permeability recovery. The effect of membrane conditioning was corroborated by multiple peak flow analysis (Figure 6-11), in which the relative loss in permeability decreased following an increase in peak number. Lebegue et al. (2008) also reported a relatively constant TMP for aerobic MBR treating synthetic wastewater when flux increased from 10 to 30 L m^{-2} h^{-1} for 2 h each day over three weeks. Such phenomena have been described through arrival of a steady-state,

in which the deposit formed during peak flow was balanced by the removal after peak flow leading to no noticeable change in TMP (Judd, 2011; Yoon, 2015).

Importantly, this study demonstrates that employing higher initial fluxes does not necessarily preclude the attainment of 'sustainable' fluxes following peak flow (Le-Clech et al., 2006); however, by specifying an initial flux below the critical flux, post-peak flow fouling is limited, as demonstrated at an initial flux of 6 L m^{-2} h^{-1} (Table 6-2, Table 6-3). To obtain similar low fouling rates for higher initial fluxes, an increased SGD_m could be employed to raise the critical flux of the suspension, although this will incur a substantial energy penalty. For example, an initial flux of 6 L m^{-2} h^{-1} and SGD_m 0.5 m^3 m^{-2} h^{-1} is equivalent to a specific gas demand per unit permeate (SGD_p) of 83 m^3 m^{-3}. Raising SGD_m to 2.0 m^3 m^{-2} h^{-1} for an initial flux of 10 L m^{-2} h^{-1} will increase SGD_p to 200 m^3 m^{-3}. Therefore, while specifying a higher initial flux, represents a capital cost reduction for membrane area of around 40 %, a considerable energy demand is incurred, equivalent to 1.79 kWh m^{-3}. In this study, an alternative pseudo dead-end filtration mode was introduced, which provided comparable d*P*/dt before and after peak flow at an initial flux of 10 L m^{-2} h^{-1}, but reduced energy demand to 0.04 kWh m^{-3} (SGD_p, 5 m^3 m^{-3}) (Figure 6-12). This is noticeably below the energy recovery typically reported for AnMBR treating municipal wastewater of 0.28 kWh m^{-3}, which is pertinent as the opportunity to achieve energy neutral sewage treatment remains the key driver for this technology (McAdam et al., 2011; Wang et al., 2018). Using the same filtration mode in anoxic MBR, McAdam et al. (2011) demonstrated that provided the volume filtered during the dead end cycle was sustained below a critical value, almost complete deposit reversibility could be achieved for fluxes in excess of the critical flux; which is similar to observations recently made by Wang et al. (2018) for AnMBR. This indicated the potential for complete deposit reversibility under super-critical fluxes during both average flow and peak flow period in AnMBR. Whilst this study illustrates comparable performance to continuous gas sparging, further work is required to establish the potential to sustain higher initial fluxes and peak fluxes in AnMBR with pseudo dead-end filtration, which has been successfully demonstrated for other MBR applications (McAdam et al., 2011; McAdam and Judd, 2008; Vera et al., 2015a). It is

therefore suggested that further capital cost reduction can be expected by increasing the attainable initial and peak flux through this pseudo dead-end filtration.

6.5 Conclusions

The impact of critical transient peak flow characteristics (peak duration, frequency and size) on membrane permeability has been evaluated, together with several reactive methods to improve permeability recovery following peak flow events. The following conclusions can be drawn:

- Enhanced permeability recovery is achieved by increasing gas sparging during peak flow. However, considerable increase in gas sparging rate (four times) is needed to shift the critical flux of the suspension, leading to a doubling of specific gas demand.
- Extending high rate gas sparging following a return to average flow, despite requiring a higher energy input, improves the kinetics of permeability recovery which may be advantageous to smaller works, typically exposed to more frequent transient flows.
- Supra-critical fluxes can be sustained for short duration; further work is required to evaluate interventions during peak flow (e.g. TMP set-point) to extend the period of operability.
- Specifying initial flux below critical flux was important for permeability recovery from a supra-critical state for continuous filtration and continuous gas sparging. To optimise membrane design (i.e. limit membrane surface area) at average flow, higher initial fluxes can only be obtained through increasing SGD_m at average flow or use of an alternative filtration mode (e.g. pseudo dead-end). However, their ability to sustain permeability in the long term following regular peak flow required validation.
- Pseudo dead-end filtration presented analogous performance at a fraction of the energy demand. Permeability recovery could be advanced by increasing SGD_m from 0.5 to 2.0 $m^3\ m^{-2}\ h^{-1}$, which would represent a comparatively negligible increase in energy due to the limited gas sparge frequency applied. With this

filtration mode, consistent supra-critical flux operation has been demonstrated in the broader literature, and warrants further examination for AnMBR to further minimise capital cost.

Importantly, this study demonstrates the potential for AnMBR membrane surface area to be specific based on average rather than peak flow, which constitutes a significant financial saving.

6.6 Acknowledgements

The authors would like to thank our industrial sponsors Anglian Water, Scottish Water, Severn Trent Water and Thames Water for their financial and technical support.

6.7 References

APHA (2005) *Standard Methods for the Examination of Water and Wastewater*. 21st edn. Washington D.C: American Public Health Association.

Barillon, B., Ruel, S.M., Langlais, C. and Lazarova, V. (2013) 'Energy efficiency in membrane bioreactors', *Water Science & Technology*, 67, pp. 2685–2691.

Butler, D. (1993) 'The influence of dwelling occupancy and day of the week on domestic appliance wastewater discharges', *Building and Environment*, 28, pp. 73–79.

Chong, S., Sen, T.K., Kayaalp, A. and Ang, H.M. (2012) 'The performance enhancements of upflow anaerobic sludge blanket (UASB) reactors for domestic sludge treatment - A State-of-the-art review', *Water Research*, 46, pp. 3434–3470.

Chu, H.P. and Li, X.Y. (2005) 'Membrane fouling in a membrane bioreactor (MBR): Sludge cake formation and fouling characteristics', *Biotechnology and Bioengineering*, 90, pp. 323–331.

Dubois, M., Gilles, K.A., Hamilton, J.K., Rebers, P.A. and Smith, F. (1956) 'Colorimetric method for determination of sugars and related substances', *Analytical Chemistry*, 28, pp. 350–356.

Giraldo, E. and LeChevallier, M. (2008) 'Membrane fouling in submerged membrane bioreactors during peak wet weather flow. Modeling for design and operation', *Proceedings of the Water Environment Federation*, 1, pp. 92–103.

Guglielmi, G., Chiarani, D., Judd, S.J. and Andreottola, G. (2007) 'Flux criticality and sustainability in a hollow fibre submerged membrane bioreactor for municipal wastewater treatment', *Journal of Membrane Science*, 289, pp. 241–248.

Hirani, Z.M., DeCarolis, J.F., Adham, S.S. and Jacangelo, J.G. (2010) 'Peak flux performance and microbial removal by selected membrane bioreactor systems', *Water Research*, 44, pp. 2431–2440.

Howell, J.A., Chua, H.C. and Arnot, T.C. (2004) 'In situ manipulation of critical flux in a submerged membrane bioreactor using variable aeration rates, and effects of membrane history', *Journal of Membrane Science*, 242, pp. 13–19.

Itokawa, H., Thiemig, C. and Pinnekamp, J. (2008) 'Design and operating experiences of municipal MBRs in Europe', *Water Science & Technology*, 58, pp. 2319–2327.

Judd, S.J. (2011) *Principles and Applications of Membrane Bioreactors in Water and Wastewater Treatment*. 2nd edn. London,UK: Elsevier.

Le-Clech, P., Chen, V. and Fane, T.A.G. (2006) 'Fouling in membrane bioreactors used in wastewater treatment', *Journal of Membrane Science*, 284, pp. 17–53.

Le Clech, P., Jefferson, B., Chang, I.S. and Judd, S.J. (2003) 'Critical flux determination by the flux-step method in a submerged membrane bioreactor', *Journal of Membrane Science*, 227, pp. 81–93.

Lebegue, J., Heran, M. and Grasmick, A. (2008) 'MBR functioning under steady and unsteady state conditions. Impact on performances and membrane fouling dynamics', *Desalination*, 231, pp. 209–218.

Lesjean, B., Ferre, V., Vonghia, E. and Moeslang, H. (2009) 'Market and design considerations of the 37 larger MBR plants in Europe', *Desalination and Water Treatment*, 6, pp. 227–233.

Lewis, W.J.T., Chance, R.M.J., Wilcox, M.C., Chew, Y.M.J. and Bird, M.R. (2012) 'Investigations of cake fouling during the cross-flow microfiltration of a model

suspension: Influence of buoyancy on deposition and shear-induced removal', *Procedia Engineering*, 44, pp. 603–606.

Lin, H., Chen, J., Wang, F., Ding, L. and Hong, H. (2011) 'Feasibility evaluation of submerged anaerobic membrane bioreactor for municipal secondary wastewater treatment', *Desalination*, 280, pp. 120–126.

Lowry, O.H., Rosebrough, N.J., Farr, A.L. and Randall, R.J. (1951) 'Protein measurement with the folin phenol reagent', *Journal of Biological Chemistry*, 193, pp. 265–275.

Martin-Garcia, I., Monsalvo, V., Pidou, M., Le-Clech, P., Judd, S.J., McAdam, E.J. and Jefferson, B. (2011) 'Impact of membrane configuration on fouling in anaerobic membrane bioreactors', *Journal of Membrane Science*, 382, pp. 41–49.

Martin Garcia, I., Mokosch, M., Soares, A., Pidou, M. and Jefferson, B. (2013) 'Impact on reactor configuration on the performance of anaerobic MBRs: Treatment of settled sewage in temperate climates', *Water Research*, 47, pp. 4853–4860.

McAdam, E.J., Cartmell, E. and Judd, S.J. (2011) 'Comparison of dead-end and continuous filtration conditions in a denitrification membrane bioreactor', *Journal of Membrane Science*, 369, pp. 167–173.

McAdam, E.J. and Judd, S.J. (2008) 'Optimisation of dead-end filtration conditions for an immersed anoxic membrane bioreactor', *Journal of Membrane Science*, 325, pp. 940–946.

McAdam, E.J., Judd, S.J., Cartmell, E. and Jefferson, B. (2007) 'Influence of substrate on fouling in anoxic immersed membrane bioreactors', *Water Research*, 41, pp. 3859–3867.

McAdam, E.J., Luffler, D., Martin-Garcia, N., Eusebi, A.L., Lester, J.N., Jefferson, B. and Cartmell, E. (2011) 'Integrating anaerobic processes into wastewater treatment', *Water Science & Technology*, 63, pp. 1459–1466.

Metcalf, G.J. (2017) *A comparative evaluation of membrane bioreactor technology at Darvill Wastewater Works*. Stellenbosch University.

Metzger, U., Le-Clech, P., Stuetz, R.M., Frimmel, F.H. and Chen, V. (2007) 'Characterisation of polymeric fouling in membrane bioreactors and the effect of different filtration modes', *Journal of Membrane Science*, 301, pp. 180–189.

Robles, A., Ruano, M.V., García-Usach, F. and Ferrer, J. (2012) 'Sub-critical filtration conditions of commercial hollow-fibre membranes in a submerged anaerobic MBR (HF-SAnMBR) system: the effect of gas sparging intensity', *Bioresource Technology*, 114, pp. 247–254.

Robles, A., Ruano, M.V., Ribes, J. and Ferrer, J. (2013) 'Factors that affect the permeability of commercial hollow-fibre membranes in a submerged anaerobic MBR (HF-SAnMBR) system', *Water Research*, 47, pp. 1277–1288.

Ruigómez, I., Vera, L., González, E. and Rodríguez-Sevilla, J. (2016) 'Pilot plant study of a new rotating hollow fibre membrane module for improved performance of an anaerobic submerged MBR', *Journal of Membrane Science*, 514, pp. 105–113.

Smith, P.J., Vigneswaran, S., Ngo, H.H., Ben-Aim, R. and Nguyen, H. (2006) 'A new approach to backwash initiation in membrane systems', *Journal of Membrane Science*, 278, pp. 381–389.

Syed, W., Zhou, H., Sheng, C., Mahendraker, V., Adnan, A. and Theodoulou, M. (2009) 'Effects of hydraulic and organic loading shocks on sludge characteristics and its effects on membrane bioreactor performance', *Proceedings of WEFTEC*. Orlando, FL.

Tchobanoglous, G., Burton, F.L. and Stensel, H.D. (2003) *Wastewater Engineering Treatment and Reuse*. 4th edn. New York: McGraw-Hill Companies.

Veltmann, K., Palmowski, L.M. and Pinnekamp, J. (2011) 'Modular operation of membrane bioreactors for higher hydraulic capacity utilisation', *Water Science & Technology*, 63, pp. 1241–1246.

Vera, L., Gonzalez, E., Diaz, O., Sanchez, R., Bohorque, R. and Rodriguez-Sevilla, J. (2015a) 'Fouling analysis of a tertiary submerged membrane bioreactor operated in dead-end mode at high-fluxes', *Journal of Membrane Science*, 493, pp. 8–18.

Vera, L., González, E., Ruigómez, I., Gómez, J. and Delgado, S. (2015b) 'Analysis of backwashing efficiency in dead-end hollow-fibre ultrafiltration of anaerobic suspensions', *Environmental Science and Pollution Research*, 22, pp. 16600–16609.

Verrecht, B., Maere, T., Nopens, I., Brepols, C. and Judd, S. (2010) 'The cost of a large-scale hollow fibre MBR', *Water Research*, 44, pp. 5274–5283.

Wang, K.M., Cingolani, D., Eusebi, A.L., Soares, A., Jefferson, B. and McAdam, E.J. (2018) 'Identification of gas sparging regimes for granular anaerobic membrane bioreactor to enable energy neutral municipal wastewater treatment', *Journal of Membrane Science*, 555, pp. 125–133.

Yoon, S.H. (2015) *Membrane Bioreactor Processes: Principles and Applications*. CRC press.

6.8 Supplementary data

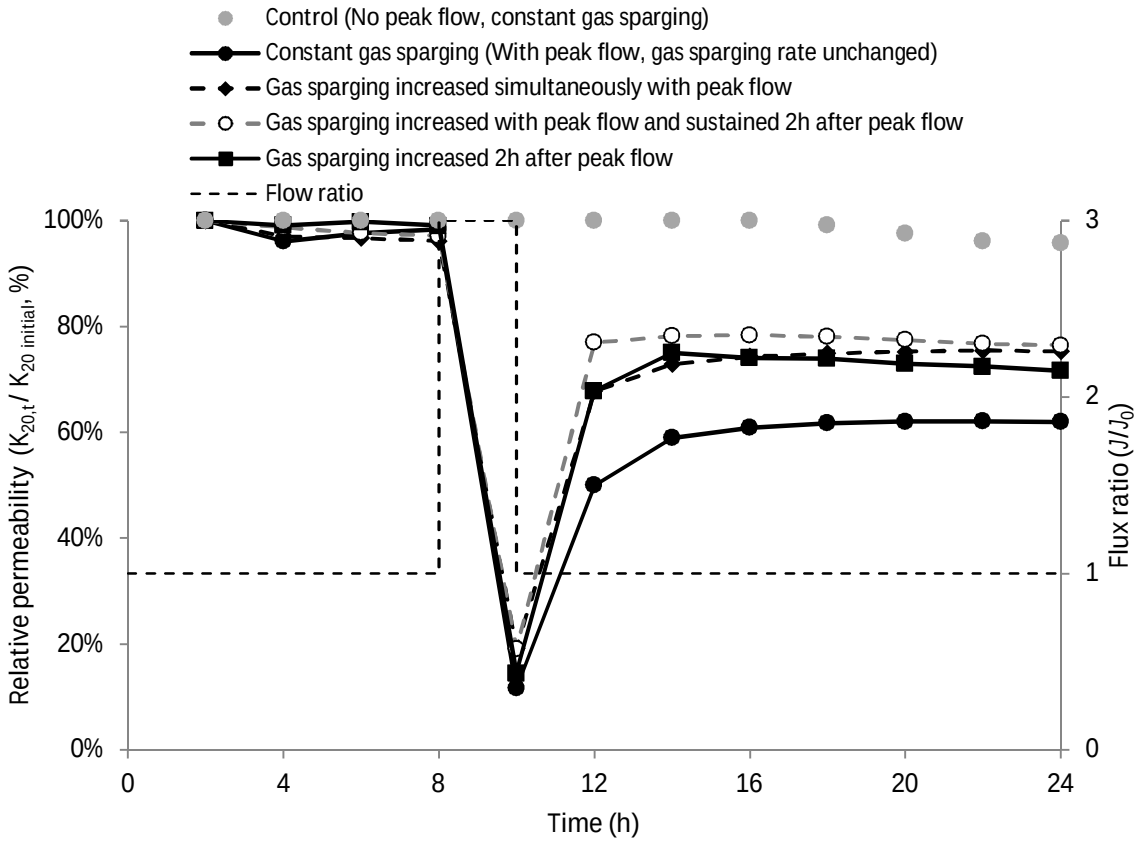

Figure S6-1. Impact of different gas sparging strategies on relative membrane permeability after flow was tripled (peak, 3Q). Initial flux, 6 L m^{-2} h^{-1}; Peak flux, 18 L m^{-2} h^{-1}. Constant specific gas demand per unit membrane area (SGD_m) of 0.5 m^3 m^{-2} h^{-1} during steady-state, and increased from 0.5 to 2.0 m^3 m^{-2} h^{-1} for set periods during specific trials (see Figure 6-2).

CHAPTER 7

Overall discussion

7 Overall discussion

In this thesis, several key challenges to implementation of anaerobic membrane bioreactor (AnMBR) for full-flow municipal wastewater treatment have been evaluated, in order to provide engineered solutions that can reduce cost, increase reliability and ultimately deliver energy neutral sewage treatment (Table 7-1). Consequently, the proposed upflow anaerobic sludge blanket (UASB) configured AnMBR with the arising knowledge from this thesis has been demonstrated (Figure 7-1). The contributions to knowledge supplied within this thesis are presented within four key aspects that support the practical implementation of UASB configured AnMBR for municipal wastewater treatment.

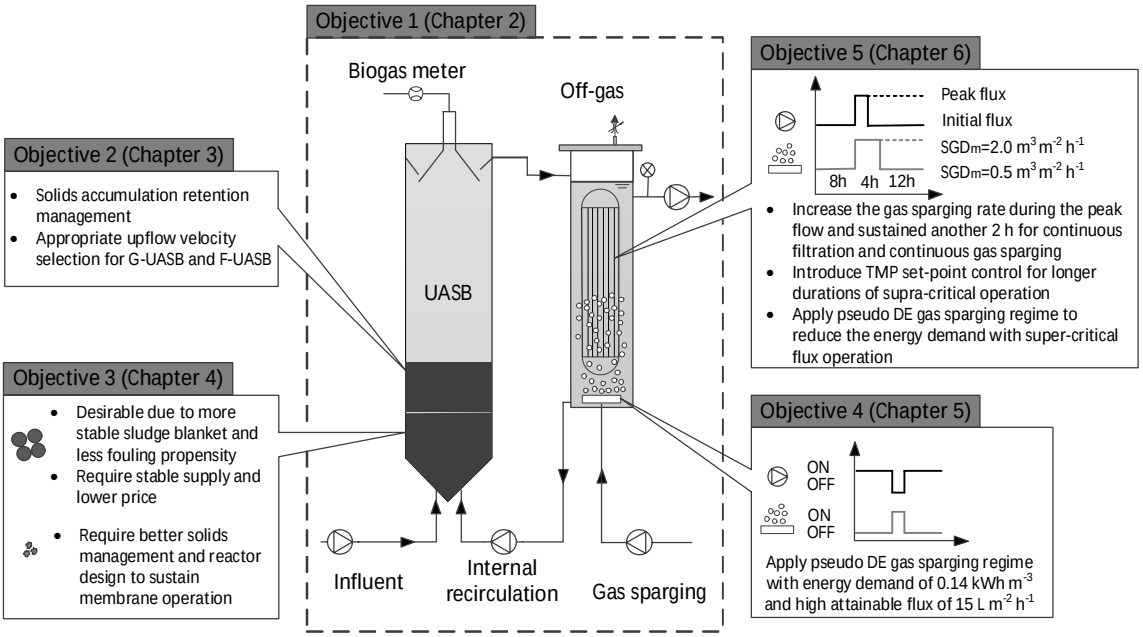

Figure 7-1. The proposed UASB configured AnMBR for municipal wastewater treatment.

Table 7-1. Proposed engineered solutions arising from the research to promote sustained operation and limit both operational and capital cost.

Design challenge	Research question	Impact	Proposed engineered solution
Solids washout	How do we sustain sludge blanket stability?	(i) High V_{up} at base (0.8-0.9 m h^{-1}) separates light sludge from granules – easy disposal and provides filtration (ii) High V_{up} within light sludge fraction destabilises sludge bed at low temperatures due to increased viscosity; this lowers settling velocity and induces washout (iii) High sludge blanket level (high SRT) increases hydrolysis and gas production washing out light solids fraction; exacerbated at higher temperatures (iv) Solids washout reduces membrane permeability under fixed hydraulic conditions	(i) Increase top section diameter to reduce V_{up} in upper layer (<0.4 m h^{-1}) for G-UASB (stratify velocity through bed); reduce V_{up} (<0.4 m h^{-1}) for F-UASB at low temperatures (ii) Reduce sludge bed height to column height ratio (around 20-30%) to enable settling (iii) Control sludge age within column through progressive withdrawal (iv) Design reactor scale to lowest temperature for wastewater treatment to increase resilience (v) Potential to increase gas sparging rate to manage in short-term
Granular sludge is limited in supply; flocculent is readily available	Does the flocculent matrix negatively influence reactor and membrane performance more than granular matrix?	(i) More methane produced from flocculent than granular at low temperatures; propose that this is due to substrate diffusion limitation in granule (ii) Light flocculent sludge washout at low temperature due to increased viscosity, exacerbated in flocculent (iii) Increase in SMP, colloids and solids in flocculent AnMBR reduces permeability; it is proposed that this is primarily linked to destabilisation of the sludge blanket (iv) Sustained permeability can be achieved with both granular and flocculent sludge using intermittent filtration (10 min on/1 min off) and cyclic gas sparging (10 s on/10 s off) (v) Low energy gas sparging regime can be deployed in both matrices; however, not possible in flocculent at low temperatures due to washout from UASB	(i) Higher methane yield in flocculent potentially due to better use of solid phase; if solid phase displaced to AD, then the net energy balance for both floc and granule will be the same (ii) Granular biomass is more resilient to system perturbation based on existing process design and selected hydrodynamics; need to increase granule source availability and improve available technology for granule production (iii) Better solids management can improve membrane robustness at low temperatures for flocculent; pseudo dead-end cycle can be reduced to compensate for higher solids and organic load following washout

Limit operational cost: membrane energy demand	Can membrane gas sparging regimes be identified to enable energy neutral operation?	(i) Conventional operation using continuous gas sparging, achieves low fouling rate but at a high energy cost (ii) Intermittent gas sparging can provide low fouling operation sufficient to achieve energy neutral sewage treatment (iii) Low solids environment makes sustainable operation all alternate pseudo dead-end gas sparging regime to be used; enables significant energy reduction (0.133 kWh m^{-3}) (iv) Negligible irreversible fouling occurred when the pseudo dead-end filtration cycle is fixed to be below 9 minutes; indicate that it is still below the critical accumulated specific mass (v) High sustainable flux can be achieved with pseudo dead-end gas sparging regime at and above critical flux, suggests operation independent of critical flux; reduction in capital cost	(i) For intermittent gas sparging, LEAPmbr or MemPulse™ could be used to reduce energy demand as this introduces higher peak shear at lower SGD_m; may also augment permeability (ii) Maintain stable sludge blanket and minimise solids washout to provide low solids environment; pseudo dead-end cycle length should be under 9 minutes to keep the accumulated specific mass below the critical value (iii) Specify membrane at or above J_c (J=15 L m^{-2} h^{-1}) (iv) Greater operational fluxes could be achievable by operating at shorter pseudo dead-end filtration cycle times (v) Lower fouling rates can be expected with a larger scale membrane due to improved hydrodynamic conditions particularly at lower SGD_m
Minimise capital cost	Can the membrane area be specified for full flow rather than peak flow?	(i) Increasing gas sparging during peak flow is effective to facilitate permeability recovery (ii) Whilst similar permeability recovery is attained for various gas sparging strategies, an improvement was achieved with SGD_m increased from 0.5 to 2.0 m^3 m^{-2} h^{-1} during peak flow and sustained for 2 h after peak flow (iii) Applying initial flux below the critical flux appears to be conducive to permeability recovery (iv) Supra-critical flux during peak flow for short duration can be managed (v) Low energy pseudo dead-end gas sparging regime provides similar potential for permeability but minimise the energy demand recovery compared with continuous gas sparging	(i) Increase gas sparging (SGD_m=2.0 m^3 m^{-2} h^{-1}) in response to an increase of peak flow (ii) Increase SGD_m from 0.5 to 2.0 m^3 m^{-2} h^{-1} during peak flow and sustain 2 h after peak flow with continuous filtration and continuous gas sparging (iii) Design the flux under critical flux when using continuous filtration and continuous gas sparging (iv) TMP set-point control strategy should be applied to facilitate permeability recovery (v) Low energy demand pseudo dead-end gas sparging regime can be applied to reduce fouling, increase permeability recovery and potentially increase the attainable flux

7.1 Can UASB configured AnMBR provide permeate quality compliance to International discharge standard?

The UASB configured AnMBR in this thesis provided compliant solids-free permeate with low total chemical oxygen demand (COD_t) of 34-41 mg L^{-1} and biochemical oxygen demand (BOD_5) of 10-13 mg L^{-1} even at low temperatures (Chapter 4, Chapter 5, Chapter 6). This is consistent with previous AnMBR studies treating municipal wastewater (Martin Garcia et al., 2013; Smith et al., 2013). The inoculum biomass may affect the permeate quality as granular biomass in UASB reactors has been shown to possess superior settling characteristics and higher specific activity (Lim and Kim, 2014), subsequently providing improved treatment performance versus flocculent UASB reactors. Interestingly, similar permeate quality from the granular AnMBR (G-AnMBR) and flocculent AnMBR (F-AnMBR) were obtained due to all solids, particulate matter and most colloidal matter retention by the membrane barrier (Chapter 4). This indicated that the expensive granules with limited supply can be replaced by the cheap and easily available flocculent inoculum biomass in UASB configured AnMBR without negatively influencing the permeate quality. Consistently high-quality permeate was also obtained during peak flow unsteady-state operation, in which the AnMBR flux temporarily increases in response to peak flow (Chapter 6). This indicated that UASB configured AnMBR is resilient to temporarily peak flow hydraulic shock, providing relatively stable permeate quality regardless of the flux fluctuations. Similar results were attained in the previous aerobic MBR (AeMBR) study with peak flow unsteady-state treating synthetic municipal wastewater (Lebegue et al., 2008). During other operational and environmental variations such as temperature and organic loading fluctuations, volatile fatty acid (VFA) accumulation can be a typical response (Leitão, 2004). This would directly affect the permeate quality as VFA cannot be normally retained by membrane (Ozgun et al., 2015). Further researches could be conducted to compare the UASB configured G-AnMBR and F-AnMBR under such operational and environmental variations.

In terms of nutrients, the ammonia concentrations even increased slightly through the AnMBR from 34±7 to 45±7 mg L^{-1}, which can be explained by the organically bound nitrogen release during the complex organic compounds degradation (Eusebi et al., 2013;

Toprak, 1995). Meanwhile, total phosphorus and ortho-phosphates concentrations of 7.5±1.5 and 6.3±1.4 mg L^{-1} were obtained in the permeate from this study. Therefore, further biological (Eusebi et al., 2013) or physico-chemical (McAdam et al., 2011; Sutton et al., 2011) downstream processes are required to meet the discharge consent for nutrients. Compared with conventional biological processes, the physico-chemical processes such as ion exchange (IEX) for nutrients removal become more attractive (Deng et al., 2014; McAdam et al., 2011; Sutton et al., 2011), as the high-quality permeate overcomes the bed clogging challenges in IEX processes (Martin-Garcia, 2010). Further investigations could be conducted to compare the characteristics of the permeate from G-AnMBR and F-AnMBR and their impact on the IEX for nutrients removal. The dissolved methane concentration in the anaerobic effluent is commonly between 10 and 25 mg L^{-1} (Cookney et al., 2012, 2016), which occupies about 40-50 % of the methane production in the UASB effluent treating municipal wastewater (Chernicharo et al., 2015; Cookney et al., 2012, 2016). Therefore, dissolved methane recovery as energy is essential to maximise the produced energy from anaerobic treatment (McAdam et al., 2011). Dissolved gas separation through membrane contactors can be considered due to high specific surface area of membrane that enables process intensification (Heile et al., 2017). The solids-free permeate with low organics makes it more attractive as it minimises the surface fouling and ensures consistently robust performance (Heile et al., 2017; Henares et al., 2017). Additionally, enhanced removal efficiencies can be achieved with comparatively low gas/liquid flow rate ratios, indicating a low energy requirement for dissolved methane recovery (Cookney et al., 2016; Heile et al., 2017). For example, Cookney et al. (2016) demonstrated that up to 98.9 % of the dissolved methane can be recovered through hollow fibre membrane contactor (HFMC) systems with net positive energy production around +0.08 kWh m^{-3}, facilitating a transition toward energy neutral sewage treatment.

A flowsheet for municipal wastewater treatment is proposed integration with AnMBR, HFMC and IEX (Figure 7-2). Compared with conventional process of A^2/O activated sludge processes (ASP) with typical hydraulic retention time (HRT) of 8 h (Tchobanoglous et al., 2003), the AnMBR in this thesis has a shorter HRT about 6 h (net

flux 13.5 L m^{-2} h^{-1}) without the need for secondary sedimentation tank. Additionally, the downstream HFMC degassing membrane and IEX processes for nutrient removal are also recognised as high rate unit processes with a short contact time of 1.5-12.5 s (Cookney et al., 2016) and an empty bed contact time (EBCT) of <30 min (Deng et al., 2014; Martin-Garcia, 2010) respectively. Therefore, a more compact sewage treatment plant with smaller footprint can be realised through this novel flowsheet application. Importantly, IEX provides the resultant product of a concentrated liquid with nitrogen and phosphorus, which has the potential to be recovered as a low-cost source of base chemicals for industrial applications (such as fertiliser) (McAdam et al., 2011).

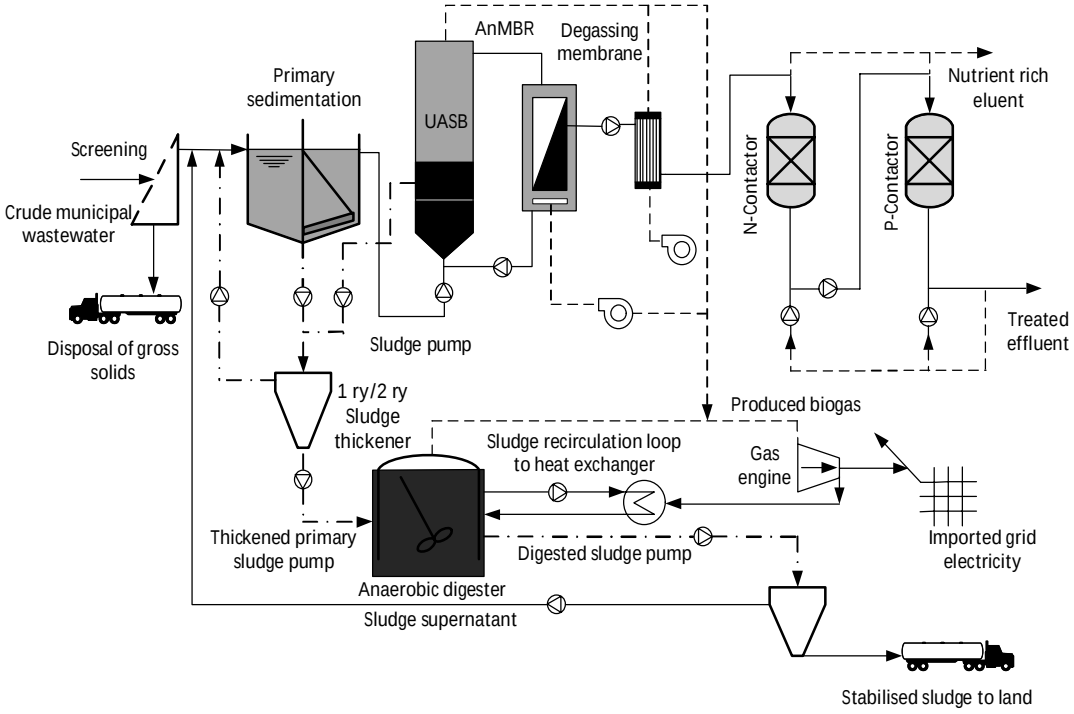

Figure 7-2. Schematics diagram of proposed flowsheet integration with anaerobic membrane bioreactor (AnMBR) (Adapted from Martin-Garcia (2010)).

7.2 Does UASB configured AnMBR provide a robust and resilient system for municipal wastewater treatment?

In UASB reactors, low temperatures increased total suspended solids (TSS) and COD concentrations in the effluent (Lew et al., 2004), which leads to solids washout sufficient to increase bulk sludge concentration in the downstream membrane tank, and may therefore influence the membrane permeability. The findings in this thesis

demonstrated that the granular UASB (G-UASB) is more stable than flocculent UASB (F-UASB) especially at low temperatures (Chapter 3). As a result, higher solids and colloidal soluble microbial products (SMPs) were observed in the downstream membrane tank of the F-AnMBR, leading to a higher membrane fouling propensity at low temperatures (Chapter 3, Chapter 4). It is therefore proposed to reduce upflow velocity (V_{up}) for F-UASB to sustain operation at low temperatures. By doing so, this thesis demonstrated similar sustained membrane operation in the G-AnMBR and F-AnMBR at low temperatures (Chapter 4). Furthermore, solids management strategies (Table 7-1) can also be applied to minimise solids washout, such as lower sludge bed height to column height ratio (around 20-30 %) to enable the solids settling and energy dissipation imparted from upflow liquid feeding and biogas release. Even solids washout from UASB to the downstream membrane tank occurred, membrane permeability can still be sustained by increasing the gas sparging rate to limit particle deposition (Chapter 5). Pseudo dead-end cycle length can also be reduced to compensate for higher solids and organic loadings, but more energy demand is required (Chapter 5).

In full-scale aerobic MBR (AeMBR), the MBR must designed to manage diurnal peaks and storm water flows (Hirani et al., 2010). In order to sustain membrane permeability, peak flow can be managed by either sustaining the average flux at peak flow through an increase in membrane surface area or temporarily increasing flux during peak flow. The latter option will constrain the capital investment in membrane surface area. A limited number of controlled studies conducted in AeMBR on the temporary increase in permeate flux to cope with peak flow, have demonstrated that response to peak flow is plausible without sacrificing membrane permeability (Hirani et al., 2010; Lebegue et al., 2008; Syed et al., 2009). This thesis indicated that UASB configured AnMBR can sustain the permeability to cope with peak flows through temporary increase of flux (Chapter 6). Several strategies such as increasing gas sparging rate during peak flow can be applied to facilitate the membrane permeability recovery after peak flow (Table 7-1). Further work is required to evaluate interventions during peak flow (such as TMP set-point control) coupled with pseudo dead-end filtration strategy to sustain the membrane permeability. Overall, this thesis demonstrated that UASB

configured AnMBR has the potential to provide a robust response to process perturbation (Chapter 3, Chapter 4, Chapter 6).

7.3 Is UASB configured AnMBR a low energy demand and low operational cost technology for municipal wastewater treatment?

The energy demand of gas sparging for membrane fouling control accounts for over two-thirds of the total energy demand (Pretel et al., 2014). The specific energy demand for membrane operation of full-scale AeMBR is typically between 0.19 and 0.70 kWh m^{-3} (Judd, 2011) and specific aeration demand per unit permeate (SAD_p) of 15-50 (Judd, 2008). In laboratory and pilot scale AnMBRs for municipal wastewater treatment, a higher specific energy demand up to 10 kWh m^{-3} (Smith et al., 2013) was reported (Chapter 2). This thesis demonstrated that conventional continuous gas sparging regime can achieve sustained membrane operation but at a high energy cost. Whilst the intermittent gas sparging regime is possible to achieve sustainable membrane operation with energy neutral sewage treatment, but it is close to the energy boundary layer (Chapter 5). The latest innovations of LEAPmbar and MEMPULSE^{TM} can be applied to further extend the gas sparging off time as this introduces higher shear stress at lower specific gas demand per unit membrane area (SGD_m) due to large amount of gas bubble release in short period of time controlled by an air chamber (Table 7-1) (Yoon, 2015). As a result, 20-30 % of the energy demand and operational cost can be further reduced, compared with commercially used intermittent gas sparging cycle of 10 s on/10 s off (Yoon, 2015). Importantly, the pseudo dead-end gas sparging regime can achieve sustained membrane operation with energy demand of 0.14 kWh m^{-3} and specific gas demand per unit permeate (SGD_p) of 14.8 m^3 m^{-3} (Chapter 5). This is only 50 % of the energy production (0.28 kWh m^{-3}) that was recovered from biogas and dissolved methane in a previous anaerobic research, treating this specific wastewater at an average temperature of 18 °C (Cookney et al., 2016). It is worth mentioning that a even lower energy demand can be expected at large scale due to improved hydrodynamic conditions to sustain membrane permeability particularly at low gas flow rate (Delgado et al., 2004). The residual energy production (0.14 kWh m^{-3}) coupled with the energy

(0.15 kWh m^{-3}) recovered from primary sludge and accumulated solids desludged from UASB reactor through anaerobic digester (AD) can be obtained. This can be utilised to support the energy demand of other systems in the flowsheet (Figure 7-2) such as the downstream degassing membrane, IEX, mechanical mixing, internal recycling and sludge treatment (Martin-Garcia, 2010; Mathioudakis et al., 2012). Accordingly, low energy demand or even energy neutral sewage treatment can be realised by applying this flowsheet integration with AnMBR for municipal wastewater treatment at ambient temperature.

7.4 What are the implications of this research on cost of AnMBR technology for municipal wastewater treatment?

The cost of commercially successful AeMBR technology has shown to be competitive with conventional activated sludge (CAS) treatment processes for medium and large municipal wastewater treatment plants (over 10,000 m^3 d^{-1}) (Brepols et al., 2010; Young et al., 2012). However, the high membrane investment cost and energy cost associated with fouling control limit the full-scale AnMBR applications for municipal wastewater treatment (Ruigómez et al., 2016). Typically lower fluxes of 5-12 L m^{-2} h^{-1} (Martin Garcia et al., 2013) can be applied in AnMBRs compared with that of 20-30 L m^{-2} h^{-1} in AeMBRs (Judd, 2011). In this thesis, a high attainable flux of 15 L m^{-2} h^{-1} (net flux of 13.5 L m^{-2} h^{-1}) can be achieved with alternative pseudo dead-end gas sparging regime (Chapter 5). It is asserted that by operating filtration in the absence of shear, fouling is less dependent upon the preferential migration of the sub-micron particle fraction and is instead governed by the compressibility of the heterogeneous cake formed, which enables higher operational fluxes to be achieved. This pseudo dead-end gas sparging regime application can therefore remarkably reduce the capital and operational cost of AnMBR for municipal wastewater treatment. More importantly, good permeability recovery of AnMBR through increasing gas sparging rate during the peak flow suggested that membrane surface area for AnMBR can be specified based on average flow instead of peak flow. This manifests in a considerable reduction in capital cost for membrane module investment in AnMBR (Chapter 6). Research into immersed AnMBR for

municipal wastewater treatment has employed a wide range of SGD_m up to 7.2 $m^3 m^{-2} h^{-1}$ (Smith et al., 2013) (Chapter 2), whilst the typical specific aeration demand per membrane surface area (SAD_m) of 0.14-0.53 $m^3 m^{-2} h^{-1}$ are applied in full-scale AeMBR (Yoon, 2015). The findings in this thesis also demonstrated a low net SGD_m of 0.2 $m^3 m^{-2} h^{-1}$ with pseudo dead-end gas sparging regime (Chapter 5), indicating considerable reductions of operational cost for energy demand and capital cost for blower purchases in AnMBR. Due to the aeration in biological compartment, more complex blower and diffuser technology are required to optimise the bubble diffusion and oxygen mass transfer in AeMBR (Yoon, 2015), leading to high capital cost for diffusion systems purchase in AeMBR. In AeMBR, typically HRTs of 5-8 h and about 12 h are applied in A/O (anoxic/aerobic) MBR and modified biological nutrient removal (BNR) MBR respectively (Yoon, 2015). A comparably lower HRT of 6 h was applied in this thesis (Chapter 5). During the unsteady-state peak flow, further lower HRT about 3 h (Initial flux of 6 L $m^{-2} h^{-1}$, peak flux of 24 L $m^{-2} h^{-1}$) can be obtained (Chapter 6). Therefore, lower capital costs are needed for concrete tank constructions in AnMBR compared with AeMBR. Overall, this thesis promotes UASB configured AnMBR as a more economically viable technology for municipal wastewater treatment, which could be comparable to the commercially successful AeMBR. However, further life cycle cost analysis must be conducted between AeMBR and AnMBR for municipal wastewater treatment in order to ascertain whether the overall costs of AnMBR can be competitive with commercially available AeMBR.

7.5 References

Brepols, C., Schafer, H. and Engelhardt, N. (2010) 'Considerations on the design and financial feasibility of full-scale membrane bioreactors for municipal applications', *Water Science & Technology*, 61, pp. 2461–2468.

Chernicharo, C.A.L., van Lier, J.B., Noyola, A. and Bressani Ribeiro, T. (2015) 'Anaerobic sewage treatment: state of the art, constraints and challenges', *Reviews in Environmental Science and Bio/Technology*, 14, pp. 649–679.

Cookney, J., Cartmell, E., Jefferson, B. and McAdam, E.J. (2012) 'Recovery of methane from anaerobic process effluent using poly-di-methyl-siloxane membrane contactors', *Water Science & Technology*, 65, pp. 604–610.

Cookney, J., Mcleod, A., Mathioudakis, V., Ncube, P., Soares, A., Jefferson, B. and McAdam, E.J. (2016) 'Dissolved methane recovery from anaerobic effluents using hollow fibre membrane contactors', *Journal of Membrane Science*, 502, pp. 141–150.

Delgado, S., Díaz, F., Vera, L., Díaz, R. and Elmaleh, S. (2004) 'Modelling hollow-fibre ultrafiltration of biologically treated wastewater with and without gas sparging', *Journal of Membrane Science*, 228, pp. 55–63.

Deng, Q., Dhar, B.R., Elbeshbishy, E. and Lee, H.S. (2014) 'Ammonium nitrogen removal from the permeates of anaerobic membrane bioreactors: Economic regeneration of exhausted zeolite', *Environmental Technology*, 35, pp. 2008–2017.

Eusebi, A.L., Martin-Garcia, N., Mcadam, E.J., Jefferson, B., Lester, J.N. and Cartmell, E. (2013) 'Nitrogen removal from temperate anaerobic-aerobic two-stage biological systems: Impact of reactor type and wastewater strength', *Journal of Chemical Technology and Biotechnology*, 88, pp. 2107–2114.

Heile, S., Chernicharo, C.A.L., Brandt, E.M.F. and McAdam, E.J. (2017) 'Dissolved gas separation for engineered anaerobic wastewater systems', *Separation and Purification Technology*, 189, pp. 405–418.

Henares, M., Izquierdo, M., Marzal, P. and Martínez-Soria, V. (2017) 'Demethanization of aqueous anaerobic effluents using a polydimethylsiloxane membrane module: Mass transfer, fouling and energy analysis', *Separation and Purification Technology*, 186, pp. 10–19.

Hirani, Z.M., DeCarolis, J.F., Adham, S.S. and Jacangelo, J.G. (2010) 'Peak flux performance and microbial removal by selected membrane bioreactor systems', *Water Research*, 44, pp. 2431–2440.

Judd, S. (2008) 'The status of membrane bioreactor technology', *Trends in Biotechnology*, 26, pp. 109–116.

Judd, S.J. (2011) *Principles and Applications of Membrane Bioreactors in Water and Wastewater Treatment*. 2nd edn. London,UK: Elsevier.

Lebegue, J., Heran, M. and Grasmick, A. (2008) 'MBR functioning under steady and unsteady state conditions. Impact on performances and membrane fouling dynamics', *Desalination*, 231, pp. 209–218.

Leitão, R.C. (2004) *Robustness of UASB Reactors Treating Sewage Under Tropical Conditions*. Wageningen University.

Lew, B., Tarre, S., Belavski, M. and Green, M. (2004) 'UASB reactor for domestic wastewater treatment at low temperatures: A comparison between a classical UASB and hybrid UASB-filter reactor', *Water Science & Technology*, 49, pp. 295–301.

Lim, S.J. and Kim, T. (2014) 'Applicability and trends of anaerobic granular sludge treatment processes', *Biomass and Bioenergy*, 60, pp. 189–202.

Martin-Garcia, I. (2010) *Sludge free and energy neutral treatment of sewage*. Cranfield University.

Martin Garcia, I., Mokosch, M., Soares, A., Pidou, M. and Jefferson, B. (2013) 'Impact on reactor configuration on the performance of anaerobic MBRs: Treatment of settled sewage in temperate climates', *Water Research*, 47, pp. 4853–4860.

Mathioudakis, V.L., Soares, A., Briers, H., Martin-Garcia, I., Pidou, M. and Jefferson, B. (2012) 'Treatment and energy efficiency of a granular sludge anaerobic membrane reactor handling domestic sewage', *Procedia Engineering*, 44, pp. 1977–1979.

McAdam, E.J., Luffler, D., Martin-Garcia, N., Eusebi, A.L., Lester, J.N., Jefferson, B. and Cartmell, E. (2011) 'Integrating anaerobic processes into wastewater treatment', *Water Science & Technology*, 63, pp. 1459–1466.

Ozgun, H., Gimenez, J.B., Evren, M., Tao, Y., Spanjers, H. and van Lier, J.B. (2015) 'Impact of membrane addition for effluent extraction on the performance and sludge characteristics of upflow anaerobic sludge blanket reactors treating municipal wastewater', *Journal of Membrane Science*, 479, pp. 95–104.

Pretel, R., Robles, A., Ruano, M.V., Seco, A. and Ferrer, J. (2014) 'The operating cost of an anaerobic membrane bioreactor (AnMBR) treating sulphate-rich urban wastewater', *Separation and Purification Technology*, 126, pp. 30–38.

Ruigómez, I., Vera, L., González, E. and Rodríguez-Sevilla, J. (2016) 'Pilot plant study of a new rotating hollow fibre membrane module for improved performance of an anaerobic submerged MBR', *Journal of Membrane Science*, 514, pp. 105–113.

Smith, A.L., Skerlos, S.J. and Raskin, L. (2013) 'Psychrophilic anaerobic membrane bioreactor treatment of domestic wastewater', *Water Research*, 47, pp. 1655–1665.

Sutton, P.M., Rittmann, B.E., Schraa, O.J., Banaszak, J.E. and Togna, A.P. (2011) 'Wastewater as a resource: A unique approach to achieving energy sustainability', *Water Science & Technology*, 63, pp. 2004–2009.

Syed, W., Zhou, H., Sheng, C., Mahendraker, V., Adnan, A. and Theodoulou, M. (2009) 'Effects of hydraulic and organic loading shocks on sludge characteristics and its effects on membrane bioreactor performance', *Proceedings of WEFTEC*. Orlando, FL.

Tchobanoglous, G., Burton, F.L. and Stensel, H.D. (2003) *Wastewater Engineering Treatment and Reuse*. 4th edn. New York: McGraw-Hill Companies.

Toprak, H. (1995) 'Removal of soluble chemical oxygen demand from domestic wastewaters in a laboratory-scale anaerobic waste stabilization pond', *Water Research*, 29, pp. 923–932.

Yoon, S.H. (2015) *Membrane Bioreactor Processes: Principles and Applications*. CRC press.

Young, T., Muftugil, M., Smoot, S. and Peeters, J. (2012) 'MBR vs. CAS: capital and operating cost evaluation', *Water Practice & Technology*, 7.

CHAPTER 8

Conclusions and future works

8 Conclusions and future works

8.1 Conclusions

This thesis explored the potential to improve the operational resilience of upflow anaerobic sludge blanket (UASB) configured anaerobic membrane bioreactor (AnMBR) treating municipal wastewater at ambient temperature, in order to achieve energy neutral sewage treatment. Overall, a highly reliable and more cost-effective UASB configured AnMBR can be achieved for full-flow municipal wastewater treatment at ambient temperature and ultimately delivers energy neutral sewage treatment. The following conclusions were drawn from this thesis:

1. A review of literature revealed significant differences with respect to biomass characteristics and fouling behaviour between aerobic and anaerobic MBRs, indicating a more challenging bulk sludge matrix in anaerobic MBRs than in aerobic MBRs. The energy production was comparable to that employed for membrane fouling control in AnMBR, suggesting that energy neutral operation is achievable for AnMBR applied to municipal wastewater treatment (Objective 1).
2. The solids accumulated in the sludge blanket of UASB reactor enhances treatment efficiency and improves biogas production during the steady-state operation. Low temperatures (average temperature of 10°C) cause the instability of the UASB reactor (Objective 2).
3. Granular inoculum biomass has good stability which exerts a positive influence on UASB performance and sustained permeability. Whilst membrane inclusion can dissipate disadvantages of flocculent biomass to deliver similar sustained membrane operation provided the sludge blanket is controlled (Objective 2, Objective 3).
4. Solids management (control the sludge blanket at a threshold between the sludge blanket development and steady-state period) and boundary condition selection (i.e. keep relatively high upflow velocity of 0.8-0.9 m h^{-1} in the UASB reactor for granular AnMBR to promote stratification of particular and granular material, whilst reducing upflow velocity to about 0.4 m h^{-1} for flocculent AnMBR at low temperatures to minimise solids washout) are required, to enable a more resilient

UASB and sustainable membrane operation at low temperatures (Objective 2, Objective 3).

5. Low energy demand (0.14 kWh m^{-3}) and high attainable flux (15 L m^{-2} h^{-1}) with sustained membrane operation can be attained in UASB configured AnMBR by pseudo dead-end gas sparging regime, sufficient to achieve energy neutral sewage treatment (Objective 4).
6. Membrane permeability has the potential to be recovered after peak flow during unsteady-state operation in UASB configured AnMBR treating municipal wastewater. Consequently, the membrane area requirement for AnMBR can be specified based on average flow providing a considerable (67 %) reduction in capital cost compared with the design based on peak flows (three times of average flow), sufficient to make AnMBR a more economically viable proposition (Objective 5).

8.2 Future works

Several key areas where future work could be beneficial have been identified from this thesis:

1. Long term trials are required with upgraded UASB reactor coupled with solids management strategies arising from this thesis to ascertain the improvement of sludge blanket stability and treatment performance, and to evidence that flocculent inoculum biomass can be a robust alternative to granular inoculum biomass for municipal wastewater treatment at low temperatures.
2. Further comparison of granular and flocculent AnMBRs could be conducted under operational and environmental variations. More microbial diversity research with temporal sampling is also warranted to further characterise granular and flocculent inoculum biomass. Additionally, the characteristics of permeate and their impacts on the downstream ion exchange for nutrients removal could also be compared between granular and flocculent UASB configured AnMBR.
3. Critical pseudo dead-end cycle length needs to be determined to have a better understanding about the fouling deposit characteristics and further tests should be conducted to assess the possibility of higher fluxes in order to further reduce the

energy demand and operational cost of AnMBR. The long-term trials with pseudo dead-end gas sparging regimes are also required.

4. Further long-term trials under unsteady-state peak flow operation should be conducted with higher initial and peak fluxes by applying pseudo dead-end filtration coupled with transmembrane pressure (TMP) set-point fouling control strategy, in order to sustain the membrane permeability and further reduce the capital cost of AnMBR.
5. Further investigations have to be conducted on life cycle cost analyses to ascertain the economic feasibility of the flowsheet integration with AnMBR for municipal wastewater treatment and to compare with commercially successful aerobic MBR.

APPENDICES

Appendices

Appendix 1: Images of pilot scale experimental rigs

Figure A- 1. 70 L upflow anaerobic sludge blanket (UASB) reactors with granular and flocculent inoculum biomass (Chapter 3 and Chapter 4).

Figure A- 2. Sludge blanket in granular UASB reactor.

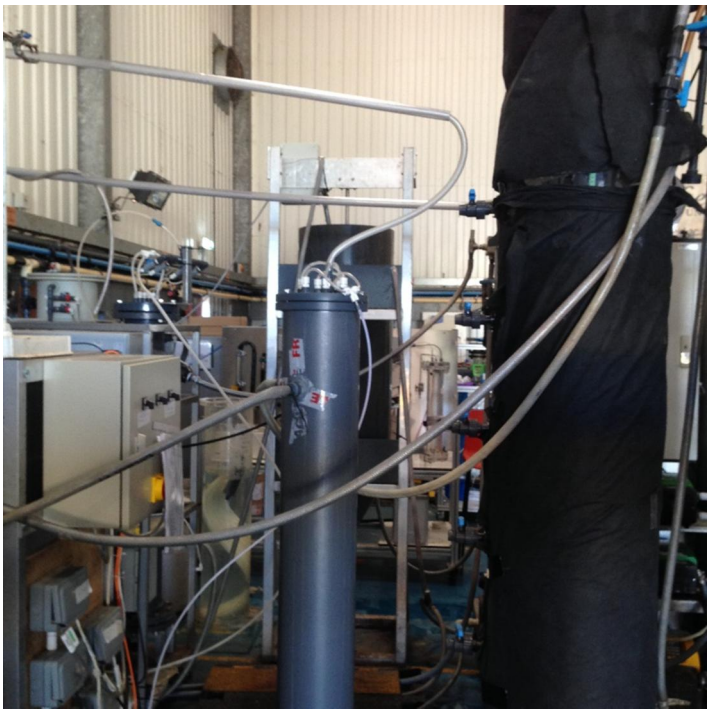

Figure A- 3. 70 L granular and flocculent UASB reactor coupled with 30 L membrane tank (Chapter 4).

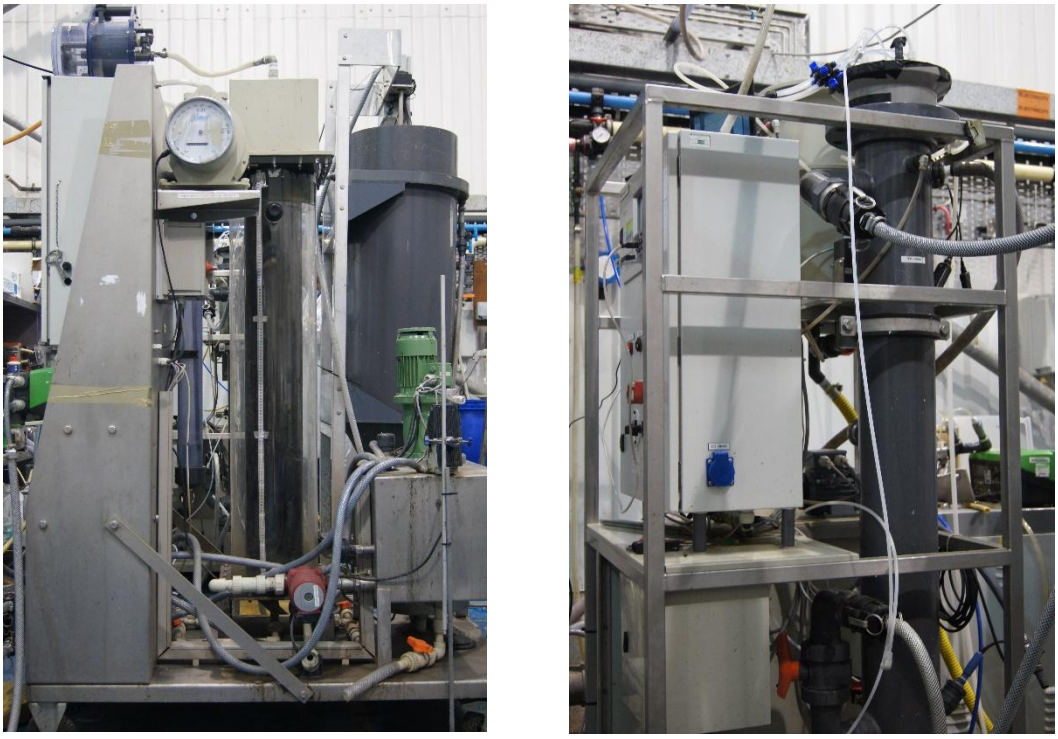

Figure A- 4. 42.5 L granular UASB reactor coupled with 30 L membrane tank (Chapter 5 and Chapter 6).

Figure A- 5. ZW-10 membrane module.

Appendix 2: Images of lab-scale membrane cell

Figure A- 6. Lab scale membrane cell (Chapter 4).